Atmospheric Dispersion Modelling Liaison Committee

Annual Report 1999/2000

INCLUDING

Review of Dispersion Over Bodies of Water

AND

Best Practice for Binning Meteorological Data

These studies were funded by the Atmospheric Dispersion Modelling Liaison Committee.

Chilton
Didcot
Oxon OX11 0RQ

Approval: January 2002
Publication: February 2002
£30.00
ISBN 0 85951 460 9

This NRPB report reflects understanding and evaluation of the current scientific evidence as presented and referenced in this document.

The following amendments have been made to this report since its first publication (February 2002)

May 2003

Title page	Price amended to £30.00
Page numbers 63–203	Addition of Annex B

PREFACE

In 1977 a meeting of representatives of government departments, utilities and research organisations was held to discuss methods of calculation of atmospheric dispersion for radioactive releases. Those present agreed on the need for a review of recent developments in atmospheric dispersion modelling, and a Working Group was formed. Those present at the meeting formed an informal Steering Committee, that subsequently became the UK Atmospheric Dispersion Modelling Liaison Committee. That Committee operated for a number of years. Members of the Working Group worked voluntarily and produced a series of reports. A workshop on dispersion at low wind speeds was also held, but its proceedings were never published.

The Committee has been reorganised and has adopted terms of reference. The organisations represented on the Committee, and the terms of reference adopted, are given in this report. The organisations represented on the Committee pay a small annual subscription. The money thus raised is used to fund reviews on topics agreed by the Committee, and to support in part its secretariat, provided by NRPB. The new arrangements came into place for the start of the 1995/96 financial year. This report describes the fifth year in which the Committee has operated under the new arrangements, and during which it placed two contracts, for reviews of modelling dispersion over bodies of water and for methods of binning meteorological data when calculating concentrations from continuous releases. The technical specifications for these contracts are given in this report, and the contract reports attached as annexes to this report. The Committee funded eight studies in previous years; they are described in its earlier annual reports.

The Committee intends to place further contracts in future years and would like to hear from those interested in tendering for such contracts. They should contact the Secretary:

Mr J G Smith
National Radiological Protection Board
Chilton
Didcot
Oxon OX11 0RQ

E-mail: justin.smith@nrpb.org

CONTENTS

ATMOSPHERIC DISPERSION MODELLING LIAISON COMMITTEE

1 ORGANISATIONS REPRESENTED ON THE COMMITTEE

Atomic Weapons Establishment, Aldermaston

British Energy

British Nuclear Fuels plc

BNFL Magnox Generation

Department of the Environment Northern Ireland

Environment Agency

Health and Safety Executive

- Hazardous Installations Directorate
- Nuclear Installations Inspectorate

Ministry of Agriculture, Fisheries and Food

Meteorological Office

National Nuclear Corporation

National Radiological Protection Board

Nycomed Amersham plc

Royal Naval College, Greenwich

Rolls Royce Power Engineering plc

Scottish Environment Protection Agency

Urenco (Capenhurst)

Westlakes Research Institute

The Chairman and Secretary are provided by NRPB.

2 TERMS OF REFERENCE

1 To review current understanding of atmospheric dispersion and related phenomena and to identify suitable models for application primarily in authorisation or licensing, in the context of discharges to atmosphere resulting from nuclear industry activities.

2 The Committee shall consist of representatives of government departments, government agencies and primarily the nuclear industry. Each organisation represented on the Committee shall pay an annual membership fee of £1000.

3 The Committee will consider selected topics. These should be selected following discussion and provisional agreement at meetings of the Committee, followed by confirmation after the meeting. Where possible, it will produce reports describing suitable models for that topic. These will reflect either the views of an Expert Working Group appointed by the Committee or the outcome of a workshop organised on behalf of the Committee. The Working Group will determine who should be invited to speak at workshops, and will subsequently review their outcome and identify suitable models.

4 The money raised from membership fees and registration fees for the workshops will be used to support the Working Group, the drafting of reports, and any other matters which the Committee may decide.

3 REPORTS OF THE COMMITTEE AND ITS EARLIER WORKING GROUP ON ATMOSPHERIC DISPERSION

Clarke, R H (1979). The first report of a Working Group on Atmospheric Dispersion: a model for short and medium range dispersion of radionuclides released to the atmosphere. Harwell, NRPB-R91

Jones, J A (1981). The second report of a Working Group on Atmospheric Dispersion: a procedure to include deposition in the model for short and medium range dispersion of radionuclides. Chilton, NRPB-R122

Jones, J A (1981). The third report of a Working Group on Atmospheric Dispersion: the estimation of long range dispersion and deposition of continuous releases of radionuclides to atmosphere. Chilton, NRPB-R123

Jones, J A (1981). The fourth report of a Working Group on Atmospheric Dispersion: a model for long range atmospheric dispersion of radionuclides released over a short period. Chilton, NRPB-R124

Jones, J A (1983). The fifth report of a Working Group on Atmospheric Dispersion: models to allow for the effects of coastal sites, plume rise and

buildings on dispersion of radionuclides and guidance on the value of deposition velocity and washout coefficients. Chilton, NRPB-R157

Jones, J A (1986). The sixth report of a Working Group on Atmospheric Dispersion: modelling wet deposition from a short release. Chilton, NRPB-R198

Jones, J A (1986). The seventh report of a Working Group on Atmospheric Dispersion: the uncertainty in dispersion estimates obtained from the Working Group models. Chilton, NRPB-R199

Atmospheric Dispersion Modelling Liaison Committee. Annual Report 1995/96. Chilton NRPB-R292

Includes annexes

- Atmospheric Dispersion at Low Wind Speed
- Application of Computational Fluid Dynamics Codes to Near-field Atmospheric Dispersion
- Rise of a Buoyant Plume from a Building Wake

Atmospheric Dispersion Modelling Liaison Committee. Annual Report 1996/97. Chilton NRPB-R302

Includes annexes

- Atmospheric Dispersion at Low Wind Speed
- Review of Models for Calculating Air Concentrations when Plumes Impinge on Buildings or the Ground

Atmospheric Dispersion Modelling Liaison Committee. Annual Report 1997/98. Chilton, NRPB-R316

Includes annex

- Portability of Weather Data for Dispersion Calculations

Atmospheric Dispersion Modelling Liaison Committee. Annual Report 1998/98. Chilton NRPB-R322

Includes annexes

- Review of Deposition Velocity and Washout Coefficient
- Review of Flow and Dispersion in the Vicinity of Groups of Buildings

4 SPECIFICATIONS FOR TECHNICAL ANNEXES

A Dispersion over bodies of water

The Atmospheric Dispersion Modelling Liaison Committee wishes to undertake a review of some aspects of dispersion modelling for releases near bodies of water. Previous work has developed a model for use particularly in submissions under Article 37 of the Euratom Treaty. This work assumed that material would travel across the water body in a straight line, and that the water body was sufficiently large that the land-to-sea and sea-to-land transition regions represented a sufficiently small part of the total travel distance that their effects could be ignored. Models have also been given for dispersion during air flow from sea-to-land where the sea surface temperature is lower than the land temperature, particularly where the release height is such that the source is in the stable (marine) air.

The Committee is interested in further work, particularly for the following situations:

Dispersion over small bodies of water, such as a lake or estuary, where the transition regions cover a substantial part of the total travel distance.

Dispersion in situations where material first travels out to sea and is subsequently returned to land, as a result of land-sea breezes. This should cover the probability of such conditions occurring in the UK, concentrations in the plume when it returns to land and the likely distance along the coast between the site and the point where the plume could return to the land.

Dispersion during air flow from sea-to-land when the sea surface temperature is warmer than the land temperature or when the release point is within the internal boundary layer.

B Recommendation for best practice on binning meteorological data

Dispersion models which utilise both statistical and sequential techniques for producing long term impact assessments of concentrations and depositions inherently give different results depending on the methodology chosen. Ad-hoc studies undertaken by the Meteorological Office have shown that these can be significant for three month simulations examining neutrally buoyant near surface releases using ADMS V2.1. Such discrepancies are affected by the categories into which met data is binned.

However powerful computers become, there will likely be a need for statistical modelling for the foreseeable future. An assessment of the most appropriate binning schemes is therefore needed, with comment on how the statistical approach may affect model output statistics. With the introduction of the use of

topographical effects in statistical runs within ADMS V3.0 this topic is of increasing interest.

Deliverable: To undertake a one year comparison between a sequential and statistical analyses of 3 release scenarios incorporating near surface non-buoyant releases; near surface buoyant releases and elevated buoyant releases.

The studies will be repeated for the standard scheme (which will be described) plus 3 other different binning methods (these will differ in binning intervals only). Results will be interpreted paying particular attention to the long-term average, 95^{th} ,97^{th} and 99^{th} percentile concentrations. The results will be analysed as is thought to be appropriate once they are available. This is likely though to include contour plots of the differences between concentration fields for the different techniques.

These comparisons will be undertaken using the ADMS V3.0 dispersion model. A report will be produced proposing the most appropriate methodology for binning met data based on the type of release. This report will include appropriate introductory material about the methods of, and errors associated with, the binning of meteorological data.

A qualitative assessment of how the binning methods are site specific will be given, with evidence provided from further limited model simulations where appropriate. This will include a qualitative discussion of the effect of complex terrain.

ANNEX A

DISPERSION OVER BODIES OF WATER

I R Cowan, D M Deaves and I G Lines
W S ATKINS CONSULTANTS

Summary

In order to determine the dispersion of pollutants over large distances, it is necessary to be able to use dispersion models confidently over a range of different underlying terrain types, and also over regions where there are changes of terrain type. The dispersion of plumes which travel over water, and over land/water interfaces, is one area in which a number of non-standard features of the dispersion characteristics need to be modelled. Hence, the main objective of this report was to review existing models and information relating to dispersion over water. Interest was focused predominantly on coastal sites, although consideration was also given to small bodies of water, such as a lake or estuary.

A literature review of published material on the subject of sea breezes, or dispersion over water was undertaken. It was clear from this study that significant advances had been made in the last decade in the understanding of the structure, occurrence and effect on dispersion of sea and lake breezes. This has been due to sets of field measurements and, in particular, computational fluid dynamics (CFD) studies. A number of different phenomena have been identified in this report, and their effect on pollution dispersion has been discussed.

An assessment was made on the current status of modelling, and this found that the most noticeable advances have been in the use of CFD for studying sea breezes. Little progress has been made in the application of box models or simpler models. Some of the current commercial implementations of box models include an allowance for some of the above phenomena, but these have been found to be small in number and are generally unvalidated. As a result, a number of suggestions have been made for ways of improving box model predictions for dispersion over water. It is suggested that the efficacy of such modifications could be judged against either field or CFD data, depending on availability.

A1 Introduction

A1.1 Background

In order to determine the dispersion of pollutants over large distances, it is necessary to be able to use dispersion models confidently over a range of different underlying terrain types, and also over regions where there are changes of terrain type. The dispersion of plumes which travel over water, and over land/water interfaces, is one area in which a number of non-standard features of the dispersion characteristics need to be modelled. The present document reviews certain particular features of such dispersion flows, relating to:

dispersion within regions of transition between roughness changes

transient and 3D dispersion effects due to sea breezes.

effects of thermal boundary layers on dispersion

The study includes a fairly wide ranging review covering all aspects of sea and lake breeze structure as well as specifically considering dispersion modelling. It includes some analysis of meteorological data which gives further insight into the characteristics which can be used to assess the possible effects on dispersion during sea breeze events.

A1.2 Definitions

The term *"sea breeze"* is used generically in this report to describe onshore local winds that are driven by surface temperature differences onshore and offshore. This includes shorelines bordering lakes and estuaries.

Two broad classes of computer modelling are considered in this report: simple models and CFD. These are briefly defined below:

A1.3 Objectives

(a) Review existing models and information relating to:

- Dispersion over small bodies of water, such as a lake or estuary, where the transition regions cover a substantial part of the total travel distance.
- Dispersion in situations where material first travels out to sea and is subsequently returned to land, as a result of land-sea breezes.
- Dispersion during air flow from sea-to-land when the sea surface temperature is warmer than the land temperature or when the release point is within the internal boundary layer.

Assessment of the way forward in situations where models are not currently available.

A1.4 Scope of work

Task 1 Review current models

The review used as its starting point the work done in this area in the early 1980's, and presented in NRPB R157 by Jones (1983). This provided much information on sea breezes and growing thermal boundary layers, and gave proposed model modifications where these were considered necessary. Account was also taken of models such as ADMS (Carruthers et al, 1992), in which there is some allowance for such effects.

A literature search was then undertaken to ensure that details of the current understanding of the relevant processes were considered. This was focused on the areas of interest identified in Section A1.1.

Task 2 Review sea breeze effects

The key features of sea breezes as they relate to dispersion modelling are;

- magnitude and duration
- vertical structure and extent
- frequency of occurrence
- temperature, geostrophic wind and relative humidity at occurrence.

The review used the information provided in Jones (1983), the Forecasters Reference Book (Met Office, 1993) and many other pertinent references found in the literature review.

Task 3 Undertake sample calculations for sea breeze effects

Three sets of calculations were made to study the effects of flow over water on dispersion:

- a calculation using ADMS (Carruthers et al, 1992), in order to model coastline fumigation.
- a calculation with HGSYSTEM (Post, 1994), to investigate the effect of roughness changes; on dispersion;
- a hand calculation of pollution recirculation as a result of a change in wind direction due to the passing of a sea breeze.

These calculations were used to assess the suitability of such models for dispersion over water.

Task 4 Assess scope for incorporating air/sea interaction effects into future model development

The output of Tasks 1-3 enabled some judgement to be given on the state of dispersion modelling in relation to air/sea interfaces, on the current level of understanding of the processes involved, and of the significance of such effects

on dispersion over bodies of water. These outputs have been considered together, to enable an assessment to be made on the potential for future development.

A2 Literature Review

A2.1 Information overview

The information obtained for this study was acquired from a number of sources, including personal contacts, internet sites, literature searches, and references from existing papers and books. This enabled more than 50 useful references to be obtained covering the various issues of interest. These have been collated into various headings, and are reviewed in Sections A2.2 - A2.5. It should be noted that some reviews appear in more than one section, since the content relates to more than one subject, and full cross-referencing has been provided between the different sub-sections.

The information from the above sources has been arranged into four main subject groups, as follows:

- structure and general effects of sea breezes;
- internal boundary layer (IBL) effects, including fumigation;
- recycling and circulation of pollution;
- other aspects of sea breezes, not covered above.

The next four subsections provide a summary of the pertinent findings from these groups of papers. The revisions are arranged in date order in each section.

A2.2 Sea breeze structure and general effects

This section covers general descriptions of sea breezes and the details of the sea breeze front.

Pearson (1973) derived a simple 2D numerical model to simulate a sea breeze over flat terrain.

Ogawa et al (1975) A wind tunnel simulation was made of the gross features of a sea breeze flow, demonstrating the significant effect of stability on turbulence levels and plume spreading rates. It was observed that stable conditions, such as might be found in the marine air transported in by a sea breeze, could increase ground-level concentrations by a factor of up to 5.

Blumenthal et al (1978) - See Section A2.4.

Simpson et al (1977) studied the occurrence of sea breezes at Lasham, 45km inland on the South coast of England, over a period of 12 years. During those 12 years, 76 sea breezes were recorded throughout the months of April to

September. This is approximately 6.3 per year. Comparing this to Thorney Island, where there were 75 sea breezes a year, implies that only 1 in 12 reach inland to Lasham. The rate of advance, the time of onset, the effect of synoptic wind conditions, and the effect of the tide are all discussed with respect to sea breezes. The structure of the sea breeze front has also been analysed in this paper using field data. A model for the rate of advancement of the front is presented.

Keen & Lyons (1978) undertook a programme of field measurements around Milwaukee, on Lake Michigan. The structure of the land/lake breeze system was analysed.

Steinberger & Ganor (1980) discussed ozone levels with reference to meteorological conditions. Interest was especially focused on the height of the base of the inversion layer, and the effect it can have on trapping pollutants close to the ground. It was stated that, in polluted urban complexes, a peak in ozone levels usually occurs around noon. However, downwind of a highly polluted city, a second peak, which can often be much higher than the first, occurs in the mid-afternoon due to transport processes such as sea breezes.

Pielke (1981) discussed basic concepts behind sea and land breeze formation. Interactions between the sea and sea breezes were also discussed briefly, and were suggested as an area being in need of further research. An example of a CFD simulation of sea breezes over Lake Michigan was given.

Jones (1983) reported the results of an NRPB working group on atmospheric dispersion, addressing the effects of coastal sites on the dispersion of radionuclides. The consensus of the working group was that dispersion in coastal regions was likely to be dominated by the effects of air stability changes that typically arise due to differences in sea and land temperature. Differences in land and sea roughness levels were not expected to be significant. In the report, a distinction was made for onshore winds between cases where the sea is warmer than the land and cases where the sea is colder than the land. For the former, a stable layer forms over the land surface, and the standard dispersion models can be applied. For the latter, as is the case in a sea breeze, an unstable layer is formed and account needs to be taken of the IBL and fumigation effects. Expressions were given for the IBL depth and the diffusion parameters, inside and above the IBL, and an example was given of a calculation of the ground level concentrations arising from stack releases inside and above the IBL. Some illustrative expressions were also given for the speed of travel of the sea breeze front and its likely effect on a plume release.

Pielke (1984) referred to sea breezes in his book on mesoscale meteorological modelling, as examples of terrain-induced mesoscale airflow systems. He presented an idealised sequence of events describing the diurnal variation of the coastal wind circulations and reviewed some results from sea breeze simulations.

Abbs (1986) presented both field data and 3D CFD simulation data for airflow over Melbourne. This included both sea breeze and bay breeze effects, due to the particular local topography. The two airflows were found to interact with each

other and with local orography, and under some conditions were found to form an inland cyclonic circulation. Good agreement was reported between the simulations and the field data, allowing the simulations to be used to explain some of the apparently contradictory field observations.

McElroy & Smith (1986) gave field data from the coastal region around San Diego and Los Angeles, where sea breezes are common, using airborne LIDAR. A mechanism was discussed for the production of pollutant layers through undercutting via sea breeze currents. This was suggested as an effective means of removing pollution from the S. California basin, where it would otherwise be trapped by a persistent inversion layer.

Ogawa et al (1986) attempted to clarify the turbulent mechanisms in the sea breeze front, and in particular fumigation, through field observations of a sea breeze front and the subsequent development of a thermal internal boundary layer (TIBL).

Helmis et al (1987) researched the structure of an experimentally measured sea breeze front over Athens, focusing on the early structure, ie before it is affected by the presence of the coastal IBL (see Section A2.3). Two fronts were studied, with different synoptic wind directions, giving different front shapes.

Kitada (1987) A 2D CFD simulation was used to study the airflow, temperature and turbulence structure ahead of and within a sea breeze flowing over flat terrain. The results illustrated a number of key features: the high stability of the marine air; the recirculating nature of the flow at the sea breeze front, with an associated peak in turbulence energy; and the growth of a thermal IBL. Typical values of the vertical diffusivity were given for air ahead of and behind the sea breeze front, and these showed a difference of up to a factor of 10, with the larger values in the mixed layer ahead of the front.

Simpson (1987) devoted a chapter of his book on gravity currents to sea breeze fronts. He presented a map of England showing the inland penetration of a set of sea breezes for a June day during which the synoptic winds were light. A criterion was suggested for the onset of a sea breeze, in terms of the difference in sea and land surface temperatures and the offshore wind speed. Some discussion was made of the structure of the sea breeze front, and of the different means of visualising the front, including radar returns from birds and insects which tend to accumulate there.

Yamada et al (1988) A coarse CFD simulation was made of a 24-hour period for conditions over Tokyo bay, showing the formation of a set of sea breezes and a convergence zone inland.

Eppel et al (1992) presented CFD simulations of sea-breeze events in the German Bight area. Comparison with field data (not shown in the paper) allegedly shows good qualitative agreement for surface winds.

Kunz & Moussiopoulos (1995) used a nested CFD model (MEMO) to simulate air flow over Athens for two specific days, both of which included sea breeze events.

A coarse-grid model was used to establish the background wind flow conditions; this information was then fed into a fine-mesh simulation for a much smaller region around Athens. Comparison of results with experimental data at six locations showed generally good agreement for wind direction and strength.

Borrego (1996) A coarse CFD simulation was made of the air quality in the region around Lisbon for a 24-hour period, during which a sea breeze was present.

Ridley (1995). See Section A2.4.

Camps et al (1996) - See Section A2.4.

Carissimo et al (1996) carried out CFD simulations of land/sea breeze evolution over a period of 24 hrs in the Athens area, using the MECURE code as part of the APSIS (Athenian Photochemical Smog Intercomparison of Simulations) project. Surface wind predictions were presented and compared with field data, and good agreement was found.

Nguyen et al (1997) A comparison was made between dispersion results from Eulerian and Lagrangian dispersion models for pollutant releases into a sea breeze event in Australia. The Eulerian model only updated its wind field once an hour, as opposed to every 20s for the Lagrangian model, and so significant differences were observed in the predicted trajectories of the plumes as the sea breeze was established. From the limited evidence available, it was concluded that the Lagrangian approach was the more versatile.

Sharan & Gopalakrishnan (1997) CFD simulations were made of the Bhopal toxic gas leak accident. These indicated that the presence of two large inland lakes close to the gas source had the effect of turning the local wind direction by 45º, which was enough to significantly effect the trajectory of the released material.

Xu et al (1997) presented field data for coastal New England, including wind rose and dry deposition rate data.

A2.3 Fumigation and IBL effects

This section focuses on the sea/land interface, and the effect on pollution dispersion of the internal boundary layer (IBL) that is often present in such regions.

Van der Hoven (1967) stated that diffusion over land was approximately three times larger than diffusion over water if the water is colder than the land. This is due to difference in surface roughness and the stability class of the airflow. Local meteorological effects such as sea breezes and IBLs were discussed in general.

Lyons & Cole (1973) dealt primarily with fumigation arising from onshore winds that are gradient wind driven, ie not lake breezes. On 15% of spring and summer days, a stable onshore flow occurs in the Chicago - Milwaukee area, ie 3 times more common than lake breezes. Observations were reported of a

fumigation episode, and a model was presented based on a Gaussian plume approach.

Peters (1975) presented two models to predict the extent of the fumigation region. They are based respectively on a boundary layer model and on a constant heat flux method. A minimal comparison with field data shows reasonable agreement for the BL model approach. Further analysis and verification was advocated.

Gifford (1976) reviewed turbulence typing schemes and discussed the differences between them. Modifications to the diffusivity values were proposed with a discussion of the means of relating stability classes to BL measures such as the Monin Obukhov length (L) and surface roughness parameter (z_o). Diffusion over water was discussed in detail, including low roughness levels and a modified L value. Diffusion in cities, in the lee of buildings, near highways and in irregular terrain was also discussed.

Raynor et al (1979) presented aircraft measurements in an IBL taken during onshore winds over Long Island. The data taken included air temperature (T), vertical turbulence intensity (σ_w) and wind speed, as well as lapse rate. Other instruments were also used to supplement the above data. The edge of the IBL was determined from traces of σ_w and T. Graphs were plotted showing turbulence and temperature structure on cross-sections through the IBL, for different wind conditions. An expression was quoted for the IBL height in terms of fetch and wind conditions. Velocity profiles were also presented for conditions prior to and during a sea breeze.

Van Dop et al (1979) showed that the discontinuity in the surface temperature at a shoreline often modifies the ABL considerably, and suggested that these effects could be incorporated into a Gaussian-plume model. They discussed the Lyons & Cole model for shoreline fumigation and presented a modified model, the main difference being a change to the lateral diffusivity coefficient. The IBL height was expressed as being proportional to the square root of the distance downwind, $H \sim x^{1/2}$. The wind direction and strength were uniform and constant in their model. Large differences (of around a factor of 3) were found for ground-level concentration predictions between the old and new models. However, it was noted that experimental data was sparse and that further validation was required.

Raynor et al (1980) undertook a study to examine current methods for predicting diffusion of pollutants from coastal nuclear power plants. Five areas were identified as being unsatisfactory - coastal IBLs; boundary layer stability classification; instrument heights and tower location; plume meander; and diffusion calculations. It was highlighted that the presence of a coastal IBL can make interpretation of tower data for stability class etc. problematic, and hence can result in non-conservative diffusion predictions. Suggestions were given for tower locations to alleviate this. References were made to studies that show that stability class is poorly correlated with lapse rate. Further inaccuracies may be

introduced into predictions of diffusion parameters due to the presence of transition regions near the coast. Uncertainties were raised about the accuracy of the plume meander expressions in coastal regions.

Misra (1980a) presented a fumigation model based on two zones: one for stable marine air, the other for the TIBL.

Misra (1980b) tested the model developed in above paper against field data for the gradient driven flow off Lake Ontario. Good general agreement was found for one single fumigation episode.

Jones (1983). See Section A2.2.

Stunder et al (1986) presented an improved model for fumigation, based on the premise that a plume emitted into stable marine air does not mix immediately down to ground-level when it arrives at the thermal IBL edge, but that this process is gradual. The Gaussian plume model of Misra (1980a) was modified using information for IBL downdrafts, and also using an empirical expression from tank tests. Since these modifications made the agreement with field data worse, the principle of immediate mixing seems sound.

Carruthers et al(1992) described the ADMS v1.0 coastline module that accounts for plume fumigation. This model can be applied under the following conditions: when there is an onshore wind, when the land is warmer than sea and when the air over the sea is stably stratified. The thermal IBL height was assumed to vary as $x^{½}$, and estimates were made for the stable boundary layer characteristics over the sea. The diffusion parameters were modified depending upon whether the plume was inside or above the IBL.

Jiang & Yu (1994) carried out a CFD study of shoreline fumigation using a second order turbulence closure model for the wind field and a Lagrangian dispersion model for the pollutant. Sensitivity tests were undertaken to assess the effects of the pollutant release height and the synoptic wind direction on plume dilution.

Lu & Turco (1994). Elevated layers of ozone are frequently observed above Los Angeles, above the base of the temperature inversion. Several mechanisms have been suggested to explain their presence; these were tested by Lu & Turco through numerical modelling. A 2D model was used to simulate sea-breezes, with and without mountains present. The formation of elevated layers was found to occur through undercutting by the stable, marine air in the sea breeze front. Anabatic mountain flows were also shown to be a viable mechanism for producing layering. It was thus shown that a combination of a sea breeze and a mountain slope flow can be highly effective in creating pollutant layering.

Lu & Turco (1995). As shown in a previous paper (Lu & Turco, 1994), sea breezes and mountain slope flows can play important roles in governing pollutant transport under stagnant synoptic conditions over the Los Angeles basin. A set of 3D CFD simulations were presented, and an elevated layer was found to form.

Lyons et al (1995). See Section A2.4.

Zhibian & Zenquan (1995) presented a shoreline fumigation model which accounts for wind shear. Observations of thermal IBLs in eastern Chinese coastal regions found that over 60% of the cases had differences in wind direction of greater than 15º between the IBL and overlying stable layer. This can result in a curve in the ground level pollutant concentration trajectory, a wider plume extent and reductions in the ground level concentrations.

A2.4 Pollution circulation and recycling

The references discussed here relate primarily to the re-circulation of pollutants caused by variations in the wind field during sea breeze events.

Blumenthal et al (1978) presented aircraft based data, taken in the Los Angeles basin during a highly smoggy day. A sea breeze was present and its effect in bringing clear air into the basin and in transporting dirty air inland was demonstrated. It was also shown that pollutant carry-over from previous days could be significant.

Ozoe et al (1983) used a simple, 2D CFD model with constant eddy diffusivity coefficients to model sea/land breeze evolution, and pollutant dispersion. A negligible geostrophic wind was assumed, so that a closed diurnal sea/land breeze circulation was formed, producing steadily more polluted conditions each day.

Uno et al (1984) presented observations of ozone levels and demonstrated that a strong relationship exists between the vertical ozone profile and the height of the temperature inversion (lid). He also showed that ozone above the inversion persists and affects the mixed layer the next day, and that sea breezes are important in determining the ozone distribution. Airborne measurements were taken over Tokyo Bay over a period of 3 days, and the pollution evolution and trajectory were studied.

McElroy & Smith (1986). See Section A2.2.

Briere (1987) applied a 2D model (3rd order closure) to sea breeze circulation.

Eastman et al (1995) used the RAMS CFD model, run in both 2D and 3D modes, to predict meteorological fields for Lake Michigan. A Lagrangian particle dispersion model (LPDM) was used to model pollutant dispersion, with a modification to account for TIBL effects. A Gaussian plume model was also applied (ISCST). Sensitivity tests were run to assess the effects of the mesh spacing and the number of the particles employed. The CFD runs showed a strong degree of pollutant recirculation along the coast of the lake, which could not be reproduced by the ISCST model.

Lyons et al (1995). A set of 3D CFD simulations with the RAMS/LPDM models were used to illustrate the influence of mesoscale vertical motions on plume dispersion. These include examples of fumigation and the effect of a sea breeze

front. The latter showed that pollutants from a coastal release can be lifted high up into the troposphere at the sea breeze front, resulting in reduced surface concentrations local to the updraft, but also potentially fumigation far downwind as the pollutants are mixed back down to ground level. Recirculation of pollutants within the sea breeze was not found to be common for simple coastline shapes. It was noted that many of these dispersion effects cannot be reproduced accurately with a Gaussian model.

Moussiopoulos et al (1995) simulated a smog pollution episode over Athens using the CFD model MEMO, coupled with a photochemical pollution model (MARS). Synoptic wind flow conditions over the Athens basin were practically stagnant. Moreover, the strength of the sea breezes was not enough to transport fresh air into the city, so that if these conditions had persisted the pollution levels would have risen steadily.

Nester (1995). As part of the APSIS project, 3D CFD simulations were made of conditions over the Athens basin for a period of 24 hours. It was shown that sea breezes are an important factor in the short-range transport of pollutants, and that air quality in the city is determined principally by the local sources. Long range transport of pollutants was dismissed as being negligible.

Ridley (1995) A CFD simulation was made of the sea breezes over Auckland during calm synoptic weather conditions. Due to the peninsular nature of the land, strong convergence occurred of sea breezes from different coastlines, coupled with a marked return flow aloft at a height of approximately 1km. This return flow was observed to be particularly affected by Coriolis forces, which acted to turn the flow to the left, thus providing the possibility of diurnal recycling of pollutants. Dispersion simulations were also undertaken, and these highlighted the importance of convergence zones in holding up and concentrating pollution.

Camps et al (1996) presented a 3D CFD study of pollutant dispersion in Tarragona (Spain) at a coastal location, with mountains inland. During the summer, the probability of sea breeze occurrence on any given day was estimated as being greater than 80%. A simulation was made of a 24 hour period, during which time both a strong sea breeze and a weak land breeze were present. Comparisons were made with field data of velocity profiles and reasonable agreement was found. Other data presented included wind direction, potential temperature, turbulence energy and the height of the mixed layer. Dispersion was studied in the simulation by releasing SO_2 from a set of elevated industrial sources near the coast. Near ground level, the sea breeze carried the pollutant inland. However, higher up (above 1000m) the return flow was found to carry the pollutant offshore, albeit at much lower concentration levels. No significant recirculation of pollutants was observed.

Latini et al (1996) CFD simulations were used to illustrate the possibility of pollution being transported from valley to valley by sea breeze circulations for cases where the valleys are parallel and face out to sea.

Romero & Ramis (1996) made numerical (CFD) simulations of SO_3 transport over the island of Mallorca during a 24 hour period in which the airflow was strongly dominated by sea breezes. The results were used to analyse the effect of a proposed new power plant, and to suggest optimal locations for siting pollution monitoring equipment. It was found that elevated layers of pollution, carried inland on the sea breeze, could subside in the evening as the land breeze was established, leading to high levels of pollution over a wide inland region.

Carizi et al (1998) used a hydrostatic, primitive equation model to simulate two sea breeze events. The agreement with the field data was not good. Dispersion was studied using a Lagrangian model, and also two Gaussian models, which had been modified to account for fumigation.

Andronopoulos et al (1999) undertook CFD studies of pollutant transport over a Mediterranean coastal area that is subject to pronounced thermal wind systems. Recycling of pollutants occurs due to diurnal wind variation. The Adrea-I model was employed for the CFD simulations, with fixed wind conditions on the landward (or upwind in terms of the background synoptic flow) domain boundaries. The sea breeze was explicitly calculated, and agreed well with field data. Reversed flow (ie a land breeze) occurred during the night-time. For simulation of the pollutant dispersion, EPA's UAM model was employed; the results showed the expected plume development and movement through the day and night.

A2.5 Other effects of dispersion over water

The three papers listed here discuss aspects of coastal dispersion that are not covered in the previous sections.

Heines & Peters (1973) studied the effect on pollutant dispersion of a temperature inversion above the stack height through use of a simplified analytical model. A constant wind field was assumed, and empirical expressions were applied for the diffusion coefficients. It was demonstrated that the ground level concentration is always increased by the presence of an inversion.

Rotunno (1983) applied linear theory to sea breezes, and focused on the effect of latitude on the flow, through the Coriolis effect.

Martin & Pielke (1983) used a linear model to study the adequacy of the hydrostatic model in simulating sea and land breezes over flat terrain. They found that the assumption becomes less valid as the intensity of the surface heating increases and as the synoptic temperature lapse rate becomes less stable.

A2.6 Recent advances in understanding of sea breezes

The Working Group on Atmospheric Dispersion produced a report in 1983 (Jones) that included a discussion of dispersion at coastal sites. The report considered two major effects of a sea breeze on dispersion. The first effect was a reduced

level of turbulence in the marine air blown onshore by the breeze, due to its generally higher level of static stability. A typical figure for plume spread offshore was given as 40% of that inland, in the absence of the breeze. The second effect was the formation of a thermal internal boundary layer (IBL), starting at the coastline, which raises the possibility of plume trapping and fumigation for releases near the coast.

A second report was produced by the Working Group in 1986 (Jones) which addressed the levels of uncertainty that might be present in dispersion calculations using the Working Group models. In particular, it advised that simple Gaussian models may not be appropriate for use in regions where surface properties vary significantly, such as near coastlines. It also stated that inclusion of sea breeze effects in probabilistic risk assessment codes had not produced significant changes in consequence predictions.

Since these reports, a large amount of effort has been expended on researching further the structure of typical sea breezes and their practical effect on dispersion in coastal regions. To illustrate this point, Table A2.1 lists the majority of the references from the previous section, sorted by date. Included in the table is an indication of what type of investigative approach was taken, ie field measurements, simple analytical modelling, or computer modelling through use of simple models (eg Gaussian plume modelling) or computational fluid dynamics (CFD).

This research has focused on the following:

gathering of more field data on sea breezes;

investigation of other ways in which sea breezes can influence pollution levels in coastal regions;

3D CFD modelling of pollution episodes, driven or affected by sea breezes.

As is reflected in the table, simple models have largely been replaced in the last decade by three-dimensional CFD calculations for researching sea breezes, since this approach can help explore in greater detail some of the spatial and transient effects of sea breezes. The only significant advance in simpler modelling appears to have been the incorporation of the effects of IBLs on dispersion into box models such as UK-ADMS (see Carruthers et al, 1992, — Section A2.3, and calculations presented in Section A5.2).

Table A2.1 List of references concerned with sea breezes, including the modelling approach employed in each study

Author	Year	Report section	Field measurements	Other	Box models	CFD
Van der Hoven	1967	2.3	✓			
Heines & Peters	1973	2.5		✓		
Lyons & Cole	1973	2.3			✓	
Pearson	1973	2.2		✓		
Ogawa et al	1975	2.2		✓		
Peters	1975	2.3		✓		
Gifford	1976	2.3			✓	
Simpson et al	1977	2.2	✓			
Blumenthal et al	1978	2.4	✓			
Keen & Lyons	1978	2.2	✓			
Raynor et al	1979	2.3	✓			
Van Dop et al	1979	2.3			✓	
Misra	1980	2.3			✓	
Misra	1980	2.3	✓		✓	
Raynor et al	1980	2.3	✓		✓	
Steinberger & Ganor	1980	2.2	✓			
Pielke	1981	2.2				✓
Jones	1983	2.2			✓	
Martin & Pielke	1983	2.5		✓		
Ozoe et al	1983	2.4				✓
Rotunno	1983	2.5		✓		
Uno et al	1984	2.4	✓			
Abbs	1986	2.2	✓			✓
McElroy & Smith	1986	2.2	✓			
Ogawa et al	1986	2.2	✓			
Stunder et al	1986	2.3			✓	
Briere	1987	2.4				✓
Helmis et al	1987	2.2	✓			
Kitada	1987	2.2				✓
Simpson	1987	2.2	✓			
Yamada et al	1988	2.2		✓		
Carruthers et al	1992	2.3			✓	
Eppel	1993	2.2	✓			✓
Jiang & Yu	1994	2.3	✓			✓
Lu & Turco	1994	2.3				✓
Eastman	1995	2.4			✓	✓
Kunz & Moussiopoulos	1995	2.2				✓
Lu & Turco	1995	2.3				✓
Lyons et al	1995	2.2				✓
Moussiopoulos	1995	2.4				✓
Nester	1995	2.2				✓
Ridley	1995	2.4				✓
Zhibian & Zengquan	1995	2.3	✓		✓	

Author	Year	Report section	Field measurements	Other	Box models	CFD
Borrego	1996	2.2				✓
Camps	1996	2.4	✓			✓
Carissimo	1996	2.2				✓
Latini et al	1996	2.4				✓
Romero & Ramis	1996	2.4				✓
Nguyen et al	1997	2.2				✓
Sharan & Gopalakrishnan	1997	2.2				✓
Xu		2.2	✓			
Carizi et al	1998	2.4			✓	✓
Adronopoulos et al	1999	2.4				✓

The CFD simulations found in the literature have concentrated on a small number of highly polluted coastal cities, such as Athens and Los Angeles, where a combination of adverse weather conditions, sea breezes and orography all combine to produce episodes during which the air quality in parts of the city deteriorates considerably.

It is noted that the development of a 3D CFD model for such a city requires considerably more detail than is necessary when applying a simple model, and that such a CFD model generally takes several days to run. This compares with several hours for a simple model. Hence use of CFD will not always be the most cost-effective means for practical studies of dispersion around industrial plant, and continued use of simple modelling, or a mixture of CFD and simple modelling, may be more appropriate.

A3 Details of sea and lake breezes

A3.1 Origins of sea and land breezes

Pielke (1984) describes the following idealised sequence of events for the diurnal evolution of the sea and land breezes over flat terrain in the absence of strong background (synoptic) winds (see Figure A3.1):

6am: calm conditions prevail; pressure surfaces are flat.

9am: strong surface heating sets up convective air currents over the land and acts to mix mass upwards; over the water, surface heating of the air is insignificant. An offshore pressure gradient is thus created at some distance off the ground, which drives an offshore flow aloft.

Noon: the offshore flow of air aloft creates a low-pressure region inland, and onshore winds (the sea breeze) develop.

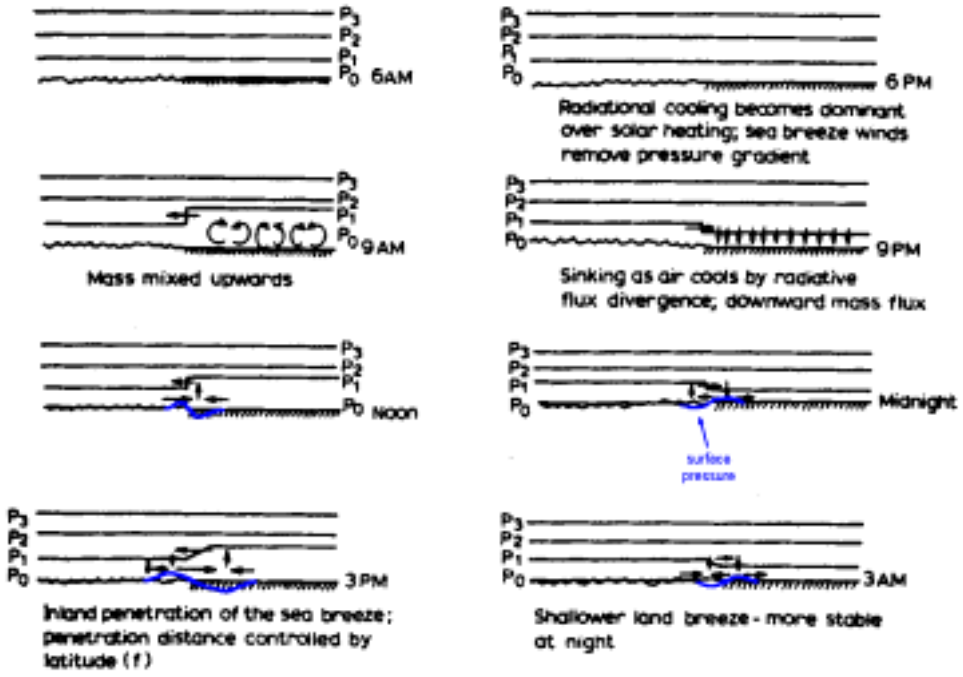

FIGURE A3.1 Diurnal evolution of the sea and land breeze systems in the absence of significant synoptic flow (reproduced with permission from Pielke, 1984). Surface pressure levels are also marked.

3pm: the sea breeze front continues to penetrate inland, advecting with it the horizontal temperature gradient.

6pm: as the sun sets, radiative heating of the land surface is replaced by radiative cooling, and the wind field removes the horizontal temperature gradient, dissipating the sea breeze front.

9pm: the air temperature over the land drops, increasing its density, and thus causing it to sink. This sets up an onshore pressure gradient and thus an onshore wind aloft.

Midnight: in response to a loss of mass above the surface over the water, a pressure minimum develops off the coast. This sets up an offshore land breeze.

3am: the land breeze penetrates offshore.

6am: the cycle repeats, if conditions are still favourable.

Pielke (1984) notes that the translucency of the sea surface and its greater ability to conduct heat away from the surface mean that the temperature of the sea surface varies to a much lesser degree throughout the day than that of the land. This differential surface temperature drives the above sea/land breeze system. However, at night the ground cooling increases the atmospheric stability, which in turn suppresses mixing, and so land breezes are generally shallower and weaker than sea breezes.

The above picture is made more complicated by the presence of a weak or moderate (Pielke quotes less ~6m/s) synoptic wind flow. A wind in the same direction as the sea breeze weakens the effects of the sea breeze, since the wind acts to diminish the horizontal temperature gradient. Conversely, a wind in the opposite direction to the sea breeze strengthens the temperature gradient and thus enhances the effects of the sea breeze.

A3.2 Differences between flow conditions over land and over water

The dispersion of pollution from a release near the coastline will be affected by the airflow conditions in the background wind. However, airflow conditions over water are often very different from those overland, due to differences in surface roughness and static stability. The sudden change in surface characteristics can have a significant effect on the spreading rate of a plume that is released into a coastal region.

A3.2.1 Surface roughness

In general, there is a marked difference in surface roughness over land and over water. To illustrate this, Table A3.1 lists the values of roughness for various different sea states, with weather conditions varying from calm to extremely stormy. The maximum likely roughness length scale over water is quoted as being 1cm, with values appropriate to relatively calm sea breeze conditions likely to be rather lower, at <1mm, for example. However, overland this level of roughness is only comparable to that of a fairly flat grassland plain. Quoted overland roughness values range up to 70cm for city centres. Hence, roughness levels overland are significantly higher than those over water.

This marked change in roughness from overland to over-water or vice versa creates an internal boundary layer (IBL), which can be considered as the extent over which the direct influence of the roughness change is experienced. Figure A3.2 illustrates such a flow.

To help assess the effect that such a roughness change might have on the wind speed and turbulence level, a simple set of calculations is presented in Table A3.2, based on data from the ESDU data book.

TABLE A3.1 Typical values of the terrain roughness parameter, z_0. Data is drawn mainly from the ESDU (1998) Wind Engineering data book; data marked with the symbol † is drawn from Snyder (1981)

Roughness length, z_0 (m)	Terrain description	
	Over water	Over land
0.00003	Sea surface for calm conditions†.	—
0.001	Inland lake in extreme storm	Snow covered farmland. Flat desert.
0.003	Rough sea in extreme storm	Flat area with short grass and no obstructions.
0.01	Very rough sea in extreme storm (50yr extreme)	Fairly level grass plain with isolated trees.
0.03	—	Open level country with few trees, few hedges and isolated buildings.
0.1	—	Countryside with many hedges, some trees & some buildings.
		Villages, outskirts of small towns.
0.3	—	Wooded country. Small towns or suburbs.
0.7	—	Forests. City centres.

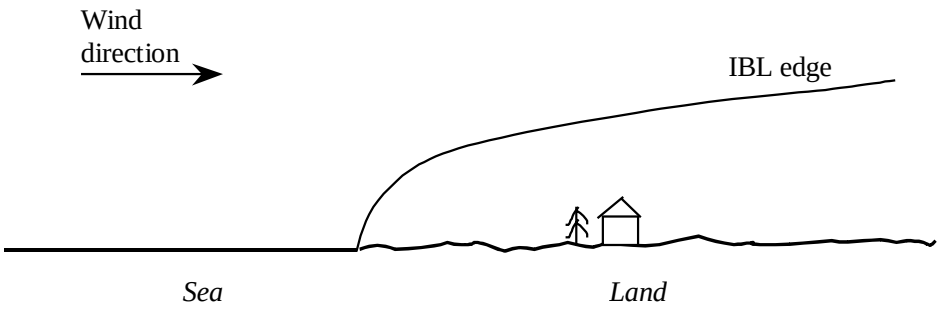

FIGURE A3.2 Schematic representation of IBL growth during an onshore wind. This IBL may be due to onshore / offshore differences in roughness and stability levels

These calculations suggest that, within 1km of the shoreline, turbulence levels (or, more properly, levels of turbulent velocity fluctuations, u', which can be expressed as u' = IU, where I is the turbulence intensity and U the mean wind speed) at a height of 10m above ground might be increased by approximately +3% over their values over water. In contrast, the mean wind speed would be reduced by approximately -11%. These variations in mean and turbulent velocity tend to vary slightly in magnitude with height until the edge of the IBL is reached, at which point wind conditions are well approximated by the over water values. For example, from Table A3.2, it appears that, within approximately 1km of the shore, the IBL height is less than 100m since the mean and turbulent velocities are little affected at this height.

The implications for dispersion in coastal regions, are that, in the absence of thermal IBL effects, plume spreading rates will increase slightly as the marine air moves inland due to the higher land surface roughness.

A3.2.2 Static stability

The atmospheric conditions that promote the generation of sea breezes also act to generate differences in static stability for the air over the land and water. Over land, conditions will be highly convective (or "unstable") during the daytime, providing the driving force behind the sea breeze development. In terms of the commonly used Pasquill-Gifford stability categories, conditions are likely to be either A or B. Over the water, the surface flux of heat into the air is much smaller, and atmospheric conditions are usually either neutrally or stably stratified, ie categories D to F.

TABLE A3.2 An example calculation for an onshore flow, based on data from ESDU. The height above the surface is denoted by z

	Sea	Land			
Distance from coastline (km):	—	0.1	1	10	600
Roughness length, z_0 (m):	0.001		0.03		
Wind speed at height of z = 10m (m/s):	5.0	4.9	4.4	4.1	3.8
Turbulence intensity at height of z = 10m:	0.12	0.12	0.14	0.16	0.18
Standard deviation of velocity fluctuations at z = 10m (m/s):	0.60	0.60	0.62	0.66	0.68
Wind speed at height of z = 100m (m/s):	6.4	6.4	6.4	5.8	5.5
Turbulence intensity at height of z = 100m:	0.08	0.08	0.09	0.11	0.13
Standard deviation of velocity fluctuations at z = 100m (m/s):	0.51	0.51	0.51	0.64	0.72

In an onshore wind, this stable marine air is transported over the land, and is slowly modified as it is heated from below. A thermal internal boundary layer (IBL) forms, with unstable air in the region close to the ground and stable marine air aloft. The fate of a plume of pollution released into a coastal region depends upon its release location relative to the IBL boundary, as is illustrated in Figure A3.3 and discussed below:

If the release point is within the IBL (top diagram in Figure A3.3), then the plume mixes rapidly in the unstable air, up to the height of the IBL. A temperature inversion at the edge of the IBL suppresses mixing beyond this boundary, and so traps pollution within the IBL. Vertical plume spreading rates are then determined by the IBL growth rate (in both space and time).

If the release point is above the IBL (lower diagram in Figure A3.3), then the initial plume development will be governed by the turbulent mixing levels in the

stable marine air which, as is shown below, are considerably smaller than those in unstable air. The initial spreading rate of plume is thus low. However, once the plume intersects the top of the IBL, then mixing levels are suddenly increased, and the pollution tends to mix rapidly down to the ground (see the review of the paper by Stunder et al, 1986, in Section A2.3).

IBLs and their effects are discussed in greater detail in Section A4.2.

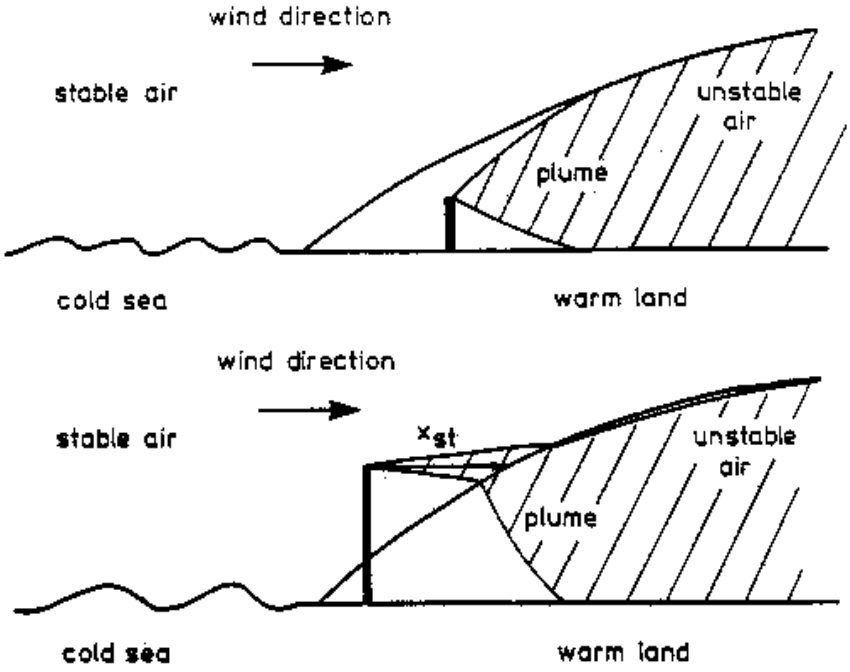

FIGURE A3.3 Schematic of plume releases into a coastal region with a thermal IBL present (from Jones, 1983). The figures illustrate the phenomena of plume trapping (top) and fumigation (bottom)

Gifford (1976) presents values for plume spreading rates for differing atmospheric conditions, as derived by Briggs. The ratios of these spreading rates to their values under neutral conditions are summarised in Table A3.3 below. This suggests that spreading rates in the IBL are a factor of three or more higher than those in the marine air. These findings are in agreement with the comments of Jones (1983), and Van der Hoven (1967), who quote ratios of spreading rates of 2.5 and 3 respectively.

TABLE A3.4 Ratio of lateral (σ_y) & vertical (σ_z) plume spreading rates to their values under neutral stability (σ_{y0} , σ_{z0}) for different atmospheric stability classes

Pasquill type	σ_y/σ_{y0}	σ_z/σ_{z0}
A	2.75	$3.33\sqrt{(1 + 0.15x)}$
B	2.00	$2.00\sqrt{(1 + 0.15x)}$
C	1.38	$1.33\sqrt{((1 + 0.15x)/(1 + 0.2x))}$
D	1	1
E	0.75	$0.5\sqrt{((1 + 0.15x)/(1 + 0.3x))}$
F	0.50	$0.27\sqrt{((1 + 0.15x)/(1 + 0.3x))}$

A3.2.3 Conclusions

Changes in surface roughness and atmospheric stability have both been shown to cause changes in turbulence levels, and thus mixing levels, in the air that is transported onshore by a sea breeze. Consideration of the magnitude of the two effects leads to the conclusion that the main change in mixing will be due to a change in stability, which is in agreement with the comments of Jones (1983).

A3.3 Sea breeze front

The form of the sea breeze front depends strongly upon the magnitude of the offshore component of the synoptic wind (Simpson, 1987). For calm conditions, the front is highly diffuse and may extend over several kilometres. However, on days on which the breeze meets an opposing wind, the front sharpens and represents a gravity current of cold air. Figure A3.4 shows a schematic representation of such a gravity current.

The sharpness of the front may change as it traverses inland. For example, Simpson et al (1977) report four occurrences in which a sea breeze passed over the south coast of England as a highly diffuse structure, causing no detectable sudden changes in wind speed and direction or humidity, before sharpening rapidly near Reading, 70km inland. An inspection of anemograms from this latter location clearly shows the sudden arrival of the sea breeze front.

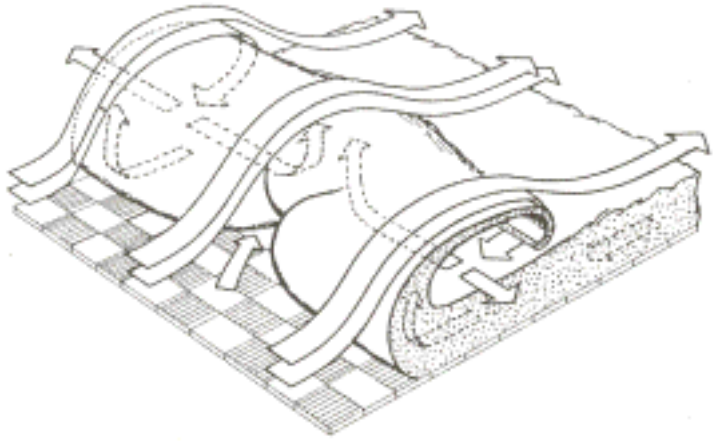

FIGURE A3.4 Schematic representation of the flow at a gravity current head, in a frame of reference that moves with the current (reproduced with permission from Simpson et al, 1977)

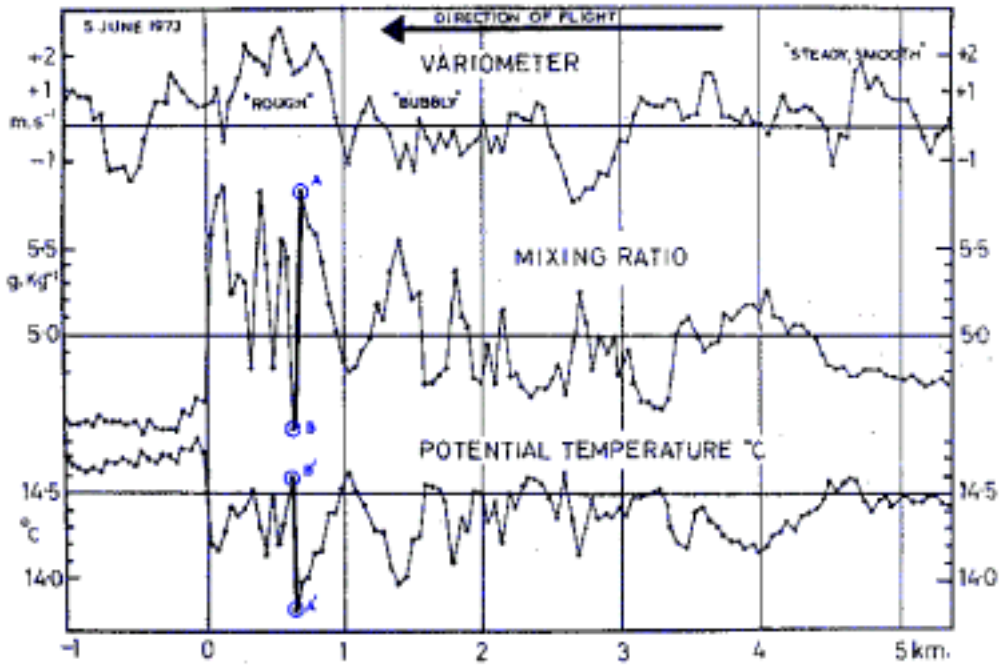

FIGURE A3.5 Traces of vertical velocity, mixing ratio and potential temperature for a horizontal traverse through a sea breeze front (reproduced with permission from Simpson et al, 1977). The front is located at zero on the abscissa, and is proceeding to the left in the graph. Points A/A' and B/B' denote undiluted marine and land air respectively

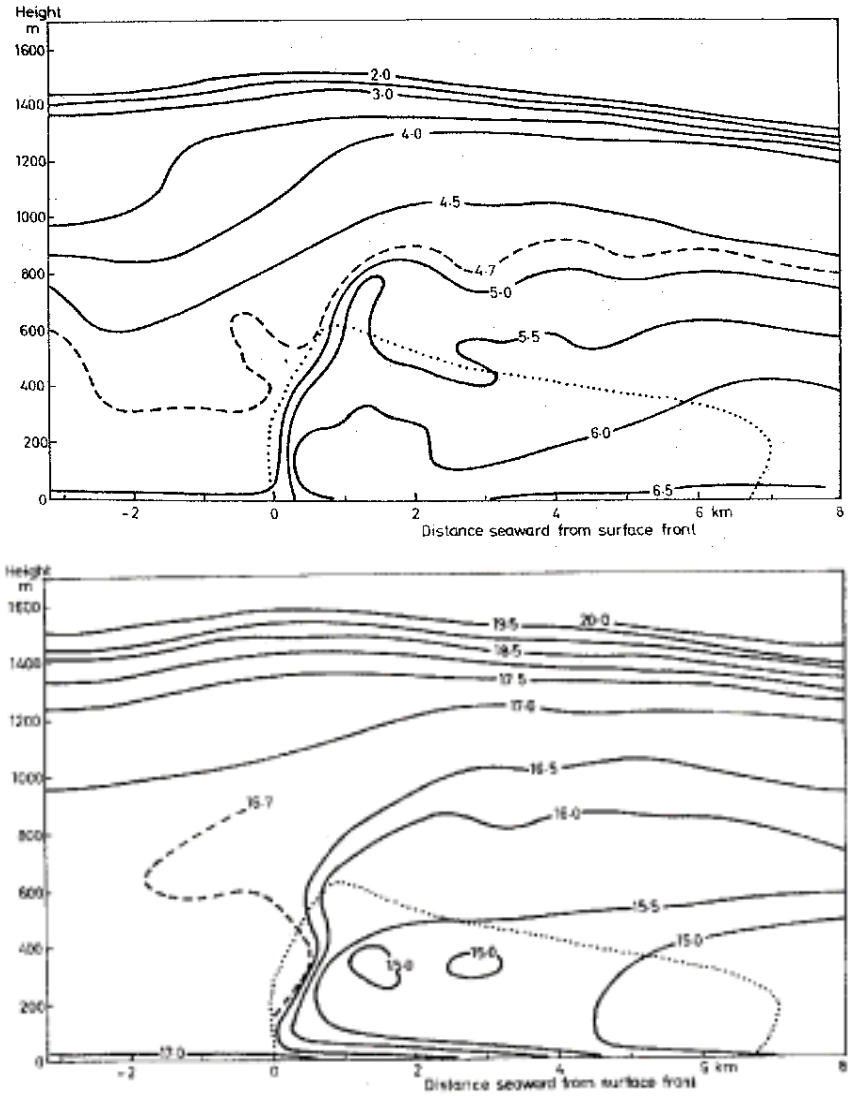

FIGURE A3.6 Contours of mixing ratio in g/kg (top) and potential temperature from field measurements of a sea breeze — see Figure A3.10 for more details. (reproduced with permission from Simpson et al, 1977)

Figure A3.5 presents field data from a traverse through a sea breeze front over the south coast of England, at a height of 600m. Ahead of the front (negative distance on the abscissa), the traces of temperature* and humidity* are relatively flat. Behind the front, rapid fluctuations occur in both quantities, which suggests the presence of strong levels of turbulence. These quantities fluctuate between values that are characteristic of undiluted marine and land air (study, for example, points A and B in the graph). Such intermittency is the result of large-scale turbulent mixing, which acts to engulf quantities of background air. Smaller-scale turbulence eventually mixes out the large fluctuations in properties, so that several kilometres behind the front the conditions are more

* Figure A3.5 actually plots the *mixing ratio* and the *potential temperature*. The mixing ratio is the ratio of water vapour to dry air, and is thus related to humidity. The potential temperature, θ, is the temperature that the air would have were its pressure, P, adjusted adiabatically to some reference value, P_0, ie $\theta = T\,(P_0/P)^{0.286}$. Usually P_0 is set to 100kPa.

homogeneous. Five kilometres behind the front, the air appears to contain a mixture of marine and land air, with approximate proportions of 1:3.

Finally, Figure A3.6 plots contours of humidity (again, as a mixture ratio) and temperature for a typical sea breeze with a sharp front. Ahead of the front, a mixed layer can be seen to extend up to approximately 800m. The location of the sea breeze front can clearly be seen from the sharp rise in humidity in the lower 200 to 400m of the atmosphere.

A3.4 Prevalence of sea breeze conditions

A3.4.1 Published data

The Met. Office Forecasters' reference book lists the following criteria for sea breeze generation:

- higher temperatures over land than sea;
- weak offshore component of wind, initially;
- convective instability over land extending up to 1500m.

It also gives examples of conditions under which sea (or lake) breezes have been observed to be present for sites in England and the USA. These data are reproduced in Figure A3.7.

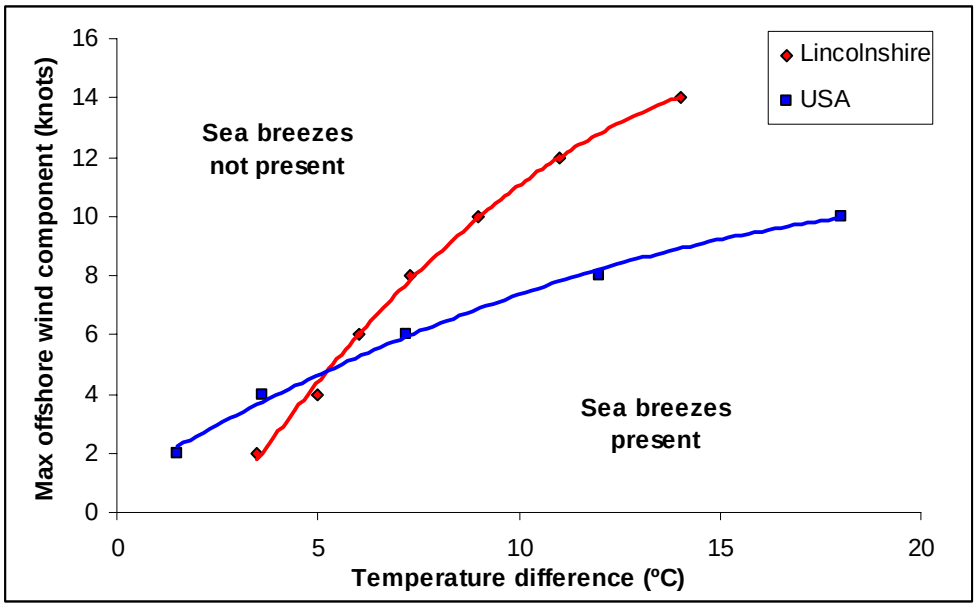

FIGURE A3.7 Observations of critical conditions for sea breeze generation, for sites in England and USA

Both Simpson (1987) and Pielke (1984) report the following criterion for the onset of sea breezes: $F_s = U^2/(C_p \Delta T) < 10$, where U is surface geostrophic wind speed, C_p is the specific heat capacity of the air (typical value is 1010 J/kgK) and ΔT is the temperature difference (°C) between the land and sea. However, rearranging this expression, one obtains the criterion (in m/s): $U < 100 \Delta T^{1/2}$, which is likely to be satisfied under most conditions. In addition, this theoretical criterion is not borne out by the observations in Figure A3.7. Hence, this expression is not believed to be of practical use.

Further field data comes from Simpson et al (1977), who report an average figure of 75 breezes per year for Thorney Island, on the south coast of England

— see the map in Figure A3.9 for further details. These breezes occur almost entirely in the six months from April to September, which gives a frequency of occurrence of once every 2.4 days for that season.

A3.4.2 Further data analysis

Hourly mean meteorological data are available for many sites throughout the UK. Such data have been analysed for the following 4 coastal sites:

Thorney Island	(S Coast, grid reference: 476000 103000)
Bournemouth Airport	(S Coast, grid reference: 411000 098000)
Hemsby	(E Coast, grid reference: 648000 317000)
Boulmer	(E Coast, grid reference: 406000 614000)

For each site, 5 years of data were used (1993-1997 inclusive). Since only wind speed, direction and temperature information was available for the (land-based) sites, with no detailed data on sea temperature or atmospheric stability, a set of criteria was developed in order to enable sea breeze events to be identified and various statistics to be drawn out.

The criteria were based on wind direction and the time of day. The following describes the logic that was used in identifying sea breezes from the meteorological data:

If the wind speed is greater than 0 calculate the change in wind direction between consecutive hours.

Check that the change in wind direction is greater or equal to the defined minimum direction swing value (ϕ) – a Valid Direction change.

If the change in wind direction is valid, check the time of change, if it is between 6am and 6pm, this is a Valid Start Trigger.

If the wind speed is greater than 0 calculate the absolute angle of the wind direction relative to the defined on-shore angle.

Check if the wind angle is within the defined angle limit ($\pm\theta°$ from normal to coastline) – a Valid Direction.

For a given hour, if we have a Valid Start Trigger and a Valid Direction, this marks the start of a Sea Breeze Event.

For subsequent hours we simply check for Valid Direction. Once the Valid Direction criterion fails, this marks the end of the Sea Breeze event – and we can calculate the start time, end time and duration of the event.

Events finishing after the defined Time Cut-off hour (T_E) are discounted; ie if the event continues to the end of the day, it is assumed to represent a change in wind direction rather than a sea breeze, and the trigger conditions are reset.

This leaves a defined set of Sea Breeze events. The initial angle and start-up wind speed are identified for each event.

The number of events identified was found to be relatively insensitive to the angle which was taken to represent onshore winds, and the criteria indicated above were used with θ set at 50°. The parameters ϕ and T_E were given values 30° and 2100hrs. This resulted in between 80 and 90 events being identified during 1996 for Thorney Island, which corresponds reasonably well with the 75 per year found by Simpson et al (1997).

Results for each of the 4 sites, averaged over the 5 years 1993-1997, are given in detail in Appendix A, and summarised in Table A3.5.

TABLE A3.5 Summary of sea breeze statistics for 4 UK sites

Site	No. of events/year	Av. duration of event (hours)	Av. wind speed at onset (m/s)
Thorney	(78) 63	(5.1) 6.1	4.0
Bournemouth Airport	(93) 67	(4.5) 5.9	3.1
Hemsby	(65) 42	(3.3) 4.5	3.2
Boulmer	(59) 35	(3.0) 4.4	3.3

Note: Bracketted numbers include events of 1 hour duration.

From the full results for these four sites in Appendix A, it can be seen that the most common event duration is only 1 hour. Since it is not clear that this represents an established sea breeze event, Table A3.5 has also included summary statistics which omit these events. Making this adjustment gives greater consistency between Thorney and Bournemouth, which are separated by only around 60km, for both numbers and durations of events.

The frequency distributions of the event durations are given in Appendix A, and an example, for Thorney Island, is shown in Figure A3.8. This shows that events lasting 8-9 hours are almost as likely as events lasting 2-3 hours, but that the frequency drops beyond 10 hours.

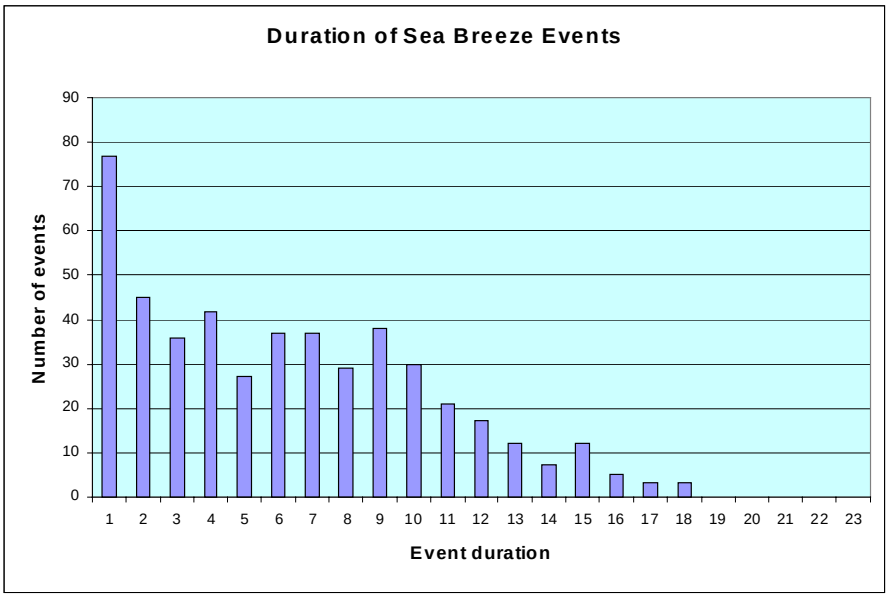

FIGURE A3.8 Frequency distribution of event duration for Thorney Island

The results presented in Table A3.5 suggest that sites on the S coast of the UK will have around 65 sea breeze events per year, lasting an average of around 6 hours. For the E coast, there are around 40 events per year, possibly declining as one travels further north, lasting an average of 4.5 hours. Wind speeds at the onset of these events are reasonably consistent at around 3-4 m/s.

A3.5 Inland penetration of sea breezes

The Met. Office Forecasters' reference book notes that the depth of the convective boundary layer (CBL) over the land has a direct influence on the sea breeze penetration. As seen from Section A3.1, the presence of the CBL over land is vital in the development of the sea breeze. However, if the air over land at the start of the day is highly stable, this CBL will be shallow and there will be little or no sea breeze penetration inland. On the other hand, if the CBL is very deep, showers and thunderstorms can form and these often act to halt the sea breeze.

Figure A3.9 presents a map of Great Britain illustrating the inland penetration of a set of sea breezes on the eastern and southern coasts of England. Figure A3.10 follows the progress inland for a front passing over Thorney Island, on the south coast. These figures demonstrate that sea breezes can travel distances of up to 100km inland.

Simpson et al (1977) reported the rate of progress of the sea breeze front passing over Lasham as being in the range of 2.8 ±0.8 m/s to 3.5 ±1.4 m/s, where the quoted error bounds are one standard deviation. However, much higher frontal advance rates, as high as 8m/s, have also been observed.

If the offshore component of the synoptic wind speed is sufficiently strong, the sea breeze front may cross the coast but become stationary further inland. For example, a critical value of 4m/s has been found for the wind-speed that will prevent a sea breeze reaching Lasham, which is 40km inland from Thorney Island — see Figure A3.9 for orientation. This may account for the observation that only one in twelve of the sea breezes that passes Thorney Island penetrates as far inland as Lasham. These data are presented in Figure A3.11.

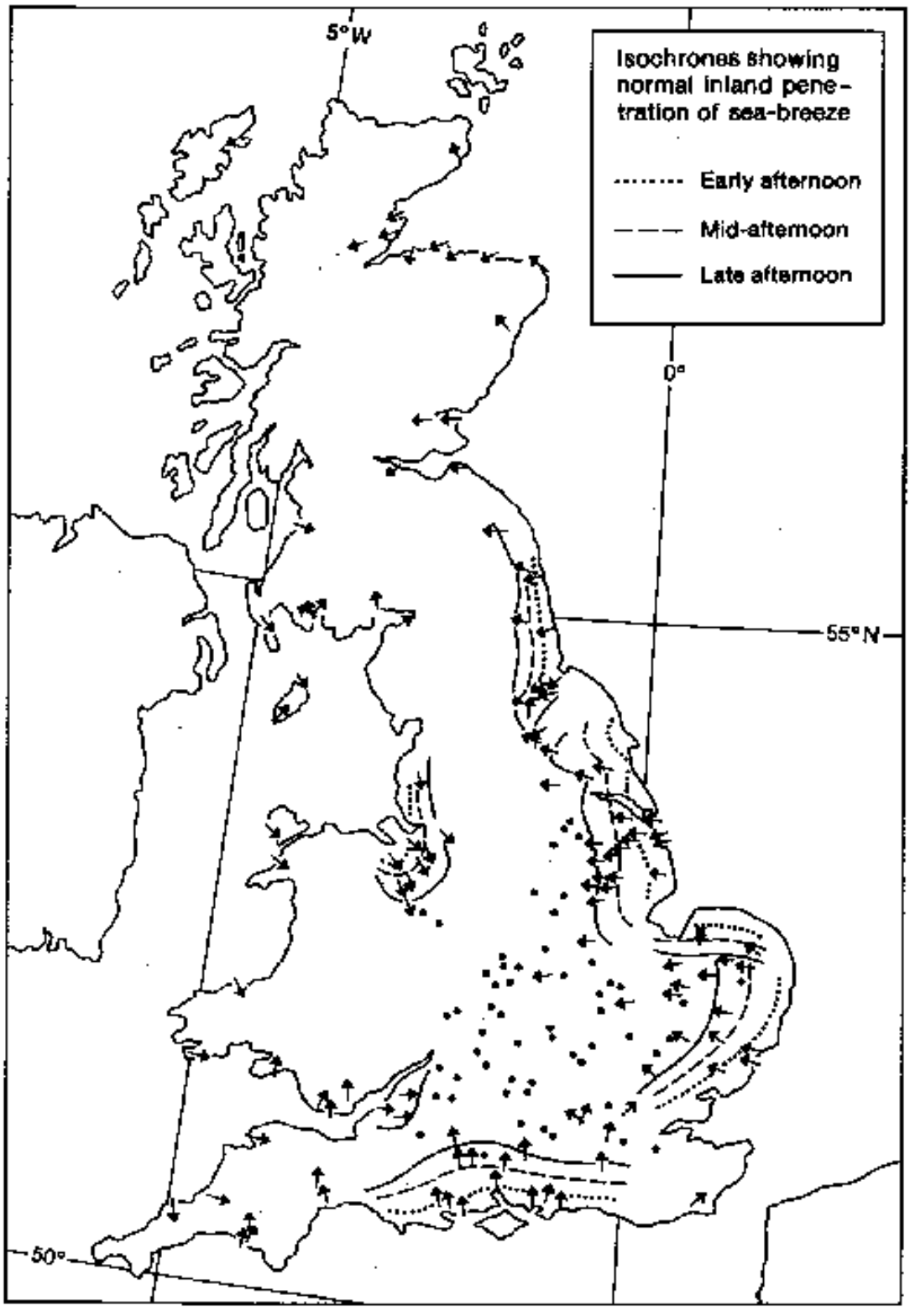

FIGURE A3.9 Map showing the position of sea breeze fronts in early, mid- and late afternoon for a summers day. The arrows denote the late afternoon local wind direction. The dots denote locations that had not been reached by the sea breezes. (With permission from the Met. Office Forecasters' reference book, Crown Copyright)

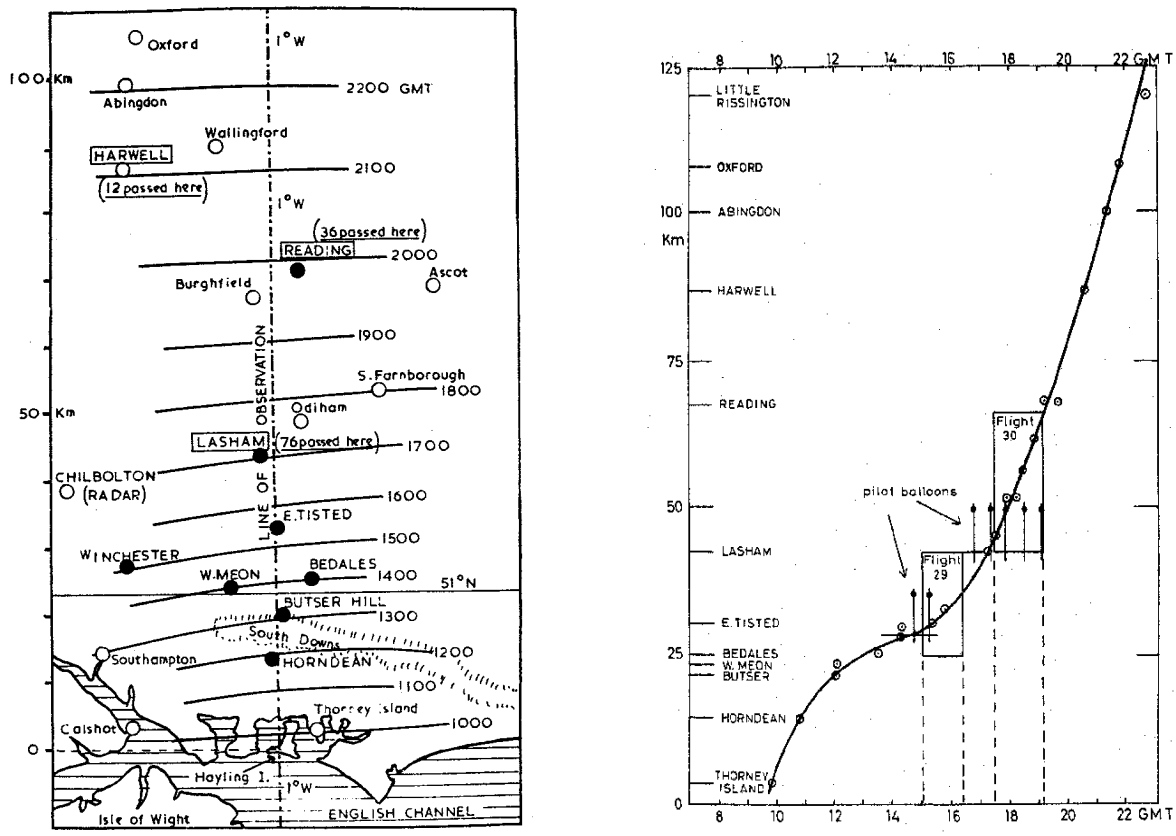

FIGURE A3.10 Progress inland of the sea-breeze fronts on the south coast of England (reproduced with permission from Simpson et al 1977). The diagram on the left shows the average progress; the graph on the right the progress for one particular breeze

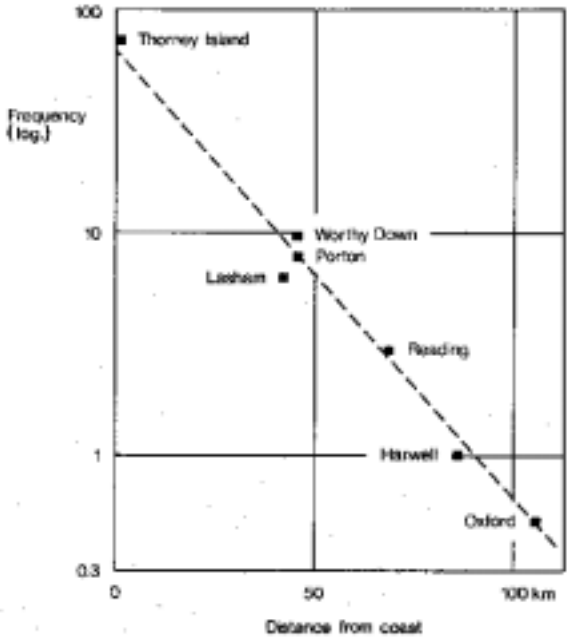

FIGURE A3.11 Frequency of penetration, in days per year, to points inland from the south coast of England. (reproduced with permission from Simpson et al 1977)

A4 Effects of Sea Breezes on Pollution Dispersion

A4.1 General comments

The effects of sea breezes on the dispersion of pollution may be grouped into *microscale* effects that are manifested in the region close to the coastline, and *mesoscale* effects whose influence is felt much further inland. These are summarised below and then discussed in more detail.

Microscale effects:

wind direction and strength changes;

an internal boundary layer (IBL) forms;

pollution may be trapped within the IBL or suddenly fumigated, depending upon the height of the release;

plume spreading rates are modified due to turbulence generated at the sea breeze front;

the sea breeze may bring in fresh or stale air from offshore.

at the onset of a sea breeze, pollutant which has been carried offshore may be blown back onshore.

Mesoscale effects:

the sea breeze can act to transport either fresh or polluted air a long distance inland, even against the synoptic wind direction;

diurnal recycling of pollution may occur, whereby the sea breeze brings ashore stale or polluted air from the previous day;

recycling of pollution may occur from sites geographically far removed;

the sea breeze can promote "layering" of pollution above the base of the PBL inversion;

sea breezes can interact with either orography or other sea breeze fronts, creating convergence zones and complex three-dimensional flow patterns.

A4.2 Microscale effects

A4.2.1 Wind direction and strength

The most obvious effect of a sea breeze is the sudden change in wind direction that occurs as the sea breeze front passes by. Prior to the passage of the front, the wind direction near ground level may be from any quarter; after its passage, the wind will be predominantly onshore. Wind strength may also pick up if conditions were previously calm.

To illustrate this, Figure A4.1 plots surface wind speed and direction measured at a coastal location on the outskirts of Athens. The coast runs from ESE to WNW, so sea breezes originate from SSW or, in terms of a bearing, approximately 200º. Data for two consecutive days are shown in the figure. On the first day (9th August), there was a moderate northerly *synoptic* wind blowing (6m/s), so that the sea breeze was late in forming and did not penetrate far inland. It passed the measurement station at approximately 1500 Local Standard Time (LST). This can clearly be seen as a sudden change in wind direction from northerly round to onshore. The breeze lasted for two hours, after which the wind swung back to a northerly direction. Overnight, the synoptic wind died down in strength, so that on the following day the sea breeze was stronger and came inland earlier in the day, at about 0800 LST. For this breeze, both a change in wind direction and a marked increase in wind strength were observed.

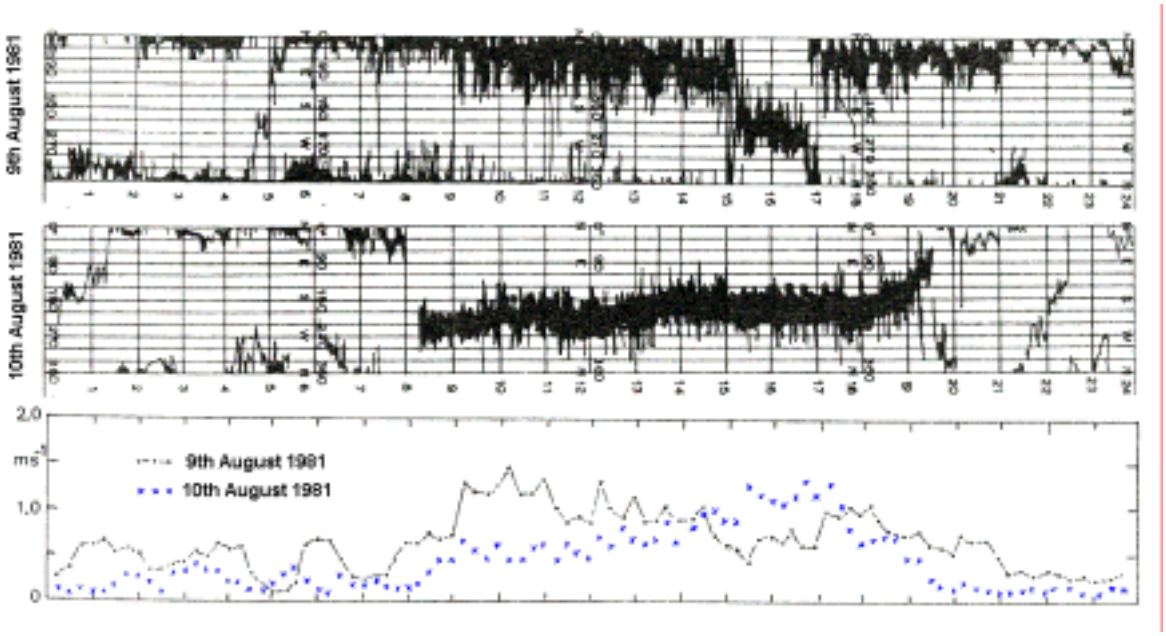

FIGURE A4.1 Traces of wind direction (top two graphs), and wind speed (bottom) for two consecutive days, at a coastal location near Athens (from Helmis et al, 1987, with kind permission from Kluwer Academic Publishers)

These transient changes in wind strength and direction can have a significant effect on the dispersion of pollution in coastal regions, since the plume trajectory and relative spreading rate will be affected. Simple box modelling of pollution dispersal must therefore account for the likelihood of changes to the wind field due to sea breeze activity.

A4.2.2 IBL development, plume trapping and fumigation

In the summer season, an onshore wind, whether it arises from a sea breeze or synoptic conditions, advects cool, marine air over the land. In sunny conditions, a thermal IBL develops close to the ground, increasing in height with distance

from the shoreline (see Figure A3.2 for an example). Air inside this IBL is unstable, although to a lesser degree than the air in the mixed layer ahead of the sea breeze front. The marine air, however, is typically stable (or at least neutrally stratified), and so a temperature inversion exists at the IBL edge.

IBL formation is also prompted by the increase in surface roughness that typically occurs at the coastline. However, as discussed in Section A3.2, roughness effects are likely to be less significant than thermal effects, and so interest is focused here on thermal IBLs.

The presence of a thermal IBL raises two issues for dispersion modelling: plume trapping, and fumigation (see the diagrams in Figure A3.3). For releases into the IBL, the inversion at the top of the IBL can effectively act as a rigid lid to plume dispersion, thus reducing spreading rates. For releases above the IBL, the initial plume spreading rate is low due to the stability of the marine air, but increases suddenly when it intersects the edge of the IBL at some distance downstream. This leads to a sudden increase in ground-level concentrations as the plume is mixed down to the ground, a process called fumigation. This was very clearly illustrated in the CFD simulations of Lyons et al (1995).

Hence, it is important for dispersion models to be able to predict IBL growth, and to take account of the differing mixing rates that are present in and above this IBL. Jones (1983) reported two expressions for calculating the thermal IBL height, one of which, Carson's model, has been employed in the ADMS box model (Carruthers et al, 1992). This can be written as:

$$h_{IBL} = \sqrt{\frac{2(1+2A_c)F}{\rho_a C_p |\gamma|}\left(\frac{x}{U}\right)} \qquad (4.1)$$

where h_{IBL} is the IBL depth at a distance x from the coastline, A_c = 2/3 is a constant, U is the offshore mean wind speed, F is the surface sensible heat flux overland, ρ_a and C_p are the air density and specific heat capacity, and γ is vertical gradient of potential temperature offshore.

As an example, assume atmospheric conditions of F = 100W/m², $\rho_a C_p$ = 1250 J/m³K, U=5m/s and γ = -0.003ºC/m. The above expression then predicts $h_{IBL} = 5.0x^{½}$, giving IBL depths of 50, 158 and 500m at distances of 0.1, 1 and 10km inland. The literature review in Section A2 found references to stacks at coastal power plant with heights up to 198m, and so there would be a strong possibility of fumigation for stack releases at a coastal site under these atmospheric conditions.

Finally, although the air in the IBL is unstable, due to convective heating from the ground, the levels of turbulence and thus mixing are significantly smaller than in the mixed layer ahead of the sea breeze front. Kitada (1987) presents data from a CFD simulation that illustrates this difference in turbulence levels: typical eddy diffusivities in the mixed layer during the afternoon range from 100m^2/s near midday to 14m^2/s in the early evening; by contrast in the IBL values range from 15m^2/s down to 7m^2/s over the same period. A possible

reason for the much smaller diffusivity levels in the IBL is that the turbulence length scales are much smaller there.

Hence a dispersion model must account for five distinct flow regions in a sea breeze:

the undisturbed mixed layer, where mixing levels are relatively high; the sea breeze front, where the flow is turbulent but recirculating; the IBL, behind the sea breeze front, where atmospheric conditions are mildly convective; the marine air, which lies offshore and above the IBL near the coast; and the return flow, high up above the sea breeze layer. Plume spreading rates will be different in each of these five regions.

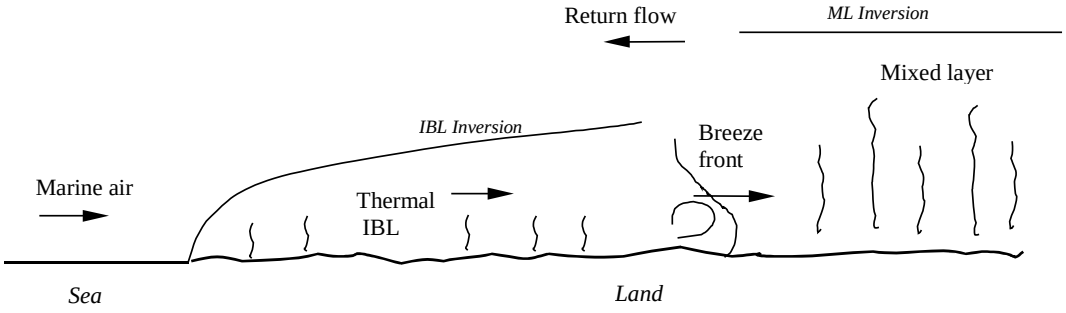

FIGURE A4.2 A schematic illustrating the five regions associated with a sea breeze

A4.2.3 Sea breeze front turbulence

No data was found in the literature for the effect of the turbulence generated by the sea breeze front on plume spreading rates. Hence, an indicative analysis is presented below, based upon the assumptions and simplifications stated.

A relatively sharp sea breeze front is assumed, with a downwind extent of 500m and a depth of 300m, moving inland at a speed of 3m/s. Turbulence levels in the region of the front are assumed to be high, with an intensity of 50%.

The time taken for the front to advect past a fixed point on the ground is thus given by: $t_1 = 500/3 = 167$s, or approximately 3 minutes.

The kinetic energy in turbulent air motions inside the front is estimated as $k_1 = 1.5\ (50\%\ 3.0)^2 = 3.4 m^2/s^2$. The dissipation rate of this turbulence can be expressed as: $\varepsilon = a\ k^{3/2}/L$, where L is the turbulence length-scale and $a(= 0.09^{3/4} = 0.16)$ is a constant.

Hence, once the sea breeze front has passed by and the turbulence generation mechanism has disappeared, the existing turbulence will decay at a rate given by: $dk/dt = -\varepsilon = -\ a\ k^{3/2}/L$.

Hence, the time taken for this turbulence to decay from k_1 down to k_2 is given by: $t_2 = (2L/a)\ (1/k_2^{½} - 1/k_1^{½})$.

Taking L = 30m, ie 1/10th the depth of the sea breeze layer, and k_2 = 1% k_1, this yields a figure of t_2 = 1830s, or approximately 30 minutes.

Hence, the enhanced turbulence due to the passing of the sea breeze front is estimated to last just over 30 minutes.

Referring back to Figure A3.5, the turbulent disturbances in the temperature and mixing ratio traces can be seen to extend for a distance of approximately 5km. Assuming a rate of progress of 3m/s for the sea breeze, this distance corresponds to a duration of 5000/3 = 1670s, or 28 minutes, which is in excellent agreement with the above analysis.

Hence, the enhanced turbulent mixing due to the passage of the sea breeze front can be expected to last on average a period of approximately 30 minutes. The increased turbulence levels, whilst they lasted, would undoubtedly increase the spreading rates for a coastal plume release. The above analysis could be used in a simple or box model to take account of this effect, by modifying plume spreading rates in line with the enhanced turbulence levels.

A4.2.4 Residual pollution

As will be discussed in the following sections, there are a number of mechanisms that can lead to high background levels of pollution in the air upstream of a release location. This "inheritance" of pollution can significantly alter the effect that a release has on ground-level concentrations downwind, since dilution of the released plume relies on mixing with clean, unpolluted air. See Section A2.4 for examples of studies of such conditions.

If the period of interest is short or the mass of upwind residual pollution is large, then conditions in the background air will be constant, and the effect of the residual pollution can be accounted for by applying an offset to the concentrations. This is demonstrated below (where Q and C are the volume flow-rate and concentration level in the plume, and subscripts "0" and "b" denote conditions at source and in the background air):

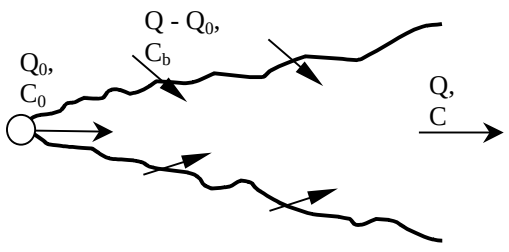

Balance of concentration:

$$Q_0C_0 + (Q - Q_0)\,C_b = Q\,C$$

$\therefore$ rearranging:

$$(C - C_b) = (C_0 - C_b)\,Q_0 / Q$$

or:

$$C' = C_0'\,Q_0 / Q$$

where C' is the excess in concentration over the background level, C_b.

Hence, a simple or box model could still be used to model the above flow conditions, provided that the release concentration and model results were offset by the background concentration. Note, however, that calculations of toxic dosage etc. would require the *true* concentration values for those gases where

the dosage ($\int C^n dt$, where t is time) is not linearly dependent on the concentration field (ie $n \neq 1$).

If the period of interest is long enough for pollution levels in the upwind air to vary significantly, then a more complex transient analysis needs to be undertaken. In terms of box modelling, a series of instantaneous puffs would need to be considered, released one by one over the period of interest.

A4.3 Mesoscale effects

A4.3.1 Inland pollution transport

As has been shown in Section A3.5, sea breezes have been observed penetrating a distance of up to 100km inland. In doing so, they can act as an effective means for transporting pollution far inland, even against the background wind flow direction. This pollution may either be residual in the marine air, or recently generated and absorbed by the sea breeze as it progresses inland.

A vivid illustration of this mechanism for pollution transport is given in Figure A4.3, which plots traces of wet and dry bulb temperature and the concentration of a pollutant (a component of a photochemical smog in this instance) over a period of four hours. The data is from a location 60 miles inland of the coastal city of Los Angeles, the source of the smog. The temperature data shows sudden changes in the wet and dry bulb temperatures. These indicate an increase in the humidity and a reduction in the air temperature, both of which are consistent with the arrival of a sea breeze. The concentration trace shows that this sea breeze contained significant levels of pollution, far exceeding the quoted US Federal air quality standard of 0.08ppm.

Under certain circumstances, the arrival of a sea breeze might be considered also to have a beneficial effect, since it can provide fresh air to strongly polluted regions inland. Simpson (1987), however, suggests that, since the sea breeze is effective in picking up and concentrating pollutants, it thus rapidly loses its "air freshening" potential, and that this aspect of the sea breeze effect is less commonly realised.

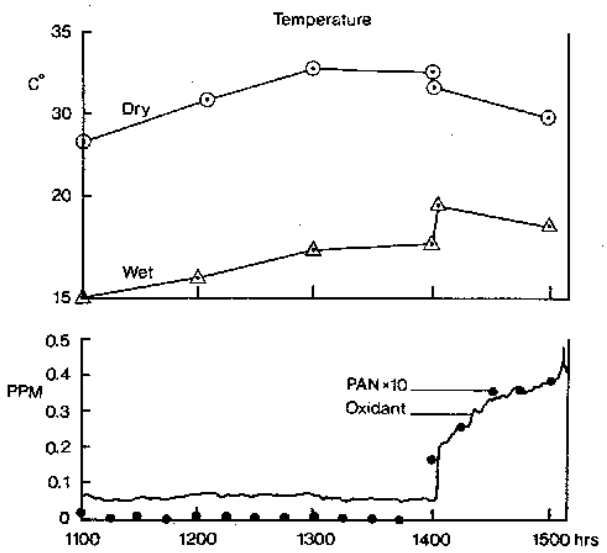

FIGURE A4.3 Traces of wet and dry bulb temperature (top graph) and concentration of a pollutant (bottom graph) for a sea breeze passing over a location 60 miles inland from the coast (reproduced with permission from Simpson, 1987). PAN is peroxyacetyl nitrate

A4.3.2 Diurnal pollution recycling

As described in Section A3.1, in calm synoptic weather conditions a sea breeze/land breeze circulation can be set up, in which a mass of marine air is blown inland during the day, picking up pollution en route, and is then blown back towards the coast at night. This provides a mechanism by which pollution levels inland can steadily rise over a period of days.

Such a mechanism has been successfully simulated by Ozoe et al (1983) and by Moussiopoulos et al (1995) using CFD modelling (see Section A2.4). Note, however, that the details of the recycled pollution depend strongly on the local terrain, weather conditions and land breeze strength, and therefore are difficult to model.

A4.3.3 Recycling of pollution from other sources

An alternative form of pollution recycling can occur when pollution from one coastal site is picked up in a sea breeze, and transported down the coast where it is fumigated. This was shown to occur in the CFD simulations of Eastman et al (1995) and Lyons et al (1995), for lake and sea breezes respectively. For the latter, the region of coastline studied (Cape Canaveral, Florida in the USA) was highly complex, and included several islands and wide rivers, as well as the mainland and sea. These features set up strong three-dimensional flows that would be impossible to recreate with a box model approach.

A4.3.4 Pollution layering effects

Lu & Turco (1994) report that low-level temperature inversions frequently occur over the southern Californian coastal region during the summer months. Elevated layers of pollution have been observed above Los Angeles, with peak concentrations occurring in the stable air above the temperature inversion. This residual pollution can return to ground level during the day through fumigation, as the convective boundary layer deepens.

Lu & Turco demonstrated through 2D and 3D CFD simulations that sea breezes were a major factor in the formation of pollution layers, through two main mechanisms (see also Figure A4.4):

Under-cutting — as the stable marine air penetrates inland, it displaces the existing airmass upwards. The return flow above the sea breeze acts to draw this air out to sea.

Interaction with mountain slope flows — if coastal mountains are present, these can promote vertical movement of polluted air though convection-driven mountain slope flows, or through interaction with the incoming sea breeze.

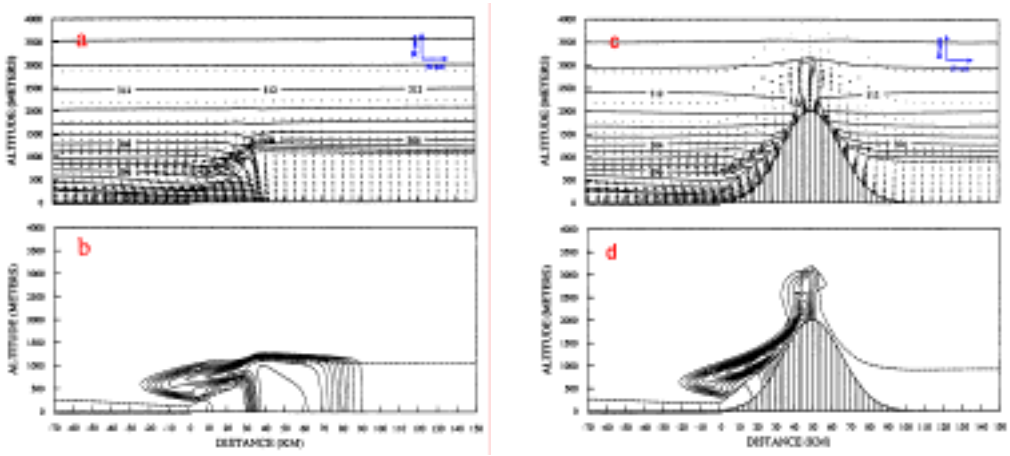

FIGURE A4.4 Two CFD simulations of pollution layering mechanisms. The left-hand figure (a, b) shows the undercutting effect of a sea breeze, on flat terrain; the right-hand figure (c, d) shows the effect of mountain slope winds, aided by a sea breeze. The upper plots (a, c) show velocity vectors and contours of potential temperature; the lower plots (b, d) show contours of pollution concentration. (The figure is taken from Lu & Turco, 1994, by permission of the American Meteorological Society)

A4.3.5 Convergence zones

When sea breezes form over small islands, peninsulae or other convex-shaped coastlines, there is the possibility that the breezes arising from different stretches of the coastline might meet, forming a convergence zone at ground-level. Such convergence zones have been shown by several authors (eg Ridley, 1995; Romero & Ramis, 1996), through CFD simulations, sometimes to result in high levels of pollution at ground-level.

Associated with a convergence zone is a vertical updraft and a set of return flows aloft. This lofting of pollutants can be followed by their fumigation later in the day as the height of the mixed layer or IBL deepens.

Such (three-dimensional) effects cannot easily be incorporated into a box model.

A5 Sample calculations

A5.1 Features modelled

As noted in Section A6.2, there has been a limited amount of box model (Gaussian plume) development which would allow the modelling of coastline or sea breeze effects. Hence, there are relatively few dispersion models which include any explicit consideration of dispersion over water or the influence of coastlines. One of the few commercially available models which does have the ability to model coastline effects is ADMS 3 (CERC, 1999).

The coastline module in ADMS 3 does not model dispersion over bodies of water, but rather it considers the effect on dispersion over land of a growing internal convective boundary layer which starts at the coastline and increases in height with increasing distance inland. It is assumed that the flow over the water is stably stratified. The coastline is treated as a straight line, and the sources must be located on land. The coastline module in ADMS is only used when all of the following conditions apply:

the sea is colder than the land;

the weather conditions on land are convective (eg Pasquill category A to C);

the wind is blowing directly onshore;

the source is higher than the internal boundary layer depth, calculated at the source location.

In all other cases, the coastline module is not used and the dispersion modelling is treated as normal dispersion over land. Use of ADMS therefore only allows the consideration of growing boundary layer effects; modelling using this code has been presented in Section A5.2.

Using the *breakpoint* facility within the dispersion modelling suite HGSYSTEM (Post 1994), it is possible to model changes in conditions; Section A5.3 presents sample results for the change from land to sea roughness and back again.

Currently, no models allow the calculation of recirculation due to changes in wind direction. Some simple calculations have been undertaken, however, using some of the data presented in Section A4.4 from real sea breeze events. These calculations show the likely along-coast spread of a plume that turns back to shore at the onset of a sea breeze, and are presented in Section A5.4.

A5.2 Internal boundary layer effects using ADMS

In order to demonstrate the influence of coastlines using ADMS, a simple test case was developed, defined as:

- 50 m high stack located 100 m inland from a straight coastline;
- passive release (ie no plume rise, as no momentum or buoyancy);
- C5 weather conditions over the land (wind at 10 m height = 5 m/s, Monin-Obukhov length = -100m, boundary layer depth = 850 m);
- wind blowing directly onshore;
- land specified to be 5ºC warmer than the sea;
- surface roughness length = 0.1 m;
- 30 minute averaging time.

Figure A5.1 shows the results in terms of the ground level plume centreline concentrations for cases with and without the coastline module. Concentrations are quoted as dispersion coefficients (units of s/m^3) which may be simply converted to real concentrations by multiplying by the continuous release rate (eg in kg/s, to give kg/m^3).

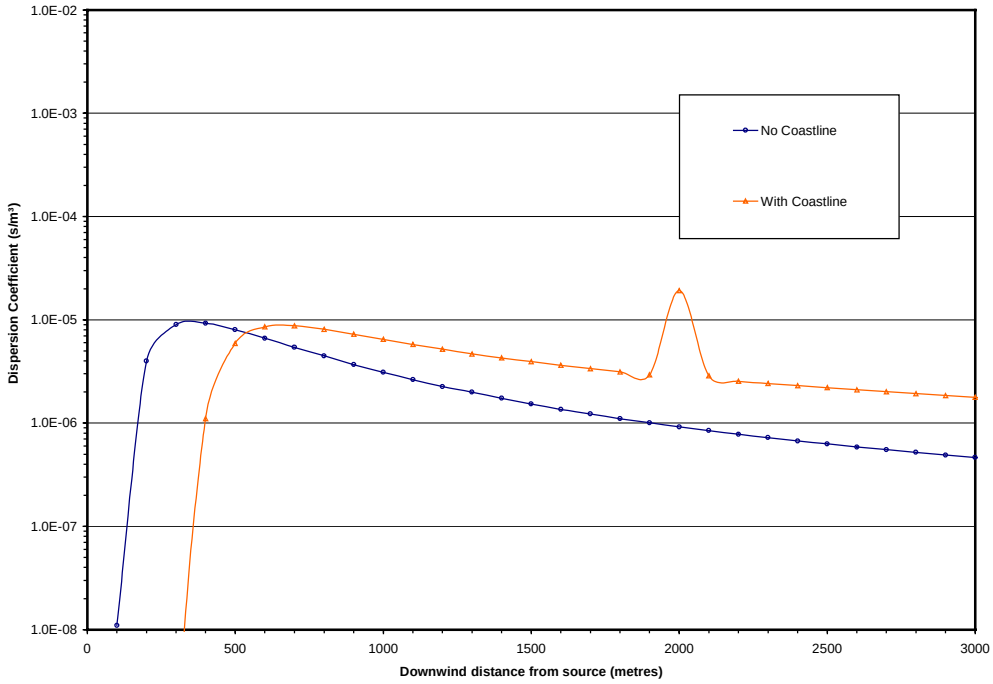

FIGURE A5.1 Comparison of Results With and Without Coastline Module Using ADMS 3 (50m stack located 100m inland in C5 weather conditions)

The results in Figure A5.1 are broadly similar to those shown in Figure A2 in NRPB-R157 (Jones, 1983). The graph shows that, when the coastline module is used, the plume remains in the stable layer for some time before intersecting the growing IBL and thereafter being fumigated and trapped within the IBL. As a result, the peak ground-level concentration is further downwind and slightly lower with the coastline module. However, downwind of the peak, concentration levels with the coastline module exceed those without, even allowing for the downwind shift in the peak. This is due to the trapping of the plume within the IBL, which limits vertical diffusion.

It is noted that there is a curious 'peak' in the concentrations predicted using the coastline module at about 2000 m downwind. This was drawn to the attention of CERC who, after some investigations, acknowledged that this effect is unphysical, being caused by the model incorrectly using a far-field concentration profile in some circumstances while the internal boundary layer is still growing. They have therefore recommended that the coastline model should not be used as present.

It is noted by CERC (1999) that the coastline module has not been validated against field data. It is also emphasised in NRPB-R157 that the results of this type of coastline model can be very sensitive to the choice of input parameters, particularly for tall stacks and buoyant plumes, where the rate of deepening of the growing internal boundary layer is very small.

A5.3 Roughness change effects using HGSYSTEM

Although the effects of roughness changes are generally of secondary importance compared with those of thermal effects (see Section A3.2), there may be cases where they are significant. For example, in releases of dense gases roughness effects are accentuated since the released gas tends to remain close to the ground, whilst for dispersion over small bodies of water thermal effects may be less significant.

An example is presented here using the dispersion model HGSYSTEM (Post, 1994), which allows the output of results at 'breakpoints'. These intermediate results can then be input to a new run using a different roughness. The example chosen here is for a 44kg/s chlorine release in the case where there is a 2km wide lake 500m downwind of the source. The land roughness is assumed to be 0.3m, appropriate for urban conditions, and the lake roughness is 0.001m. The results are shown in Figure A5.2, from which it can be seen that concentration would be increased by a factor of around 2-3 over the lake. Beyond the lake, this difference reduces with distance.

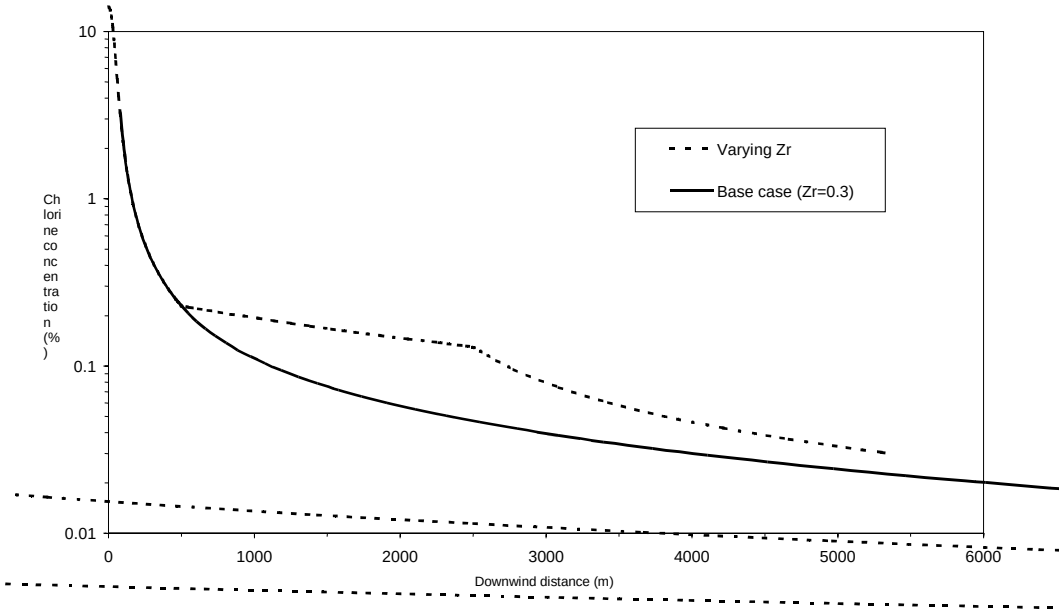

FIGURE A5.2 Effects of lake roughness on dispersion of large chlorine release

A5.4 Consideration of recirculation

It had originally been intended to use ADMS 3 with some sequential meteorological data for selected coastal sites in the UK. The standard hourly sequential meteorological data for two sites was obtained. Plots of the average concentration using this data can easily be calculated (with or without the coastline module) and the results would provide an indication of the effect of sea breezes, in so far as these episodes are captured in the hourly meteorological data. Indeed, as discussed in Section A4.2.3, the initial sea breeze disturbance lasts about 30 minutes, suggesting that hourly mean data is too coarse to resolve the detail at the establishment of the event.

However, it is emphasised that ADMS 3 is not able to model puffs of material travelling out to sea and back again. Furthermore, if ADMS is to be used with its coastline module, then the meteorological input data must include the difference between the sea and land surface temperatures, which is not normally included in standard meteorological data files. The simplest solution is to specify a constant sea temperature (eg 16ºC in August, 14ºC in September, etc), which allows ADMS to calculate the difference using the air temperature specified in the standard hourly meteorological data. However, given the concerns with the ADMS coastline module described in Section A5.2, it was not felt worthwhile to perform any detailed modelling with ADMS using the sequential meteorological data.

As an alternative, some simple calculations can be undertaken to determine possible puff trajectories, and hence the likely along-coast range of any pollutant. The following assumptions are made:

Average wind speed during breeze establishment	= V(m/s)
Angular change during onset	= $+\theta_0$ to $-\theta_0$ (° from coastline)
Duration of onset	= T(secs)

Angle θ varies linearly with time t.

Calculations can then be undertaken on the basis of one of the following two assumptions on wind speed:

a) Wind speed magnitude (V) remains constant over time T

a) Wind component parallel to shore (V cosθ) remains constant over time T.

The distance along the coast at which a puff emitted at the start of this event will return to land is given by:

$$x_L = \int_0^T u\,dt$$

where

$$u = V\cos\theta = V\cos\theta_o\left(1 - \frac{2t}{T}\right) \quad \text{for case a)}$$

$$u = V\cos\theta_o \quad (=\text{constant}) \quad \text{for case b)}$$

Hence:

$$x_L = VT\frac{\sin\theta_o}{\theta_o} \qquad \text{a)}$$

$$= VT\cos\theta_o \qquad \text{b)}$$

The variation of x_L/VT with θ_o is given in Table A5.1.

TABLE A5.1 Normalised coastline trajectory distances

Initial wind angle θ_o	30	45	60	75	90
x_L/VT case a)	0.95	0.90	0.83	0.74	0.64
x_L/VT case b)	0.87	0.71	0.50	0.26	0.00

Clearly releases which occur prior to the onset of the sea breeze would have travelled further out to sea, and could be driven further along the coastline. However, since concentrations in such cases would be correspondingly reduced, the above general calculations can be used to give an indication of the distance along the coastline to which 'recirculation' effects may be felt. Taking $\theta_o \approx$ 45-60°, V $\approx$ 3.5m/s and T = 1800s, it can be seen that x_L will range from 3150 to 5690m. It should be noted that any lateral spread would be added to the above. The maximum distance given above corresponds to a trajectory distance of 6300m, at which a typical σ_y value would be around 500-1000m, giving a total distance affected of order 6km.

A5.5 Discussion

In summary, models such as ADMS are capable of modelling some of the complex effects of coastlines, although they do not deal explicitly with issues such as sea breeze effects, except in so far as such effects are captured by the available meteorological data. Nor does ADMS deal explicitly with dispersion of material over bodies of water. There are also some residual concerns relating to some of the current ADMS coastline module results which have yet to be fully explained, suggesting that such models should be used with caution. HGSYSTEM is able in principle to model some of the roughness change effects, although it is best applied to ground level dense gas releases.

In practice, there is therefore very little amongst current simple modelling capability which allows the effects of coastlines or sea breezes to be assessed. Nevertheless, some simple calculations, based upon data obtained from sea breeze events at 4 UK coastal locations (see Section A3.4.2), have enabled some estimates to be made of the likely along-coast spread of pollutant during the onset of a sea breeze.

A6 Assessment of current modelling

A6.1 Modelling types

Table A2.1 presented a summary of the sea breeze references that were identified in the literature review, and indicated the types of approach that had been taken in each case. A small number of papers (marked "Other" in the table) used simple analytical methods to study certain aspects of sea breeze structure; these are disregarded here since they offer little or no information on dispersion. The remainder of the papers are concerned with either field measurements or computer simulations.

Interest in this section is focussed on computer modelling of dispersion. The studies are broadly divided into those using *simple models* and those based on *CFD*.

Simple models can be further subdivided into Gaussian plume models and box models. Gaussian plume models are based upon a generic solution of the convection/diffusion equation, combined with empirical plume width parameters. A box model, also sometimes referred to as an integral model, is a computational model that simulates the dispersion of a plume or puff of gas through calculation of the evolution of a small number of integral statistics, such as plume width or puff mass. Empirical expressions are used to relate the movement and rate of entrainment, and thus dilution, of the plume or puff. Local variations in the background flow field, for example due to changes in terrain shape, must be explicitly and empirically accounted for in the model, where possible.

A computational fluid dynamics (CFD) simulation explicitly calculates the spatial wind field for the modelled geometry, and then uses this wind field to determine

the dispersion of the released gas. Specific empirical relations are not needed to model the plume evolution, although some assumptions are necessary to model the wind field turbulence. Local variations in the background flow field are generally calculated implicitly by the CFD model.

In the following discussion, reference is made back to Section A2.1, which discussed the effects that sea breezes can have on dispersion, and on the ability of the various modelling approaches to account for these effects.

A6.2 Simple models

Little progress has been reported in the development of simple models for dispersion in coastal regions. Of the issues raised in Section A2.1, only one seems to have been addressed — IBL growth and fumigation. Misra (1980b) demonstrated that acceptable accuracy can be obtained with a simple model for both the location and magnitude of the ground level peak concentration. A number of papers (Stunder et al, 1986; Zhibian & Zenquan, 1995) have tried to improve upon this model, but with limited or no effect.

Simple models could, in principle, be used to study the other microscale effects of sea breezes, such as changes in wind direction and strength and recycling of pollution, and some of the mesoscale effects, such as inland transport and diurnal recycling of pollution. The results from the literature search suggest that this has not been done thus far; it is likely that the main reason for this is that current simple models are not well suited to such investigations.

Just one commercially available model (ADMS 3) was identified which included a specific coastline model. This has been considered in Section A5.2, which includes some sample calculations. Although these were useful in demonstrating the effects of the IBL on dispersion, they also revealed some inadequacies, acknowledged by the code's vendor (CERC), in the matching of the modelling with far-field effects. As a result, it is clear that this feature of ADMS needs to be treated with considerable caution.

A6.3 CFD

In Table A2.1 the references are listed in chronological order, and it is immediately apparent that there has been an explosion of interest in applying CFD to sea breezes during the last decade. This is partly a reflection of the advances in CFD modelling techniques, partly a result of the increased ease of availability of the computing resources necessary for CFD, but also perhaps partly an indication that the complexity of the processes involved imply that CFD modelling is needed to explore the subject in any detail.

CFD is able to model all of the effects of sea breezes identified in Section A2.1. Indeed, the majority of the mesoscale effects of sea breezes can probably only be tackled confidently through use of CFD, since variations in terrain characteristics, coastline shape etc. can all cause variations in the three dimensional wind field and thus in the dispersion of the released gas. A series of

studies for coastal cities such as Athens, Los Angeles and Melbourne, have shown that CFD is an appropriate prognostic tool for studying air quality over large regions.

It should be noted that the use of CFD is a much more expensive modelling approach than the use of simple models, typically by around an order of magnitude or more. This is due to the longer time required to set up, run and post-process the data from the model, as well as the greater requirement for computer resources.

A7 Conclusions

A7.1 Current understanding of sea breezes and dispersion over water

It is clear from the review undertaken in this study that significant advances have been made in the understanding of sea breeze structure and occurrence over the last decade. These have been due mainly to series of field measurements and theoretical studies using CFD. A number of complex interacting phenomena have been identified whose effects on pollution dispersion may be understood separately, but which may be difficult to combine effectively in practice.

A7.2 Current status of modelling

Whilst various simple models allow the modelling of a small number of the effects of coastlines and sea breezes etc, there is no single model which satisfactorily combines all the features required. For example, the ADMS model includes a "coastline" module for studying fumigation at the shoreline, but, as discussed in Section A5.2, there are some uncertainties in the output of the current version, and it should therefore be used with some caution.

CFD modelling has been applied to various problems of dispersion over water, and has been shown to be capable of modelling most of the relevant effects. It is noted that CFD is most appropriate for conditions where the wind flow pattern is complex and 3D, due to topography, sea breeze convergence, coastline shape etc. Specific case studies have been undertaken demonstrating these capabilities, but more general application of CFD requires significant modelling skill and large computing and man-power resource.

A7.3 Scope for model development

The complexities of the physics to be modelled imply that it would be difficult to modify a simple (Gaussian) model in order to take account of all the effects that are likely to influence dispersion over water. However, whilst CFD is in principle much more suited to the problem, its current application is most likely to be to

specific sites or regions. Hence, the following simple modelling "improvements" are suggested as having potential for investigation;

Allowance for variable wind direction and strength; parameterisation of typical variations in such quantities for sites in the UK.

Further investigation of the effect of the enhanced short-term mixing that is experienced at the sea breeze front, and possible incorporation into a box model.

Incorporation of a facility for accounting for residual pollution, ie pollution left over from the previous day, or transported from somewhere upwind.

Improved facilities for modelling large changes in surface roughness, such as might occur at the edge of a lake in an urban environment. Development of modelling guidelines may be appropriate here.

Assessment of the variabilities in plume spreading rates due to the above effects, and comparison of these with the variabilities due to uncertainty in the synoptic atmospheric conditions.

Any of the above studies would need to include comparisons with field data, or possibly CFD simulations if they were more easily available or more comprehensive.

The result of the above set of studies would be an improved, relatively low cost method for analysing the effects of water bodies on dispersion, and also a better understanding of the applicability and limitations of such an approach.

A8 References

Abbs, DJ (1986). "Sea-breeze interactions along a coastline in southern Australia: observations and numerical modelling study", *Monthly Weather Review, pp 831-848.*

Adronopoulos, S, Passamichali, A, Gounaris, N & Bartzis, JG (1999). "Evolution and transport of pollutants over a Mediterranean coastal area and Biogenic VOC emissions influence on ozone levels", *J. Appl. Met, in Press.*

Blumenthal, DL, White, WH & Smith, TS (1978). "Anatomy of a Los Angeles smog episode: pollutant transport in the day-time sea-breeze regime", *Atmos. Environment, vol 12, pp 893 – 907.*

Borrego, C (1996). 'Atmospheric pollution in coastal zones: mesoscale modelling as applied to air quality studies', *pp 56-69.*

Briere, S (1987). "Energetics of daytime seabreeze circulation", *J Atmos Sci, vol 44, pp 1455-1474.*

Camps, J (1996). "Numerical modelling of pollutant dispersion in sea breeze conditions", *Annales Geophysicae- European Geophysical Society, vol 14/6, pp 665-677 .*

Carissimo, B (1996). "Local Simulations of land-sea breeze cycles in Athens based on large-scale operational analyses", *Atmos. Environment, vol 30/15, pp 2691-2704 .*

Carizi, G, Cinotti, S, Giovanni, I, Levy, A & Presotto, L (1998). "Numerical simulation of atmospheric diffusion in sea breeze conditions", *5th Int Conf on Harmonisation with Atmos. Disp. Mod. for Regulatory Purposes, pp 211-218.*

Carruthers, DJ, Weng, WS & Apsley, DD (1992). "Coastline model - the thermal internal boundary layer", *ADMS2 Technical Specification, UK ADMS 1.0 p15/01E/92, pp 1-7.*

CERC, 'ADMS 3 User Guide', February 1999.

Deaves, DM, (1981) "Computations of wind flow over changes in surface roughness", *J. Ind. Aero., vol 7, pp 65-94.*

Eastman, JL, Pielke, RA & Lyons, WA (1995). "Comparison of lake-breeze model simulations with tracer data", *J. Appl. Met, vol 34, pp 1398-1418.*

Eppel, DP (1993). "Nonstationary 3-D Simulation of Air Flow and Pollutant Transport in the Coastal Region of Northern Germany and the Oeresund", *Nato Challenges Of Modern Society, vol 17, pp 133.*

Engineering Sciences Data Unit (1998). "Wind engineering data." Volume 1b.

Garrat, JR. (1990). "The internal boundary layer – a review", *Boundary Layer Met. vol 50, pp 171-203.*

Gifford, FA (1976). "Turbulent diffusion-typing schemes: a review", *Nucl. Safety, vol 17, pp 68-86.*

Heines, TS & Peters, LK (1973). "The effects of a horizontal impervious layer caused by a temperature inversion aloft on the dispersion of pollutants in the atmosphere", *Atmos. Environment, vol 7, pp 39 – 48.*

Helmis, CG, Asimakopoulos, DN, Deligiorgi, DG & Lalas, DP (1987). "Observations of sea breeze fronts near the shoreline", *Boundary Layer Met, vol 38, pp 395-410.*

Jiang, W (1994). "Study on the Thermal Internal Boundary Layer and Dispersion of Air Pollutant in Coastal Area by Numerical Simulation", *Advances In Atmospheric Sciences, vol 11/3, pp 285.*

Jones, JA (1983). "Models to allow for the effects of coastal sites, plume rise and buildings on dispersion of radionuclides and guidance on the value of deposition velocity and washout coefficients", *5th Report of a Working Group on Atmospheric Dispersion.* NRPB-R157.

Jones, JA (1986). 'The uncertainty in dispersion estimates obtained from the working group models.' *7th Report of a Working Group on Atmospheric Dispersion. NRPB-R199.*

Keen, CS & Lyons, WA (1978). "Lake/land breeze circulations on the western shore of Lake Michigan", *J Appl. Met. vol 17, pp 1843 – 1855.*

Kitada, T (1987). "Turbulence structure of sea breeze front and its implication in air pollution - application of k-e turbulence model". *Boundary-Layer Met., vol 41, pp 217-239.*

Kunz, R & Moussiopoulos, N (1995). "Simulation of the Wind Field in Athens Using Refined Boundary Conditions", *Atmos. Environment, vol 29/24, pp 3575.*

Latini, G, Polonara, F & Vitali, G (1996). "Sea-breeze modelling of middle Adriatic sea coast". *Envirosoft 96, pp 351-359.*

Lu, R & Turco, RP (1994). "Air Pollutant Transport in a Coastal Environment. Part I: Two-Dimensional Simulations of Sea-Breeze and Mountain Effects", *Journal Of The Atmospheric Sciences, vol 51/15, pp 2285.*

Lu, R & Turco, RP (1995). "Air pollutant transport in a coastal environment - II. Three-dimensional simulations over Los Angeles basin", *Atmos. Environment, vol 29/13, pp 1499.*

Lyons, WA & Cole, HS (1973). "Fumigation and plume trapping on the shores of Lake Michigan during a stable onshore flow", *J App/. Met., vol 12, pp 494 – 510.*

Lyons, WA, Pielke, RA, Tremback, CJ, Walko, RL, Moon, DA & Keen, CS (1995). "Modelling impacts of mesoscale vertical motions upon coastal zone air pollution dispersion", *Atmos. Environment, vol 29/2, pp 283.*

Martin, CL & Pielke, RA (1983). "The adequacy of the hydrostatic assumption in sea breeze modelling over flat terrain", *J Atmos Sci, vol 40, pp 1472-1481.*

McElroy, JL & Smith, TB (1986). "Vertical pollutant distributions and boundary layer structure observed by airborne lidar near the complex south Californian coastline", *Atmos. Environment, vol 20, pp 1555 – 1566.*

The Met. Office, (1993). "Forecasters' Reference Book.", *2nd Edition.*

Misra, PK (1980a). "Dispersion from tall stacks into a shoreline environment", *Atmos. Environment, vol 14, pp 397 – 400.*

Misra, PK (1980b). "Verification of a shoreline dispersion model for continuous fumigation", *Boundary-Layer Met., vol 19, pp 501 – 507.*

Moussiopoulos, N (1995). "Numerical Simulation of Photochemical Smog Formation in Athens, Greece", *Atmos. Environment, vol 29/24, pp 3619.*

Nester, K (1995) "Influence of Sea Breeze Flows on Air Pollution Over the Attica Peninsula", *Atmos. Environment, vol 29/24, pp 3655.*

Nguyen, KC Noonan, JA, Galbally, IE & Physick, W (1997). "Predictions of plume dispersion in complex terrain: Eulerian versus Lagrangian models", *Atmos. Environment, vol 7, pp 947-958.*

Ogawa, Y, Ohara, T, Wakamatsu, S, Diossey, PG & Uno, I (1986). "Observations of lake breeze penetration", *Boundary Layer Met, vol 35, pp 207-230.*

Ogawa, Y, Griffiths, R & Hoydysh, WG (1975). "A wind-tunnel study of sea breeze effects". *Boundary Layer Met, vol 8, pp141-161.*

Ozoe, H, Shibata, T, Sayama, H & Ueda, H (1983). "Characteristics of air pollution in the presence of land and sea breeze – a numerical experiment", *Atmos. Environment, vol 17, pp 34 – 42.*

Pasquill, F and Smith, FB, 'Atmospheric Diffusion', 3rd Edition, 1983.

Pearson, RA (1973). "Properties of the sea breeze front as shown by a numerical model", *J. Atmos. Science, vol 30, pp 1050 – 1060.*

Peters, LK (1975). "On the criteria for the occurrence of fumigation inland from a large lake", *Atmos. Environment, vol 9, pp 809 – 816.*

Pielke, RA (1981). "An overview of our current understanding of the physical interactions between sea and land breeze and coastal waters", *Ocean. Management, vol 6, pp 87 – 100.*

Pielke, RA (1984). "Mesoscale meteorological modelling", *Academic Press.*

Post, L (1994). "HGSYSTEM 3.0 Technical reference manual". *Shell Research Ltd., Report No. TNER 94.059.*

Raynor, GS, Sethuraman, S & Brown, RM (1979). "Formation and characteristics of coastal internal boundary layers during onshore flows", Boundary-Layer Met., vol 16, pp 487–514.

Raynor, GS, Michael, P, & Sethuraman, S (1980). "Meteorological measurement methods and diffusion models for use at coastal nuclear reactor sites", *Nuclear Safety, vol 21, pp 749 – 765.*

Ridley, RN, (1995). "Lagrangian particle dispersion simulations in cases of sea-breeze convergence". *Math. Computer Modelling, vol 21, pp 137-142.*

Romero, R & Ramis, C (1996). "A numerical study of the transport and diffusion of coastal pollutants during the breeze cycle in the Island of Mallorca", *Annales Geophysicae- European Geophysical Society, vol 14/3, pp 351-363 .*

Rotunno, R (1983). "On the linear theory of the land and sea breeze", *J Atmos Sci, vol 40, pp 1999-2009.*

Sharan, M & Gopalakrishnan, SE (1997). "Bhopal gas accident: a numerical simulation of the gas dispersion event". *Environmental Modelling & Software, vol 12, pp 135-141.*

Simpson, JE (1977). "Inland penetration of sea-breeze fronts", *Quart J Roy Met Soc, vol 103, pp 47-76.*

Simpson, JE (1987). "Gravity currents", *Ellis Horwood Pub., pp 48 - 63.*

Snyder, WH (1981). "Guideline for fluid modelling of atmospheric diffusion." *US EPA Report EPA-600/8-81-009.*

Steinberger, EH & Ganor, E (1980). "High ozone concentrations at night in Jerusalem and Tel-Aviv", *Atmos. Environment, vol 14, pp 221 – 225.*

Stunder, M, Sethuraman, S, Misra, PK & Salcota, H (1986). "Downwind non-uniform mixing in shoreline fumigation processes", *Boundary Layer Met., vol 34, pp 177 – 184.*

Uno, I, Wakamatsu, S, Suzuki, M & Ogawa, Y (1984). "3D behaviour of photochemical pollutants covering the Tokyo Metropolitan area", *Atmos. Environment, vol 18, pp 751 – 761.*

Van der Hoven, I (1967). "Atmospheric transport and diffusion at coastal sites", *Nuclear Safety, vol 8, pp 490 – 499.*

Van Dop, H, Steenkist, R & Nieuwstadt, FTM (1979). "Revised estimates for shoreline fumigation", *J Appl Met, vol 18, pp 133-137.*

Yamada, T Bunker, SS & Niccum, E (1988). "Numerical simulations of long-range pollutant transport from coast to inland mountainous region". *Los Alamos National Laboratory Report DE88005383/GAR.*

Xu, X (1997). "Characteristics of winds and their effect on dry deposition at the Connecticut coastline of Long Island Sound", *Atmos. Environment, vol 31, 22, pp 3729-3735 .*

Zhibian, L & Zengquan,Y (1995). "A Shoreline Fumigation Model with Wind Shear", *Atmos. Environment, vol 29/22, pp 3373.*

Appendix A

Analysis of Sea Breeze Data from 4 UK Sites

Site Name: Thorney Island

Range of data: April - September 93-97

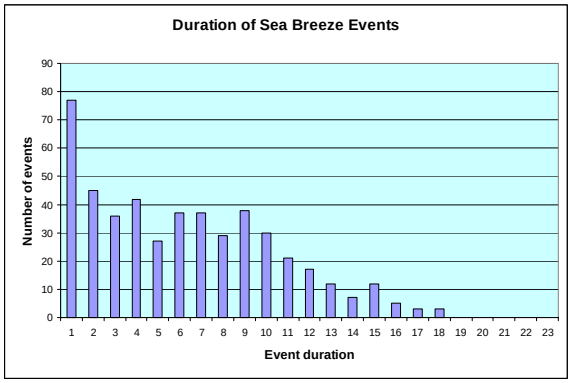

Site variables

Onshore wind angle	180
Maximum angle from onshore angle	50
Discount events finishing after	21
Minimum swing into onshore sector	30

Statistics

Number of sea breeze events	392
Average event duration	5.1
Maximum event duration	13
Minimum event duration	1
Earliest event start time	6
Latest event start time	18
Earliest event end time	7
Latest event end time	21
Total duration of all events	1994
Total hours with no data	1957
Average initial angle re: onshore angle	8.4
Average absolute initial angle re: onshore	25.9
Average windspeed over initial hour	4.0
Maximum windspeed over initial hour	12.9
Minimum windspeed over initial hour	0.5
Maximum windspeed over all data	18.5

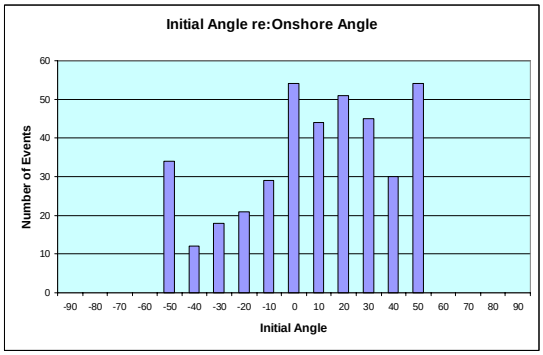

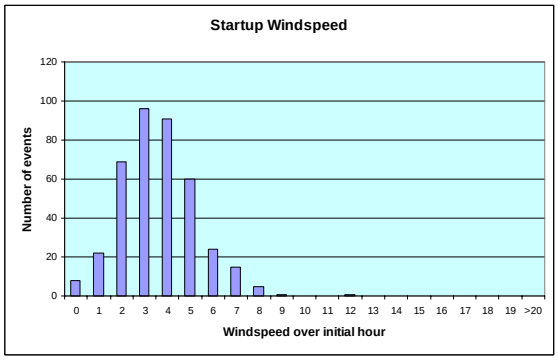

Site Name: **Boulmer**
Range of data: April - September 93-97

Site variables

Onshore wind angle	260
Maximum angle from onshore angle	50
Discount events finishing after	21
Minimum swing into onshore sector	30

Statistics

Number of sea breeze events	293
Average event duration	3.0
Maximum event duration	15
Minimum event duration	1
Earliest event start time	6
Latest event start time	18
Earliest event end time	7
Latest event end time	21
Total duration of all events	873
Total hours with no data	46
Average initial angle re: onshore angle	-6.3
Average absolute initial angle re: onshore	29.4
Average windspeed over initial hour	3.3
Maximum windspeed over initial hour	9.8
Minimum windspeed over initial hour	0.5
Maximum windspeed over all data	25.7

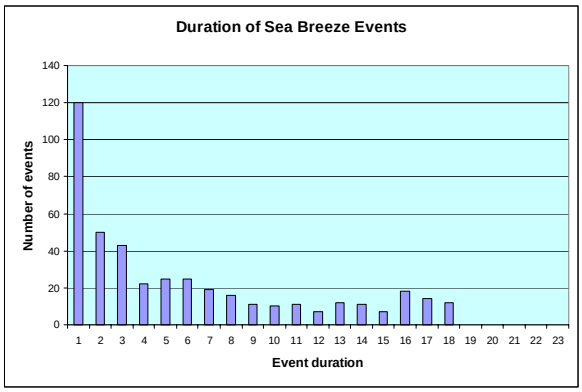

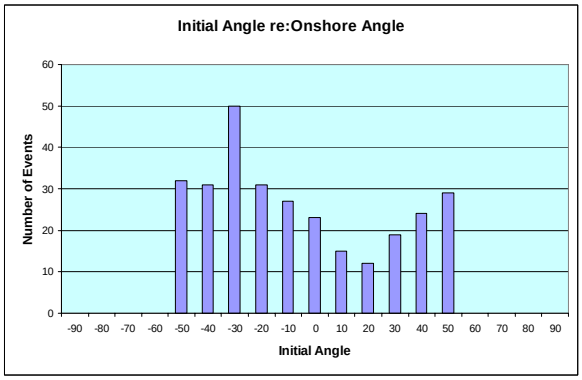

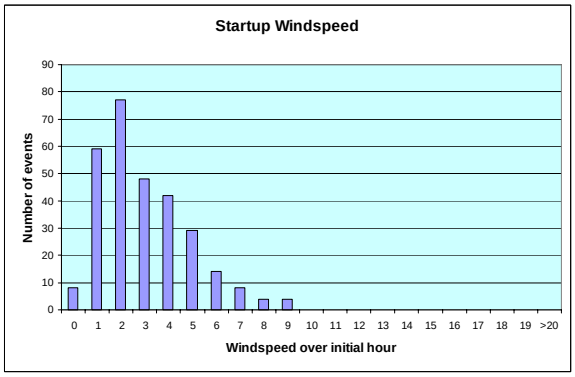

Site Name: **Hemsby**
Range of data: April - September 93-97

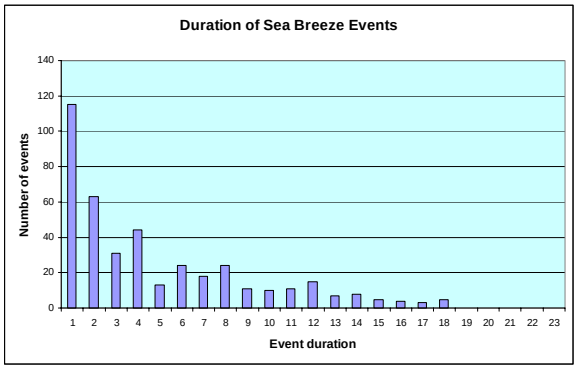

Site variables

Onshore wind angle	250
Maximum angle from onshore angle	50
Discount events finishing after	21
Minimum swing into onshore sector	30

Statistics

Number of sea breeze events	325
Average event duration	3.3
Maximum event duration	15
Minimum event duration	1
Earliest event start time	6
Latest event start time	18
Earliest event end time	7
Latest event end time	21
Total duration of all events	1061
Total hours with no data	222
Average initial angle re: onshore angle	-1.8
Average absolute initial angle re: onshore	26.7
Average windspeed over initial hour	3.2
Maximum windspeed over initial hour	10.3
Minimum windspeed over initial hour	0.5
Maximum windspeed over all data	18.5

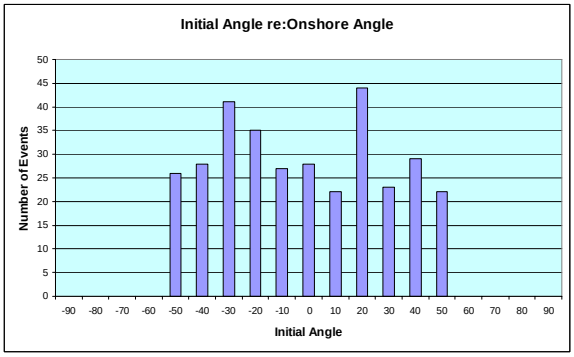

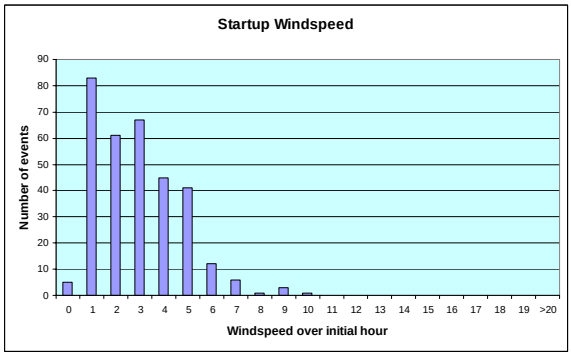

Site Name: **Bournemouth Airport**

Range of data: April - September 93-97

Site variables

Onshore wind angle	170
Maximum angle from onshore angle	50
Discount events finishing after	21
Minimum swing into onshore sector	30

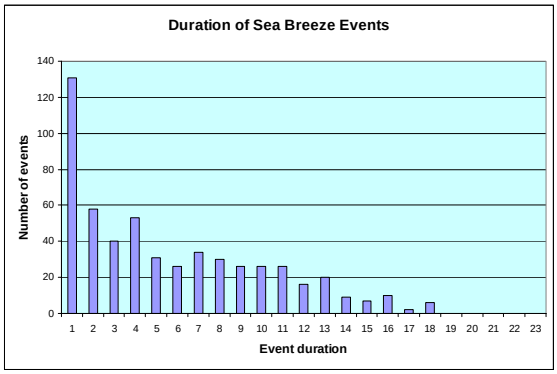

Statistics

Number of sea breeze events	467
Average event duration	4.5
Maximum event duration	15
Minimum event duration	1
Earliest event start time	6
Latest event start time	18
Earliest event end time	7
Latest event end time	21
Total duration of all events	2094
Total hours with no data	77
Average initial angle re: onshore angle	4.2
Average absolute initial angle re: onshore	25.7
Average windspeed over initial hour	3.1
Maximum windspeed over initial hour	10.8
Minimum windspeed over initial hour	1.0
Maximum windspeed over all data	25.7

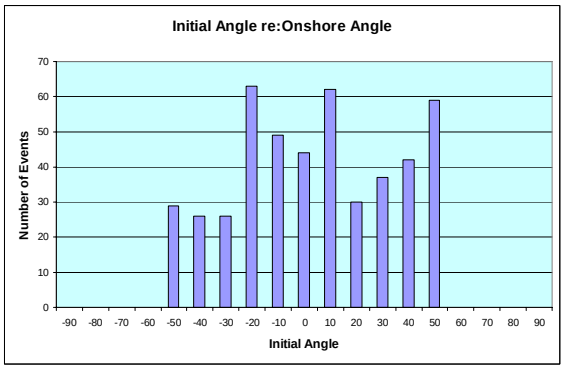

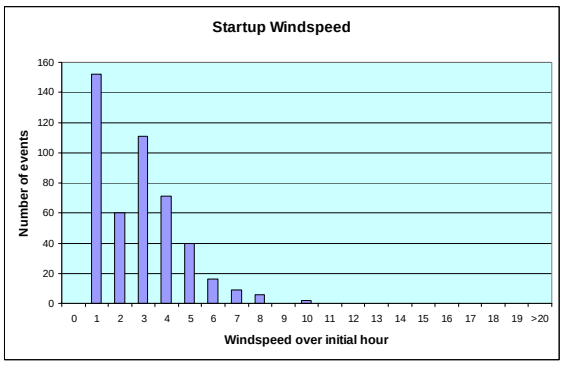

ANNEX B

RECOMMENDATION FOR BEST PRACTICE ON STATISTICAL BINNING OF MET DATA FOR DISPERSION MODELLING PURPOSES

N Nelson
THE METEOROLOGICAL OFFICE

EXECUTIVE SUMMARY

As air quality legislation governing the management of air quality in the U.K. becomes more stringent there is a greater need to understand more of the constituent processes that form the overall air quality management strategy. One such component is the use of atmospheric dispersion models. Dispersion modelling occupies an important position in the management process, with model results used to make important regulatory decisions concerning the operation of industry. As a result a better understanding of the reliability of model predictions is required. It has been noted that on occasions the results offered by dispersion models vary depending on the form of input met data used, and in particular, depending on whether the data is raw hourly sequential or statistically processed into classes or 'bins'. As a consequence the Atmospheric Dispersion Modelling Liaison Committee has commissioned this study to investigate why the discrepancies exist and whether or not they can be minimised by altering the scheme used to compile the input met data.

The study investigated the results obtained for the two different types of met input files when applied to a variety of emission release scenarios using the ADMS model. Both statistical and sequential met files are routinely supplied by the Met Office. It was found that, rather than being associated with the statistical processing of the met data per se, the largest discrepancies noted in the study were due to the absence of a specific met parameter in the statistical data, namely ambient temperature. It was found that the results were not particularly sensitive to the ambient temperature itself, but to the difference between ambient and release temperature.

The report concludes that refining the statistical processing scheme would not bring about a significant reduction in the discrepancies noted and hence the standard statistical processing method is adequate for most purposes. However, care should be taken regarding releases which are sensitive to the exact difference between ambient and release temperatures, e.g. for release temperatures close to ambient with a significant mass being released. In such an event it may well be more appropriate to use statistical met data rather than sequential. This is due to the way in which the ambient temperature is treated in the two types of input files rather than because of the statistical processing itself.

B1 Introduction

The use of dispersion models within the regulatory system for air quality has increased over the past ten years. Many air quality standards as presented in the National Air Quality Strategy (NAQS) have been set for the concentration of specific pollutants as measured by the network of pollution monitors. However, within the framework of air quality management, the use of predictive dispersion models has benefited areas of planning, regulation and compliance estimation in the absence of observations.

In designing the National Air Quality Objectives it has become appropriate to adopt percentile compliance for those standards that have short averaging times (The United Kingdom National Air Quality Strategy 1997). This approach has become a standard for setting European air quality limit values. In practice this means that if an objective for the 99.9th percentile was set then 99.9 % of measurements recorded for the pollutant in question during the relevant period (normally a year), must be at or below the specified level for that pollutant. This approach recognises that there are occasions where it is not practicable to demand 100% compliance to the standard, as there exists certain factors outside our normal control. Exceptional weather is an example or uncontrollable natural sources (fallout from volcanic eruptions). Also certain social and cultural practices would otherwise have to be banned (Guy Fawkes Night).

Percentile values are therefore of particular importance in dispersion modelling. In 1995 the Expert Panel on Air Quality Standards recommended a standard for airborne PM_{10} (airborne particulate matter of aerodynamic diameter less than 10 micrometers) of 50 $\mu g/m^3$, recorded as a running 24-hour average (EPAQS 2001). The value was accepted and adopted by the Government in the National Air Quality Strategy in 1997 (The United Kingdom National Air Quality Strategy 1997) as a provisional objective, to be achieved at the 99th percentile by 2005. The standard has now been accepted as an objective but measured as a fixed 24-hour mean, not to be exceeded more than 35 times per year. The timescale for this objective to be achieved is 2004. Other examples include Sulphur Dioxide measured as a 15-minute mean; the objective to be achieved by 2005 is 100 ppb as the 99.9th percentile. Also the objective for ozone, measured as a running 8 hour mean, is 50 ppb at the 97th percentile by the year 2005 (The Air Quality Strategy 2000), although this particular pollutant does not form part of the NAQS review and assessment procedure.

Current standard dispersion models can use hourly sequential or statistically binned meteorological data to give long-term impact assessments of pollutant concentrations and depositions. A straightforward process is used when hourly sequential data is employed. In this case the dispersion model is provided with meteorological data for successive hours. The dispersion is calculated for each hourly set of data, and quantities such as the long-term mean and / or various percentiles of concentration are calculated in much the same way as they would be calculated for long-term sequences of observed concentrations. The use of

statistically binned met data requires a slightly more complex process. Rather than be supplied with a set of 'real data' the model is provided with a set of representative meteorological conditions, each with a frequency of occurrence associated with it. These frequencies are used to 'weight' the results in calculating long-term averages or percentiles. The statistical data is usually produced from sequential data by grouping the hourly values into classes or bins, and counting how many cases occur in each bin. This use of statistical data reduces the number of occasions that have to be considered and hence the computational costs.

The need to use statistical data for some studies is likely to remain for the foreseeable future despite increases in computer power, partly because of alternative uses for that power – such as more sophisticated building downwash or terrain calculations.

Generally, analyses using statistical data cannot be expected to duplicate exactly the hourly treatment of the sequential data, as some of the meteorological detail will be lost in the categories into which the data is binned. To ensure that any discrepancies between the two types of data are kept to a minimum it is essential to estimate at least the size of the error that occurs with the current binning scheme. It is also appropriate to investigate whether altering the binning procedure can reduce this error. However it should be recognised that the optimal scheme is likely to be different for different dispersion scenarios and it is not very practical to change the approach for different problems

Over the years some concerns have been raised regarding the difference between results obtained from the two types of met data. Furthermore, small ad-hoc studies (presented by a range of different model users at meetings) have revealed significant differences for three-month simulations examining neutrally buoyant near surface releases using ADMS version 2.1. B.M.Davies and D.J.Thomson (1997) investigated the sensitivity of model results to specific pre-processing of the met data. The study concluded that there was very little difference found in predictions of long-term mean concentrations using statistical and sequential datasets, and that for the situations analysed, the binning scheme used by the Met Office was adequate. It was also found that better concentration estimations were achieved when binned heat flux values were used instead of the reciprocal Monin-Obukhov length in the input parameters. This study however used an earlier version of ADMS (V. 1.5) and investigated only high buoyancy emission sources. It was also concluded that results using 3 and 5 years of statistical meteorological data compared well with 10-year datasets. The aim of this study is to use the current version of ADMS to investigate some of the discrepancies that exist between analyses using statistically binned and hourly sequential met data and to look at ways in which they might be reduced by altering the binning procedure.

B2 Methodology

B2.1 The dispersion model

The study was conducted using ADMS version 3.0. Some of the discrepancies noticed in past analyses were obtained using earlier versions of ADMS. In case these discrepancies were a result of the underlying science/coding of the earlier version leading to a greater sensitivity to the type of met data, some cases were also run with ADMS version 2.2 for comparison. In an attempt to keep the complexity to a minimum, the model was run assuming a single point source release over flat terrain of constant roughness length. The more complex effects of buildings, coasts and topography that ADMS can account for were not included. Also, the deposition processes (wet and dry) were not investigated.

In essence ADMS adopts the following method for calculating the long-term percentiles of concentration. Each line of met data is analysed in turn and the resulting concentrations calculated. The concentration is stored for each output point along with the frequency with which that concentration occurs (for sequential data the frequency associated with each case is always 1). The concentrations are then sorted into descending order to form a probability distribution function. The highest value of this function gives the 100^{th} percentile value (concentration). The lower percentile values are calculated using linear interpolation according to the cumulative frequency. In this way values of, for example, the 98^{th} percentile are calculated at each point. In this study the main emphasis is placed on the spatial peak of the values of any given percentile although some contour plots of percentiles showing the spatial variations are also presented.

The method used to store the values varies according to the type of met data being used and the value of the percentile being requested. High percentile values from hourly sequential data are stored in a linked list in such a way as to be ordered from the highest to the lowest values as they are stored. For example, for a one-year dataset consisting of 8760 hours of data, only the top 2% of values (i.e. 176 hours) will be stored for a request of a 98^{th} percentile. For lower percentiles requested from hourly sequential and for all statistical data, all the concentrations and their frequency of occurrence are stored.

B2.2 Meteorology

Three one-year datasets for the years 1994, 1995 and 1996 were used in the analysis. For each year both statistical and hourly sequential data were used. The data was extracted from the Met Office Data Archive for the met station Elmdon. Elmdon is situated near Birmingham; the site details are summarised in table B1 below:

TABLE B1 Elmdon site details

Station latitude	52 Degs 27 min North
Station longitude	01 Degs 44 min West
Height above mean sea level	98 metres
Anemometer height above ground level	10 metres
Observing Frequency	Hourly

For the three years chosen the collection of data was almost 100 % complete. The total number of hours (excluding calms, variable direction and unavailable data) used to compile the statistical datasets were 98.6% for 1994, 95.8% for 1995 and 94.9% for 1996 of the total number of available hours.

The sequential datasets offer the chronological hour by hour values of specific parameters as measured at the site. The sequential data used included information regarding:

- The year year (T_{year});
- The Julian Day Number day (T_{day});
- The hour of the day hour (T_{hour});
- The near surface temperature T_0 (°C);
- The wind speed U ($m.s^{-1}$);
- The wind direction ϕ (Degrees);
- The precipitation rate P (mm/hr);
- Cloud amount CL (oktas) and
- The relative humidity RHu.

The wind data recorded are hourly averaged and the hourly precipitation amount includes contributions from water falling as snow or hail etc. Note however that although precipitation and relative humidity information was present in the input file, these values are not relevant to the study as the parts of ADMS which make use of them – namely the wet deposition and plume visibility modules – were not used.

The statistical datasets were constructed using the standard procedure employed by the Met Office for producing statistical met datasets for ADMS. In this procedure, heat flux ($F_{\theta 0}$) and boundary layer depth (H) were calculated for each hour of data. For each hour five met parameters, namely wind speed, wind direction, surface heat flux, boundary layer height and precipitation, are retained and the rest of the data discarded. Categories or 'bins' are then introduced for each of the five parameters. The number of categories varies according to the met parameter as follows:

- Hourly averaged wind speed - U 5 classes
- Hourly averaged wind direction - ϕ 12 classes
- Surface sensible heat flux - $F\theta_0$ 7 classes
- Boundary layer height - H 7 classes
- Hourly precipitation - P 3 classes

and the upper limits of the classes are as follows:

U – 3 6 10 16 ∞ (Knots)

ϕ - 15 45 75 105 135 165 195 225 255 285 315 345 (Degrees)

$F_{\theta 0}$ - -30 -10 0 50 100 150 ∞ ($W.m^{-2}$)

H - 100 200 300 500 800 1200 ∞ (m)

P - 0 6 ∞ (tenths of mm)

Each hour of met data is then assigned to one of the (5x12x7x7x3) 8820 categories depending on which combination of the U , ϕ , $F_{\theta 0}$, H and P classes the data falls into, and the number of hours of data falling into each of these 8820 categories is computed. In essence the approach can be summarised by saying that the model constructs a 5-dimensional frequency table. The met input file is constructed by giving a set of met data for each of the 8820 multi-dimensional categories (using representative values of U, ϕ, etc) and associating the corresponding frequency with the set of data. When the dataset is used by ADMS, dispersion is calculated for each of the 8820 sets of data and the frequency information is used to weight the results in calculating long-term means and percentiles. In practice there are fewer than 8820 cases because many of these will be empty - e.g. stable cases with light winds and deep boundary layers or strong winds with shallow boundary layer.

For each of the U, $F_{\theta 0}$, H and P bins, the representative value is chosen as the mean value of all the cases falling in that bin. ϕ however is handled quite differently in that the representative values are chosen to be the mid-point of each bin. A possible way to improve the binning scheme which does not involve increasing the number of bins, is to use, for example, a different value of U for each of the 8820 combination of bins based on the average wind speed for all the cases falling in that combination of bins. However that would mean ADMS would have to calculate each case from scratch which would reduce the speed advantage offered by statistical met over sequential (see below). Consequently this has not been investigated here. A typical ten-year statistical dataset contains about 2000 hours of met data compared with the max possible in a sequential dataset of 87600 (over the ten years). This is significantly less than the number of hours in a year (8760 – as used for an annual sequential dataset) and so statistical binning reduces the computing time significantly even if just a single year is being considered. In addition, if the terrain is uniform with no buildings etc considered, ADMS does not need to calculate everything for each case. For example if only ϕ and P change, this will only effect the direction of the plume and the wet deposition calculations.

Values that are equal to the upper limit of a particular class are placed within that class. The wind speed values used for defining the classes are given in knots because the observations are recorded and stored in knots to the nearest knot. However the values given in the dataset for input to ADMS are converted to $m.s^{-1}$. Notice that with the statistical dataset we pre-calculate the boundary layer height, H and the surface sensible heat flux, $F_{\theta 0}$ instead of allowing ADMS to derive this itself from Julian day number, hour of day, cloud cover and

temperature. There are two reasons for this. Firstly it is important when calculating H to allow for the gradual build up in height during the day and knowledge of the recent history regarding met conditions is therefore needed for estimating H. In statistical datasets there is no information on the sequence of the met conditions and so ADMS would be unable to allow for this if it had to estimate H. Secondly, the replacement of H and $F_{\theta 0}$ by Julian day number, hour etc would make the multi-dimensional frequency table 7 dimensional. The resulting large number of cases would increase the required ADMS running time to the point where there would be little or no advantage over using sequential data.

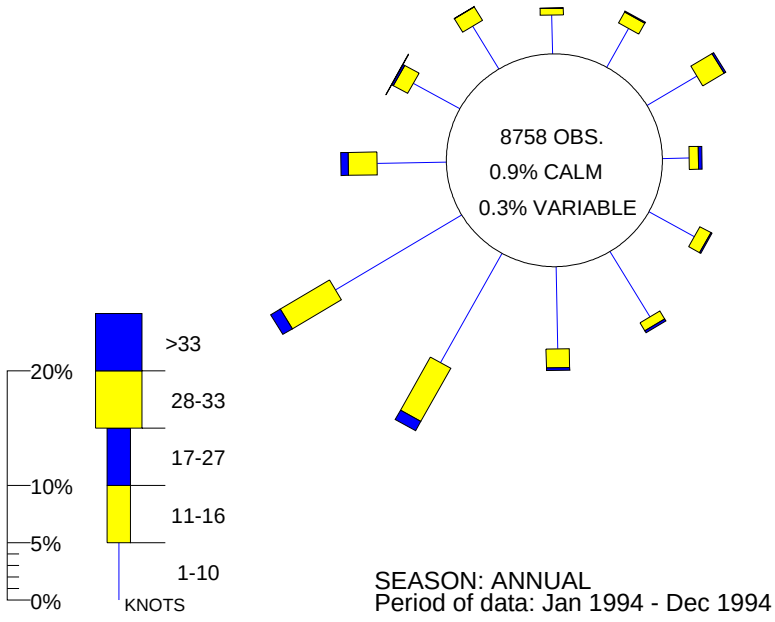

FIGURE B1a Elmdon Windrose for 1994

WIND ROSE FOR ELMDON
N.G.R: 4171E 2837N ALTITUDE: 98 metres a.m.s.l.

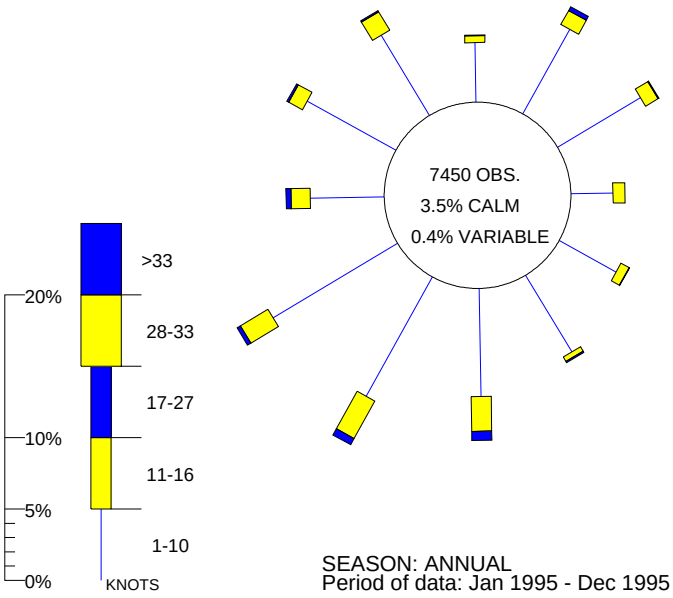

FIGURE B1b Elmdon Windrose for 1995

WIND ROSE FOR ELMDON
N.G.R: 4171E 2837N ALTITUDE: 98 metres a.m.s.l.

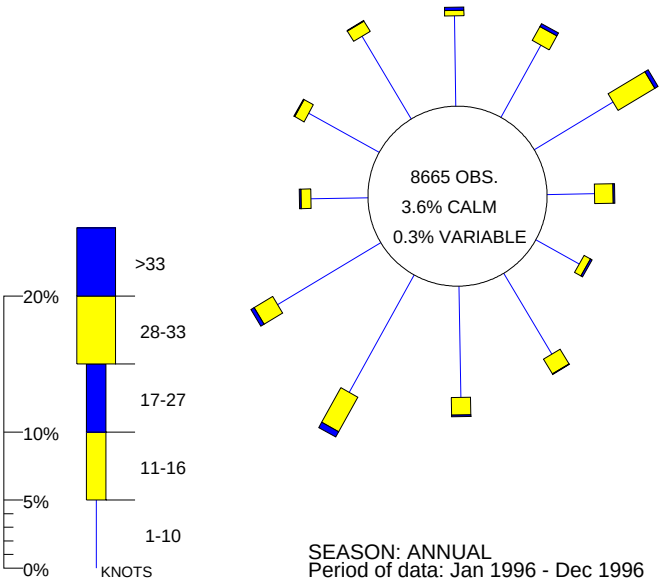

FIGURE B1c Elmdon Windrose for 1996

In the wind rose diagrams (Figs 1a – c) north is at the top of the diagram. There are 12 arms extending from the central circle, each representing a 30-degree segment of wind direction. The length of the arm is proportional to the amount of time (in hours) the wind blew from that particular wind segment. The different thicknesses of the arms represent different wind speed classes (the key to the classes is at the bottom left of the diagram). Because the length of each arm will vary per rose, the length of the scale will be adjusted. Therefore each scale is unique to the rose it is shown against. As long as the recording instrumentation is working correctly for every hour of the year there will be 8760 readings used to compile each annual wind rose. Exceptions to this occur when there is not sufficient wind to move the wind vane and to record a wind speed on the anemometer (referred to as calm conditions). Or when there is only just enough wind to move the wind vane (so recording a wind direction) but not to record a wind speed on the anemometer – usually because the wind speed is below the start up speed of the anemometer (referred to as variable conditions).

- Wind directions are expressed in degrees from true north and represent the direction from which the wind is blowing;
- Speeds are in knots (nautical mph), with 1 knot = 1.15 mph, or 0.515 $m.s^{-1}$;
- The centre of the circle gives information about the number of observations used in compiling each rose, the percentage of the time when the winds were calm and the percentage of the time with variable winds.

The three years chosen exhibit little real significant differences. For all years winds from the south-west are the most common, but is more marked in 1994. 1995/96 show more winds from the north-east than 1994. There is also fewer calms recorded in 1994.

B3 Study 1

The method used calculated the dispersion from three types of point source releases:

- A buoyant release from a 150m stack (simulating a power station source);
- A less buoyant release from a 10m stack and
- A buoyant release from a 10m stack.

A summary of the release details are given in table D2 below:

TABLE B2 Release scenarios

Source	Height (m)	Width (m)	Exit Velocity (ms^{-1})	Exit Temp (^0C)
1	150	7	15	150
2	10	1	1	40
3	10	1	15	150

The pollutant used was an inert gas (adopting the ADMS default values – the same as air) released at a rate of 1 kg/sec over the flat terrain with a roughness length of 0.1m. The dispersion calculations were based on an hourly averaging time period. The output grid size varied according to the release height, velocity

and temperature. The resolution was varied so to ensure that the 'true' peak value had been recorded. On occasions when the maximum concentration coincided with the first grid point the resolution was increased so to ensure that the peak concentration was not in fact closer to the source. The source was always placed at the origin (0,0).

B3.1 Study 1 results

It was originally suggested in the contract that 95th, 97th, 99th percentiles of concentration and long term average concentrations should be investigated. The results for these initial runs using ADMS version 3.0 are shown in Appendix A. Similar runs were made using ADMS version 2.2 and these results can be seen in Appendix B.

For ADMS version 3.0 there was generally good agreement between the two datasets for sources 2 and 3. This was true for all the percentile groups and the long term average values. For the different percentile groups, sources 2 and 3 showed an average discrepancy of 1.67% (the difference between sequential and statistical expressed as a percentage of the sequential value) with one exception (source 2, 99th percentile for 1995 gave a 9.8% difference). Discrepancies for the long-term average concentrations were generally higher – sources 2 and 3 averaged about 6% difference.

With the exception of one particular value, the percentile results for source 1 gave a higher average 16.7% difference between the two datasets. The worst discrepancy occurred for the 95th percentile value for Source 1 in 1994. Here the difference, expressed as a percentage of the sequential value, was as much as 47%. The results for source 1 long-term average concentrations showed a 15% fractional difference. Generally the higher percentage differences were associated with Source 1 for each of the different percentile and long-term average concentration results.

The results for ADMS version 2.2 showed generally higher fractional differences between the two datasets. For the 95th and 97th percentile groups, sources 2 and 3 showed average discrepancies of 19.8%. This compares with an average discrepancy of 4.3% for the 99th percentile group. The long term average concentrations for sources 2 and 3 average 8.7% fractional difference.

As with version 3.0 the worst discrepancies were noted for source 1. For the 95th and 97th percentile groups, source 1 averaged 192% fractional difference between the two datasets. The 95th percentile result for 1996 shows a fractional difference of almost 300%. The 99th percentile result averages at a much reduced 43% difference for source 1. The long-term average results show a peak fractional difference for 1994 of 102%.

It is clear that the earlier version of ADMS is more sensitive to differences between the two datasets and that this problem has been reduced for version 3.0. With the exception of the 95th percentile result for the elevated source (source 1) the results from version 3.0 show reasonable agreement between the two datasets. Wishing to investigate still further, potential problems with the other sources, and acknowledging the infrequent use of the 95th percentile in the NAQS, a decision was made to concentrate on version 3.0 and to extend the study to include the higher

percentiles. The more extreme percentiles should offer a more stringent test of the binning procedure because extreme events are due to extreme or perhaps unusual conditions that may not be well represented by the binned values. ADMS was therefore run and a comparison made between the spatial peak values of 99.9th and 100th percentile of concentrations for each of the types of met data.

B3.2 Study 1 summary

Figure B2a below summarise the results for the spatial peak of the 100th percentiles of concentration for all 3 sources for the 3 study years, for both statistical and sequential cases. The concentration units are $\mu g.m^{-3}$.

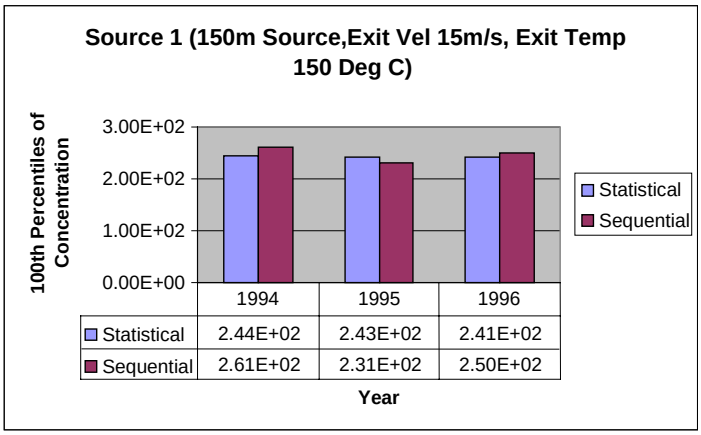

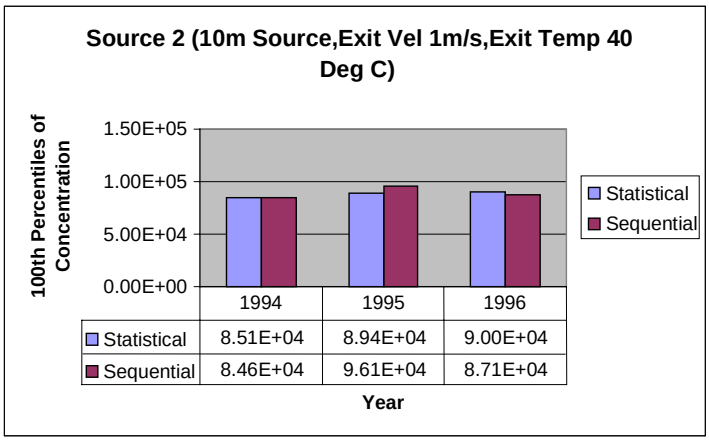

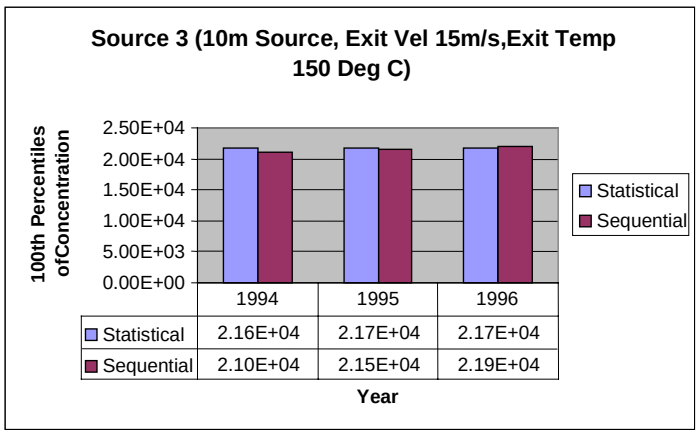

FIGURE B2a Comparison of peak 100th percentile of concentrations for statistical and sequential datasets during the study period

The charts for the 99.9th percentiles of concentration are summarised in Figure 2b below. Again the results are presented for all 3 sources for the 3 study years and for both statistical and sequential cases. The concentration units are $\mu g.m^{-3}$.

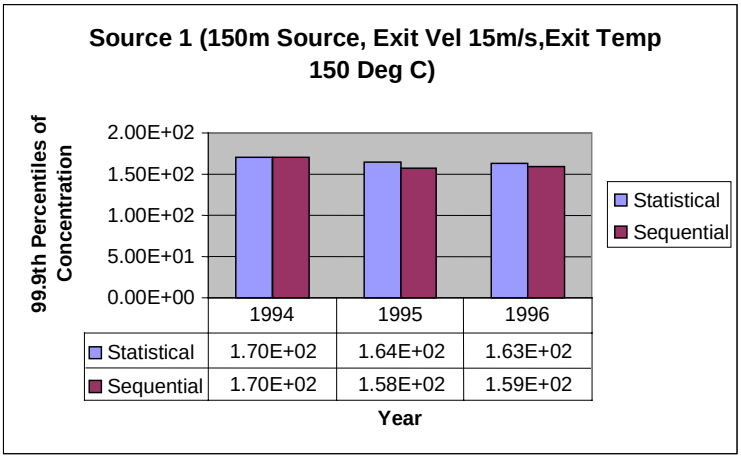

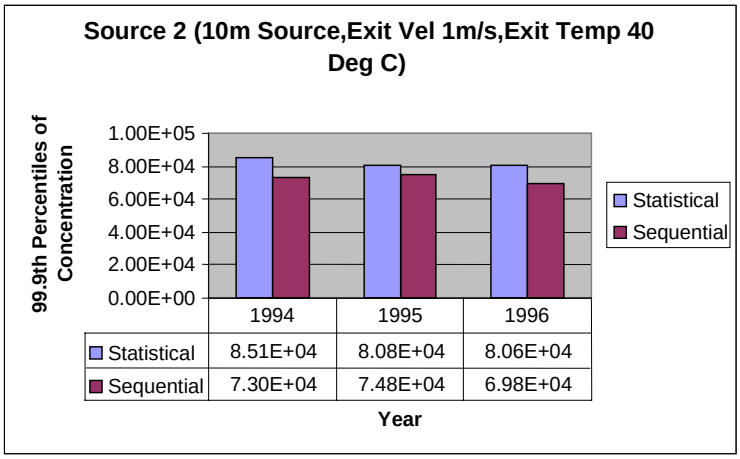

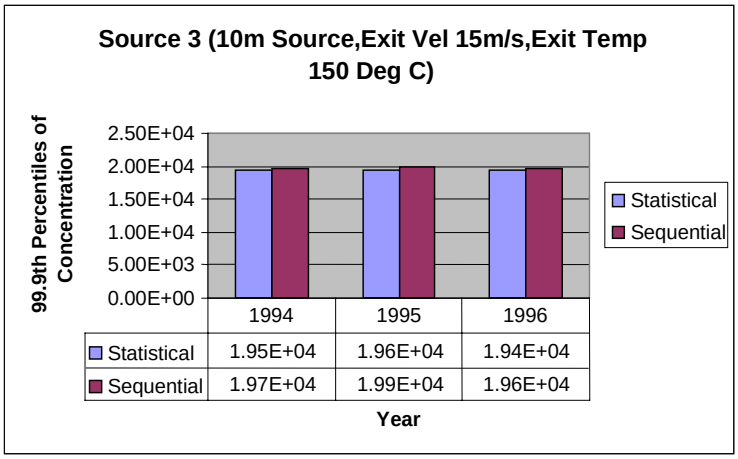

FIGURE B2b Comparison of peak 99.9th percentile of concentrations for statistical and sequential datasets during the study period

It can be seen that for all three years there is generally good agreement between the sequential and statistical datasets. In some instances the sequential runs provide higher spatial peak concentrations and in others the statistical is greater. The difference in all cases however was marginal (differences ranging from 0.6% of the sequential value to 7% for 100th percentile values and from 0.4% to 16.5% for the 99.9th). A summary of the average differences expressed as a percentage of the sequential value is shown in Table B3 below. One last attempt was made to identify significant differences with the 95th, 97th and 99th percentiles of concentration. These also resulted in very good agreement between statistical and sequential datasets (See Appendix C). It was therefore considered that a new set of release details should be investigated to see if discrepancies would emerge from varying release heights or temperatures and velocities etc.

TABLE B3 Summary of the difference between statistical and sequential results expressed as a percentage of the sequential value

100^{th} Percentile	1994	1995	1996
Source 1	6.5%	5.2%	3.6%
Source 2	0.6%	6.9%	3.3%
Source 3	2.8%	0.93%	0.91%
99.9^{th} Percentile			
Source 1	0.4%	3.8%	2.2%
Source 2	16.5%	8.0%	15.5%
Source 3	1.1%	1.5%	0.9%

B4 Study 2

A series of runs were undertaken with different release temperatures, heights and release velocities. The release heights were varied from 100m down to 10m. For each height a release containing a buoyant emission but with small exit momentum and a less buoyant release coupled with an increased momentum were used. The following table summarises the release characteristics;

TABLE B4 Summary of release characteristics

Case	Release hight (m)	Release vlocity (m/s)	Release tmperature (°C)
A	100	9	15
B	100	1	40
C	75	9	15
D	75	1	40
E	50	9	15
F	50	1	40
G	30	9	15
H	30	1	40
I	10	9	15
J	10	1	40

For these cases the release diameter was kept at 1m, rate of release at 1 kg/sec and the roughness length at 0.1m.

B4.1 Results for B.D.F.H&J

Figures B3a – 3c below summarise the results from the cases with high buoyancy and reduced momentum (i.e. cases B, D, F, H and J) for the 3 study years. Values for both statistical and sequential spatial peak concentrations are shown together with the differences between the two. The contoured results for these runs can be seen in Appendix D Figs D1a to D1f through to D5a to D5f.

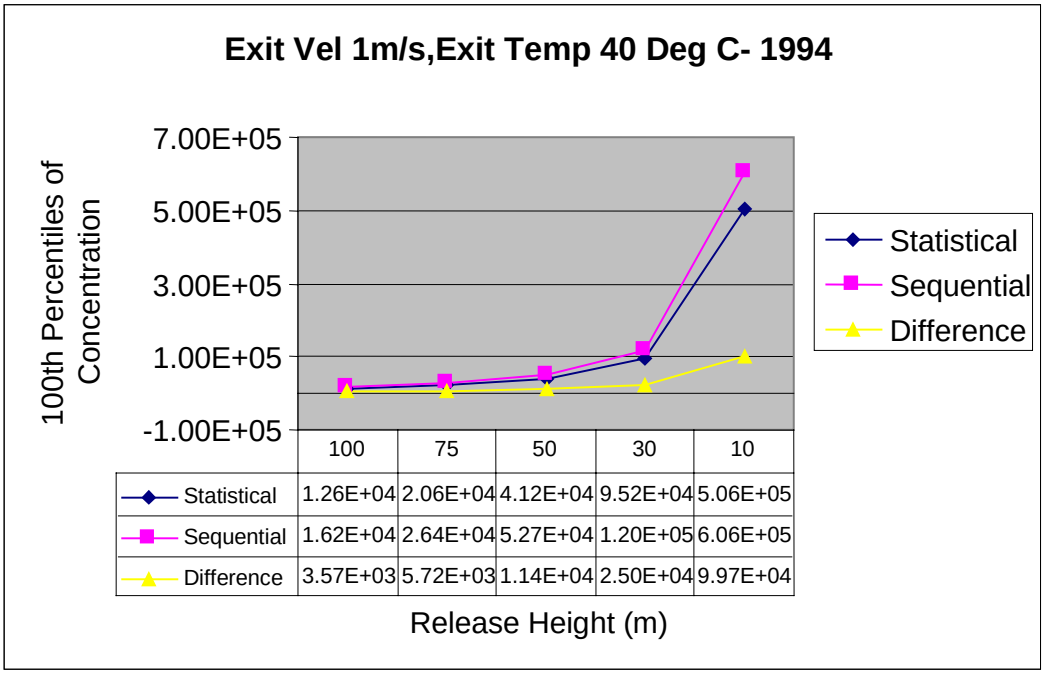

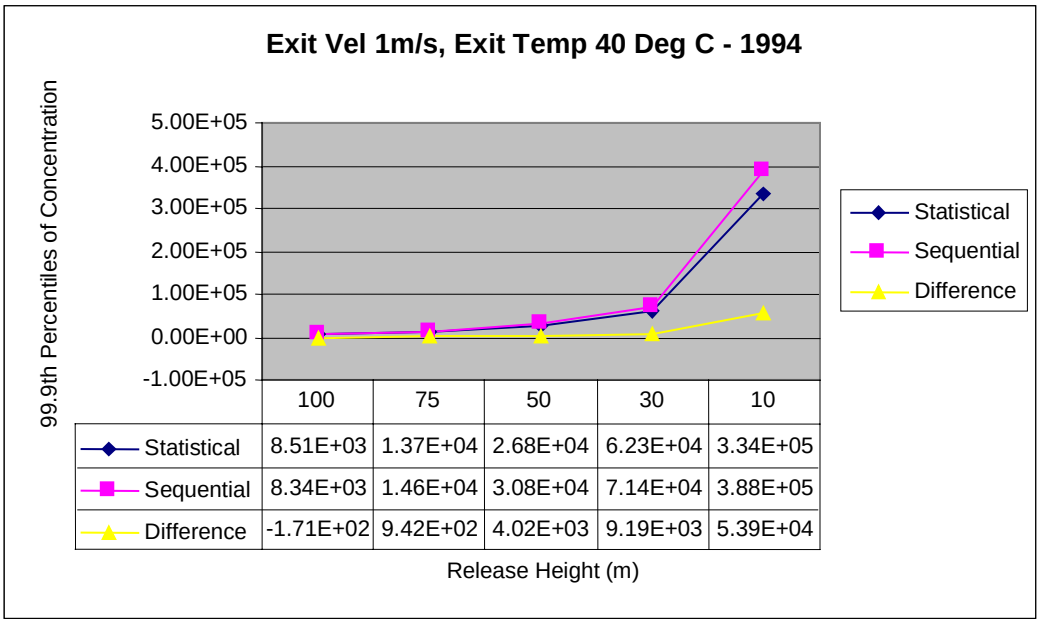

FIGURE B3a Comparison of peak 100th and 99.9th percentiles of concentration at varying release heights for 1994

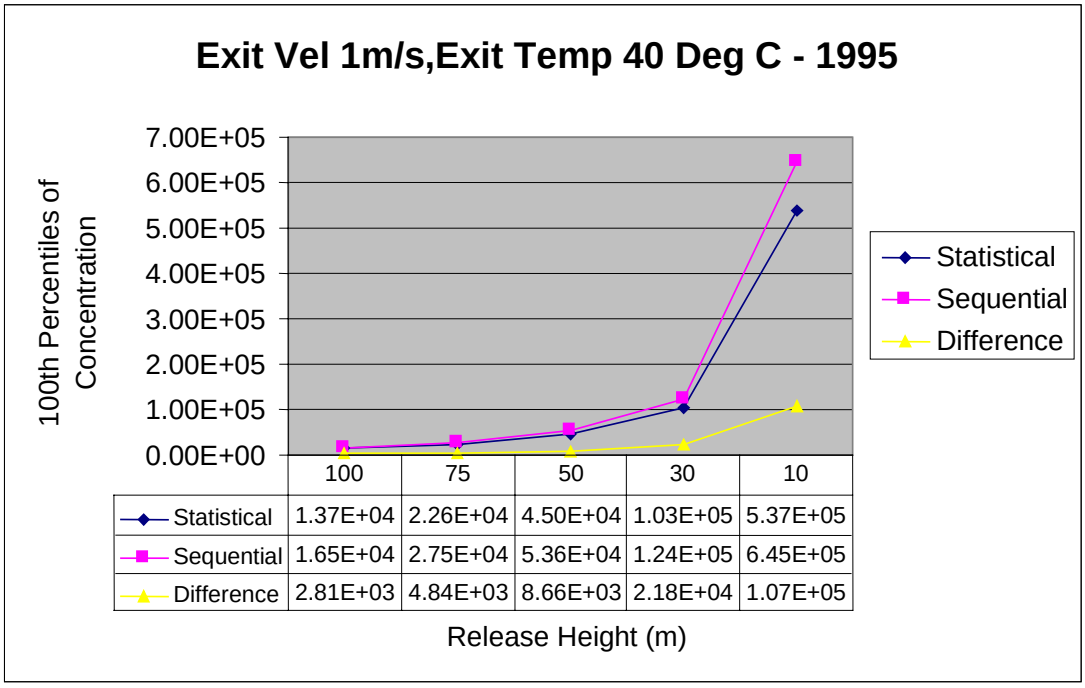

	100	75	50	30	10
Statistical	1.37E+04	2.26E+04	4.50E+04	1.03E+05	5.37E+05
Sequential	1.65E+04	2.75E+04	5.36E+04	1.24E+05	6.45E+05
Difference	2.81E+03	4.84E+03	8.66E+03	2.18E+04	1.07E+05

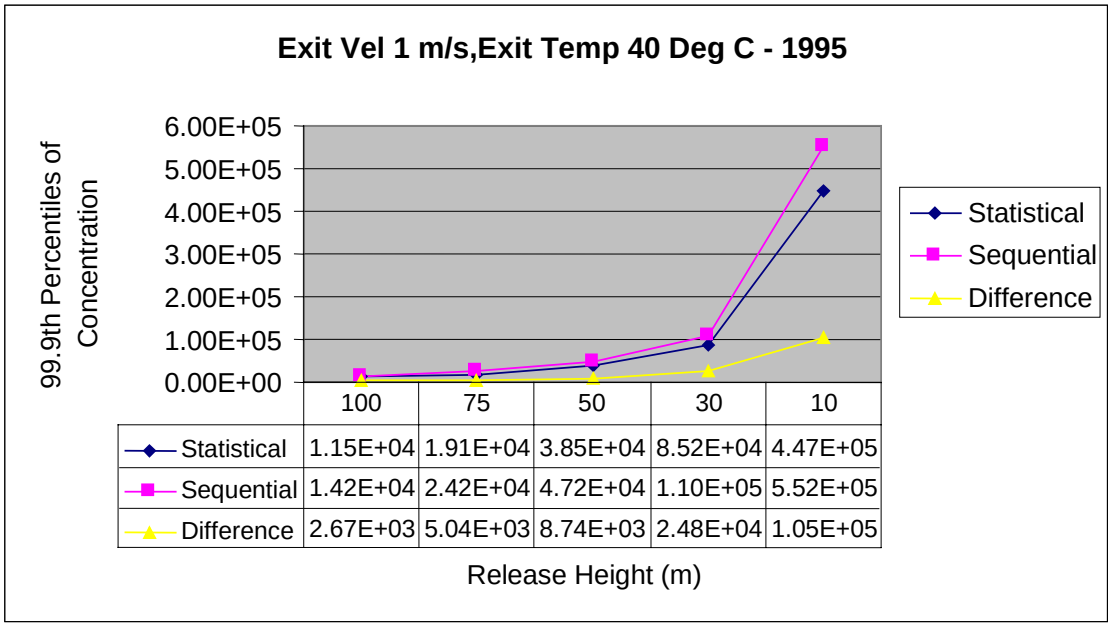

	100	75	50	30	10
Statistical	1.15E+04	1.91E+04	3.85E+04	8.52E+04	4.47E+05
Sequential	1.42E+04	2.42E+04	4.72E+04	1.10E+05	5.52E+05
Difference	2.67E+03	5.04E+03	8.74E+03	2.48E+04	1.05E+05

FIGURE B3b Comparison of peak 100th and 99.9th percentiles of concentration at varying release heights for 1995

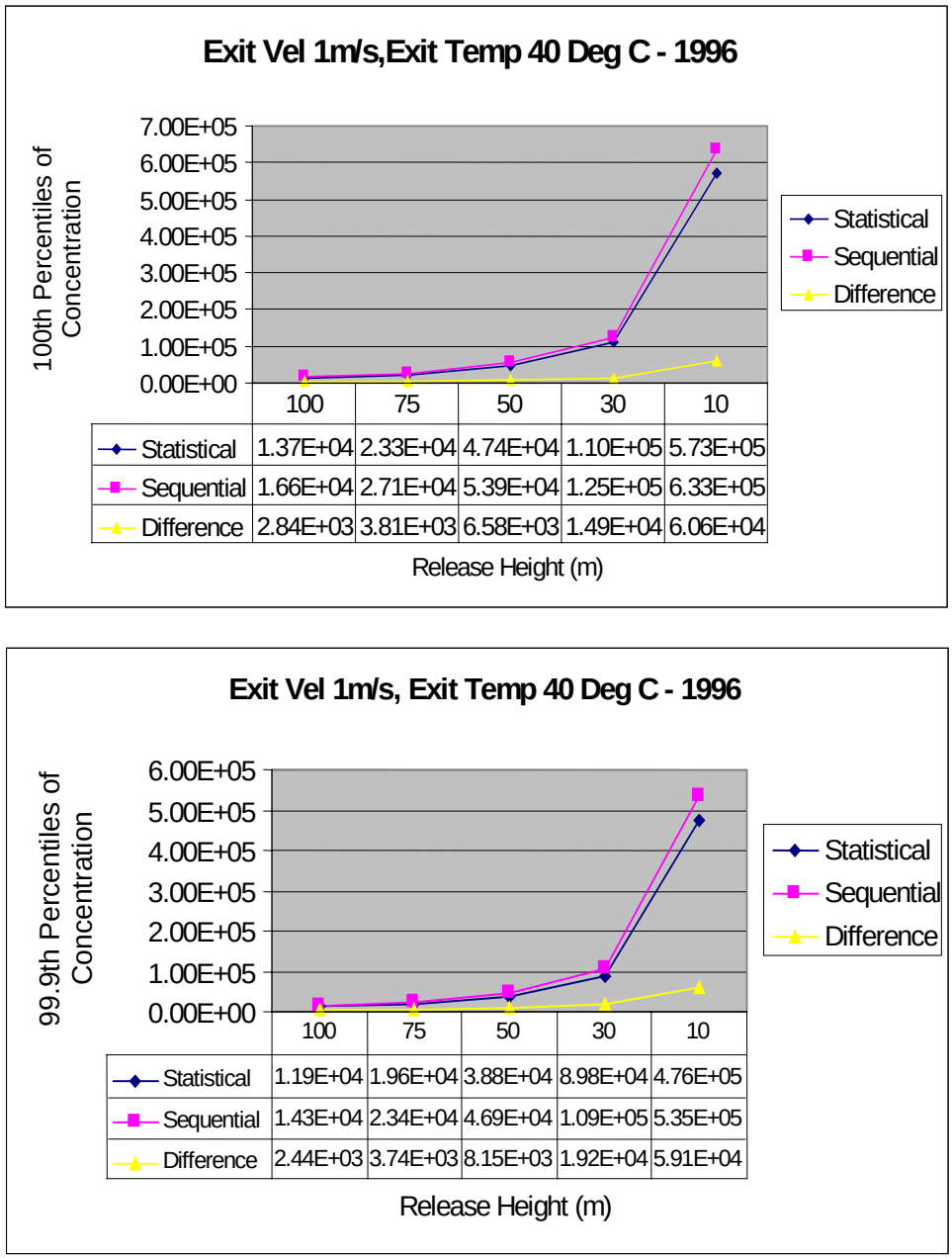

FIGURE B3c Comparison of peak 100th and 99.9th percentiles of concentration at varying release heights for 1996

The results for cases B, D, F, H and J show generally good agreement between statistical and sequential runs although somewhat larger fractional differences than were seen in the cases considered in section 3. The sequential runs produce higher concentrations with just one exception occurring for the 99.9th percentile value - 100m release for 1994. In this case the statistical value was marginally higher.

Expressing the difference between statistical and sequential results as a percentage of the sequential value gives an average percentage difference for the 100th percentile of 16.8 %. The worst percentage difference of 22% occurs for the 100m release height in 1994.

For the 99.9th percentile results, the average percentage difference was 15%. In this case, the worst percentage difference was 22.5% and occurred for the 30m-release height in 1995. The average differences expressed as a percentage of the sequential value are shown in table B5 below.

TABLE B5 Summary of the average difference between statistical and sequential results expressed as a percentage of the sequential value

Percentile	1994	1995	1996
100th	20.5%	17.0%	13.0%
99.9th	9.6%	20.0%	15.8%

B4.2 Results for A,C,E,G&I

Results for the other cases (A,C,E,G,I) where the buoyancy was reduced but the momentum increased are shown in Figures B4a – D4c below. The contoured results for these runs can be found in Appendix E, Figs E1a to E1f through to E5a to E5f.

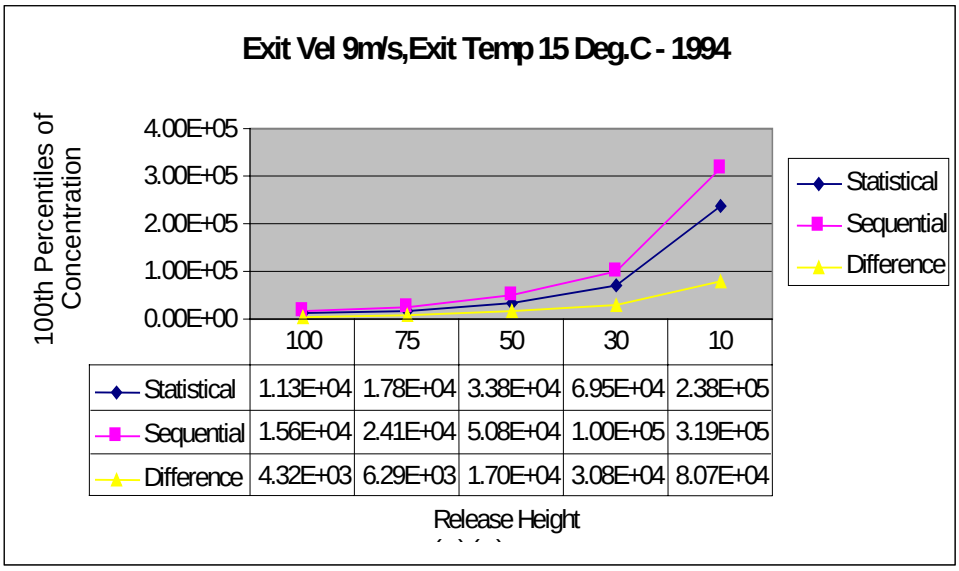

	100	75	50	30	10
Statistical	1.13E+04	1.78E+04	3.38E+04	6.95E+04	2.38E+05
Sequential	1.56E+04	2.41E+04	5.08E+04	1.00E+05	3.19E+05
Difference	4.32E+03	6.29E+03	1.70E+04	3.08E+04	8.07E+04

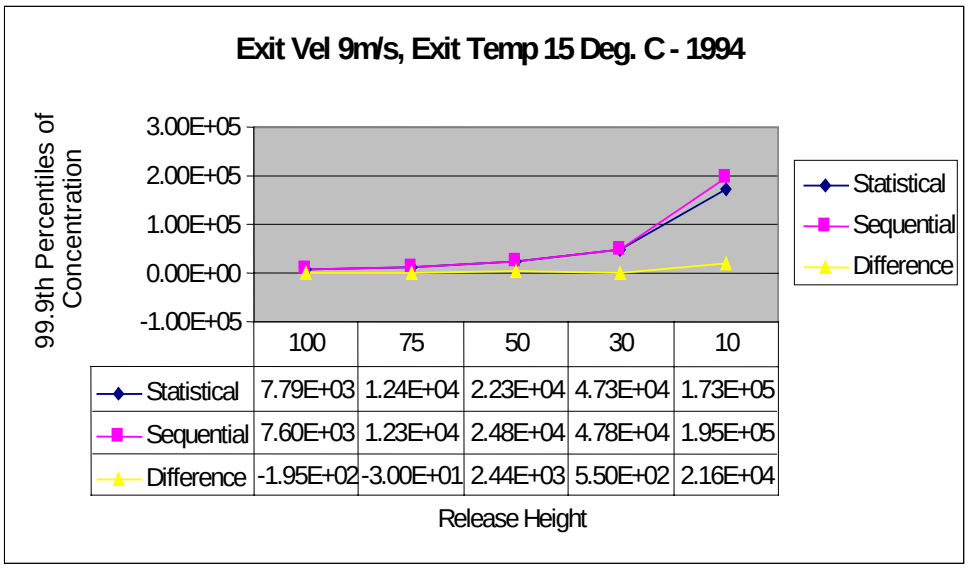

	100	75	50	30	10
Statistical	7.79E+03	1.24E+04	2.23E+04	4.73E+04	1.73E+05
Sequential	7.60E+03	1.23E+04	2.48E+04	4.78E+04	1.95E+05
Difference	-1.95E+02	-3.00E+01	2.44E+03	5.50E+02	2.16E+04

FIGURE B4a Comparison of peak 100th and 99.9th percentiles of concentration at varying release heights for 1994

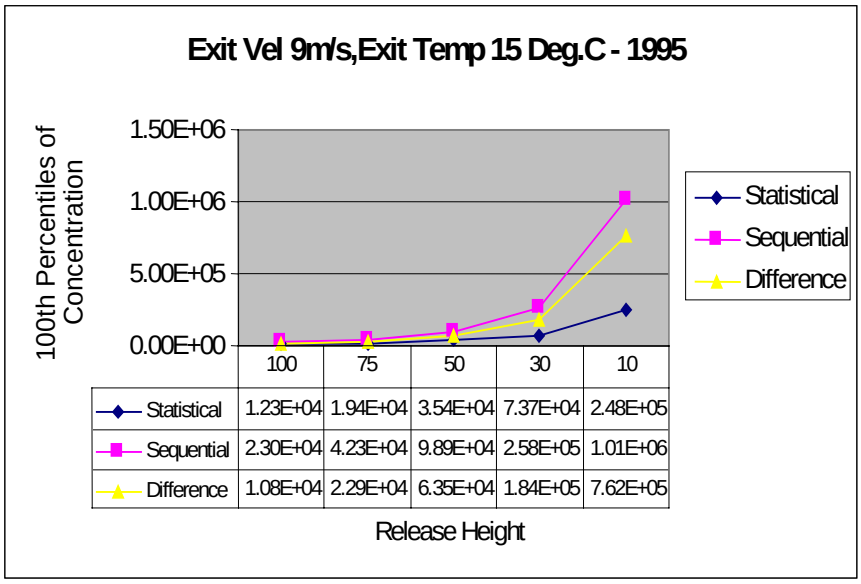

	100	75	50	30	10
Statistical	1.23E+04	1.94E+04	3.54E+04	7.37E+04	2.48E+05
Sequential	2.30E+04	4.23E+04	9.89E+04	2.58E+05	1.01E+06
Difference	1.08E+04	2.29E+04	6.35E+04	1.84E+05	7.62E+05

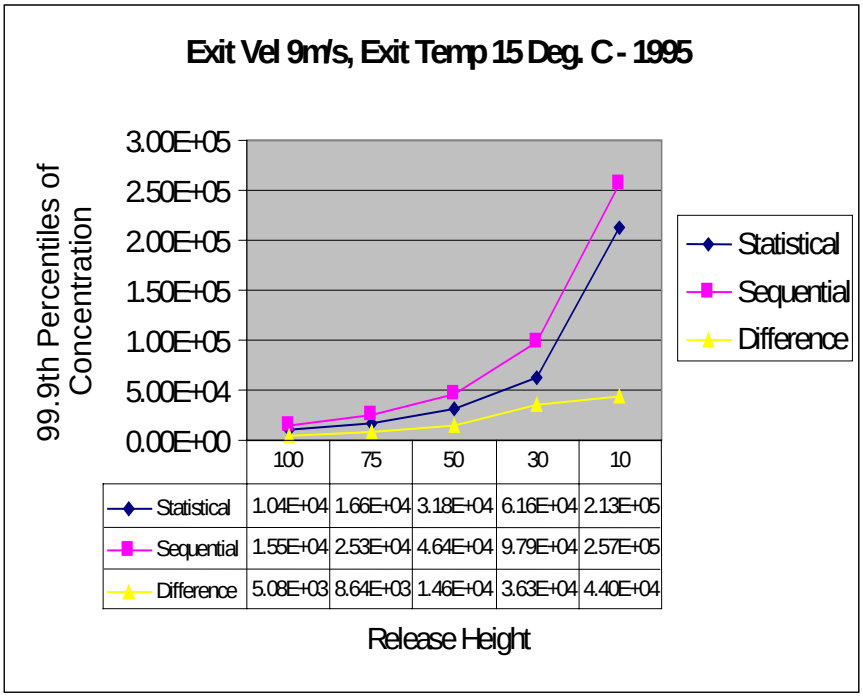

	100	75	50	30	10
Statistical	1.04E+04	1.66E+04	3.18E+04	6.16E+04	2.13E+05
Sequential	1.55E+04	2.53E+04	4.64E+04	9.79E+04	2.57E+05
Difference	5.08E+03	8.64E+03	1.46E+04	3.63E+04	4.40E+04

FIGURE B4b Comparison of peak 100th and 99.9th percentiles of concentration at varying release heights for 1995

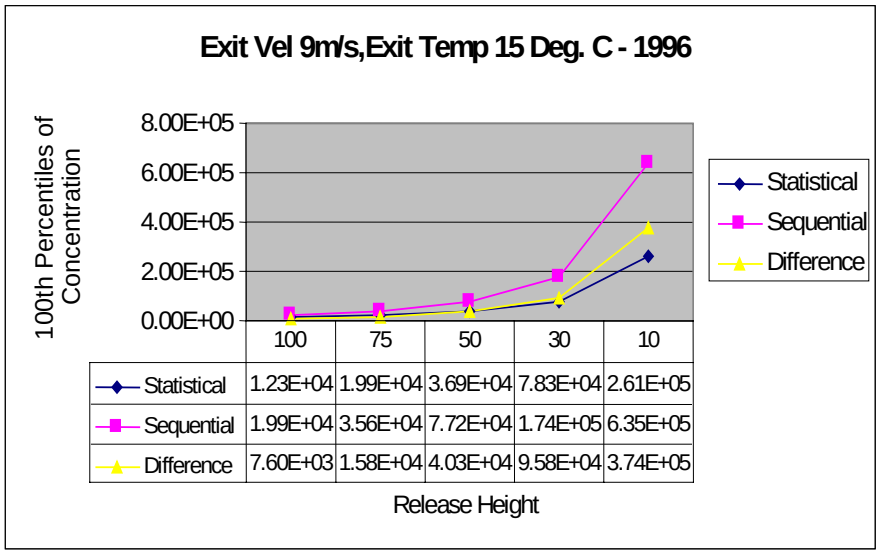

	100	75	50	30	10
Statistical	1.23E+04	1.99E+04	3.69E+04	7.83E+04	2.61E+05
Sequential	1.99E+04	3.56E+04	7.72E+04	1.74E+05	6.35E+05
Difference	7.60E+03	1.58E+04	4.03E+04	9.58E+04	3.74E+05

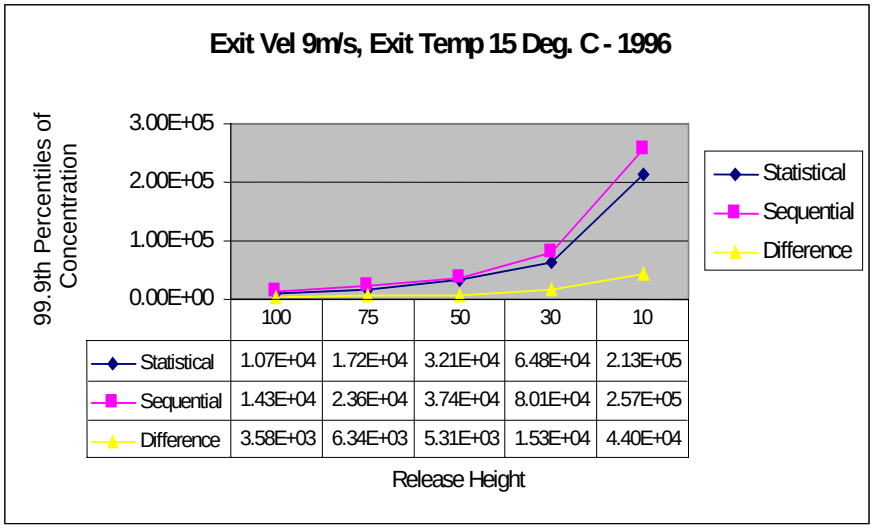

	100	75	50	30	10
Statistical	1.07E+04	1.72E+04	3.21E+04	6.48E+04	2.13E+05
Sequential	1.43E+04	2.36E+04	3.74E+04	8.01E+04	2.57E+05
Difference	3.58E+03	6.34E+03	5.31E+03	1.53E+04	4.40E+04

FIGURE B4c Comparison of peak 100th and 99.9th percentiles of concentration at varying release heights for 1996

As with the previous set of runs the above cases resulted in generally higher concentrations for the sequential cases. The difference between the statistical and sequential results was more significant – the average difference (expressed as a percentage of the sequential value) for the 100th percentile cases was 47% (c.f. 16.8% from the previous case runs) and a worst case difference of 75% which occurred for the 10m release height for 1995.

The average difference for the 99.9th percentile cases was 18.6%, which was only slightly higher than those mentioned in the previous case (see 4.1.1). The worst case difference was 37% and occurred for the 30m-release height for 1995. The differences are noticeably more pronounced for the 100th percentile cases. A summary of the average difference expressed as a percentage of the sequential value is shown in table B6 below.

TABLE B6 Summary of the average difference between statistical and sequential results expressed as a percentage of the sequential value

Percentile	1994	1995	1996
100th	28.6%	49.7%	62.4%
99.9th	4.9%	20.5%	30.5%

The discrepancies between the two datasets are at their greatest for the 100th percentile runs for the cases of higher momentum and lower buoyancy (i.e. exit velocity – 9 ms^{-1}, exit temperature 15ºC). The discrepancies for the 99.9th percentile runs were not as marked between the two cases run (c.f. Tables B5 and B6).

B4.3 Additional Run: High Buoyancy and Momentum

As a final check it was decided to perform one last run where the exit momentum and buoyancy were both high for the low-level source. Hence the following release values were run:

Case K

Release Height (m)	Release Velocity (m/s)	Release Temperature (°C)
10	15	150

The contoured results for this scenario can be found in the Appendix E – Figures E6a to E6f. The actual spatial peak concentration values can be seen in the following two graphs of Figure D5.

It can be seen that case K gives good agreement between statistical and sequential runs. With the exception of two cases the sequential results were always marginally higher than the statistical. The differences were close to zero in any case. When these results are compared to the previous cases concerning the 10m-release height it can be seen that the effect of increasing both momentum and buoyancy results in a reduced discrepancy between the statistical and sequential datasets.

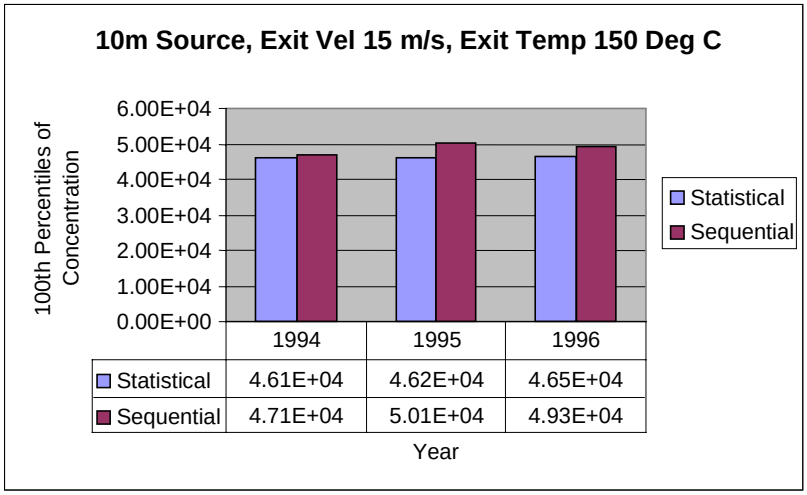

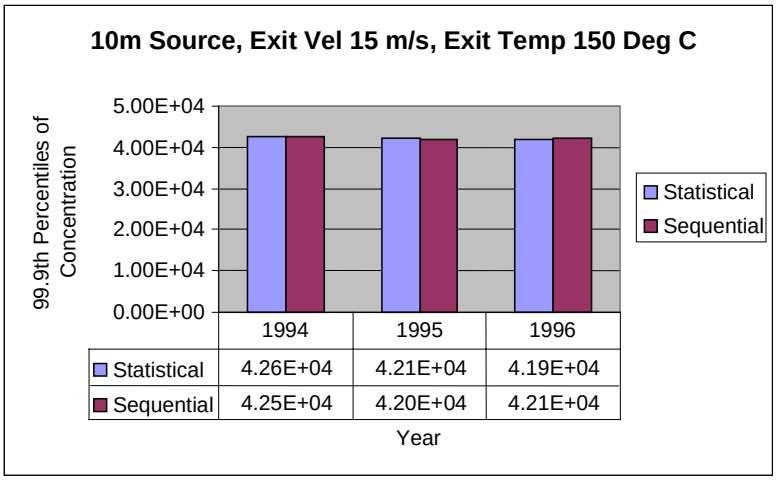

FIGURE B5 Comparison of peak 100th and 99.9th percentiles of concentration for case k

B4.4 Summary and discussion

In order to investigate the effect of release characteristics on the peak 100th and 99.9th percentile concentrations using sequential and statistical met data, the source exit temperature and velocity were varied for a range of release heights. Discrepancies were found for the spatial peak values of the 100th and 99.9th percentile between the statistical and sequential analyses. These discrepancies were at their most marked for cases of high exit momentum and low buoyancy, i.e. for exit velocities of 9m/s and temperatures of 15°C. For one run where the release was given increased buoyancy and momentum, the difference between the sequential and statistical cases was minimal.

The contoured results in Appendix D and E show a pattern consistent with that expected. As the release height decreases so too does the distance between the source and the location of the spatial peak value. Due to the nature of the statistical calculations the contours tend to be more circularly symmetric compared to the sequential contour results. This is especially true for the 100th

percentile cases and is expected because, provided the worst bin (more precisely the worst combination of U, $F\theta_0$ and H bins) occurs at least once for each wind direction, then the 100th percentiles should occur independent of direction.

B5 Study 3

The discrepancies identified in the last section showed some to be as high as 75%, and so potentially very important. To investigate them further, the input met data was analysed for those occasions where the results gave significant differences. One of the suite of output files obtained from each ADMS 3 run is the '.max' file. This contains the spatial maximum value of the ground level mean concentration field and of each of the percentiles requested. It also records the position of the maximum value along with the met calculation line that gave rise to the maximum. Each met calculation line can be viewed in the '.mop' file. This contains the met input parameters and calculated met output values for each line of met data present in the met file. The values of the met parameters which make up the set of binned elements were recorded, i.e. wind speed (U), wind direction (ϕ), surface heat flux ($F_{\theta 0}$) and boundary layer height (H), see section 2.2.3 for units. Tables 7 – 11 below show these input met parameters that correspond to the maximum concentration obtained for each model run. The cases shown below are runs taken from Study 2 that resulted in significant discrepancies between statistical and sequential datasets. They correspond to the cases A,C,E,G and I of the runs shown in section 4.2 above. The cases shown in section 4.1 did not result in very large discrepancies and are not included here.

TABLE B7 Binned Met Parameters for Case A

Case A	Line No.	Percentile	U	ϕ	$F_{\theta 0}$	H
94 Statistical	124	100	1.3	210	116.6	643
	114	99.9	1.3	90	70.2	986
95 Statistical	170	100	1.2	270	116.7	642
	174	99.9	1.2	150	116.7	981
96 Statistical	176	100	1.2	0	118	640
	154	99.9	1.2	240	69.9	640
94 Sequential	4811	100	1.0	90	76.96	572.27
	4786	99.9	1.5	120	69.96	1002.93
95 Sequential	5610	100	1.0	190	6.4	897.46
	5296	99.9	1.0	110	66.73	1042.97
96 Sequential	4819	100	1.0	180	1.32	915.04
	4788	99.9	1.0	240	101.01	763.67

TABLE B8 Binned Met Parameters for Case C

Case C	Line No.	Percentile	U	ϕ	$F_{\theta 0}$	H
94 Statistical	125	100	1.3	240	116.6	643
	103	99.9	1.3	150	70.2	393
95 Statistical	169	100	1.2	150	116.7	642
	159	99.9	1.2	120	69.7	981
96 Statistical	175	100	1.2	30	118	390
	153	99.9	1.2	210	69.9	640
94 Sequential	4834	100	1.0	190	5.36	202.15
	6877	99.9	1.5	140	78.61	359.37
95 Sequential	5059	100	1.0	130	0.37	1022.46
	4907	99.9	1.0	110	94.19	636.72
96 Sequential	4819	100	1.0	180	1.32	915.04
	6207	99.9	1.0	250	58.3	834.96

TABLE B9 Binned Met Parameters for Case E

Case E	Line No.	Percentile	U	ϕ	$F_{\theta 0}$	H
94 Statistical	122	100	1.3	90	116.6	643
	122	99.9	1.3	90	116.6	643
95 Statistical	170	100	1.2	270	116.7	642
	141	99.9	1.2	30	69.7	642
96 Statistical	175	100	1.2	30	118	390
	154	99.9	1.2	240	69.9	640
94 Sequential	4834	100	1.0	190	5.36	202.15
	5436	99.9	1.5	140	107.04	770.51
95 Sequential	5059	100	1.0	130	0.37	1022.46
	4913	99.9	1.0	160	47.48	1101.56
96 Sequential	4819	100	1.0	180	1.32	915.04
	5053	99.9	1.0	240	98.54	766.6

TABLE B10 Binned Met Parameters for Case G

Case G	Line No.	Percentile	U	ϕ	$F_{\theta 0}$	H
94 Statistical	95	100	1.3	30	70.2	251
	77	99.9	1.3	150	22.5	643
95 Statistical	128	100	1.2	120	69.7	250
	143	99.9	1.2	90	69.7	642
96 Statistical	175	100	1.2	30	118	390
	176	99.9	1.2	0	118	640
94 Sequential	4834	100	1.0	190	5.36	202.15
	4909	99.9	2.1	110	71.16	584.96
95 Sequential	5059	100	1.0	130	0.37	1022.46
	4912	99.9	1.0	130	60.47	1061.52
96 Sequential	4819	100	1.0	180	1.32	915.04
	6446	99.9	1.0	180	70.22	539.06

TABLE B11 Binned Met Parameters for Case I

Case I	Line No.	Percentile	U	ϕ	$F_{\theta 0}$	H
94 Statistical	109	100	1.3	60	70.2	250
	67	99.9	1.3	120	28.8	154
95 Statistical	127	100	1.2	90	69.7	250
	144	99.9	1.2	120	69.7	642
96 Statistical	175	100	1.2	30	118	390
	146	99.9	1.2	0	69.9	640
94 Sequential	4834	100	1.0	190	5.36	202.15
	5049	99.9	1.5	120	67.68	377.93
95 Sequential	5059	100	1.0	130	0.37	1022.46
	5054	99.9	1.0	150	76.67	857.42
96 Sequential	4819	100	1.0	180	1.32	915.04
	4832	99.9	1.0	230	35.18	208.98

It can be seen that in all the cases where significant discrepancies occur, the sequential data corresponding to the worst case has a very low surface heat flux i.e. 0.37, 1.32 or 6.4 W.m-2 (in contrast the worst case statistical values are 69.7, 118 or 116.7 W.m-2 respectively). It is slightly surprising that in these cases the heat flux for the worst sequential case lies outside the heat flux bin for the worst statistical case. However, this is clearly not impossible if the concentration varies non-monotonically with heat flux. In some sequential cases the very low surface heat flux is associated with a deep boundary layer. It is not unusual for this to occur, especially in the late afternoon. Many of the instances above occur at 6.00pm when the surface heat flux is low. It is only after the Sun has dipped below the horizon and the surface heat flux changes sign to a negative value that we expect the daytime boundary layer to break down and be replaced by a new developing stable boundary layer that will evolve close to the ground (a more detailed account of the effect of surface heat flux on boundary layer height can be found in Carson, 1973). The statistical data is not resolved sufficiently to capture these low values with the relevant heat flux line spanning the range 0 to 50 W.m-2 (see section 2.2.3).

Calm or variable wind speed events would be expected to change the observed results above, but the detailed investigation of calms is outside the scope of this report and would constitute a report on its own. The wind roses for each year showed only a small percentage of such events.

B6 Study 4

It was thought therefore that the results might be improved by re-binning the statistical data with an extra heat flux category so as to represent these lower heat flux values more accurately. It was noted that although this re-binning would represent the heat flux more accurately, it did not necessarily follow that it would also lead to improved agreement between statistical and sequential results. A recalculation of the binned data was carried out with the 0 to 50 $W.m^{-2}$ heat flux category divided into the categories 0 to 10 $W.m^{-2}$ and 10 to 50 $W.m^{-2}$. This gave 8 classes with the following upper limits;

$F_{\theta o}$. -30 -10 0 10 50 100 150 32767 $W.m^{-2}$

The runs were made for cases A and C to investigate whether this would result in a significant change. The results for these runs can be seen in Figures B7a and B7b below.

B6.1 Results for Case A*& C* - (A & C Re-binned)

CASE	Release height (m)	Release velocity (m/s)	Release Temperature (°C)
A*	100	9	15
C*	75	9	15

Contour plots of the 100th and 99.9th percentiles for this scenario can be found in the Appendix F - Figs F1a to F1f and F2a to F2f. For convenience the re-binned statistical results are shown with the equivalent sequential results. Visually there are only very small differences between the statistical re-binned contours and the original statistical runs. In general the overall shape is the same but the original results show a more uniform radial pattern for the 100th percentiles. A comparison of the actual peak values between the re-binned and original cases can be seen in the following graphs:

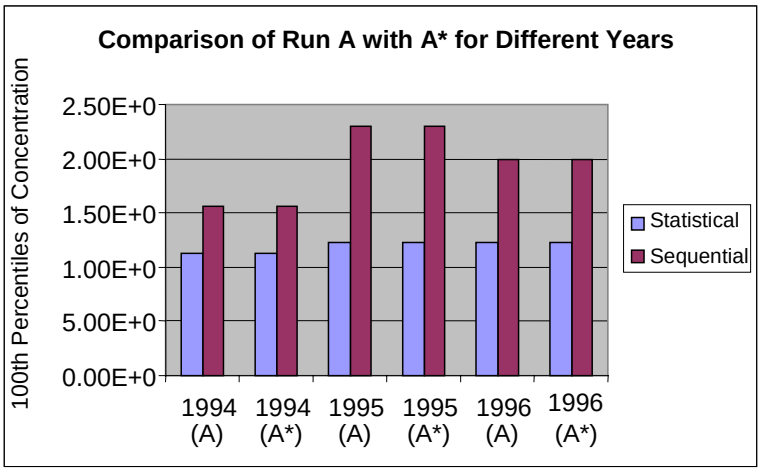

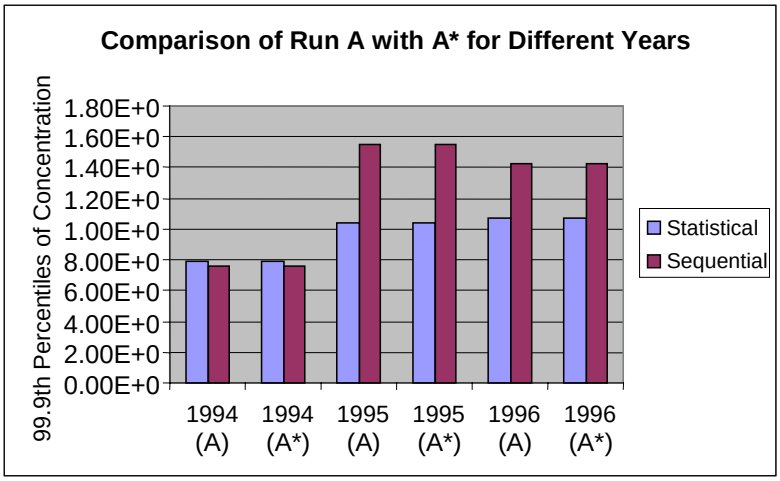

FIGURE B7a Comparison of Case A* with the original results of Case A for the 100th and 99.9th percentiles of concentration

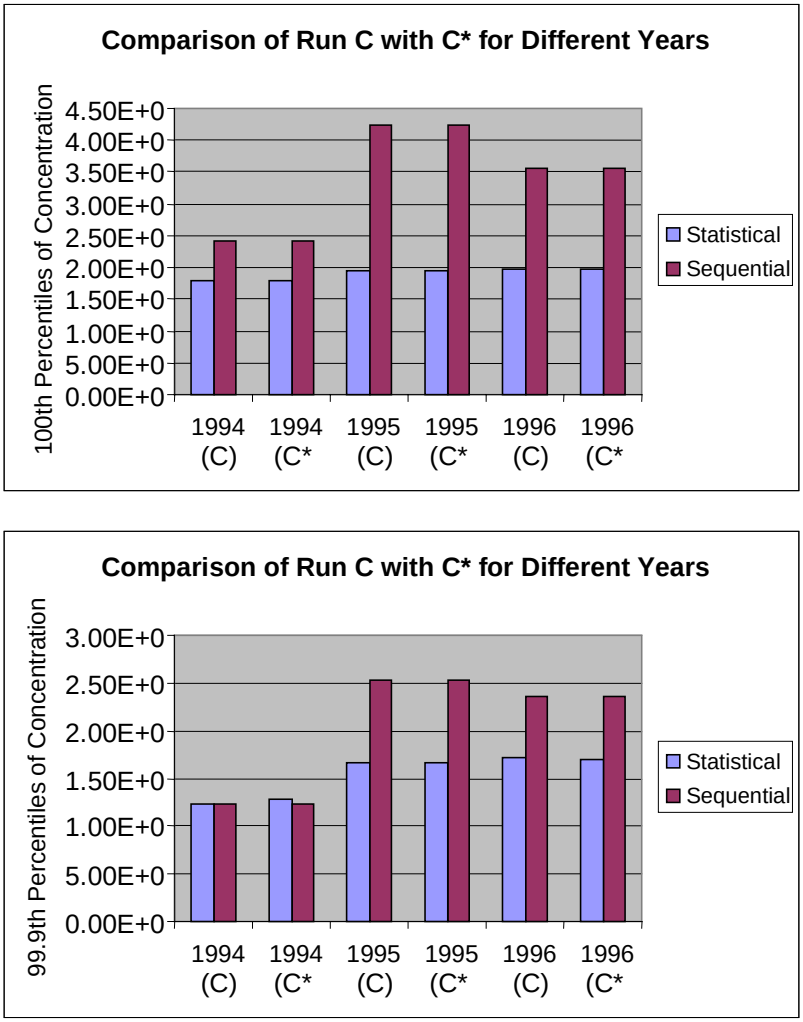

FIGURE B7b Comparison of Case C* with the original results of Case C for the 100th and 99.9th percentiles of concentration

It can be seen that the alteration of the number of binned classes has not improved the agreement between the statistical and sequential datasets. This was true for all the re-binned cases suggesting that the surface heat flux was not the main determining factor for the discrepancy between the two datasets. Indeed, the binning scheme is not sensitive to the changes to heat flux categories.

B7 Study 5

The surprising lack of improvement from re-binning the data led us to consider other possible causes of the discrepancies. The actual weather parameters that are input to ADMS differ between statistical and sequential data, as shown in the table below.

TABLE B12 Input Met Parameters for statistical and sequential datatsets

	T_{year}	T_{day}	T_{hour}	T_0	U	ϕ	P	CL	RHu	H	$F\theta_0$
Stat					√	√	√			√	√
Seq	√	√	√	√	√	√	√	√	√		

For the current computations relative humidity (RHu) and precipitation rate (P) are irrelevant, the year (T_{year}) is not actually used by ADMS, the Julian day number (T_{day}), the hour (T_{hour}) and cloud amount (CL) are used by ADMS only for calculating the boundary layer height (H) and surface heat flux ($F\theta_0$), and the surface temperature (T_0) is used both for calculating H and $F\theta_0$ and for the dispersion calculation itself. Once ADMS has completed its met pre-processing and calculated H and $F\theta_0$, we see that the variables available are essentially the same for the two cases except for the absence of T_0 for the statistical case – here ADMS will assume a default of 15ºC.

In order to investigate the discrepancies further, we selected case A (exit velocity 9m/s, exit temperature 15°C for 100m release height). We then took the met lines which gave rise to the peak 100th percentile for the sequential case (see table 7) and asked which combination of statistical bins this met line would fall in. We then took the line in the statistical dataset corresponding to these bins (i.e. for U, etc) and altered it so that the values of U, etc were equal to those in the sequential dataset. In other words, we altered the statistical dataset so as to remove any error due to the size of the bins in representing this hour of met. Somewhat suprisingly, the results were little changed. As a result we concluded that the difference is not due to the size of the bins, but can only be due to either the absence of temperature in the statistical input dataset or a processing problem within ADMS.

In order to investigate the discrepancies further, it was planned to alter the sequential dataset until it resembled the input from a statistical dataset. Case A (exit velocity 9m/s, exit temperature 15C for 100m release height) was selected and the sequential data was edited to input only the day which was responsible for the peak 100th percentile value. A series of runs were then performed making various alterations for each run. Five model runs were made with the following alterations to the data;

Run 1 - sequential run of 24 hours responsible for the peak 100th percentile was made;

Run 2 - met file edited so the hour responsible for peak value was only input to model run;

Run 3 - met file further altered to include boundary layer depth (H) and surface heat flux ($F\theta_0$) as derived from processing the sequential dataset (i.e. derived from 'mop' output file for run 1);

Run 4 - the met file was edited to remove T_{year} , T_{day} , T_{hour} , RHu , and CL, and finally

Run 5 - the value for T_0 was removed

A summary of the results for cases A and G are shown below in tables B13 and B14.

TABLE B13 Results for H, $F\theta_0$, T_0 and spatial peak 100th percentile for Study 5 on Case A

Run	Peak 100th %ile	H	$F\theta_0$	T_0
1	$2.30x10^4$	897.46	6.4	29.7
2	$2.19x10^4$	1198.24	6.4	29.7
3	$2.30x10^4$	897.46	6.4	29.7
4	$2.30x10^4$	897.46	6.4	29.7
5	$9.06x10^3$	897.46	6.4	15

TABLE B14 Results for H, $F\theta_0$, T_0 and spatial peak 100th percentile for Study 5 on Case G

Run	Peak 100th %ile	H	$F\theta_0$	T_0
1	$2.56x10^5$	1022.46	0.37	29.1
2	$2.52x10^5$	1350.59	0.37	29.1
3	$2.56x10^5$	1022.46	0.37	29.1
4	$2.56x10^5$	1022.46	0.37	29.1
5	$2.48x10^4$	1022.46	0.37	15

B7.1 Study 5 – comments

- **Run 1**; The 24 hours that produced the original maximum 100th percentile value was run. As expected the first run replicated the peak values of $2.30x10^4$ $\mu g.m^{-3}$ and $2.56x10^5$ $\mu g.m^{-3}$ for Case A and G respectively.
- **Run 2**; It is interesting to note that the second run which used only the one-hour of data responsible for the peak value resulted in a slightly reduced peak value. This was expected as the value for the boundary layer depth will depend on the history of the meteorology (in Run 2 this is not provided as input and ADMS has to make some assumptions). It can be seen that the value calculated for this run is deeper than in Run 1. This will therefore result in a greater mixing volume and thus a slightly smaller peak concentration. Note also that for both runs the values for $F\theta_0$ and T_0 are the same (as expected).
- **Run 3**; In Run 3 where H and $F\theta_0$ are included as part of the input data stream the peak concentration estimated by the model is again $2.30x10^4$ $\mu g.m^{-3}$ for Case A and $2.56x10^5$ $\mu g.m^{-3}$ for Case G. This is as expected because the only influence of the meteorological history is on H. By specifying H in the input file, results are the same whether the whole day or just the individual hour are included.
- **Run 4**; Run 4 removed the values for the year, day, hour, cloud cover and humidity. This again resulted in the same peak concentration for both cases. Again this is to be expected as the removed variables either play no role or are used only for estimating $F\theta_0$ and H when the latter are absent.

- **Run 5**; Run 5 finally removed the near surface temperature T_0 from the input stream. This last removal is significant as it effectively changes the sequential input data stream to include exactly the same parameters as a statistical dataset i.e. U, ϕ, p, H and $F\theta_0$. The results of this run showed a reduced peak concentration of 9.06×10^3 $\mu g.m^{-3}$ for Case A and 2.48×10^4 $\mu g.m^{-3}$ for Case G. Both H and $F\theta_0$ are the same as other runs but the value for T_0 has been reduced to 15°C – this is the ADMS default used when T_0 is not input (and happens to be the same as the plume exit temperature).

The above shows that the ADMS calculations of percentiles are sensitive to the value used for surface temperature. The exit release temperature of the runs that exhibited the most discrepancies was 15°C. In the two events analysed above, the ambient temperatures were 29.7°C and 29.1°C for the 100m and 30m-release height respectively. It is possible that under these conditions with a sequential dataset, ADMS treats the emerging effluent as a denser than air release (emerging gas temperature 15°C with the ambient temperature higher by about 14°C or so). The sequential data will of course provide ADMS with the specified ambient temperature (~ 29°C) and ADMS will know the release temperature (15°C), so it is possible that ADMS will treat the release as cold and dense relative to the ambient conditions. In the statistical case however, ADMS does not know the ambient temperature and uses a default of 15°C, so in this case the emerging gas is at ambient temperature and is treated as a neutrally buoyant release. In one instance therefore ADMS treats the gas as a neutrally buoyant release and in the other as denser than air. This is confirmed when a plot of the plume centreline position is made for the two cases. Taking first Case A (exit velocity 9m/s, exit temperature 15C for a 100m release height), Figure D8a below shows the plume centreline position when the surface temperature is included (i.e. as with a standard sequential data input).

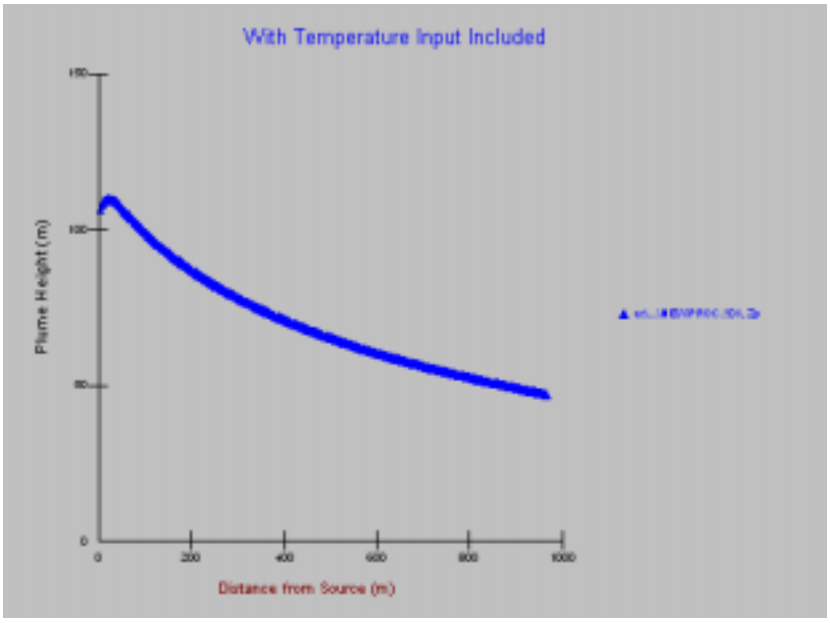

FIGURE B8a Variation of Case A plume centreline height with distance from source with temperature input included

It can be seen straight away that the plume in this case drops quite rapidly towards the ground resulting in the higher concentrations recorded in runs 1 to 4 in table 13 above. The gas is emerging at a temperature cooler than its surroundings.

When the surface temperature is excluded (i.e. similar to statistical data input) the results are illustrated in Figure 8b below:

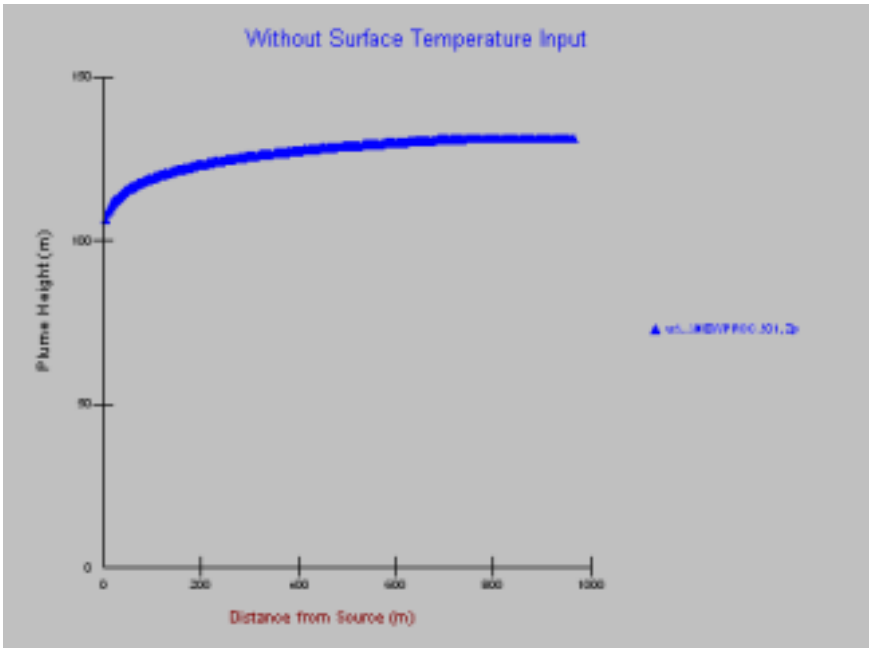

FIGURE B8b Variation of Case A plume centreline height with distance from source without temperature input

In this case the plume begins to rise immediately on release – resulting in the reduced value obtained in run 5 in Table 13. In this case the gas is emerging at similar temperature to ambient and is not therefore treated as denser than air.

Turning now to the lower release case, Case G (30m release height with exit velocity 9m/s and exit temperature 15°C), Figure 9a below shows the centreline plume height for the occasion when the surface temperature was included (i.e. standard sequential data input).

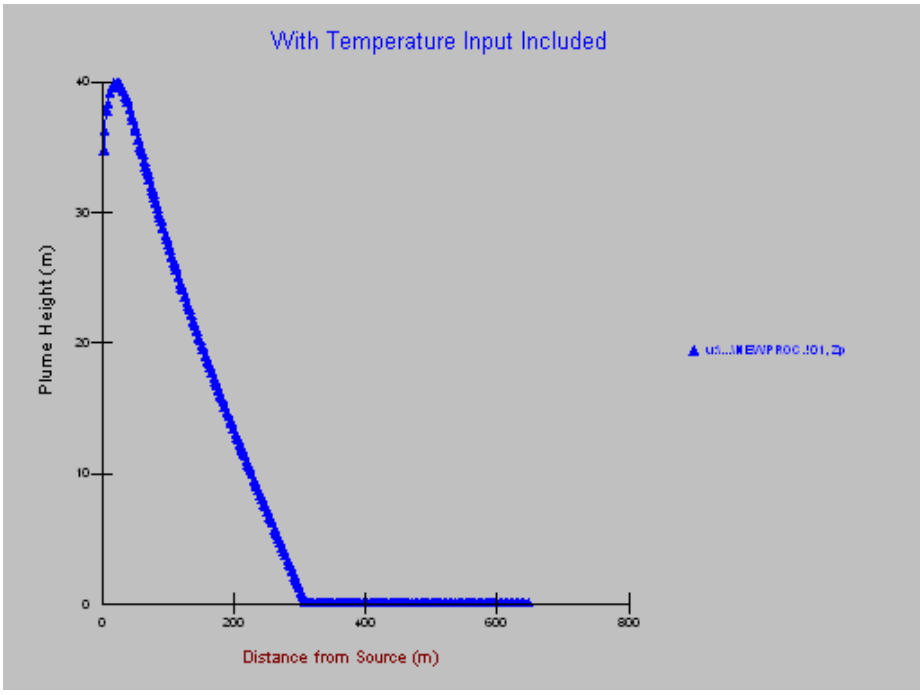

FIGURE B9a Variation of Case G plume centreline height with distance from source with temperature input included

As expected the plume drops quite rapidly to the surface after an initial small rise. The plume grounds within 300m of the source. This then corresponds to the higher concentrations recorded in runs 1-4 of Table 14 above.

Figure 9b below illustrates the centreline plume position for the occasion when the temperature data is not included and a default of 15°C used by the model (as in a statistical data input)

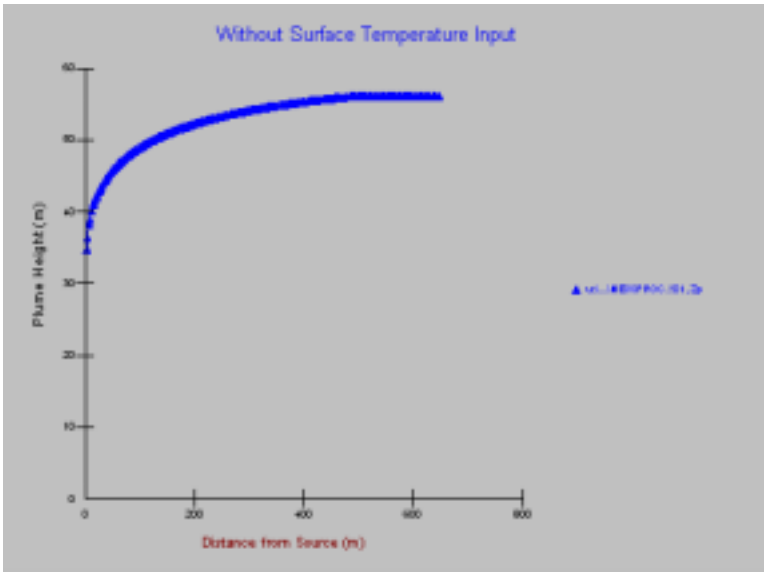

FIGURE B9b Variation of Case G plume centreline height with distance from source without temperature input

As seen with Case A, the plume can be seen to rise immediately on release which would explain the reduced concentration recorded in Run 5 of Table14. In this case the emerging gas is treated as a neutrally buoyant release.

B8 Discussion

The analyses performed and recorded in this study has shown that under certain conditions the expected spatial peak percentiles of concentration may be expected to differ depending on whether statistical or hourly sequential data was used. The difference between the results from the two types of met data appears to be more pronounced in lower release height situations. Generally speaking analyses using sequential data predicts the higher concentration of the two. Ordinarily one would assume that the sequential dataset would offer the more accurate representation of conditions as every hourly condition is presented for analysis, unlike the statistical case where some of the meteorological detail is lost to the statistical 'smoothing'. However for the cases with the biggest discrepancies the critical meteorological parameter appears to be one which is not included in the statistical binning procedure – i.e. surface temperature.

The main discrepancies occur when the effluent release temperature is lower than the ambient. Sequentially generated results suggest that the emerging gas is treated as denser than air and is quickly transported to ground level. Statistical calculations however will not have an indication of the hourly variations in ambient temperature; instead they use a default of 15°C. This means that for a release temperature of about 15°C the model will not know whether the ambient temperature is higher and will treat the release as neutrally buoyant. In reality, releases that are close to ambient temperature are more likely to vary their temperature as the ambient temperature varies rather than remaining at a fixed temperature. The sequential runs would keep the exit temperature static but allow the gas to be treated as a denser than air release when the ambient temperature rises well above that of the effluent. Perhaps in reality this gas would be at ambient and should be treated as neutrally buoyant. Under these conditions therefore there may be a case for trusting the statistical results over those obtained from the sequential analyses.

Because the biggest discrepancies which we have found are due not to the choice of category ranges but due to the inclusion or absence of ambient temperatures in the met input, there would be very little point in altering the current category ranges. The alternative would be to attempt to include the ambient temperature within the set of parameters that are statistically binned. However, the inclusion of another parameter would add another dimension to an already complicated multi-dimensional frequency table and would reduce or eliminate the current advantage in computational time which statistical data has over sequential. In any case, as discussed above, it seems likely that, except in situations where a release temperature is fixed in absolute terms rather than relative to ambient

temperatures, the results are likely to be better if ambient temperature is not included in the input.

B9 Conclusions

Comparisons between results obtained with statistical and sequential datasets in ADMS have been made. The largest differences that were found occurred for release temperatures close to ambient and were due, not to the binning process per se, but to the absence of temperature in the statistical input datasets. In such situations we believe that the statistical results may actually be the more appropriate because ADMS does not allow the release temperature to vary with ambient temperatures. In practice it seems likely that most such releases would so vary. The same effect might also explain the more moderate differences found with 40°C releases in section 4.

The study investigated potential differences between the datasets using three single years of met input data. There were some small but significant year to year variations that were evident in some of the results (i.e. generally comparing 1994 spatial peak values with 1995 and 1996). The consideration therefore of a single year alone may not be adequate for impact assessments. With limited resources and multiple years the advantage of statistical datasets over sequential in terms of computing time is then even larger. An analysis using several years of statistical data may well be better than one year of sequential.

Generally, the analyses of the 95^{th}, 97^{th} and 99^{th} percentiles of concentration along with some long-term average concentrations using ADMS Version 3.0, revealed good agreement between the statistical and sequential input datasets. The analyses performed with the earlier version of ADMS (Version 2.2) resulted in higher discrepancies between the two datasets.

We conclude that we have not been able to uncover any evidence that the current binning scheme is inadequate, except for the use of release temperatures close to ambient which do not vary with ambient temperature (probably quite unlikely in reality). For these cases there seems little alternative but to use sequential data. In addition there is a strong case for encouraging model developers to allow the option of source temperature varying with ambient temperatures. In any case, care should be taken when modelling dispersion of emissions whose temperature is close to ambient, but not affected by small ambient variations.

B10 Suggestions for future work

The biggest differences were found in cases where the choice between statistical and sequential data interacts with the plume rise scheme incorporated in ADMS.

It might prove to be a suitable project to investigate the merits of using statistical data and modelling plume rise or using sequential data and ignoring efflux velocity. This study would obviously investigate issues related to the workings of ADMS rather than strictly the met data. For this reason it was not covered in this project but might offer a useful exercise for future work.

In tables 7 to 11 the highest concentrations are associated with wind speeds mainly in the range 1 to 2 $m.s^{-1}$. The correct treatment of plumes in calm or near calm conditions has traditionally caused many problems within dispersion modelling. Investigating how the results might change for different methods of calm treatment was outside the scope of this study but could form part of a future investigation.

B11 Acknowledgements

The author would like to express his gratitude for the time and guidance offered by Dr David Thomson throughout this study.

B12 References

The United Kingdom National Air Quality Strategy Dept of the Environment March 1997 The Stationary Office Ltd

Expert Panel on Air Quality Standards – Airborne Particles 2001, Department of the Environment, Transport and the Regions, Scottish Executive, National Assembly for Wales, Department of the Environment in Northern Ireland. Published by The Stationary Office Ltd – London.

The Air Quality Strategy for England, Scotland, Wales and Northern Ireland – *Working Together for Clean Air*; Department of the Environment, Transport and the Regions, 2000.

Carson D.J., 1973. 'The development of a dry inversion-capped convectively unstable boundary layer' Quart.J.R. Met. Soc. Vol, 99, pp. 450 – 467.

Davies B.M. & Thomson D.J., 1997: 'Investigating the importance of pre-processing in estimating dispersion climatology' Int.J.Environment and Pollution, Vol. 8, Nos. 3-6

APPENDIX A

Figures A1, A2, A3 & A4 95^{th},97^{th} & 99^{th} Percentiles of concentration & long term average concentration using ADMS Version 3.0

Source	Release Height (m)	Exit Velocity (ms^{-1})	Exit Temp (^0C)
1	150	15	150
2	10	1	40
3	10	15	150

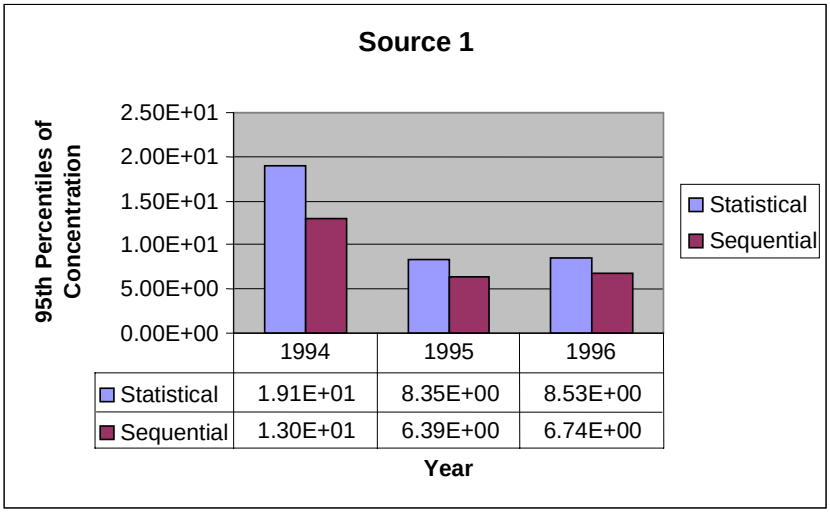

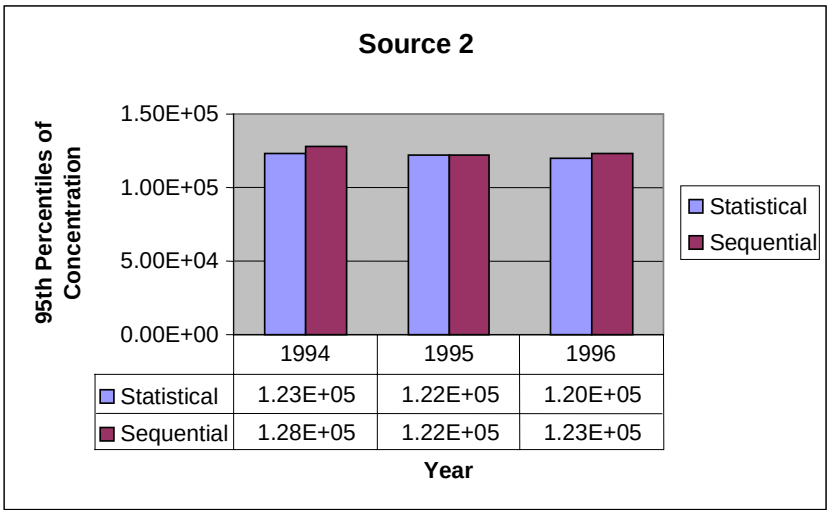

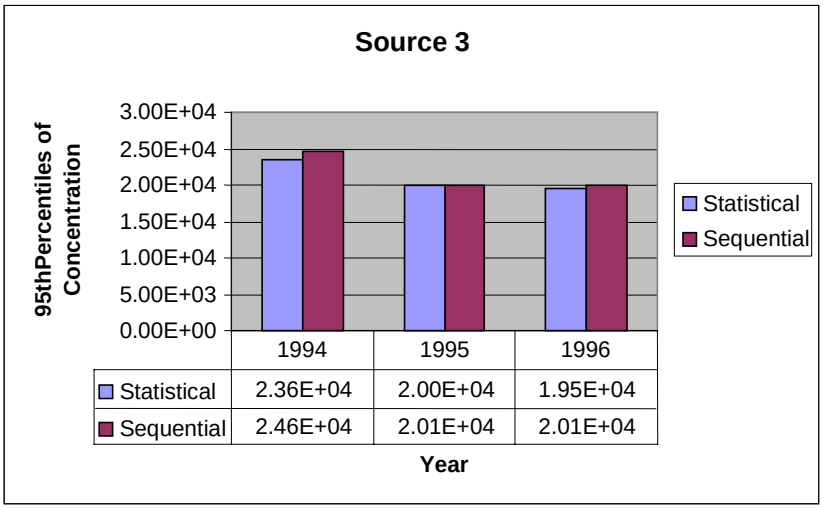

FIGURE A1 Comparison of peak 95th percentile of concentrations for statistical and sequential datasets during the study period

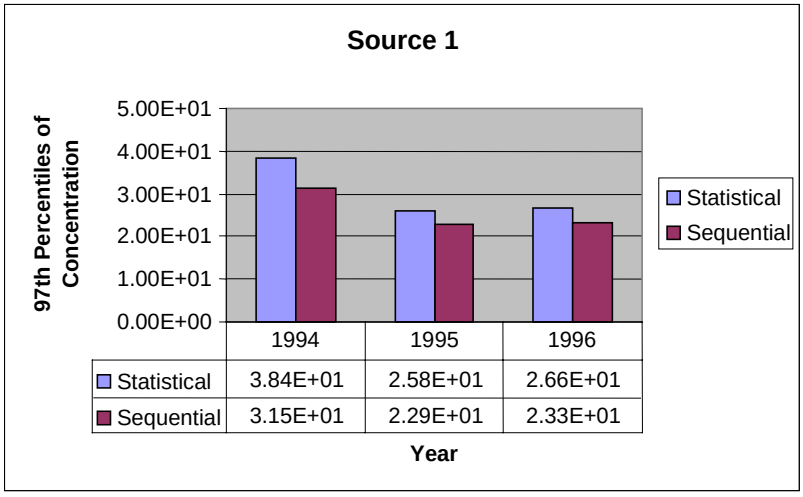

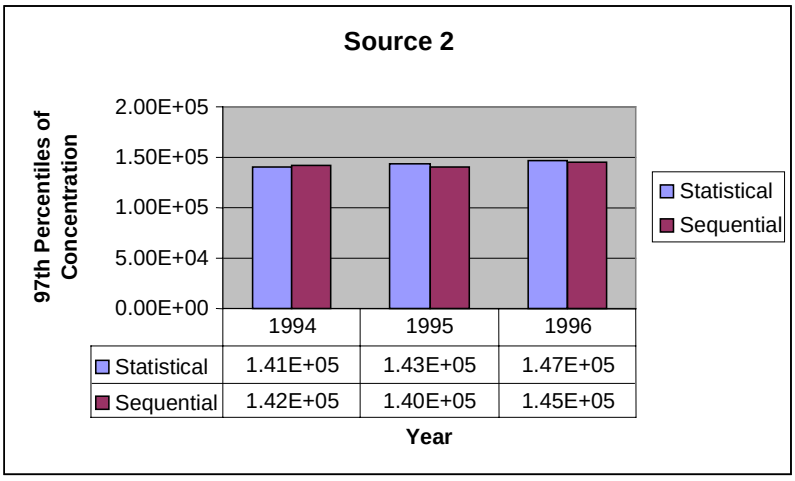

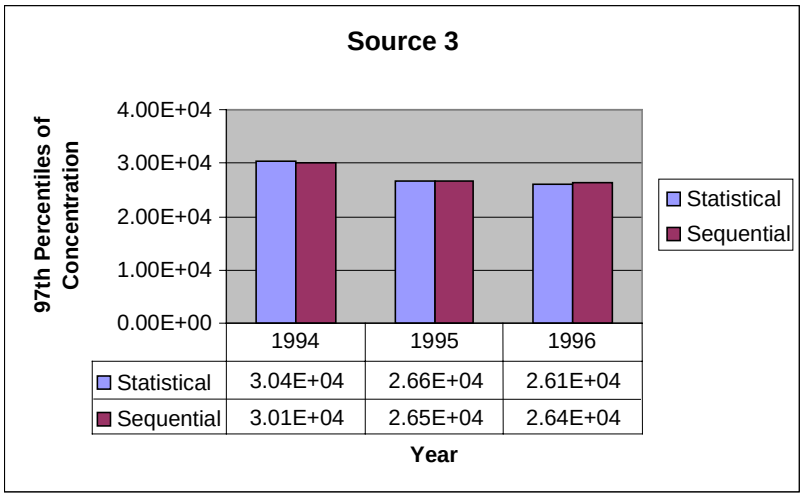

FIGURE A2 Comparison of peak 97th percentile of concentrations for statistical and sequential datasets during the study period

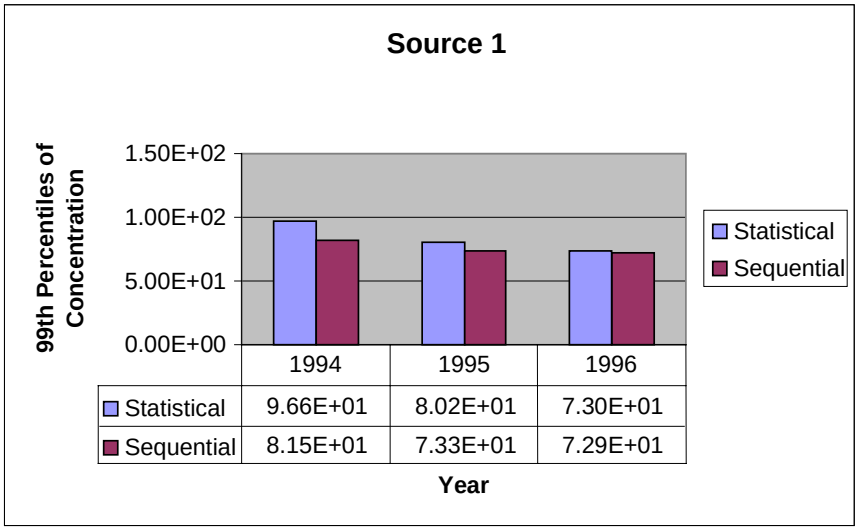

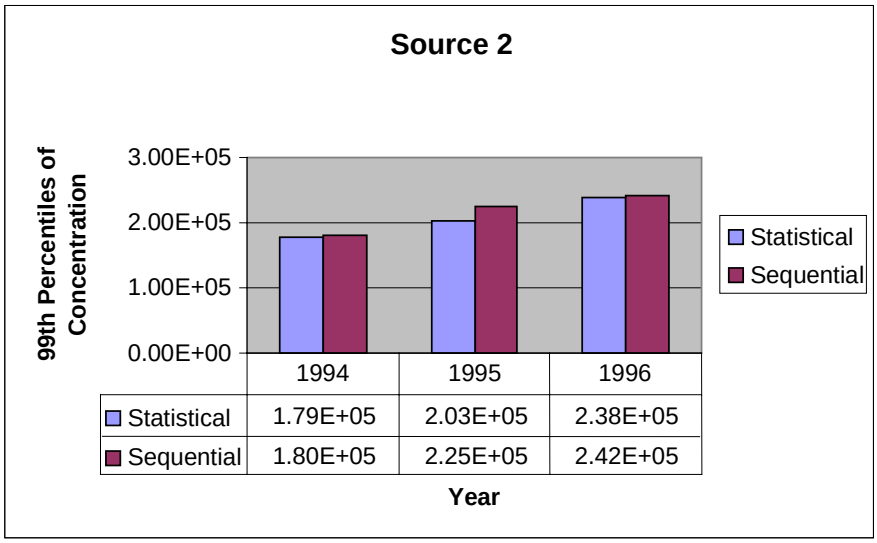

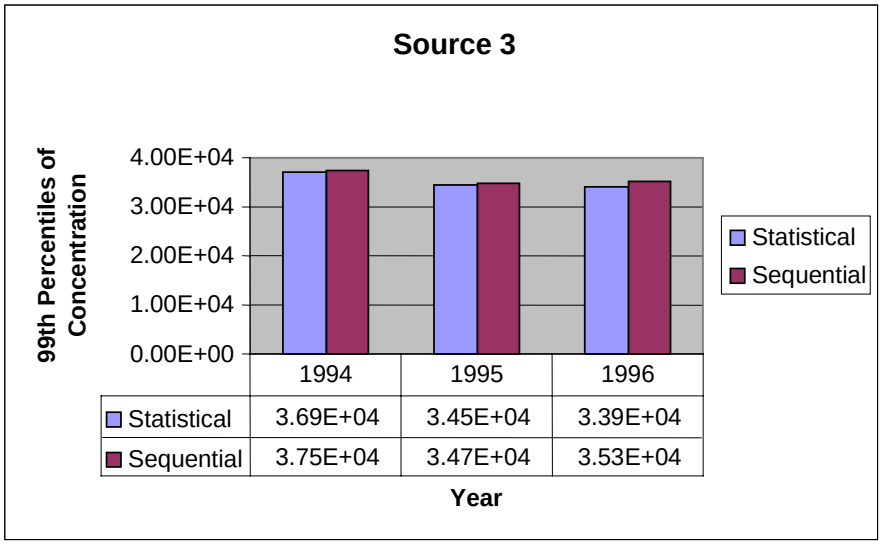

FIGURE A3 Comparison of peak 99th percentile of concentrations for statistical and sequential datasets during the study period

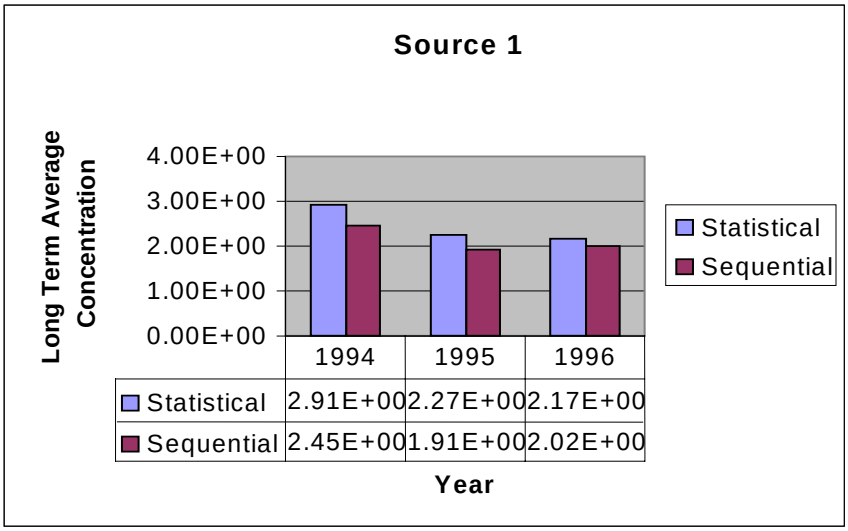

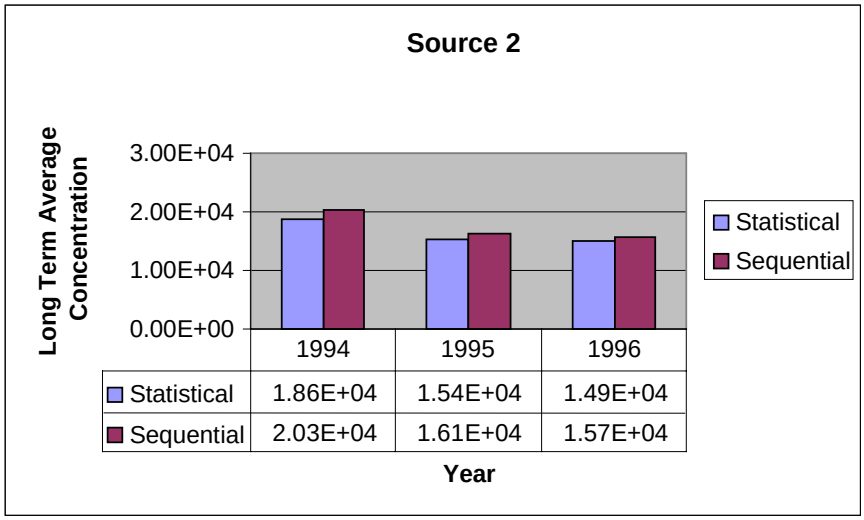

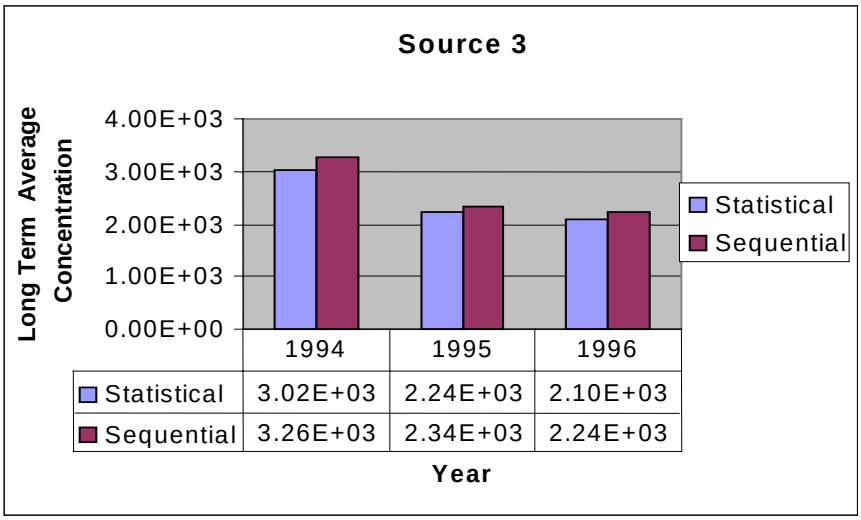

FIGURE A4 Comparison of peak long term average concentrations for statistical and sequential datasets during the study period

APPENDIX B

Figures B1, B2, B3 & B4 95th,97th & 99th percentiles of concentration & long term average concentration Using ADMS Version 2.2

Source	Release Height (m)	Exit Velocity (ms^{-1})	Exit Temp (^0C)
1	150	15	150
2	10	1	40
3	10	15	150

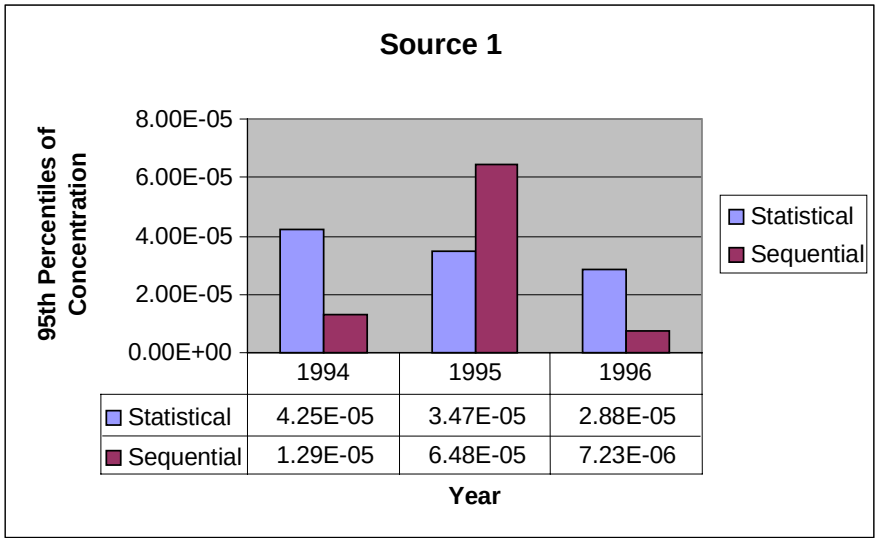

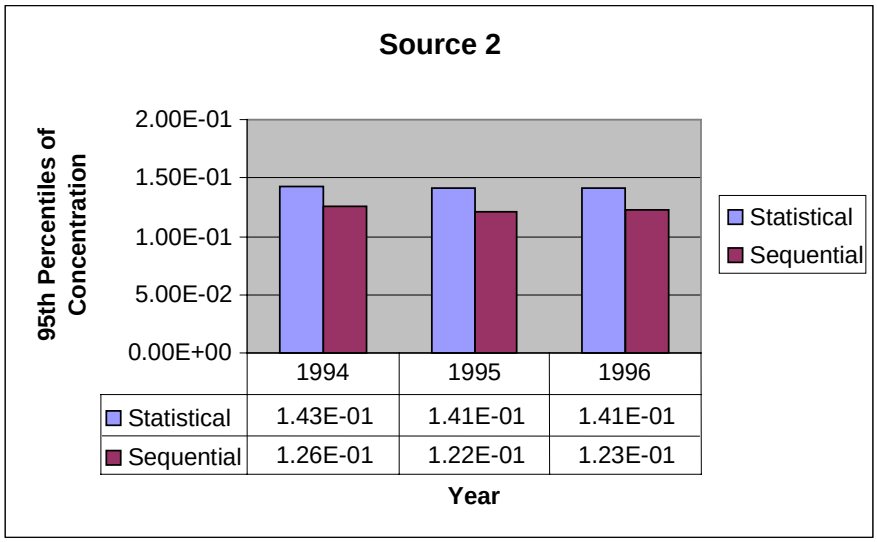

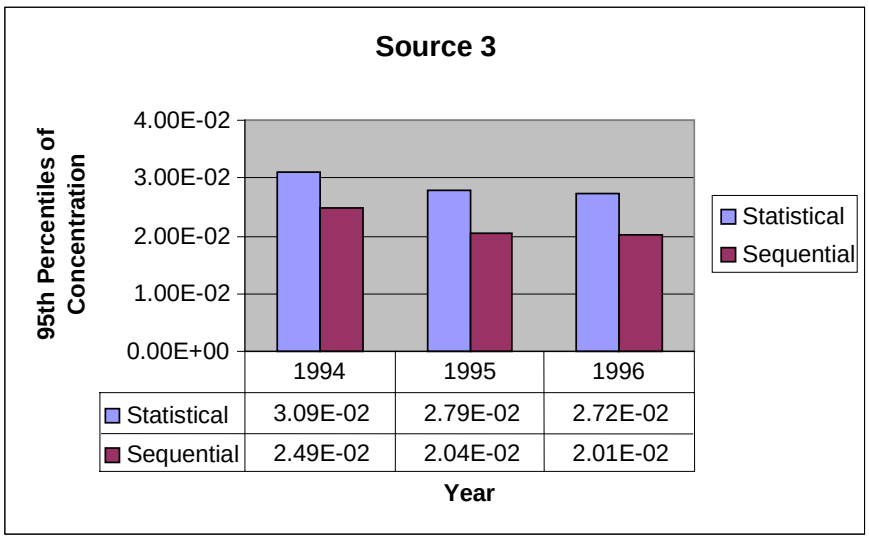

FIGURE B1 Comparison of peak 95th percentile of concentrations for statistical and sequential datasets during the study period

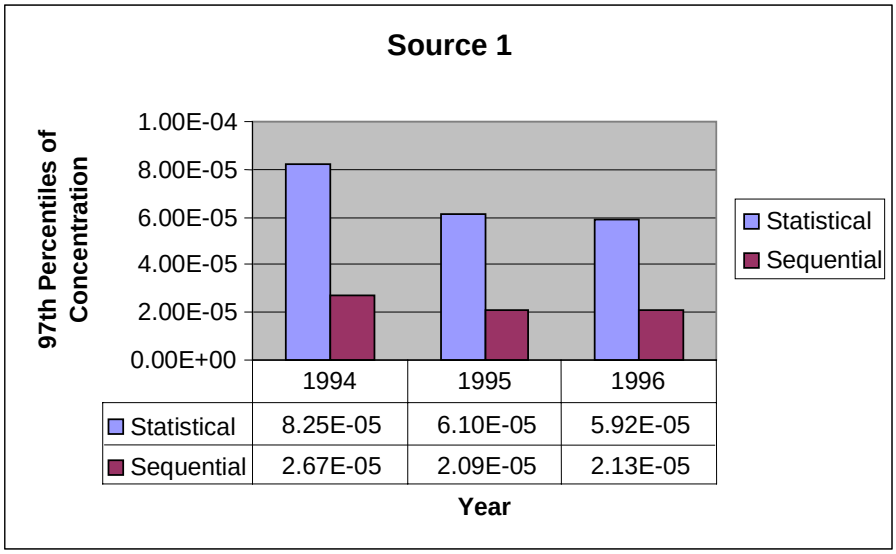

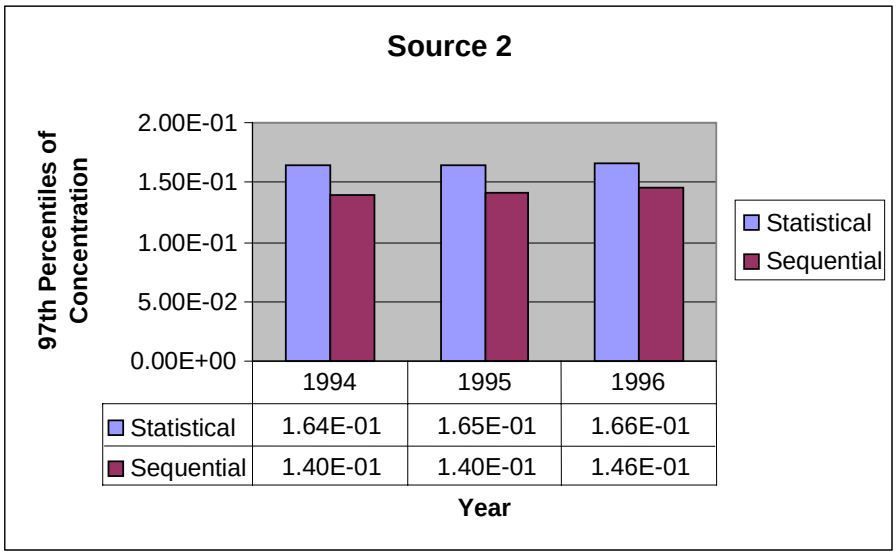

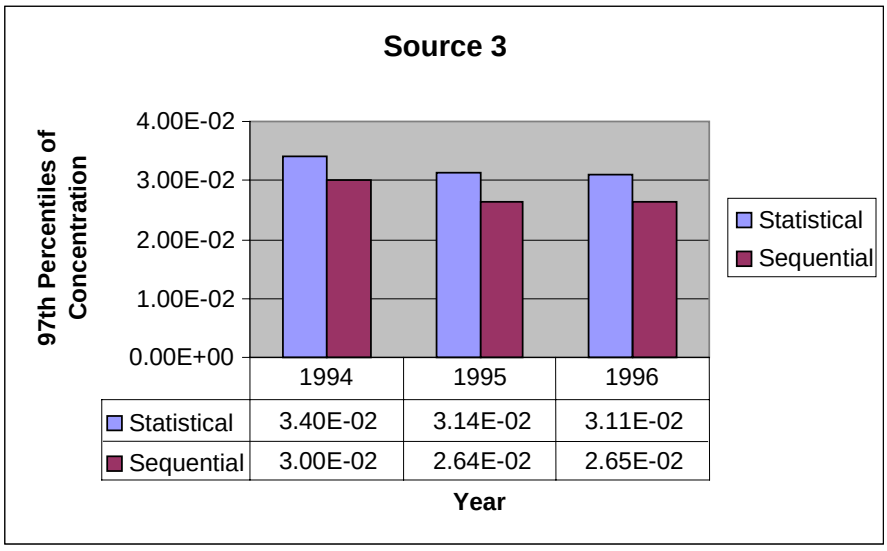

FIGURE B2 Comparison of peak 97th percentile of concentrations for statistical and sequential datasets during the study period

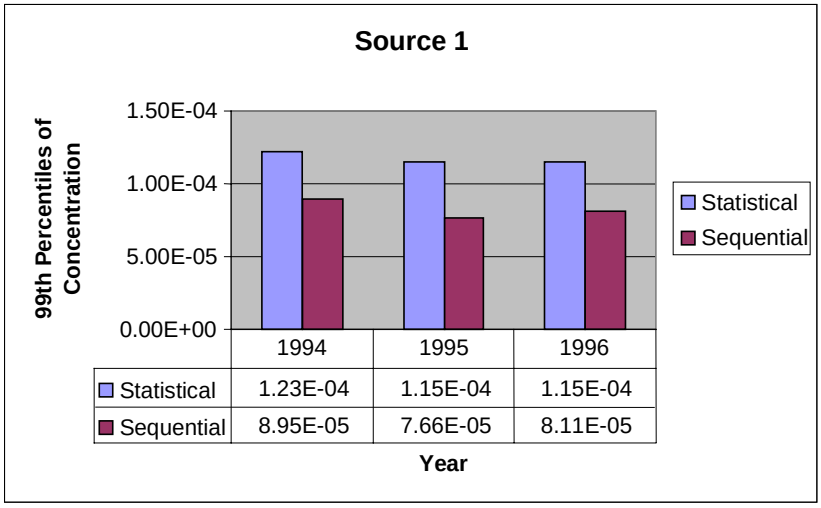

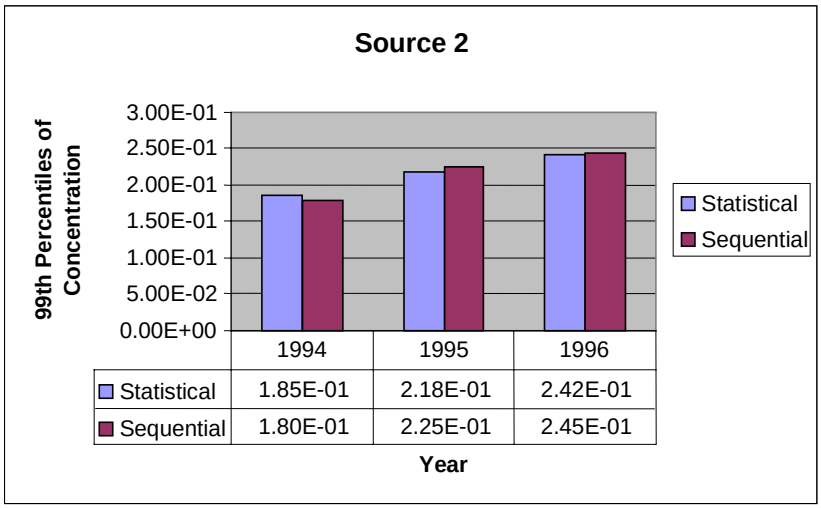

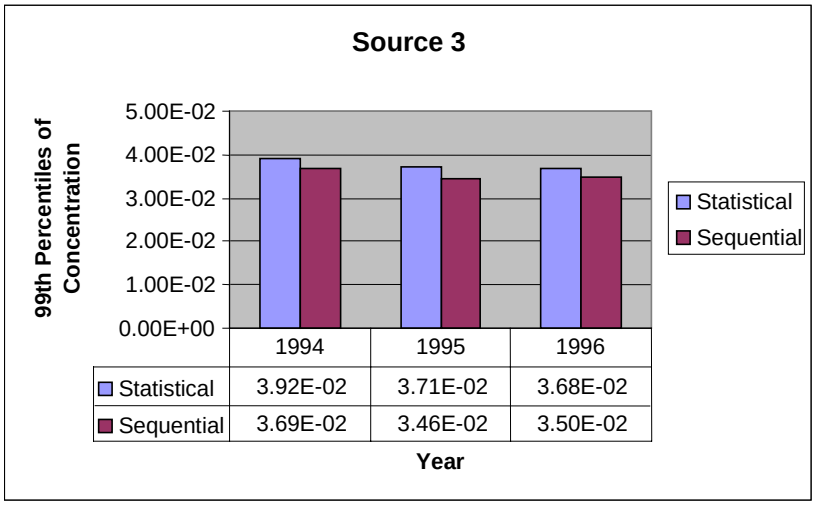

FIGURE B3 Comparison of peak 99th percentile of concentrations for statistical and sequential datasets during the study period

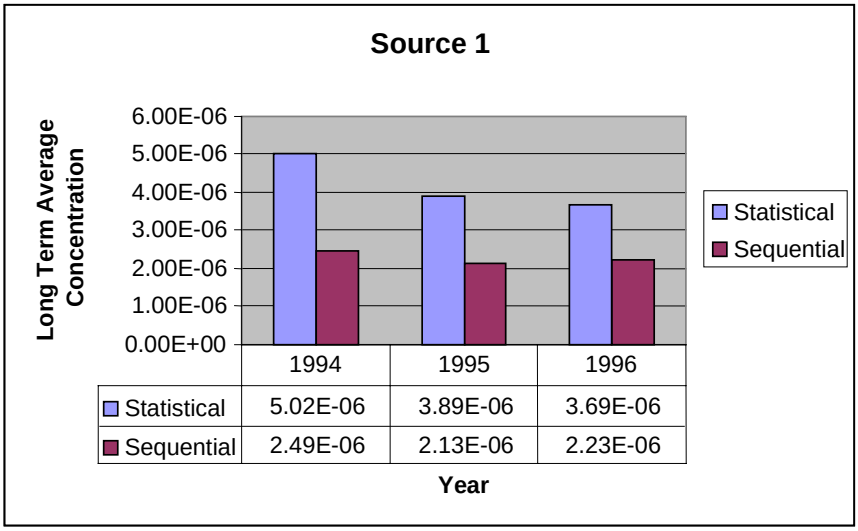

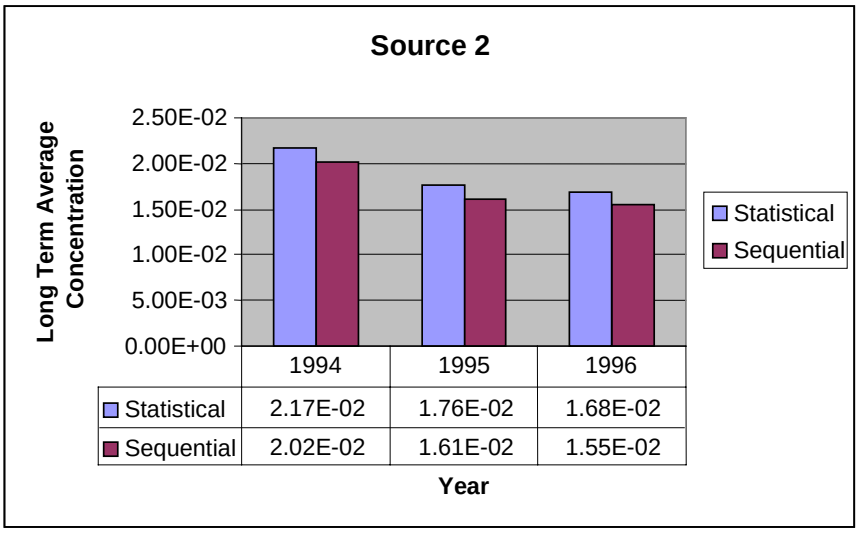

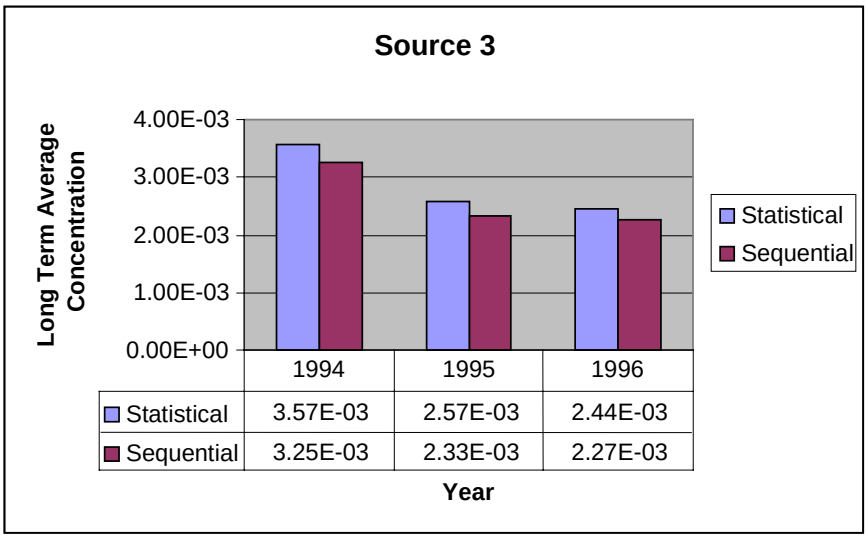

FIGURE B4 Comparison of peak long term average concentrations for statistical and sequential datasets during the study period

APPENDIX C

Figures C1, C2 & C3 95th,97th & 99th Percentiles of concentration using ADMS Version 3.0

Source	Release Height (m)	Exit Velocity (ms^{-1})	Exit Temp (^0C)
1	150	15	150
2	10	1	40
3	10	15	150

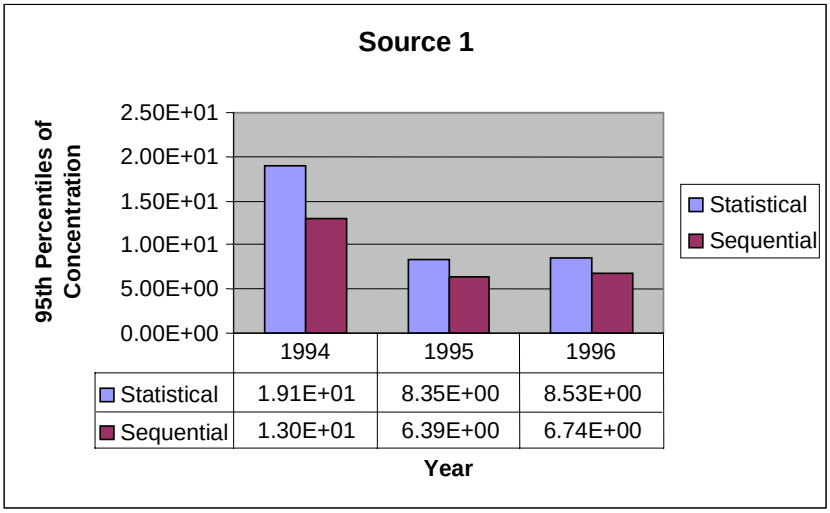

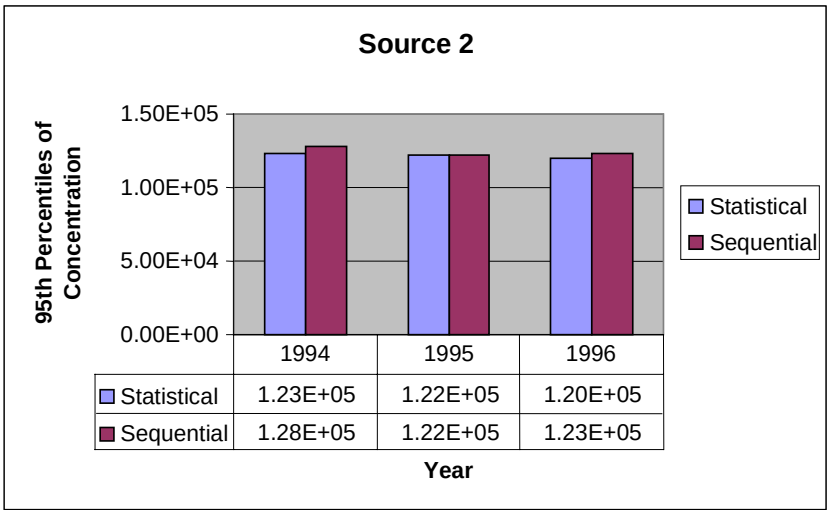

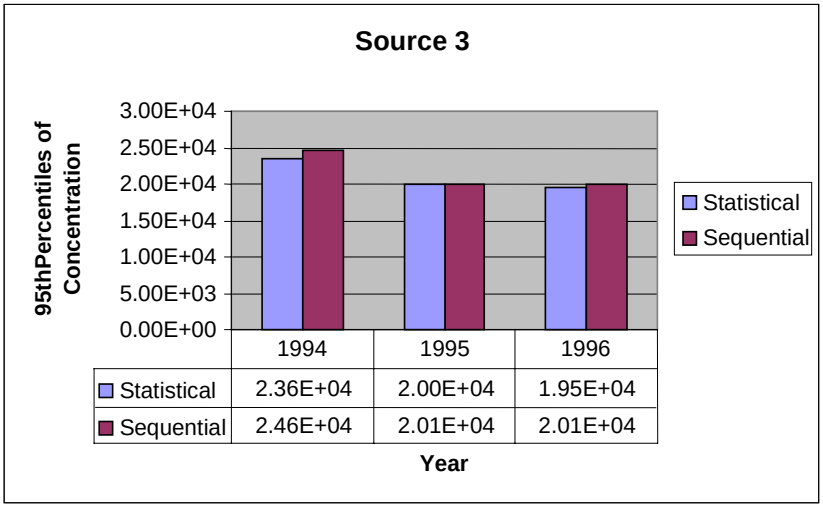

FIGURE C1 Comparison of peak 95th percentile of concentrations for statistical and sequential datasets during the study period

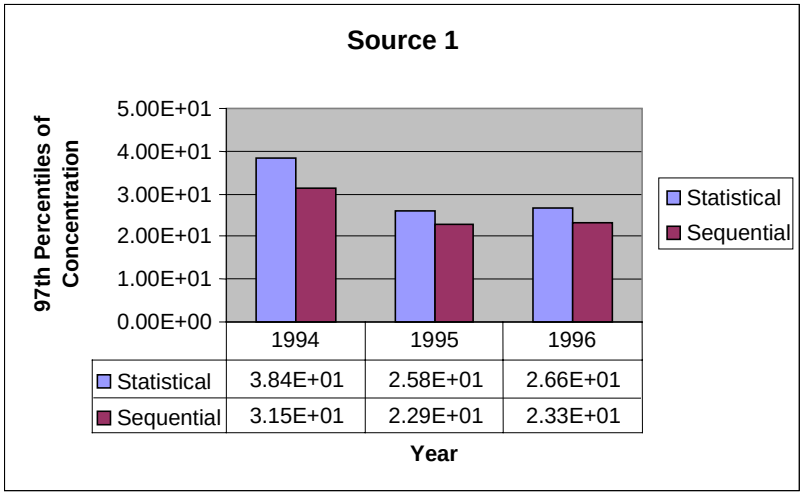

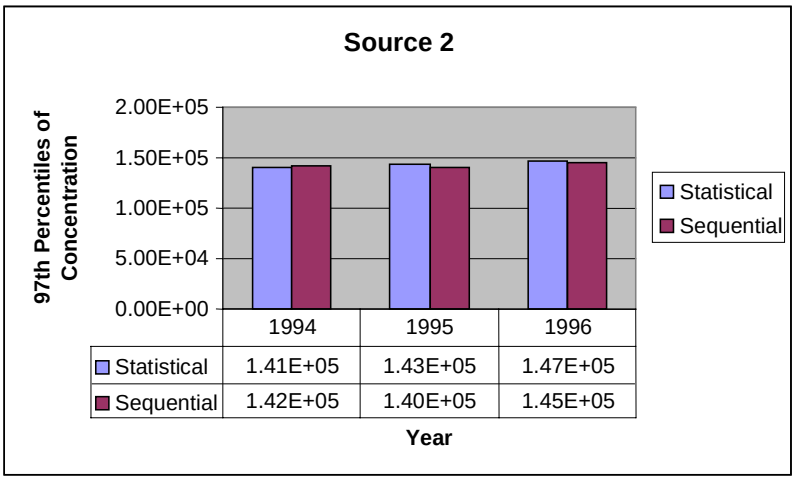

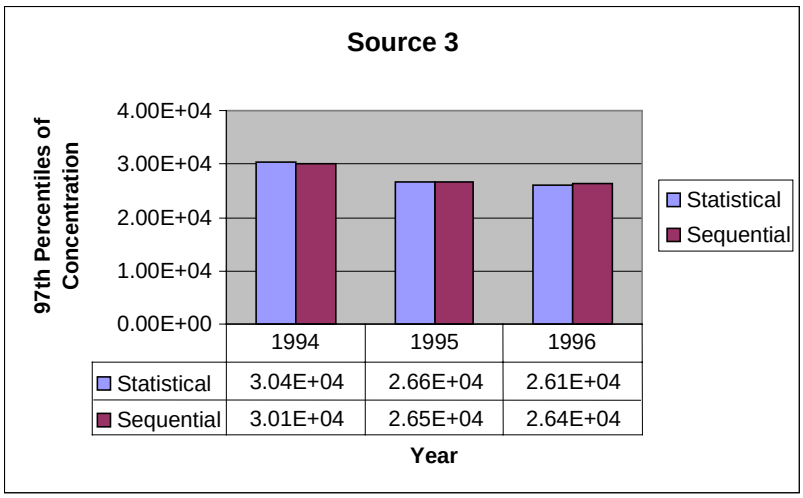

FIGURE C2 Comparison of peak 97th percentile of concentrations for statistical and sequential datasets during the study period

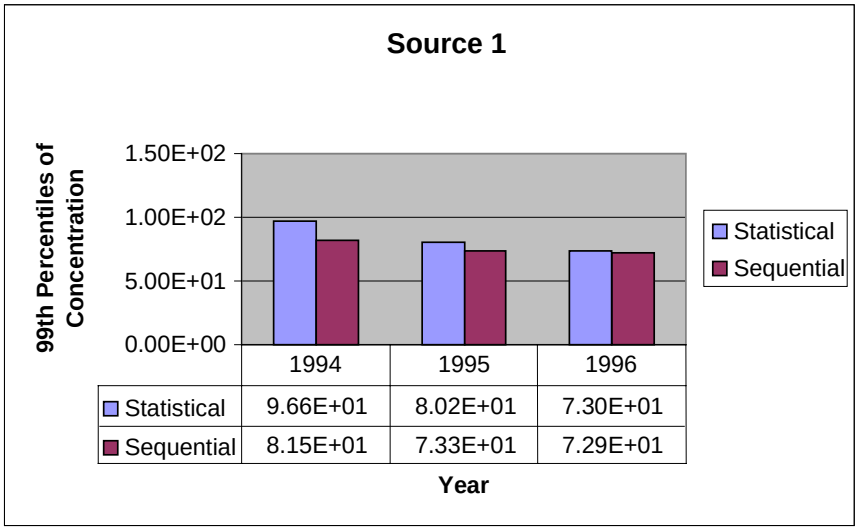

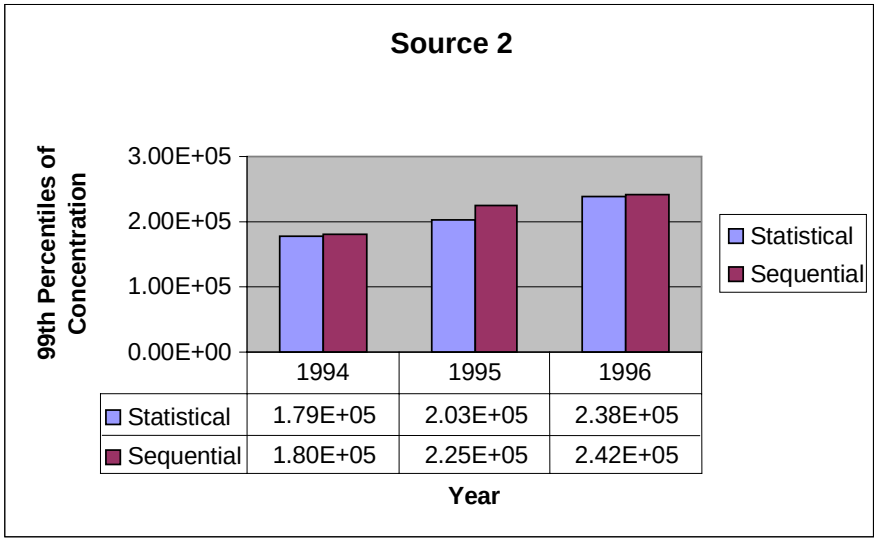

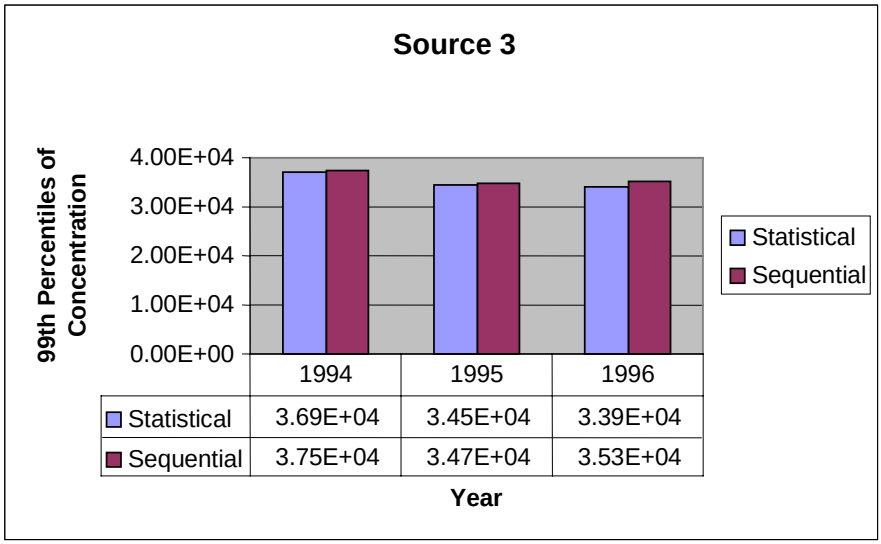

FIGURE C3 Comparison of peak 99th percentile of concentrations for statistical and sequential datasets during the study period

APPENDIX D

Figures D1a to D1f

Case B

Release Height	Release Velocity	Release Temperature
100m	1m/s	40°C

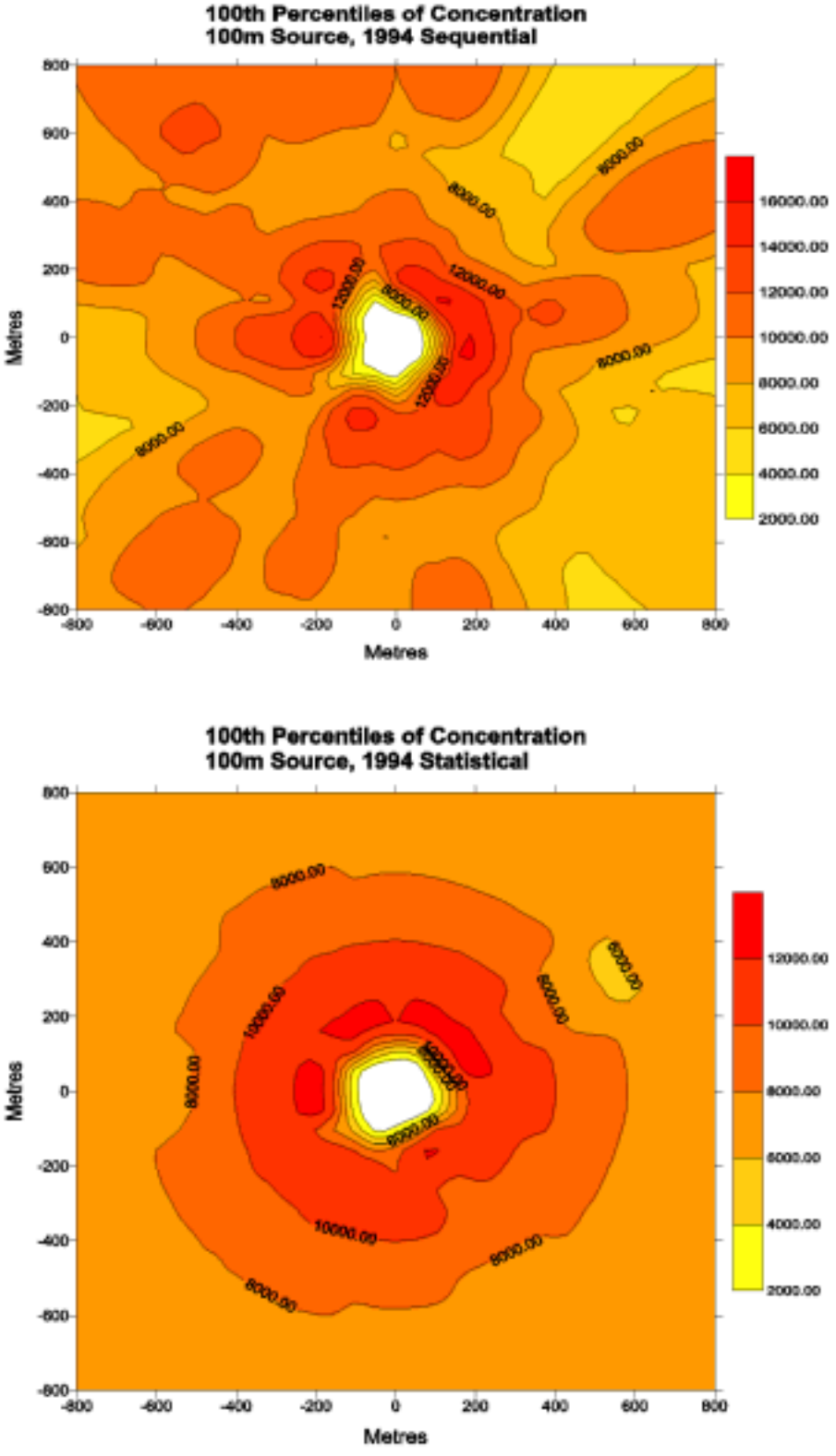

FIGURE D1a 100th Percentiles of concentration for 100m source using 1994 sequential and statistical data

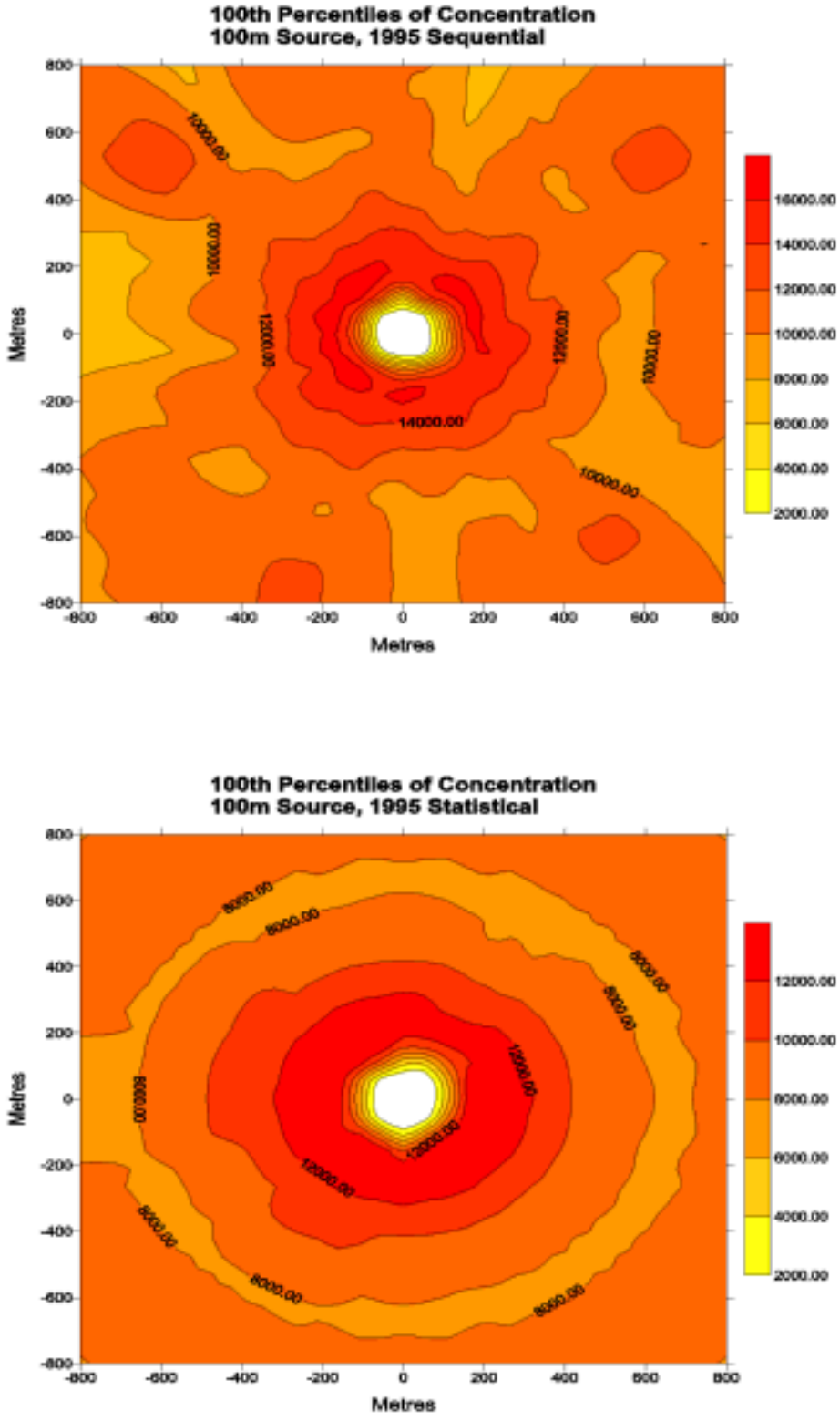

FIGURE D1b: 100th Percentiles of concentration for 100m source using 1995 sequential and statistical data

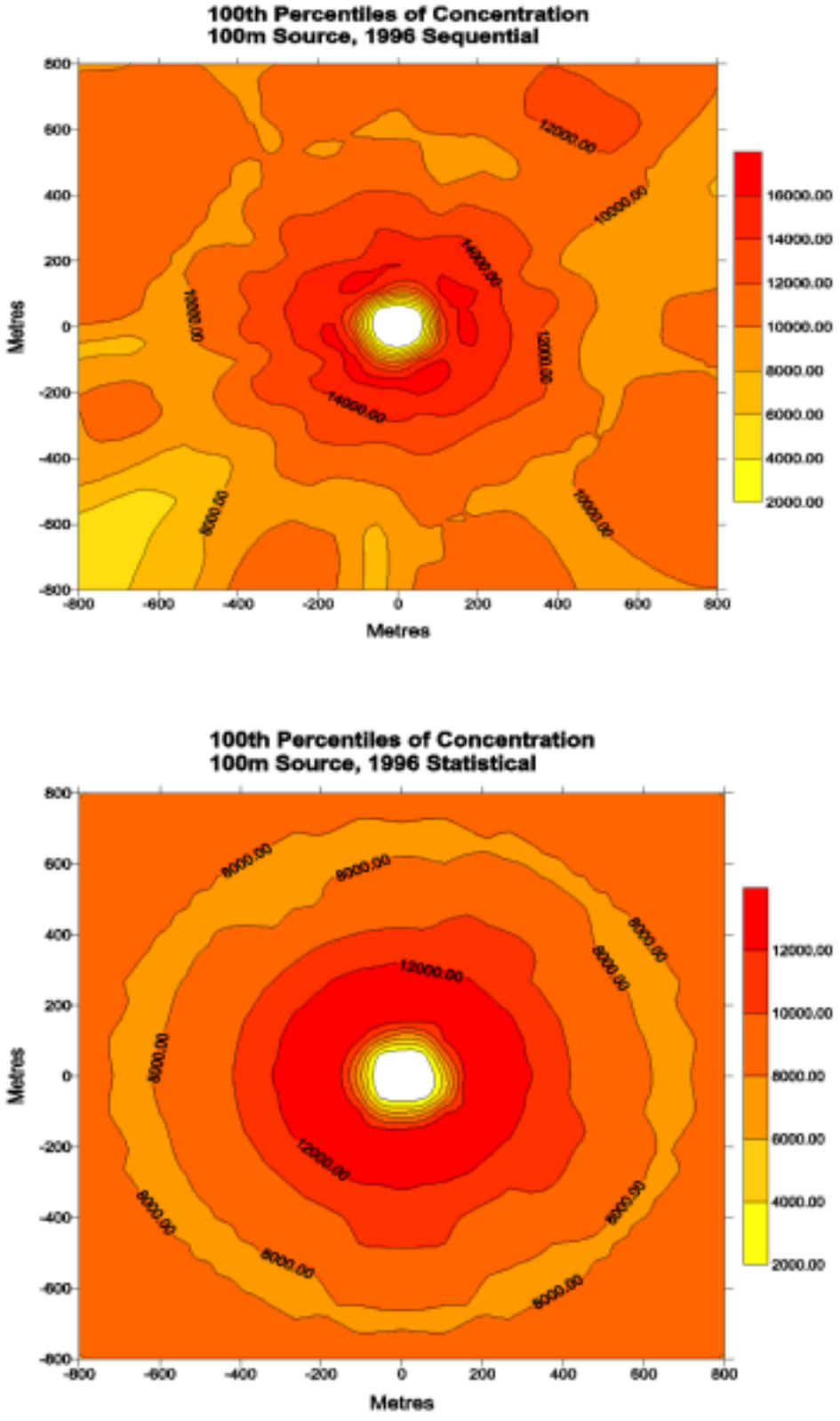

FIGURE D1c: 100th Percentiles of concentration for 100m source using 1996 sequential and statistical data

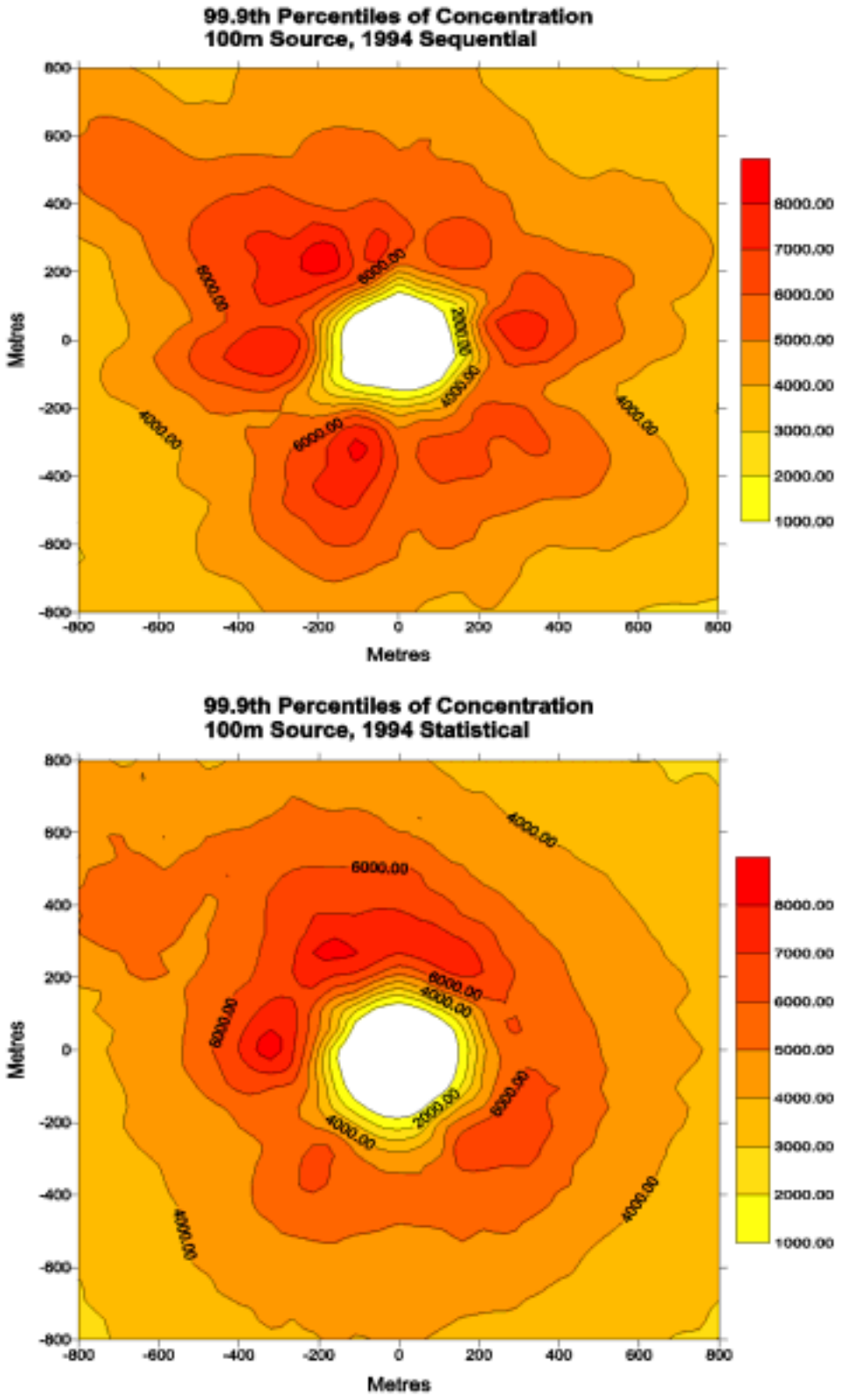

FIGURE D1d 99.9th Percentiles of concentration for 100m source using 1994 sequential and statistical data

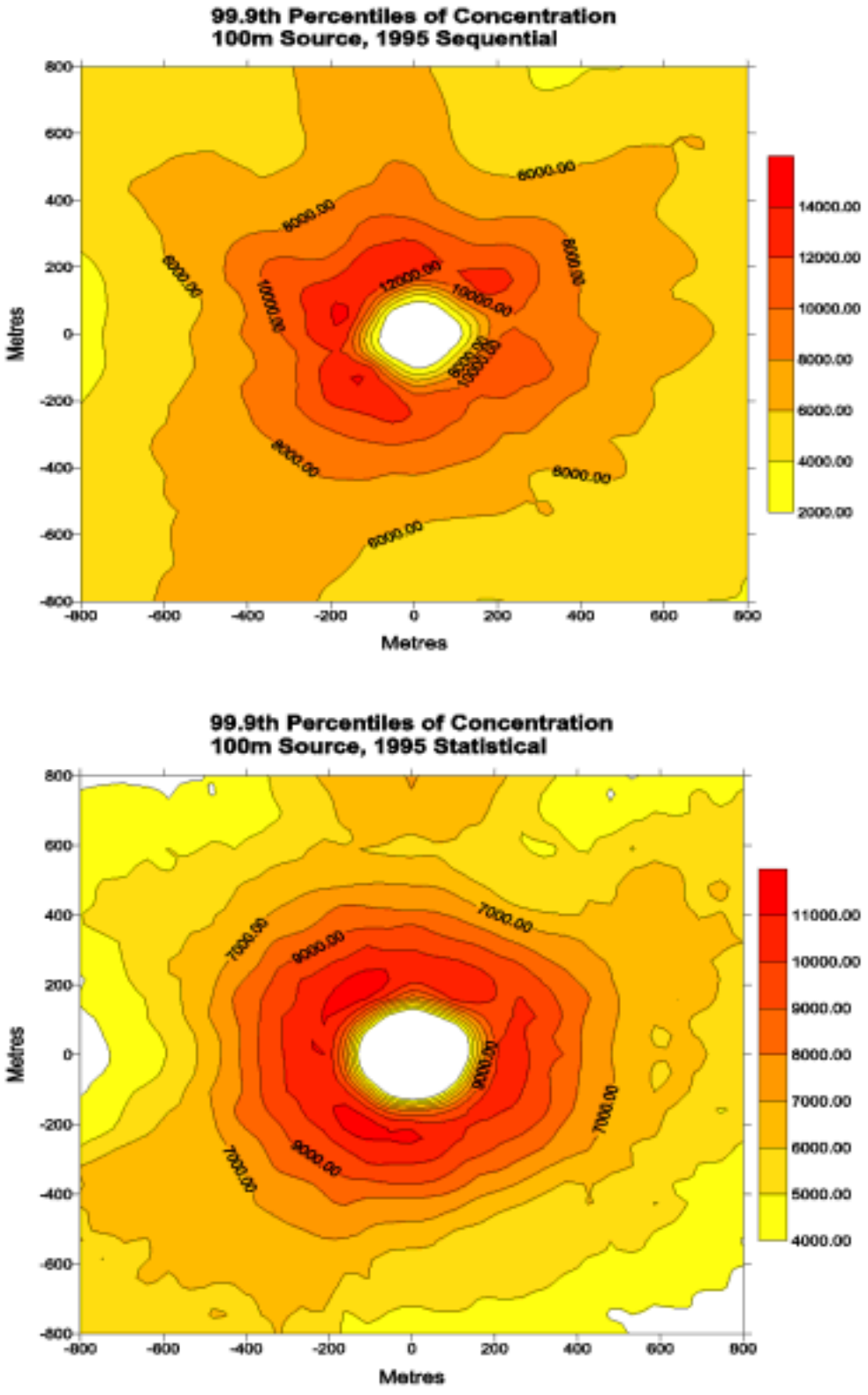

FIGURE D1e 99.9th Percentiles of concentration for 100m source using 1995 sequential and statistical data

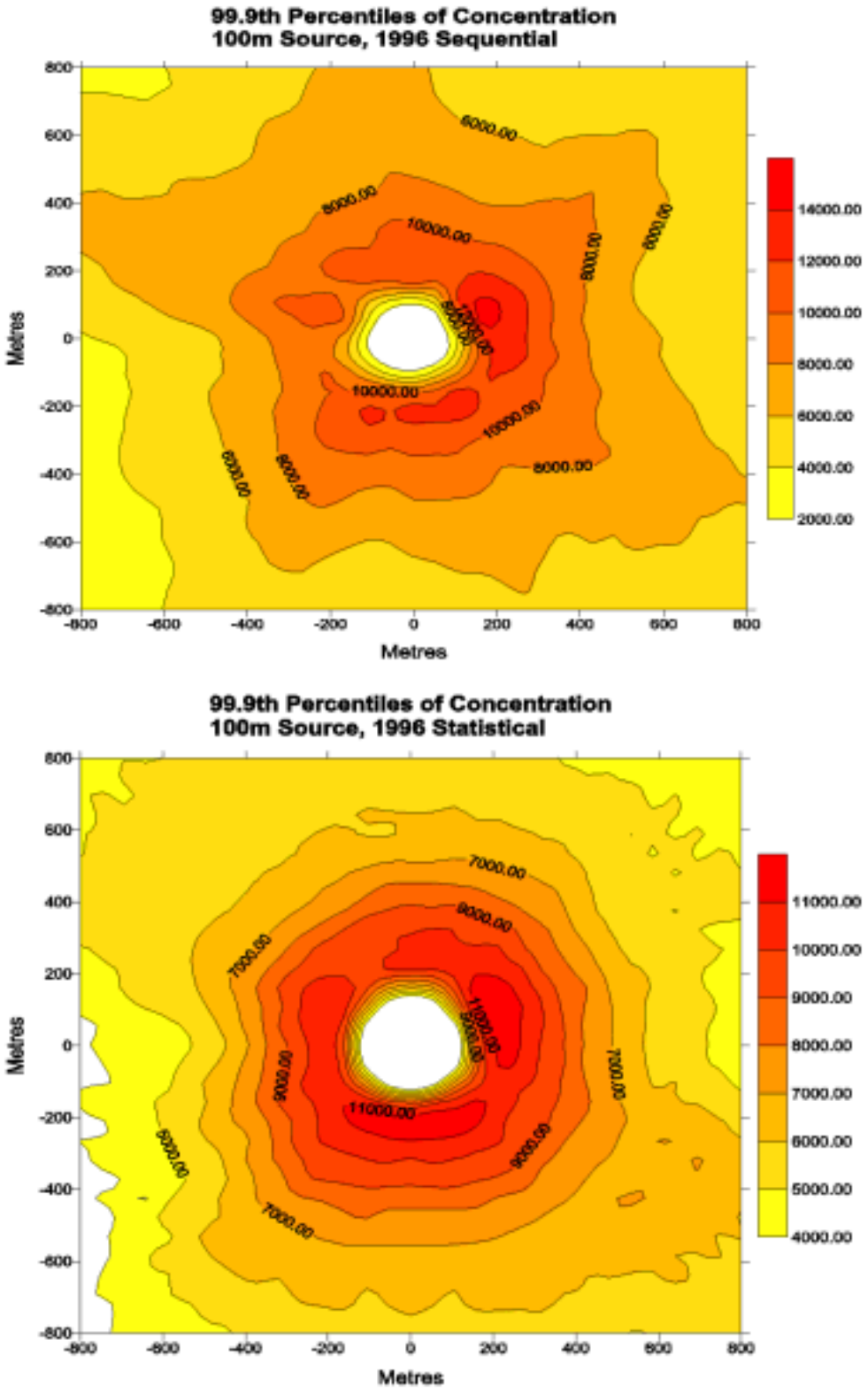

FIGURE D1f 99.9th Percentiles of concentration for 100m source using 1996 sequential and statistical data

Figures D2a to D2f

Case D

Release Height	Release Velocity	Release Temperature
75m	1m/s	40°C

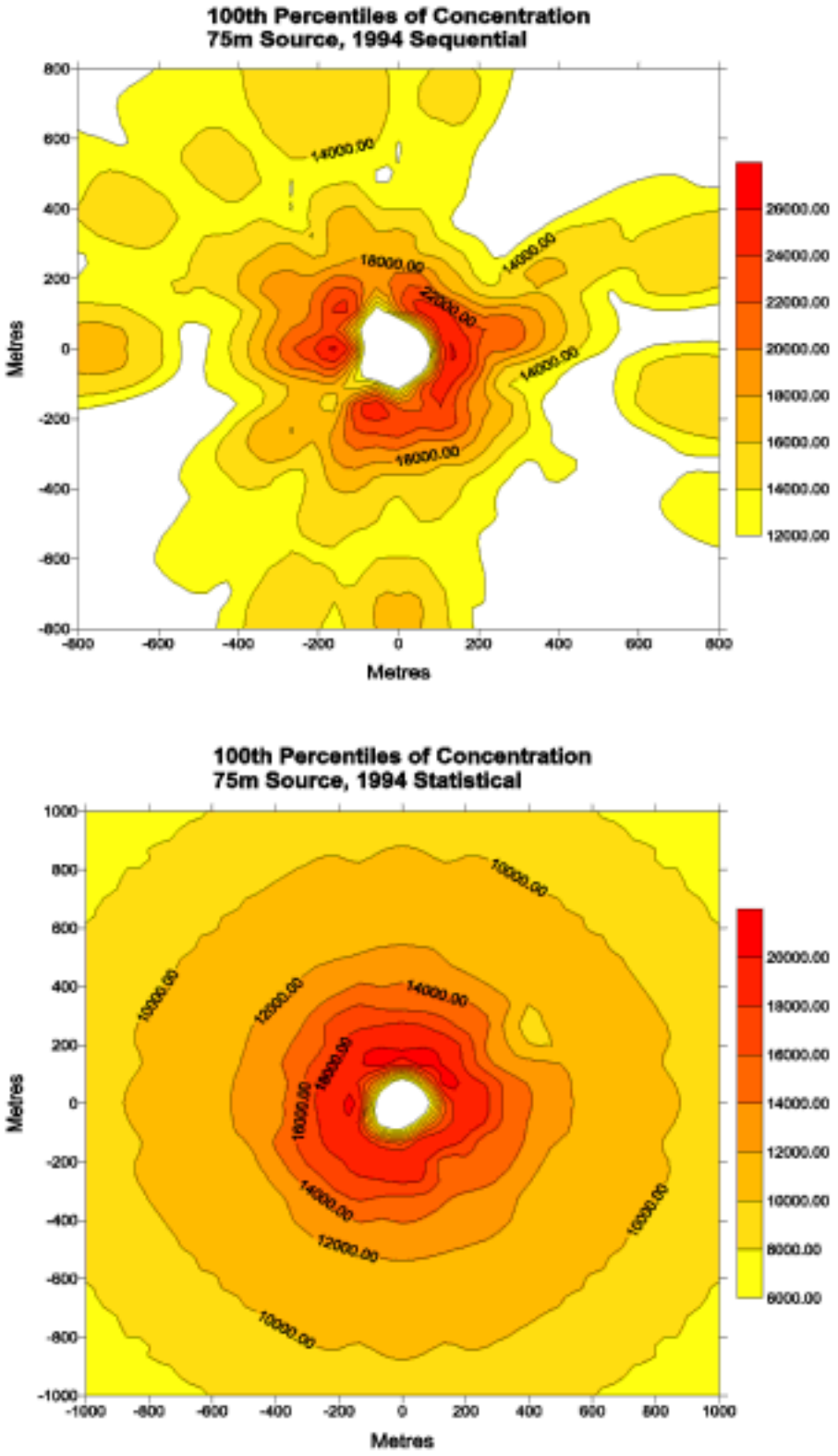

FIGURE D2a 100th Percentiles of concentration for 75m source using 1994 sequential and statistical data

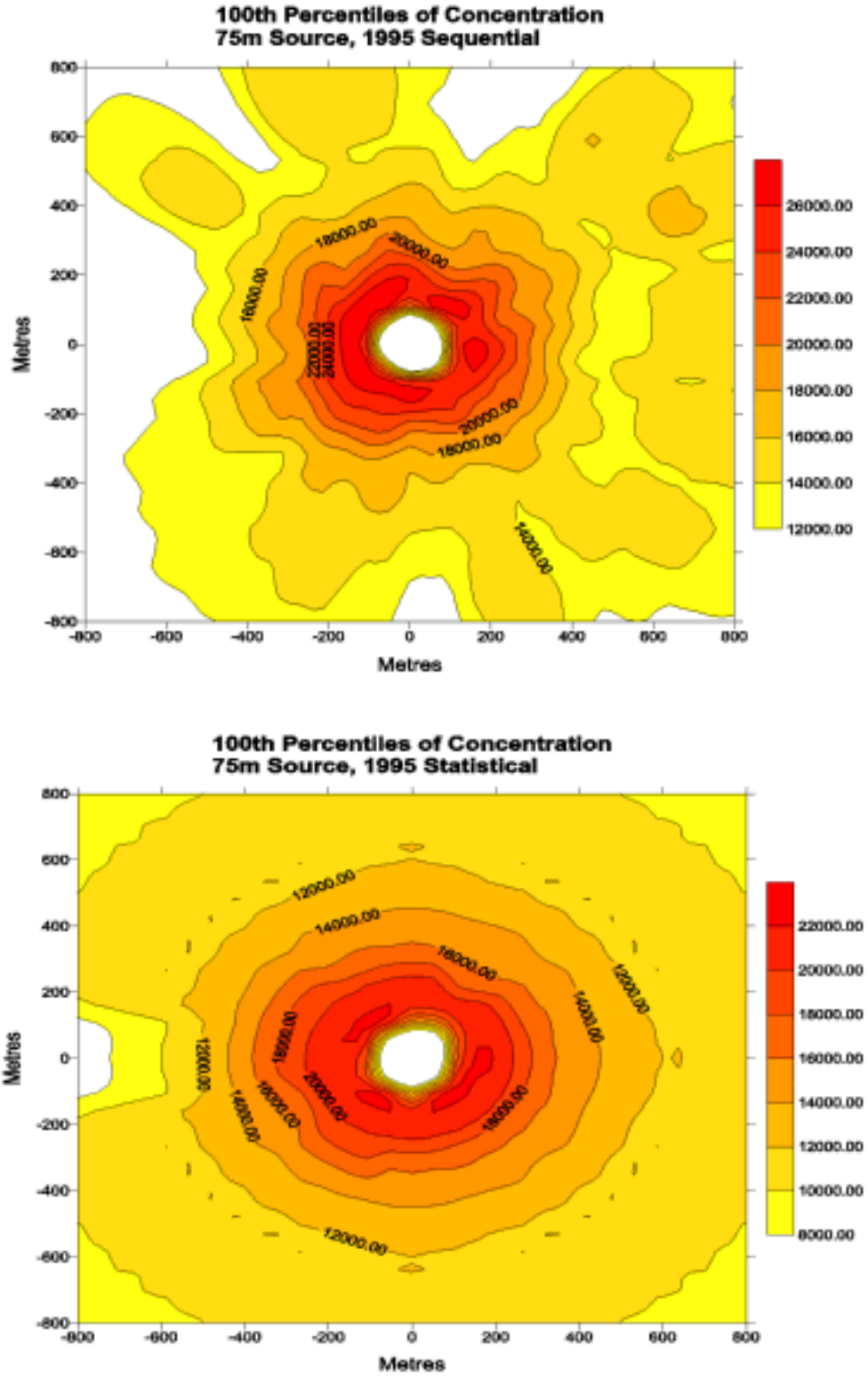

FIGURE D2b 100th Percentiles of concentration for 75m source using 1995 sequential and statistical data

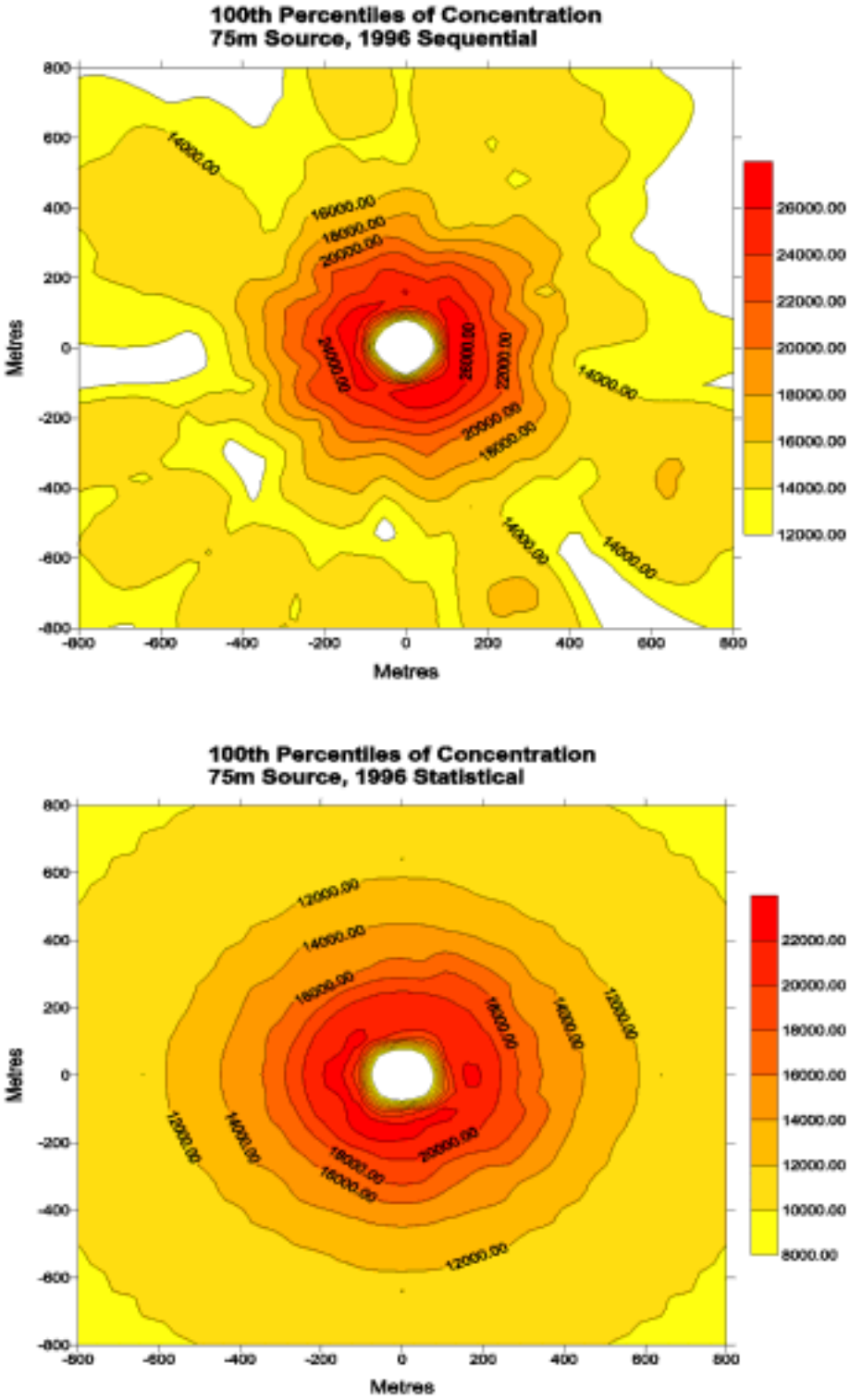

FIGURE D2c 100th Percentiles of concentration for 75m source using 1996 sequential and statistical data

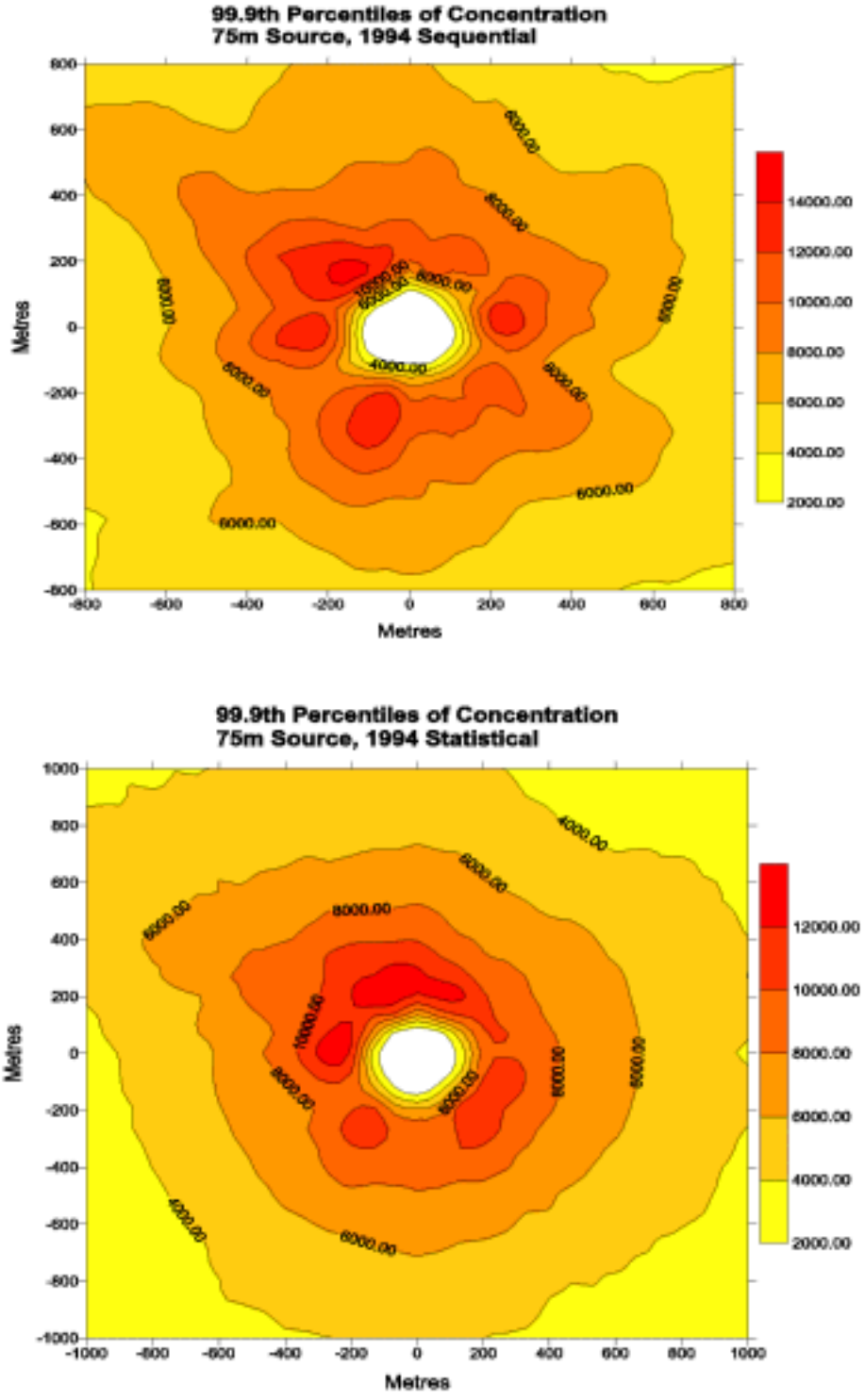

FIGURE D2d 99.9th Percentiles of concentration for 75m source using 1994 sequential and statistical data

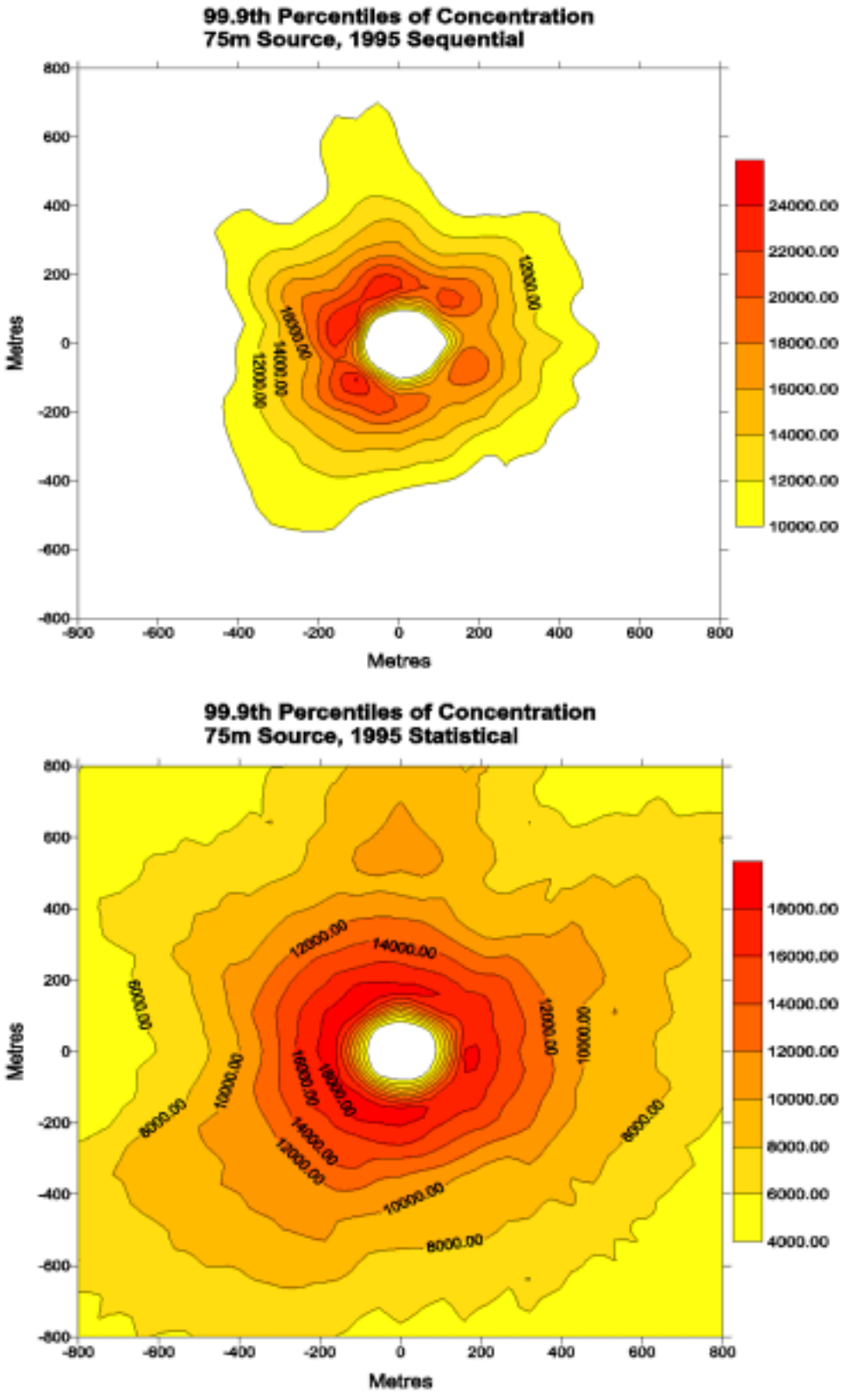

FIGURE D2e 99.9th Percentiles of concentration for 75m source using 1995 sequential and statistical data

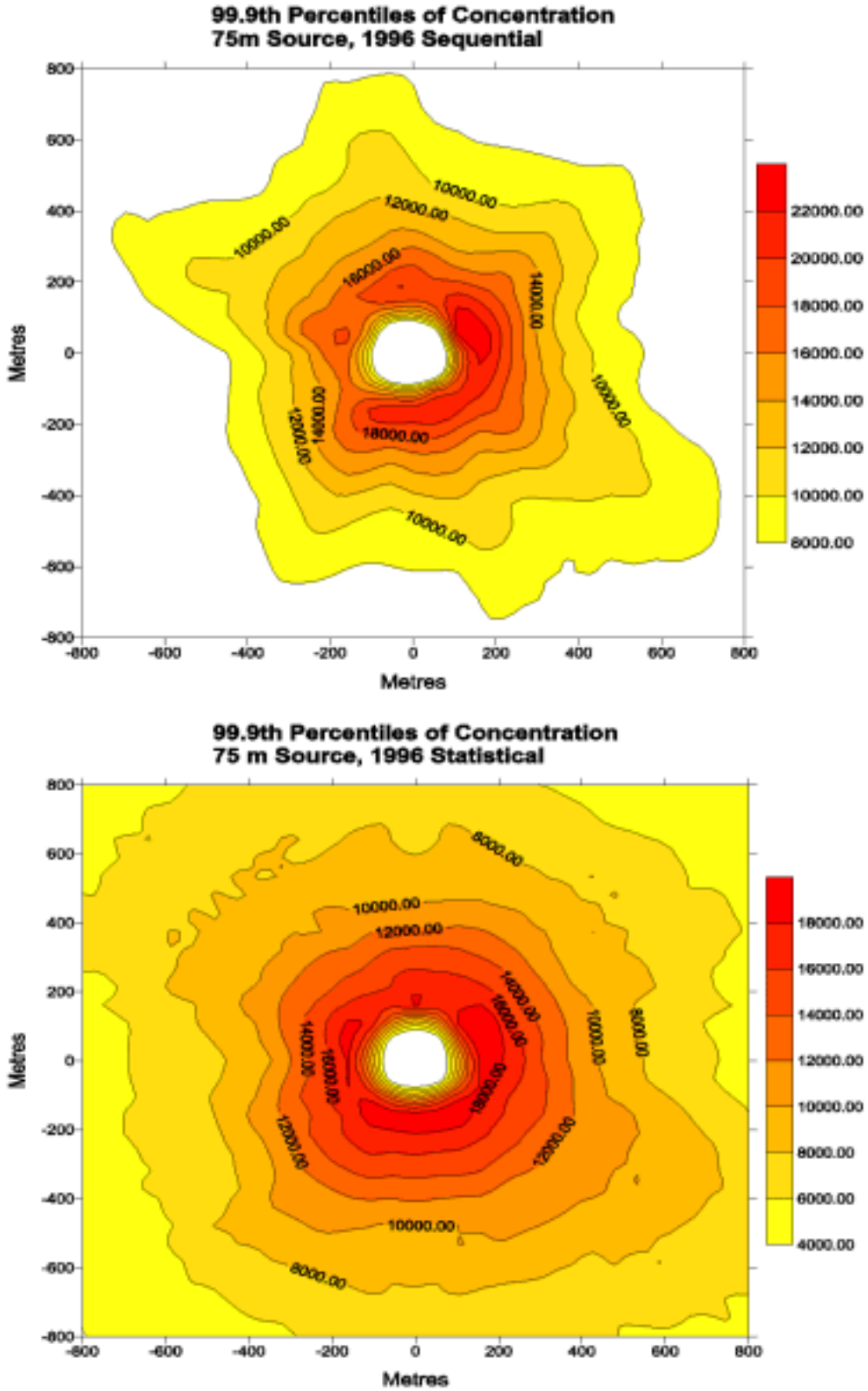

FIGURE D2f 99.9th Percentiles of concentration for 75m source using 1996 sequential and statistical data

Figures 3a to 3f

Case F

Release Height	Release Velocity	Release Temperature
50m	1m/s	40°C

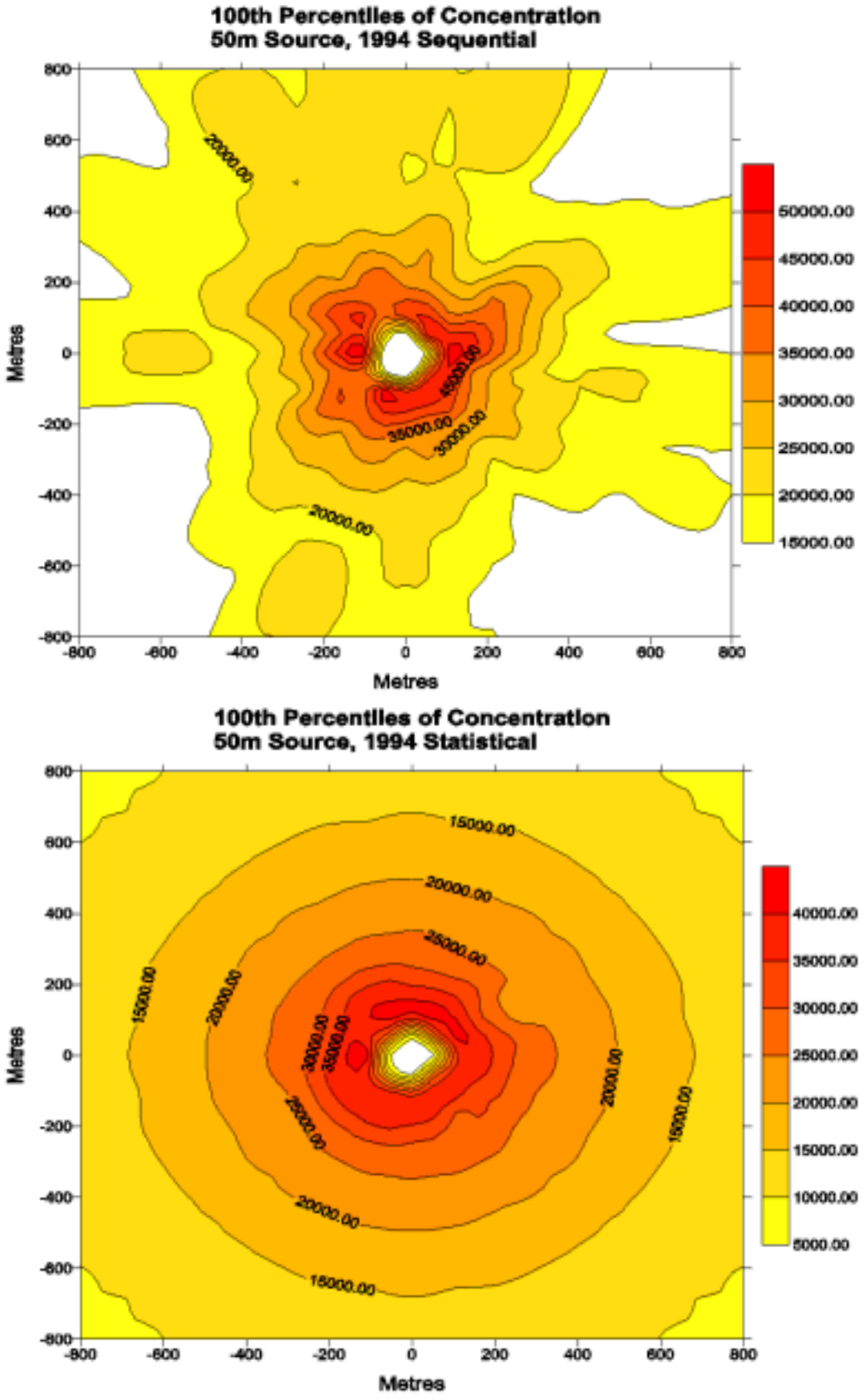

FIGURE D3a: 100th Percentiles of concentration for 50m source using 1994 sequential and statistical data

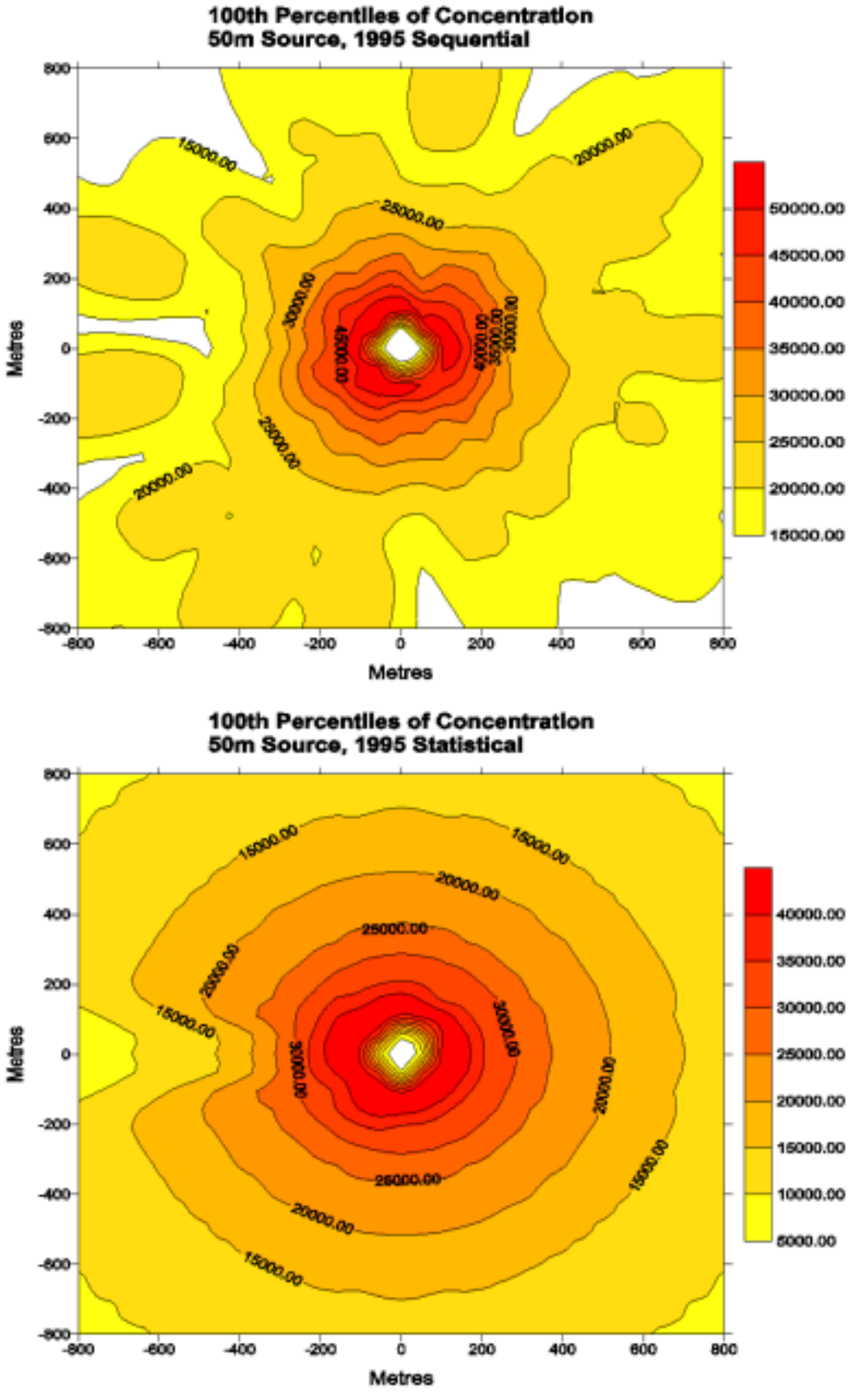

FIGURE D3b 100th Percentiles of concentration for 50m source using 1995 sequential and statistical data

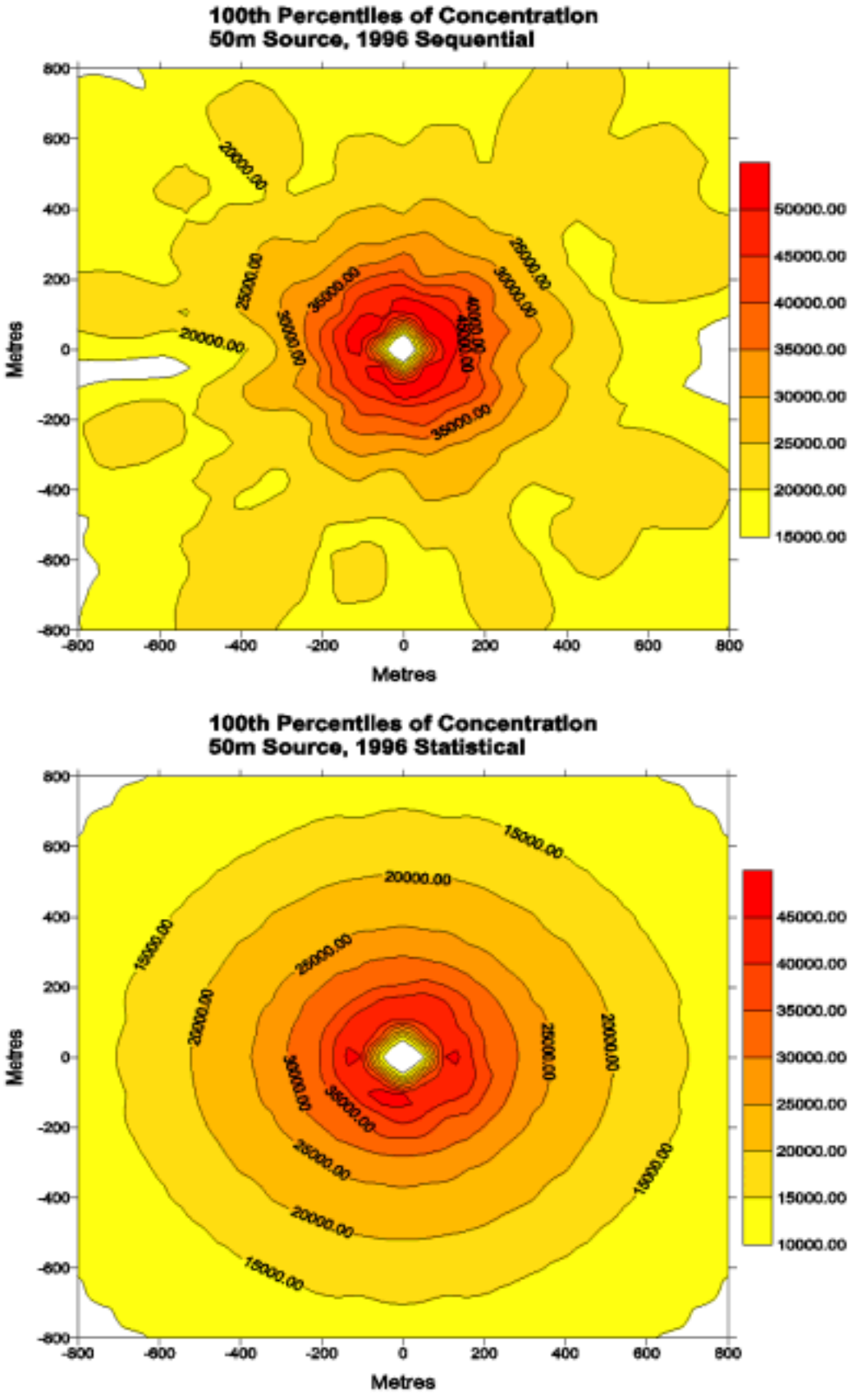

figure D3c 100th Percentiles of concentration for 50m source using 1996 sequential and statistical data

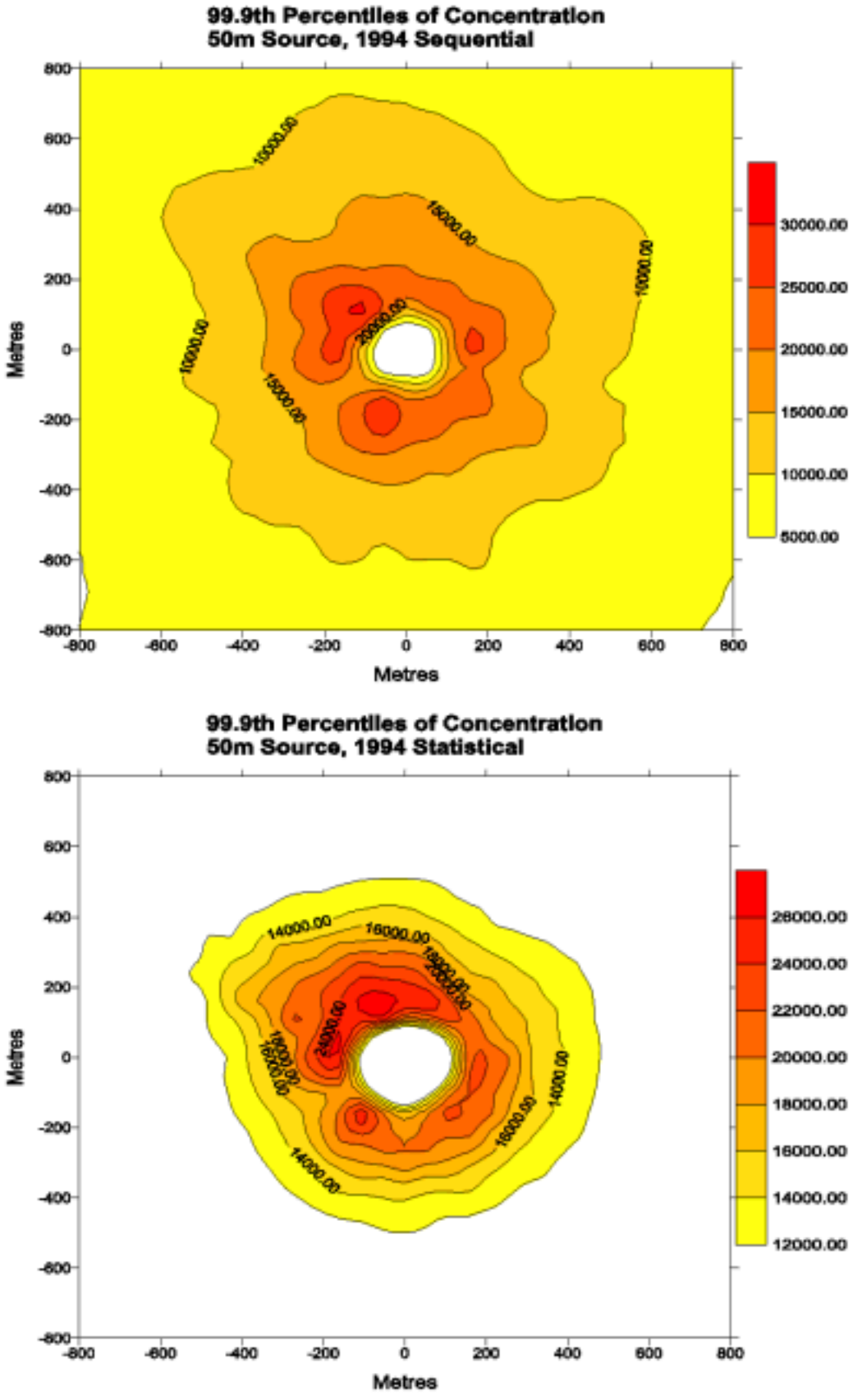

FIGURE D3d 99.9th Percentiles of concentration for 50m source using 1994 sequential and statistical data

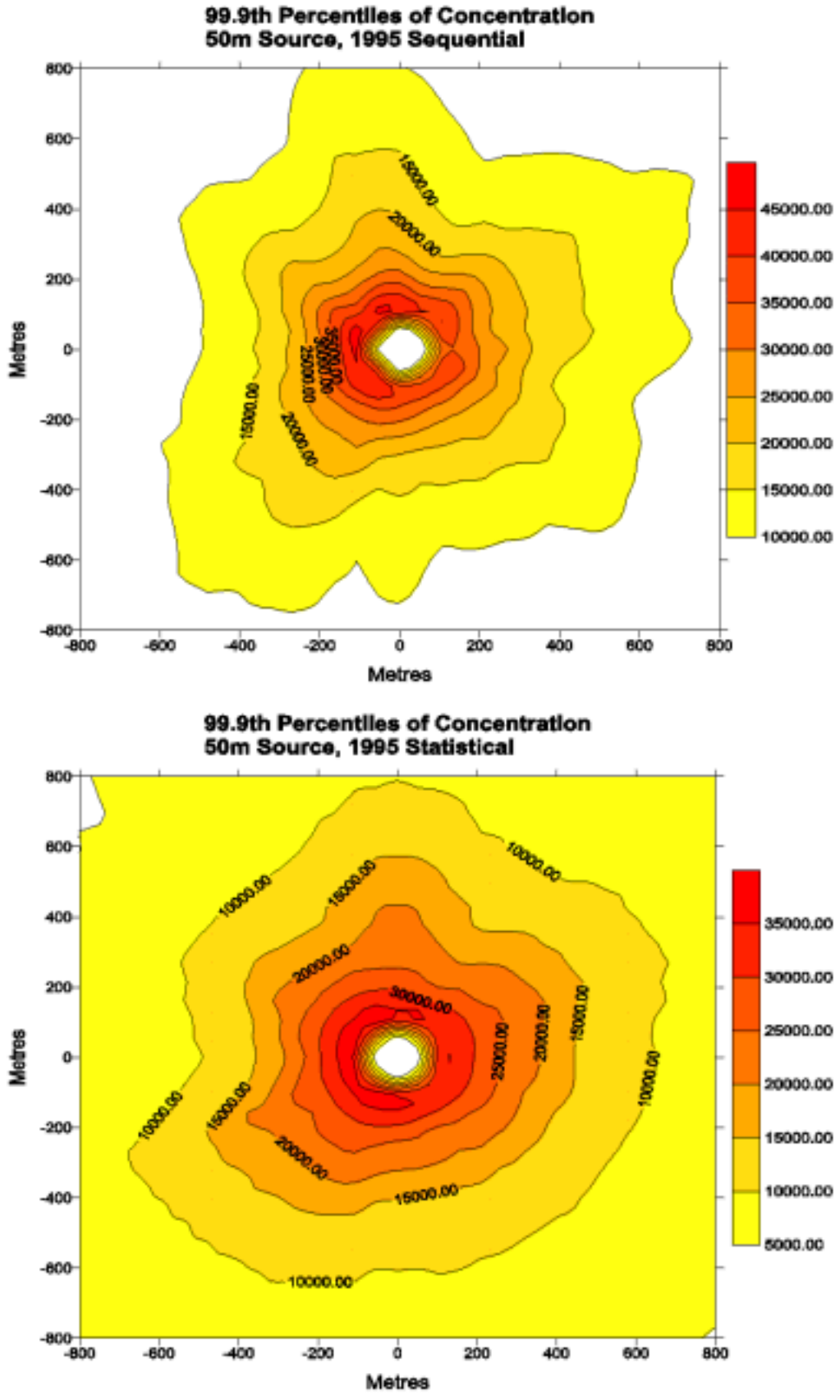

FIGURE D3e 99.9th Percentiles of concentration for 50m source using 1995 sequential and statistical data

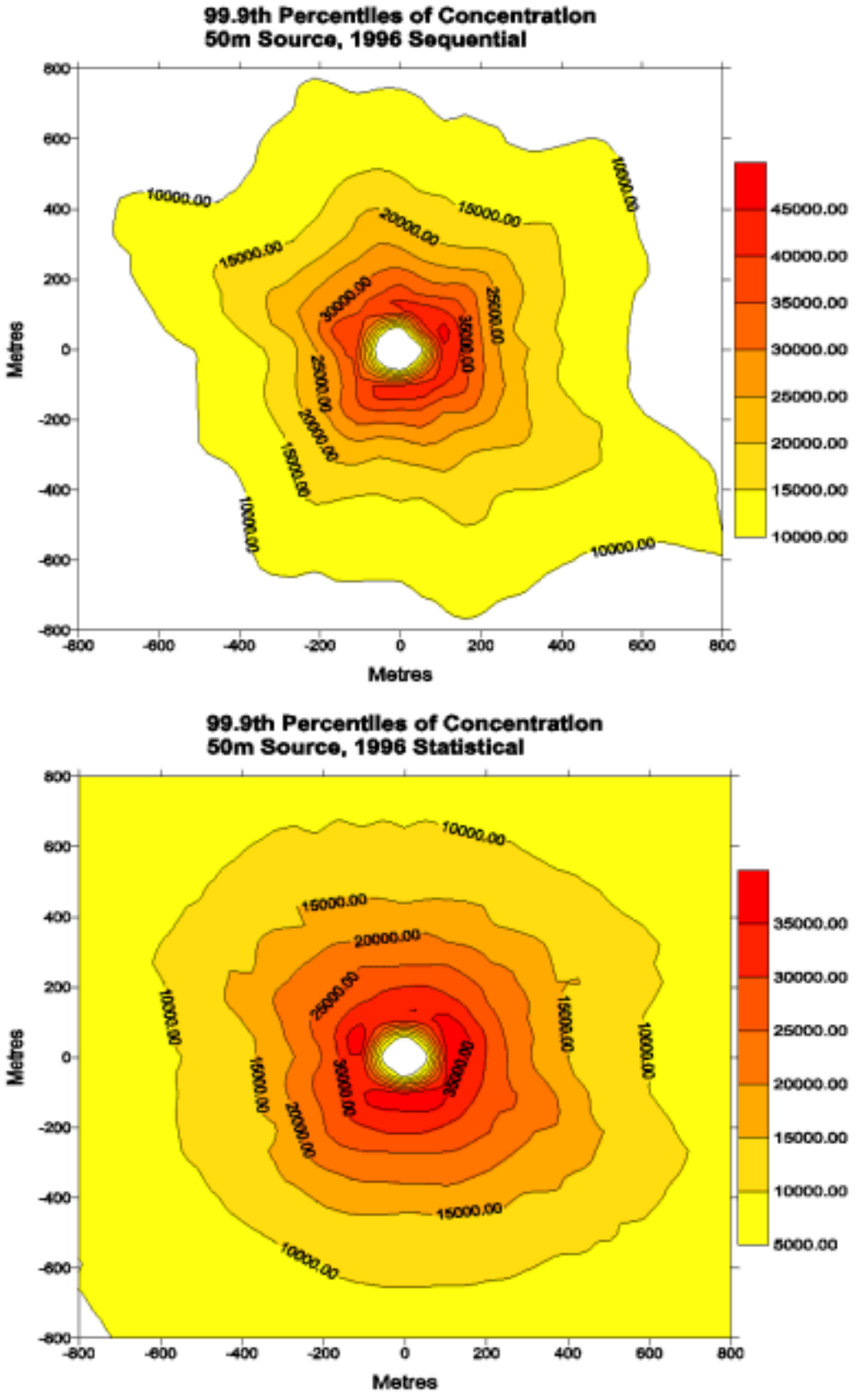

FIGURE D3f 99.9th Percentiles of concentration for 50m source using 1996 sequential and statistical data Figures D4a to D4f

Case H

Release Height	Release Velocity	Release Temperature
30m	1m/s	40°C

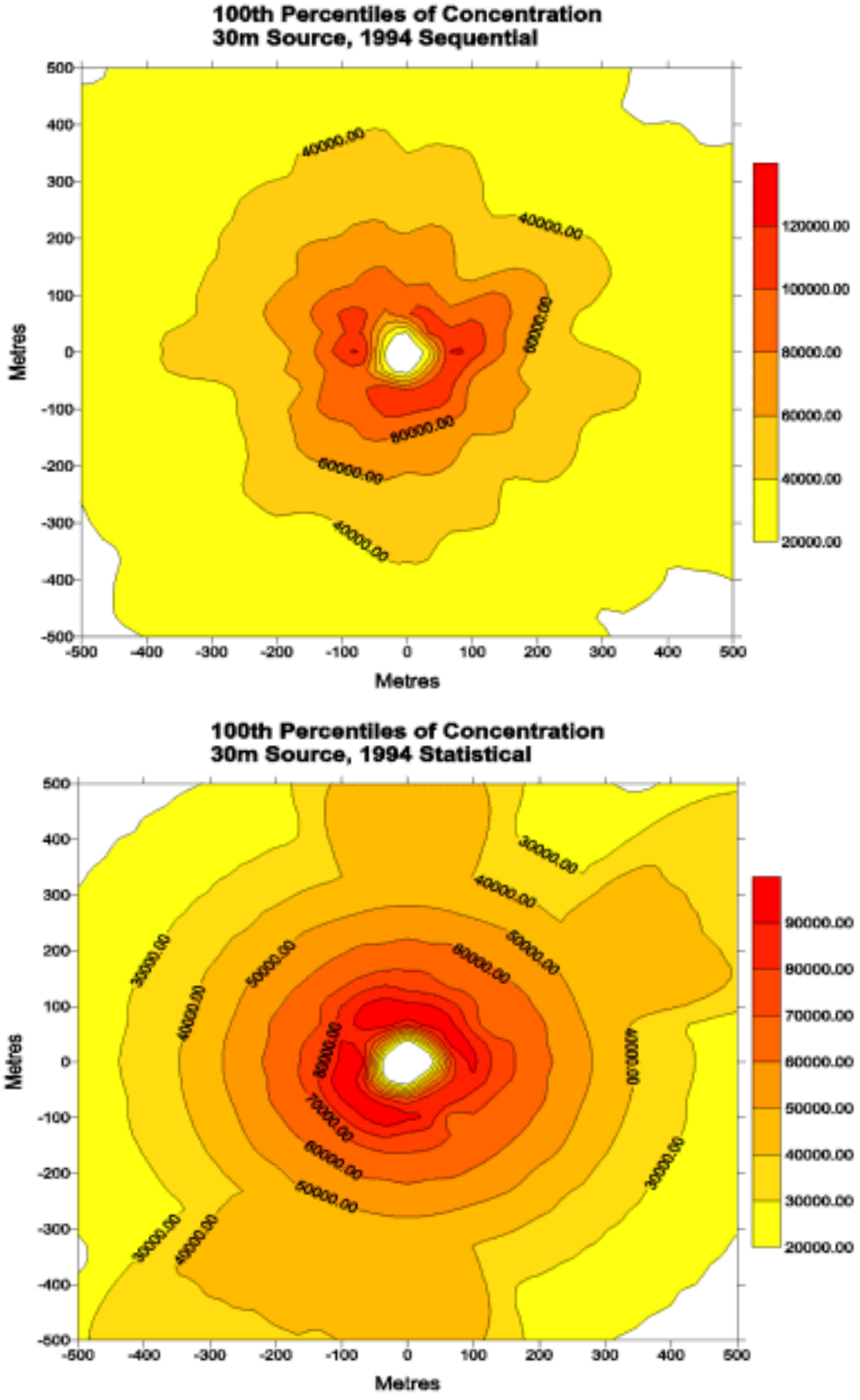

FIGURE D4a: 100th Percentiles of concentration for 30m source using 1994 sequential and statistical data

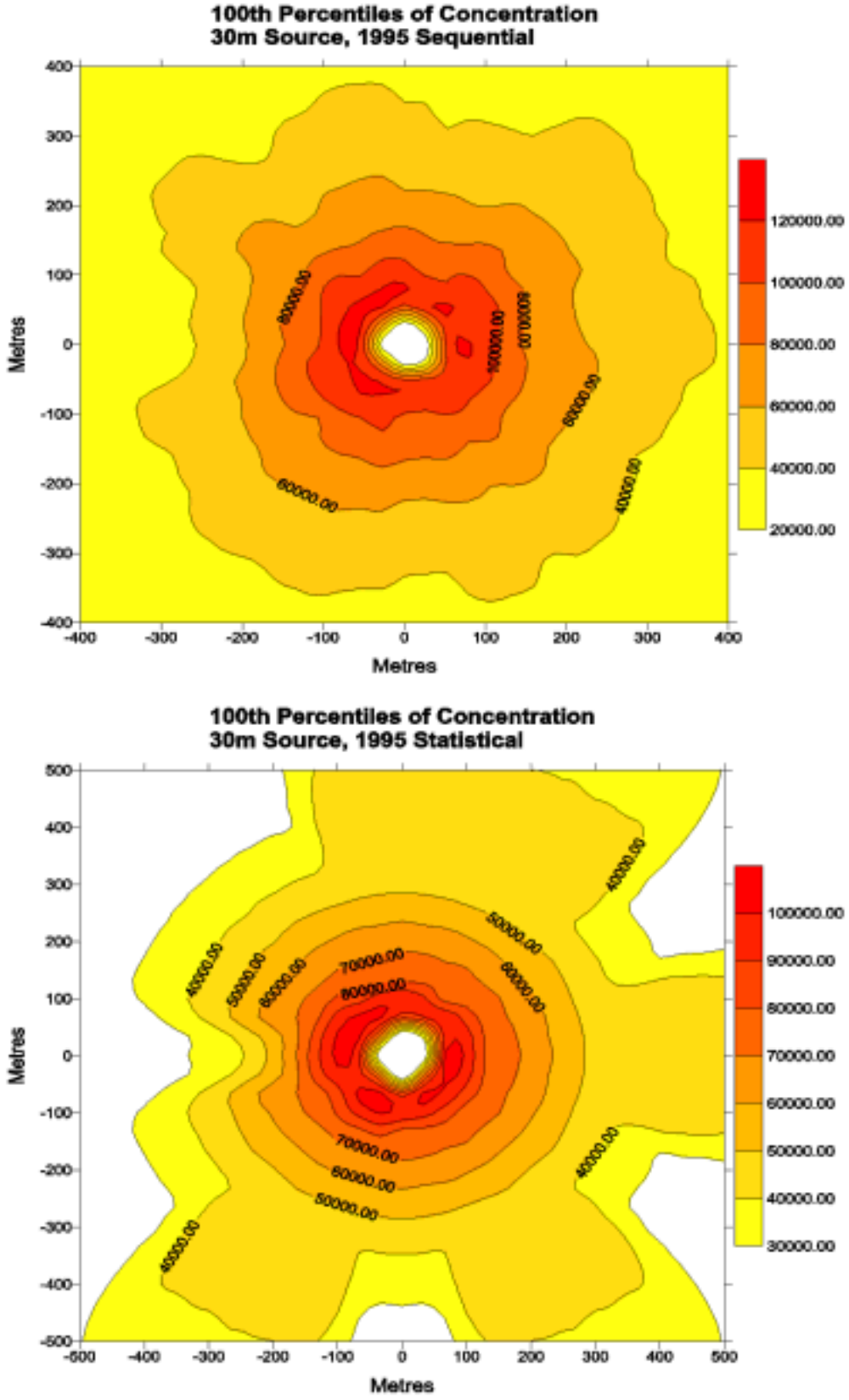

FIGURE D4b: 100th Percentiles of concentration for 30m source using 1995 sequential and statistical data

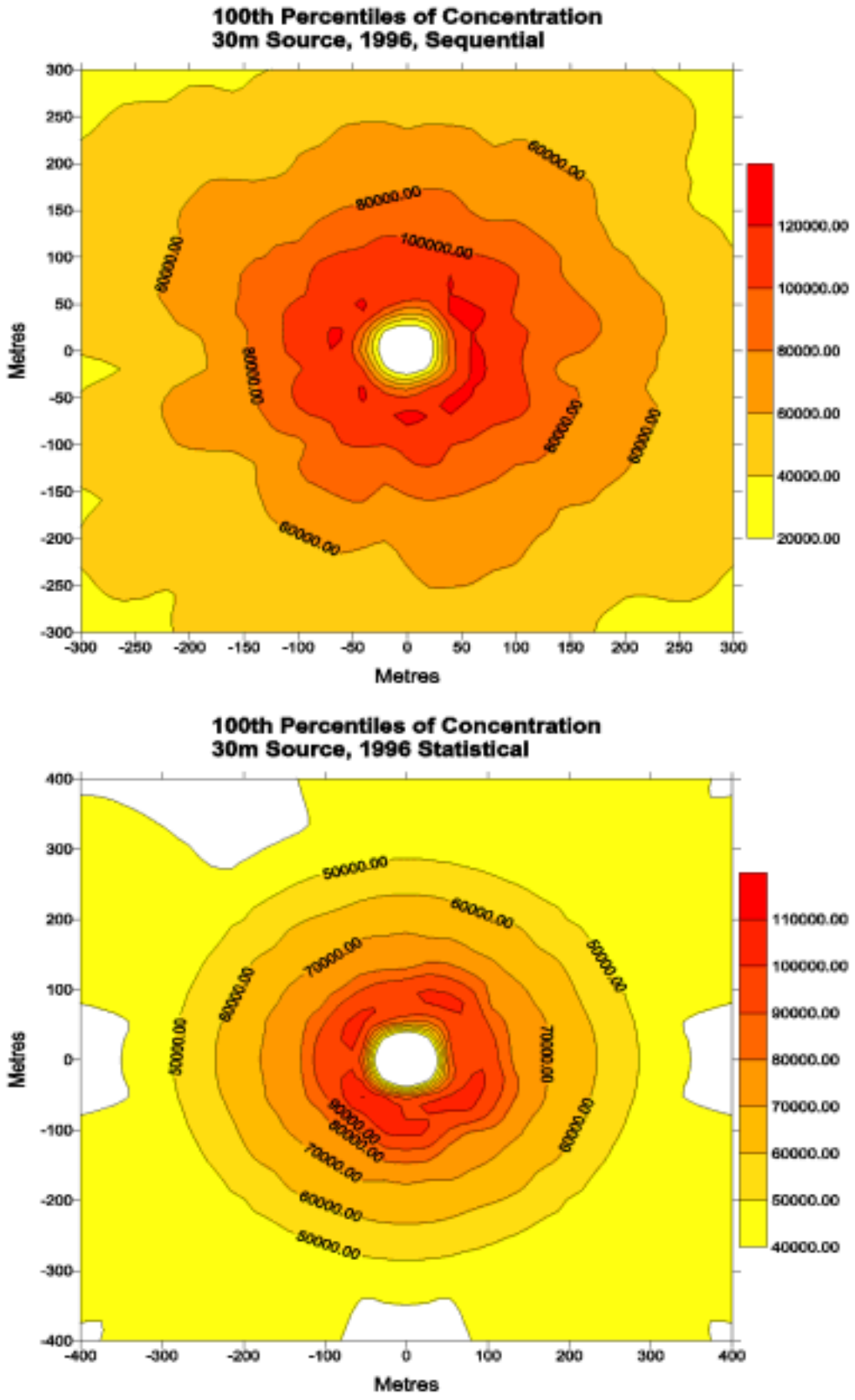

FIGURE D4c: 100th Percentiles of concentration for 30m source using 1996 sequential and statistical data

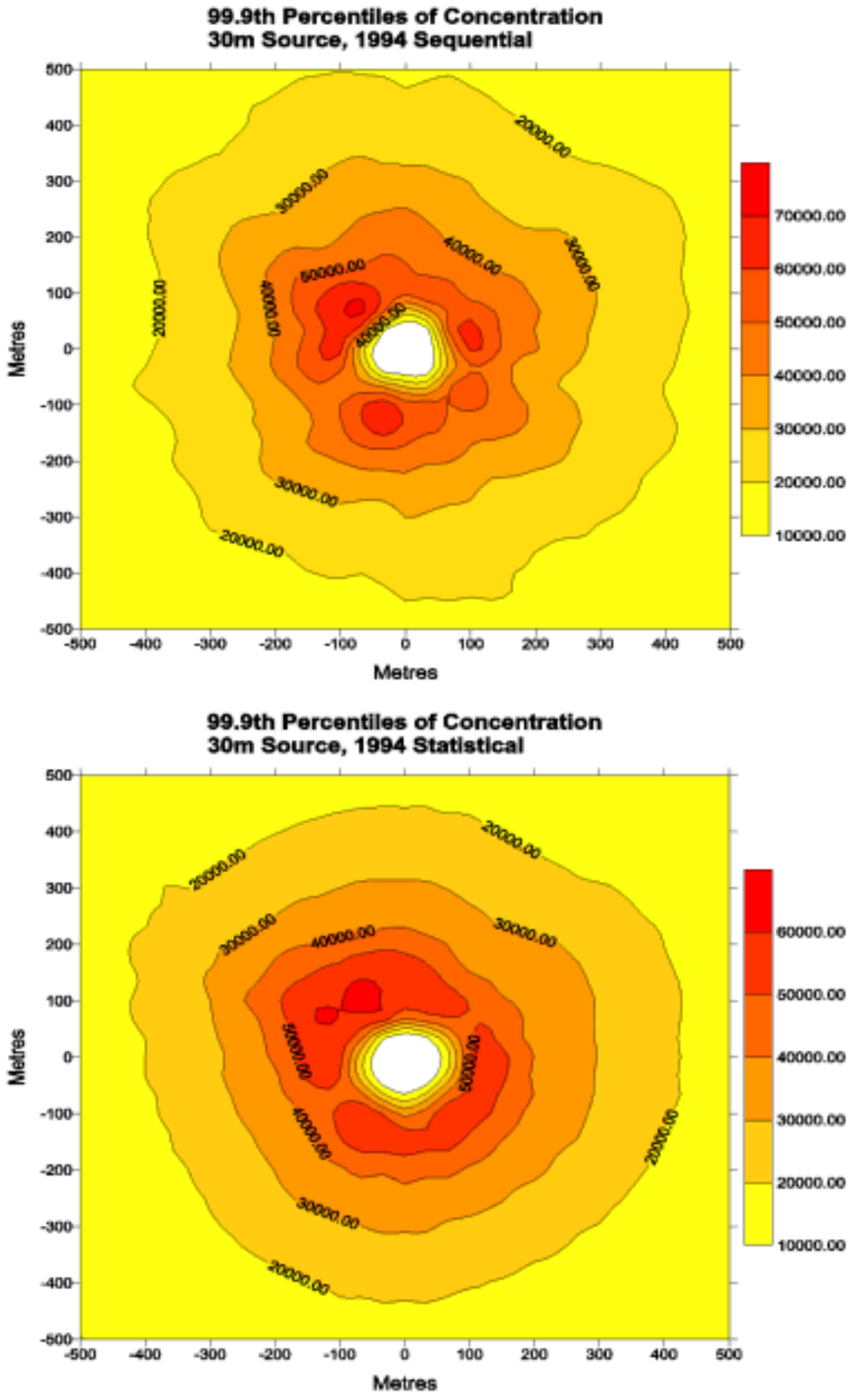

FIGURE D4d: 99.9th Percentiles of concentration for 30m source using 1994 sequential and statistical data

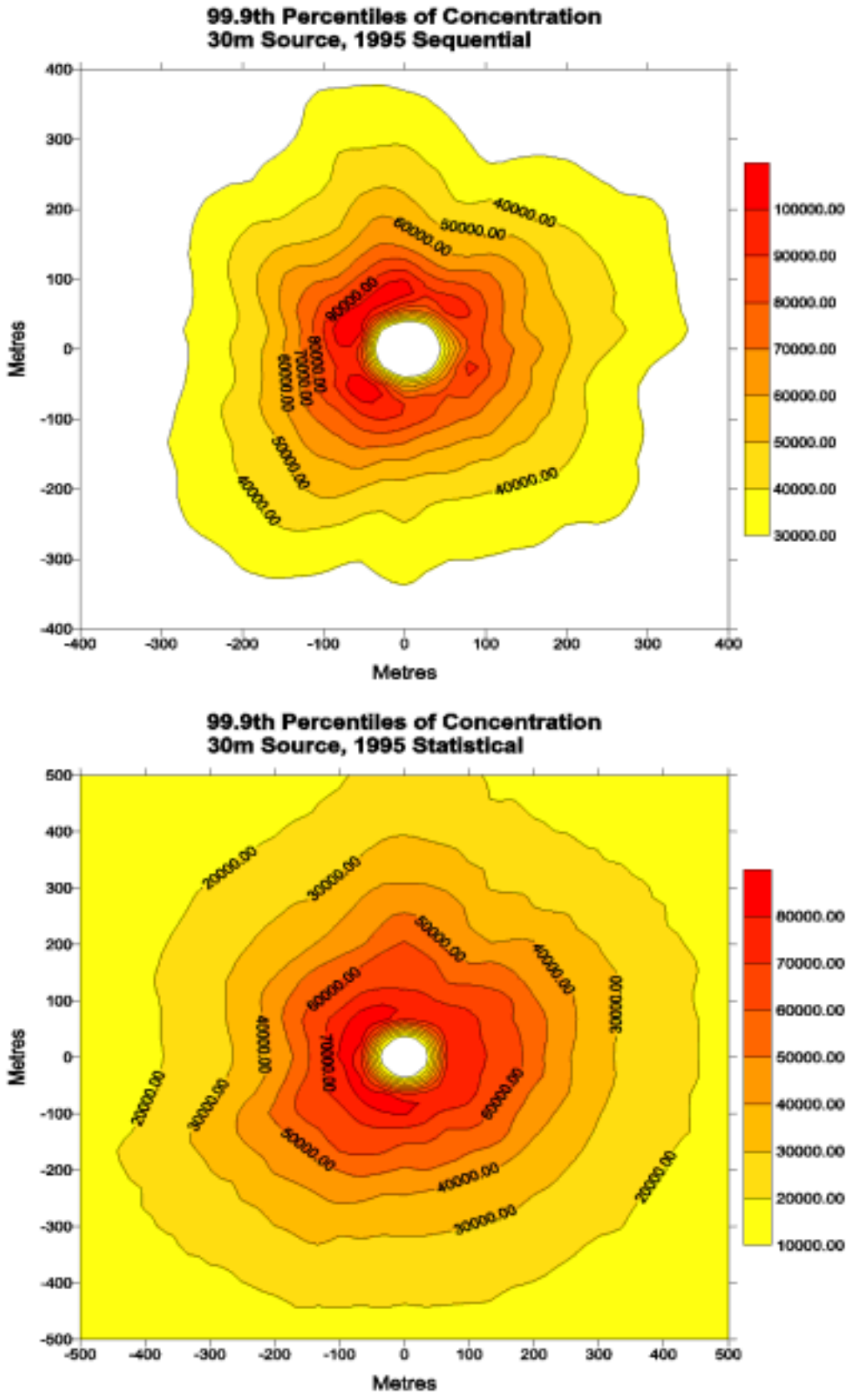

FIGURE D4e: 99.9th Percentiles of concentration for 30m source using 1995 sequential and statistical data

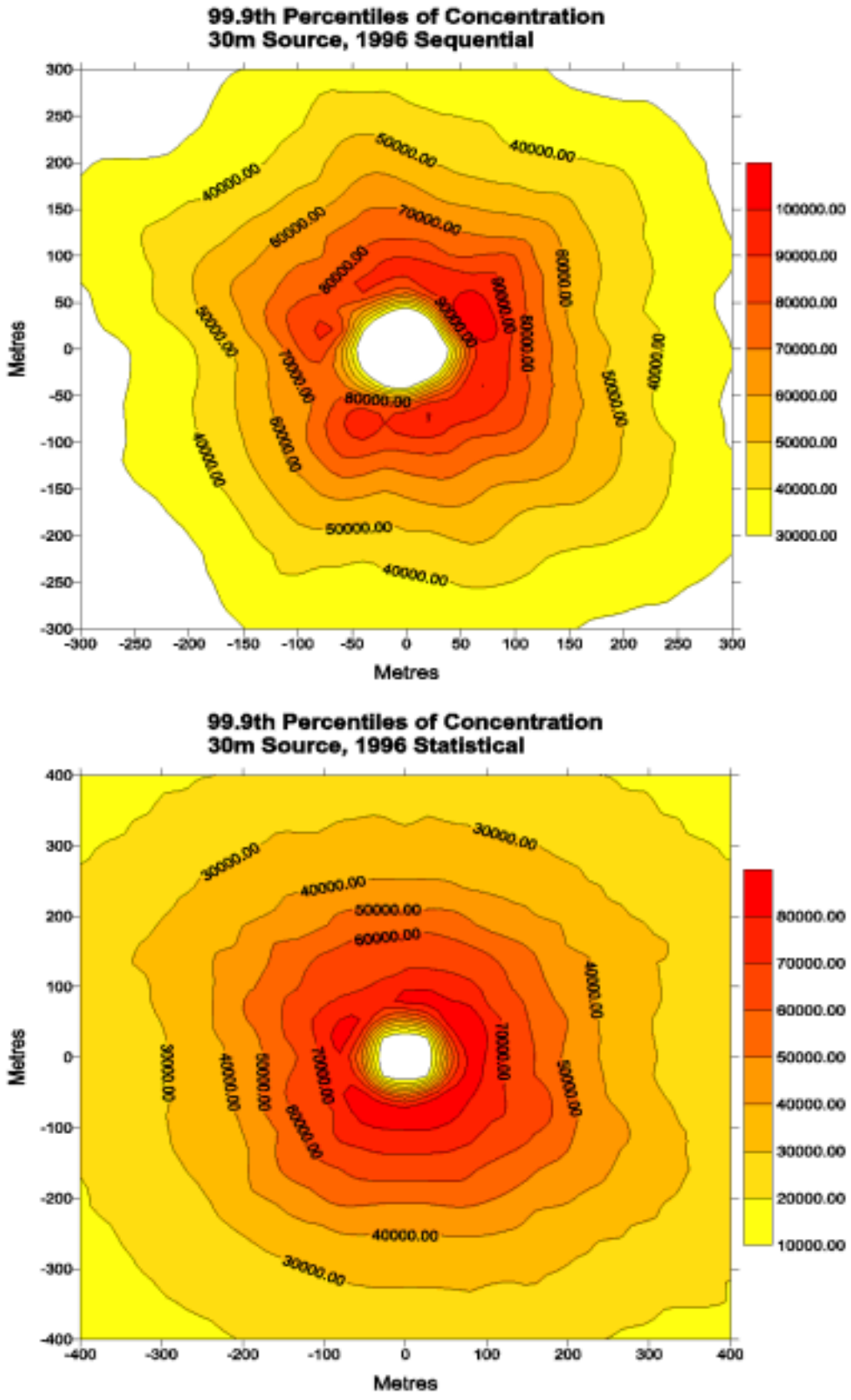

FIGURE D4f: 99.9th Percentiles of concentration for 30m source using 1996 sequential and statistical data

Figures 5a to 5f

Case J

Release Height	Release Velocity	Release Temperature
10m	1m/s	40°C

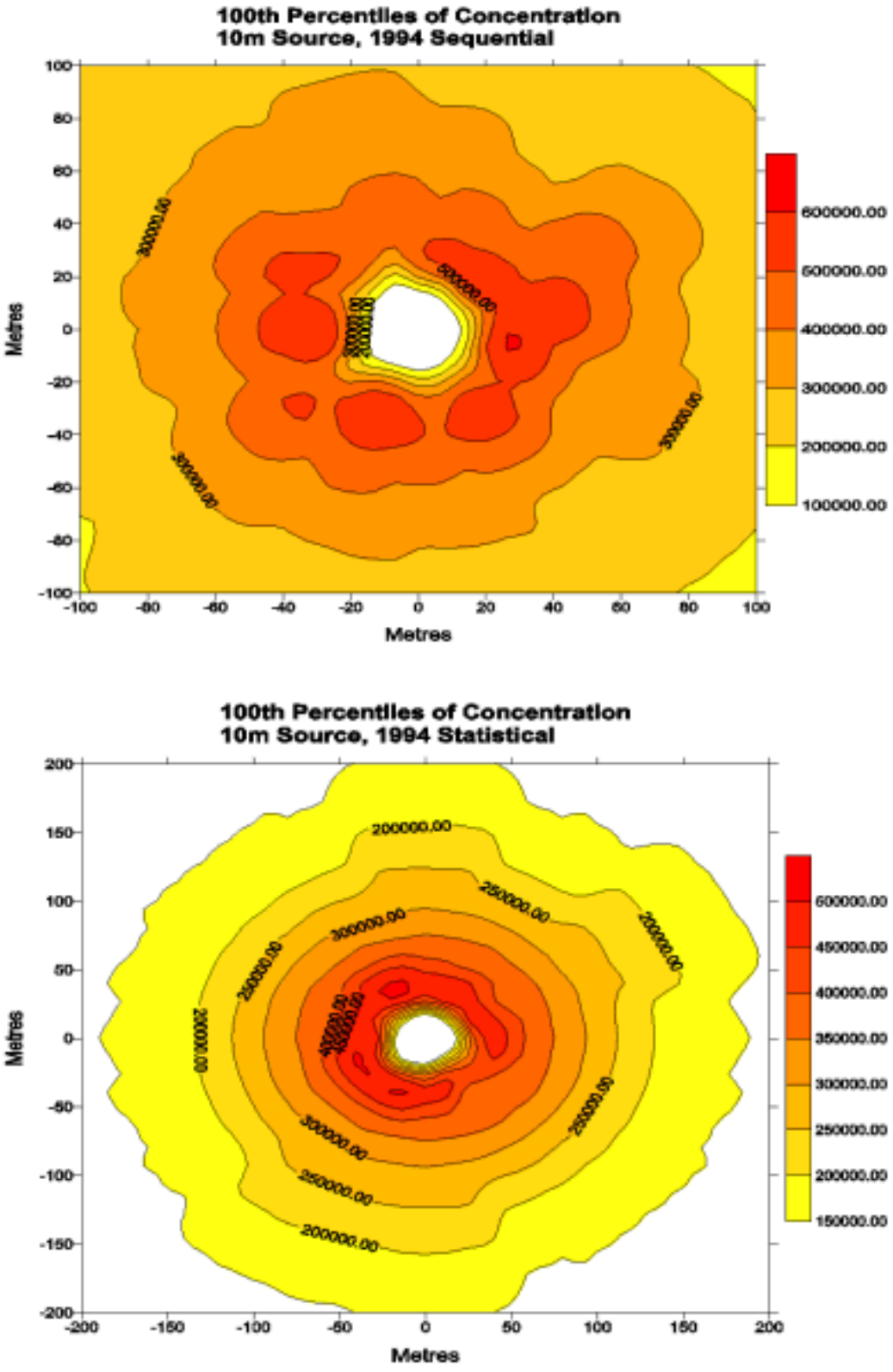

FIGURE D5a: 100th Percentiles of concentration for 10m source using 1994 sequential and statistical data

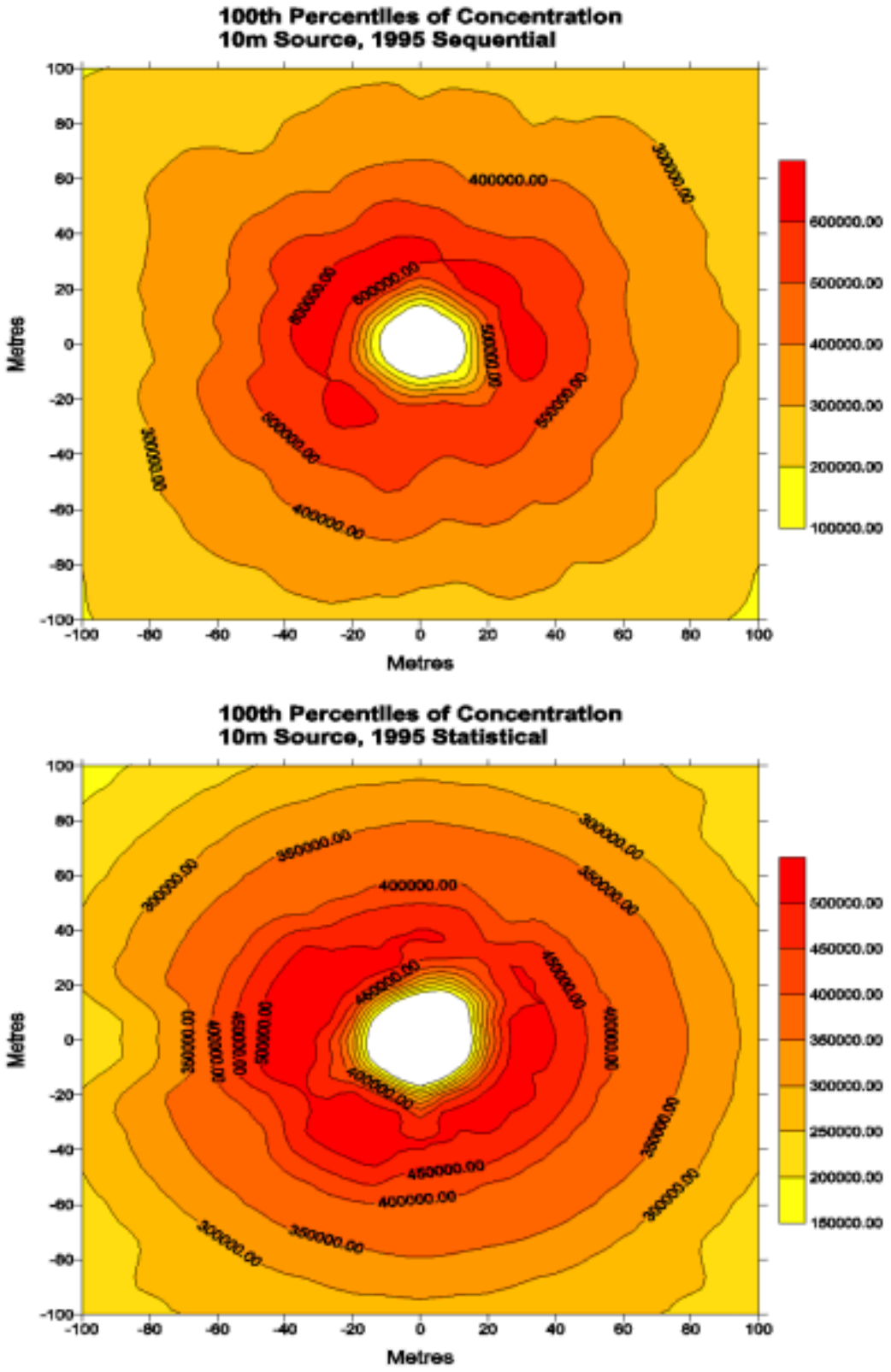

FIGURE D5b: 100th Percentiles of concentration for 10m source using 1995 sequential and statistical data

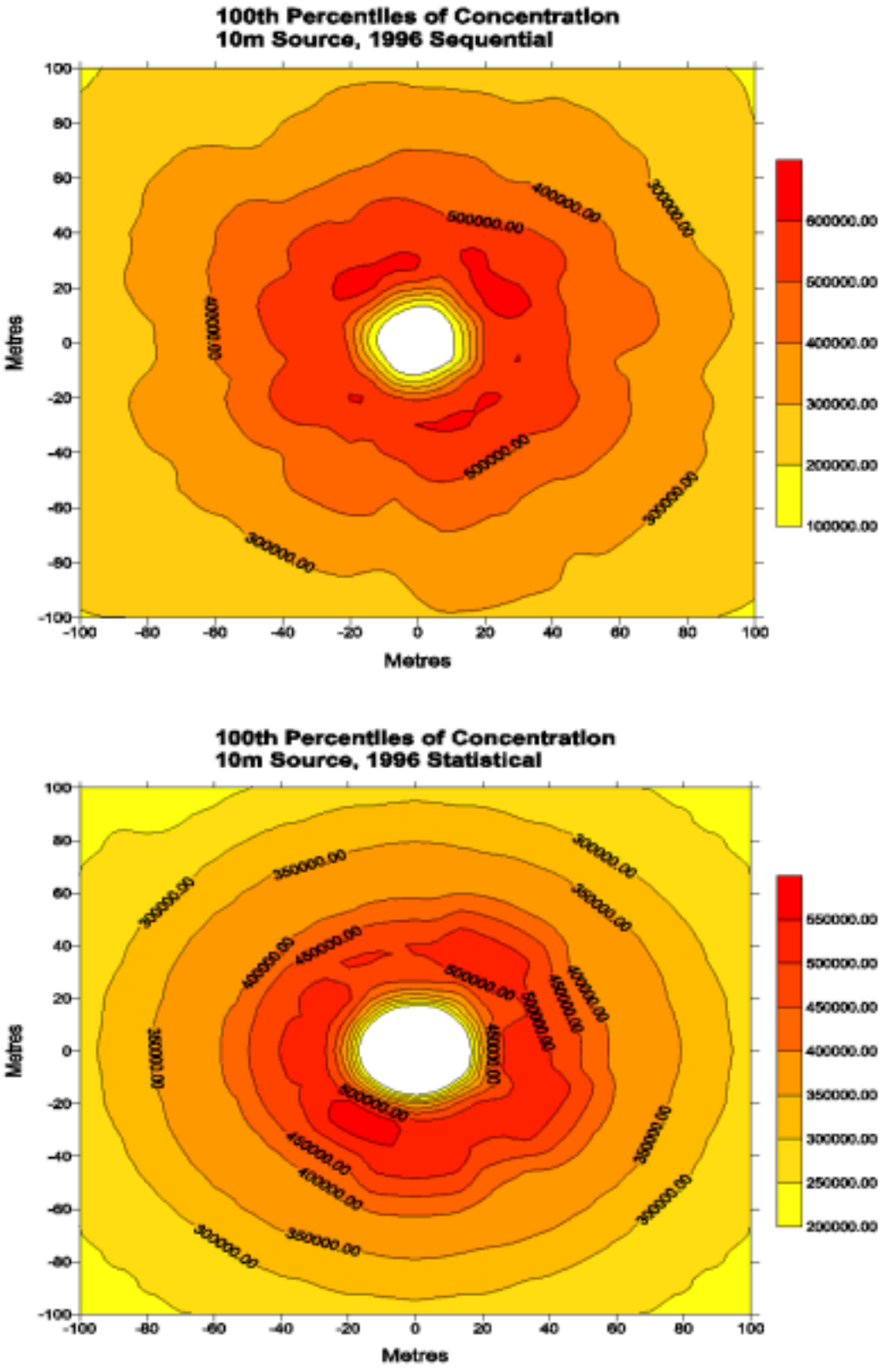

FIGURE D5c: 100th Percentiles of concentration for 10m source using 1996 sequential and statistical data

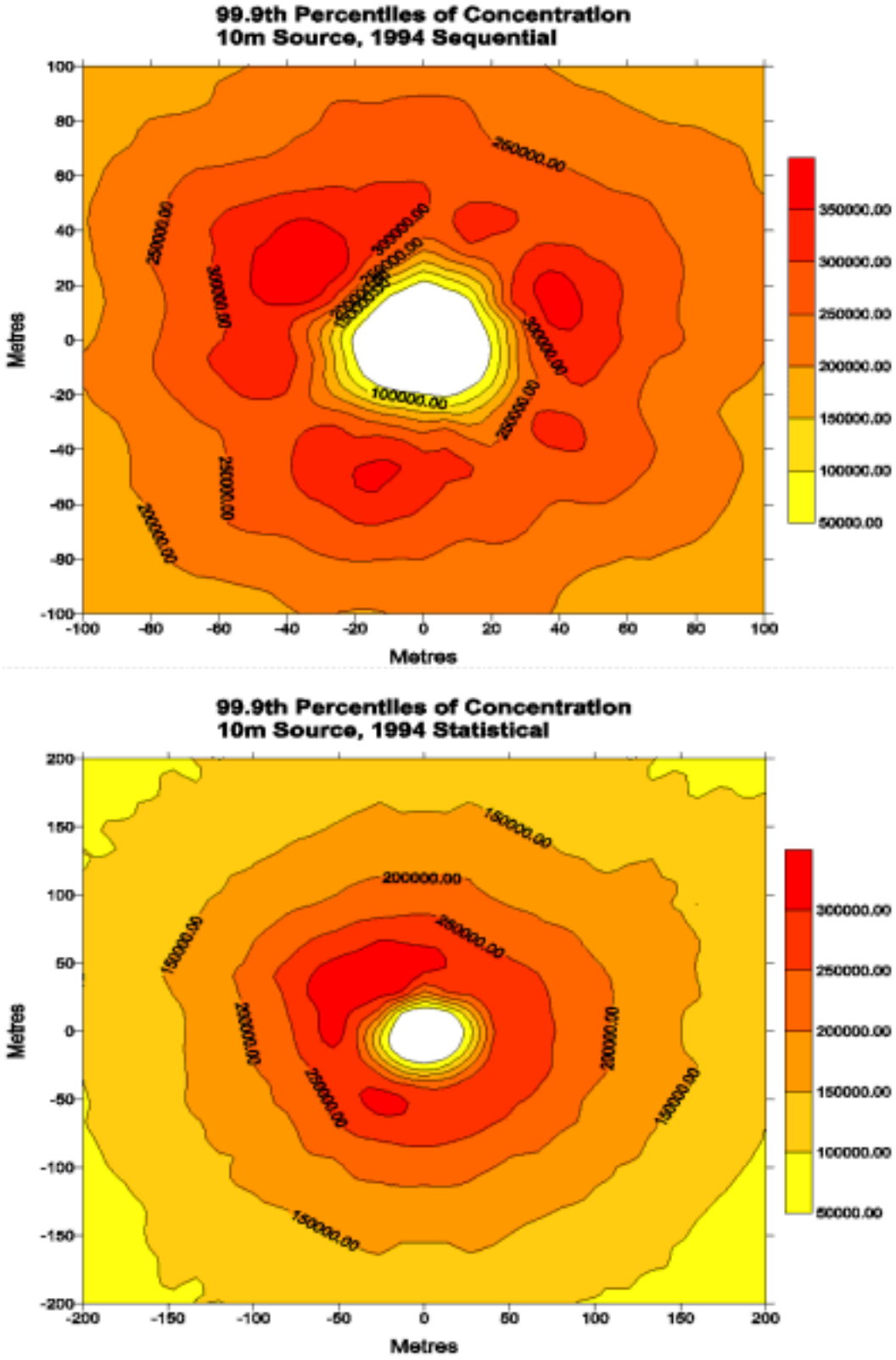

FIGURE D5d: 99.9th Percentiles of concentration for 10m source using 1994 sequential and statistical data

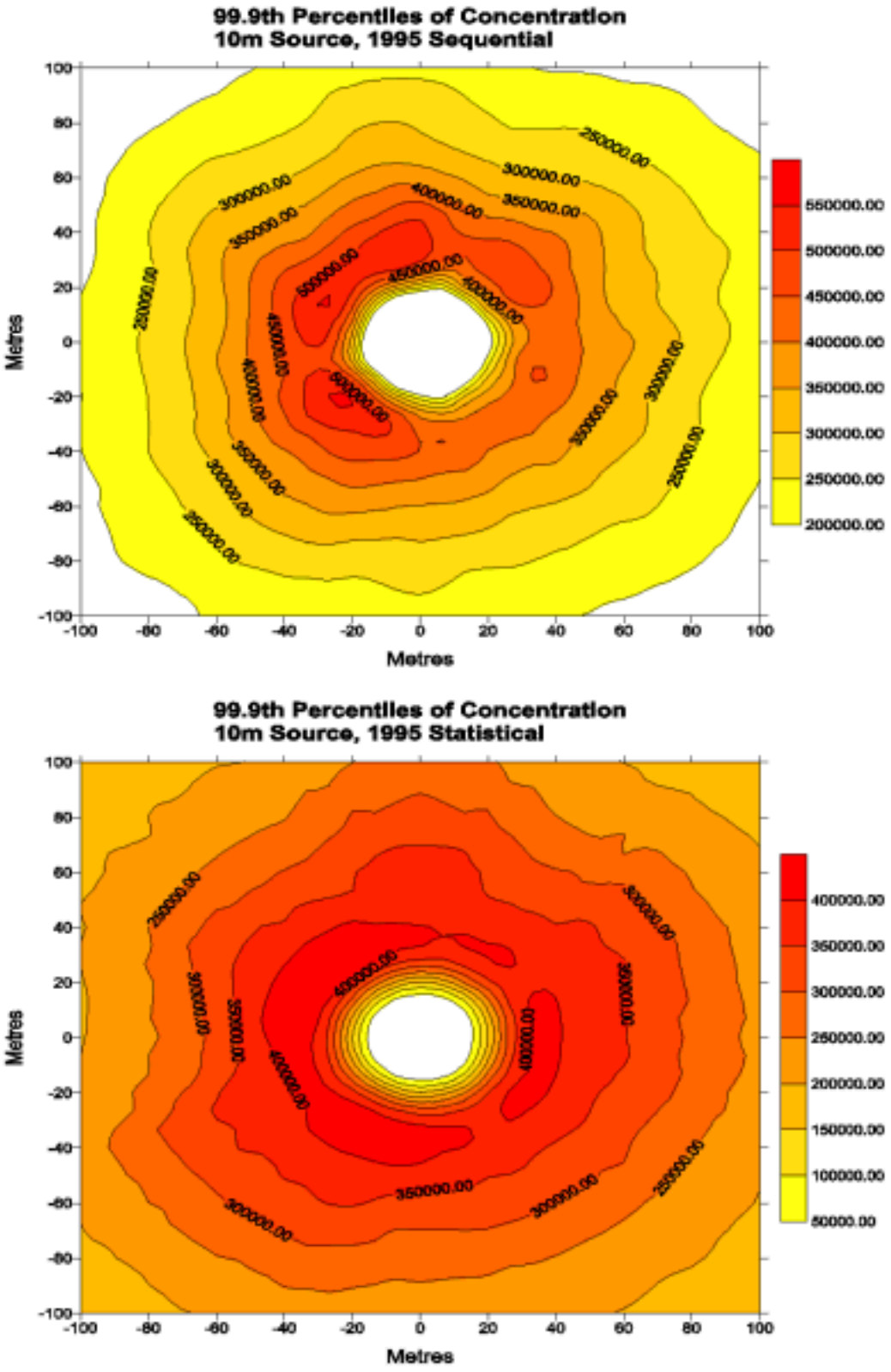

FIGURE D5e: 99.9th Percentiles of concentration for 10m source using 1995 sequential and statistical data

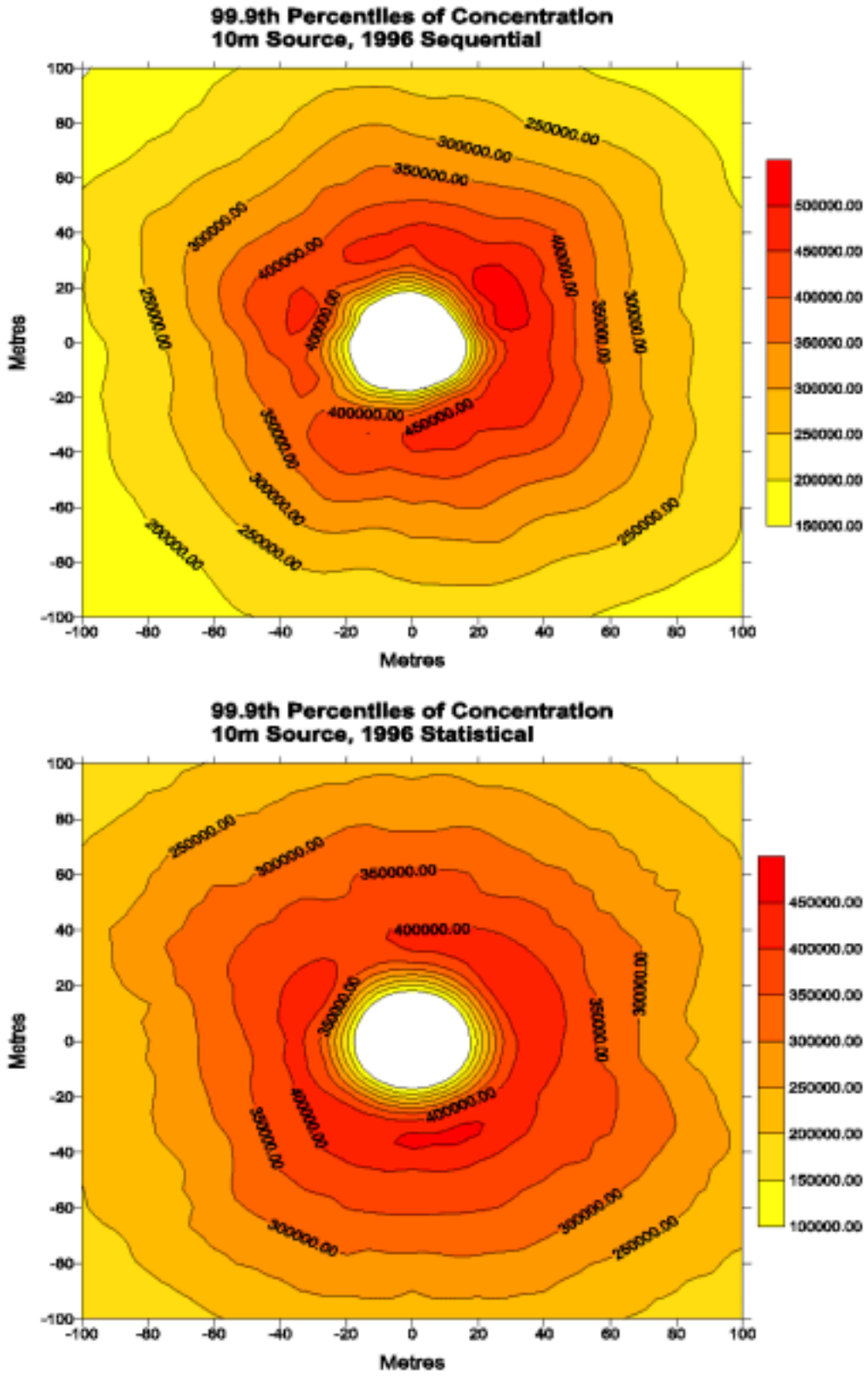

FIGURE D5f: 99.9th Percentiles of concentration for 10m source using 1996 sequential and statistical data

APPENDIX E

Figures E1a to E1f

Case A

Release Height	Release Velocity	Release Temperature
100m	9m/s	15°C

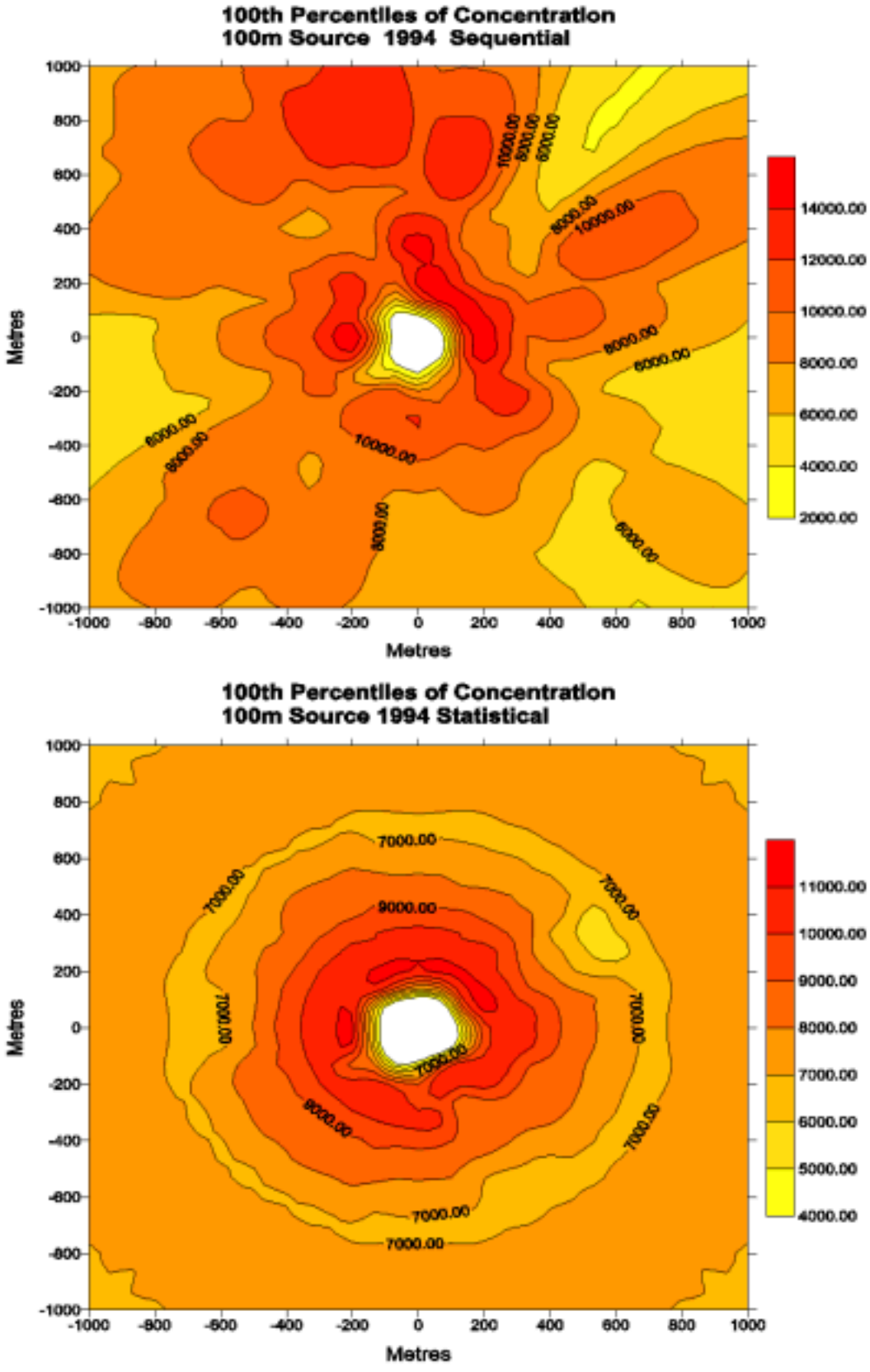

FIGURE E1a: 100th Percentiles of concentration for 100m source using 1994 sequential and statistical data

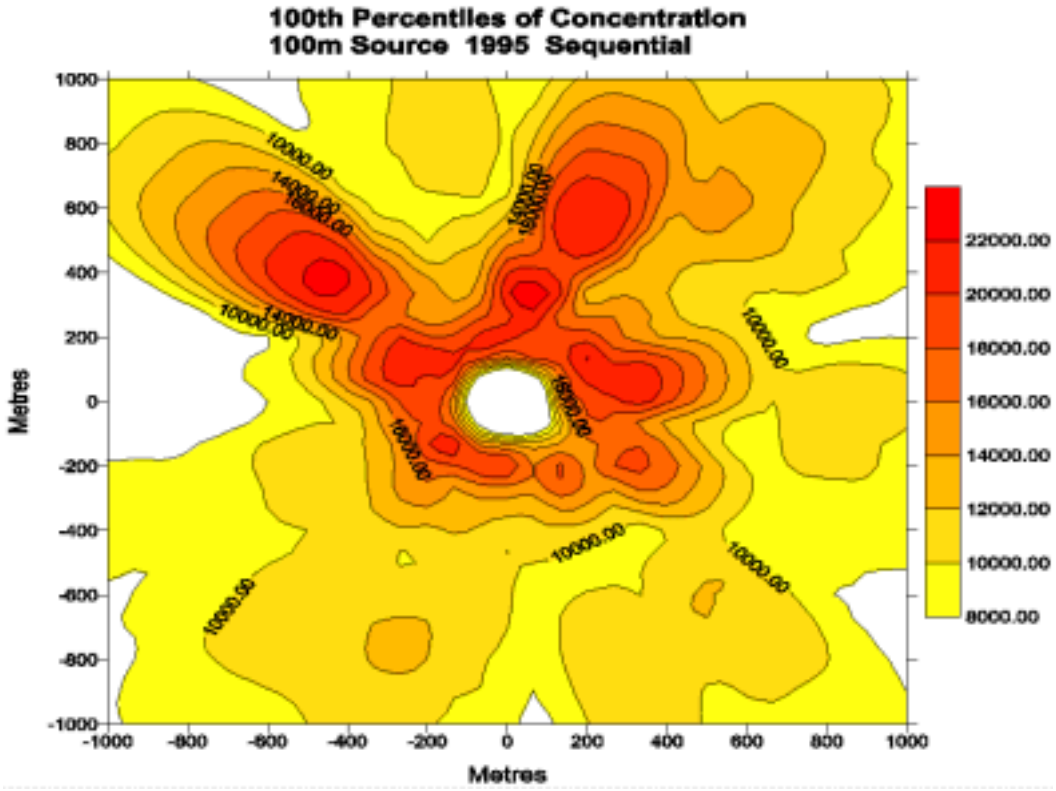

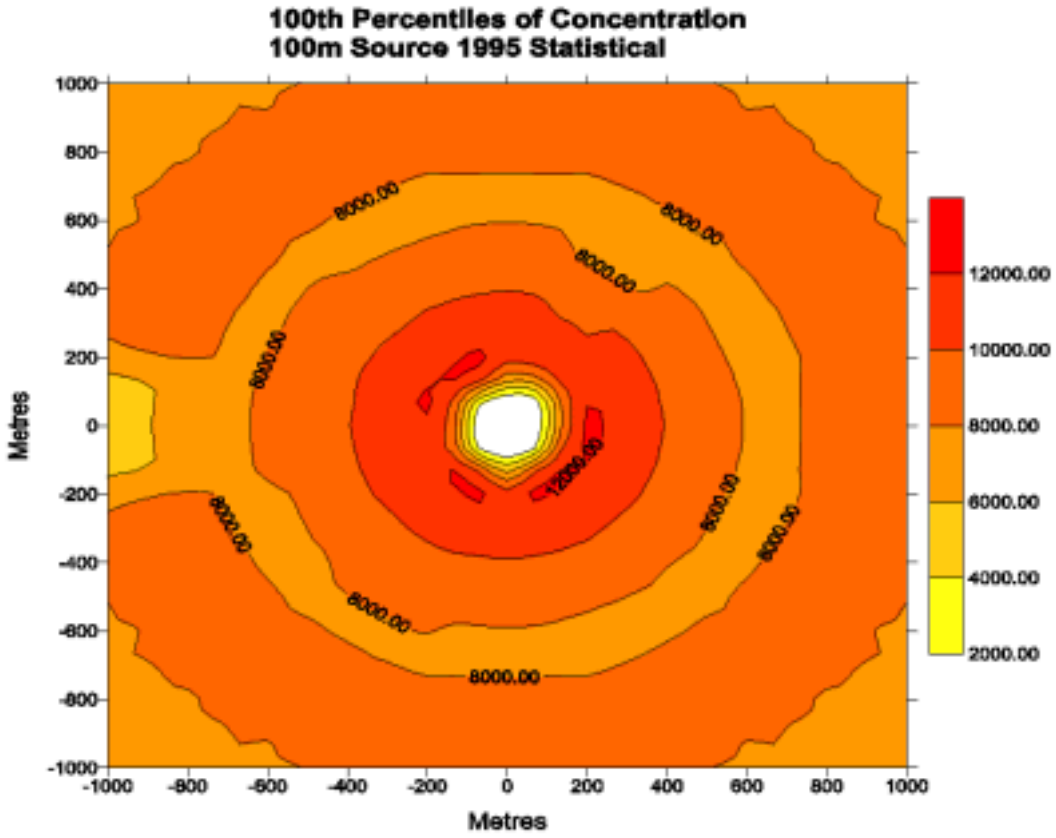

FIGURE E1b: 100th Percentiles of concentration for 100m source using 1995 sequential and statistical data

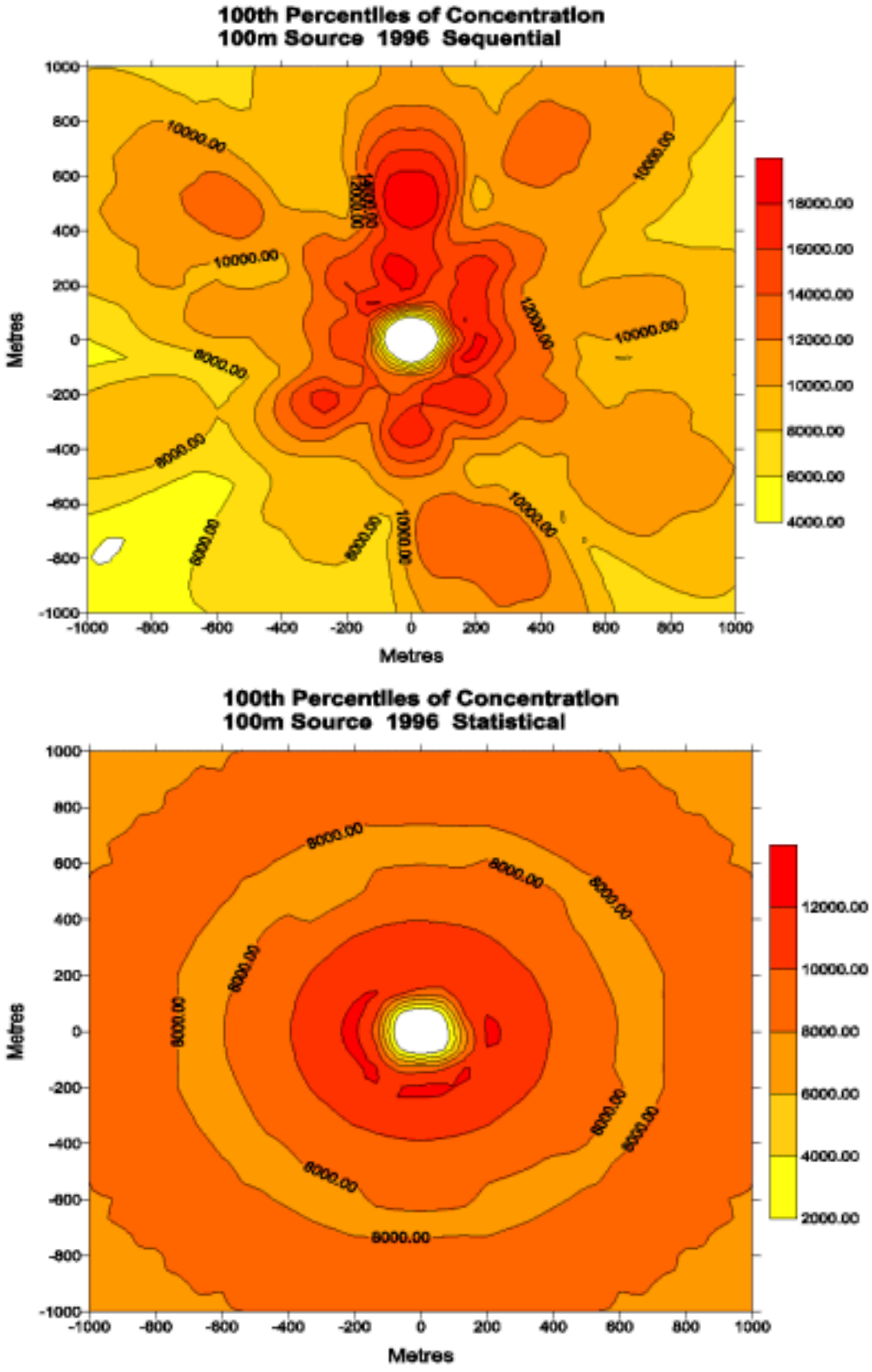

FIGURE E1c: 100th Percentiles of concentration for 100m source using 1996 sequential and statistical data

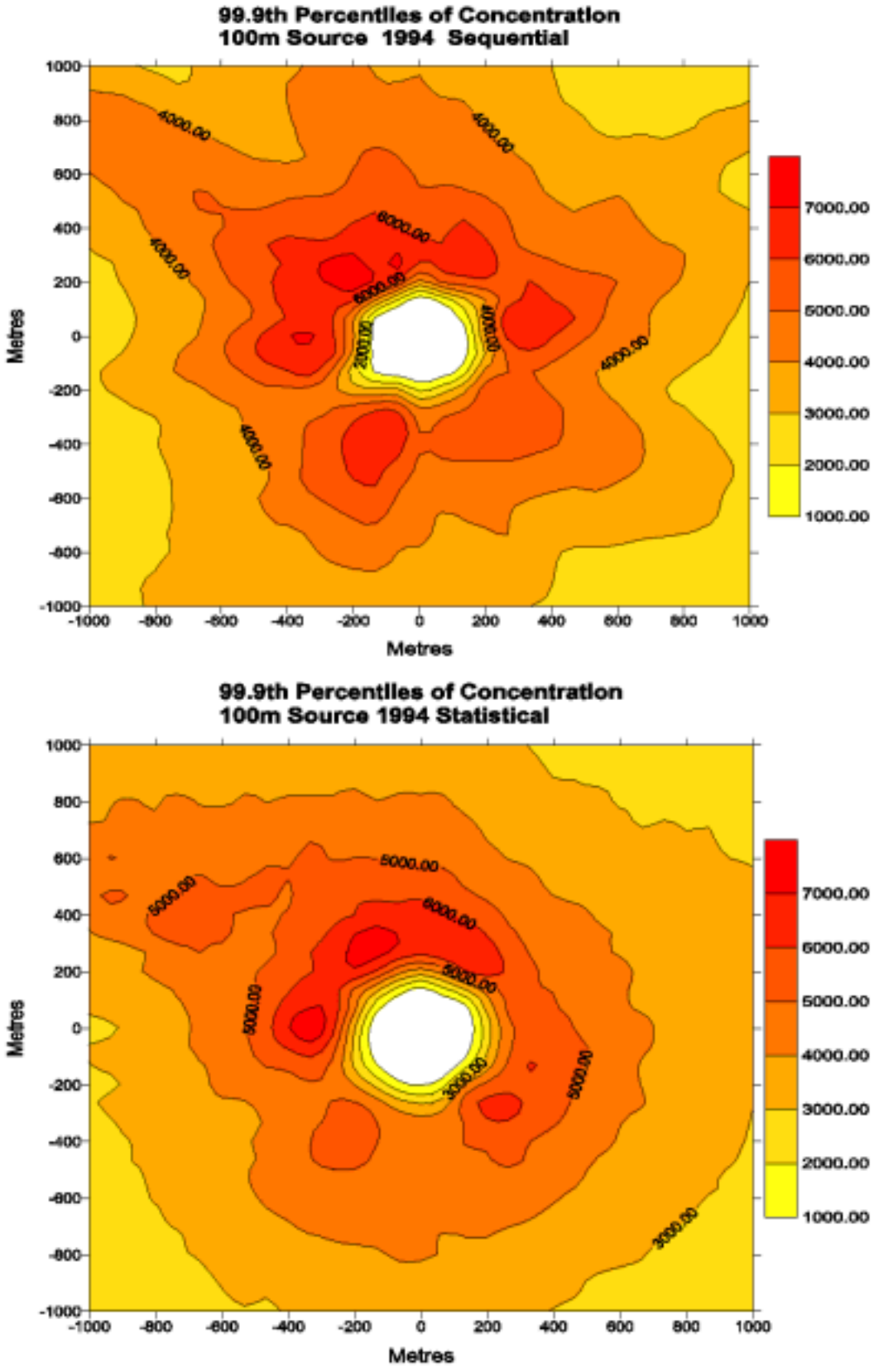

FIGURE E1d: 99.9th Percentiles of concentration for 100m source using 1994 sequential and statistical data

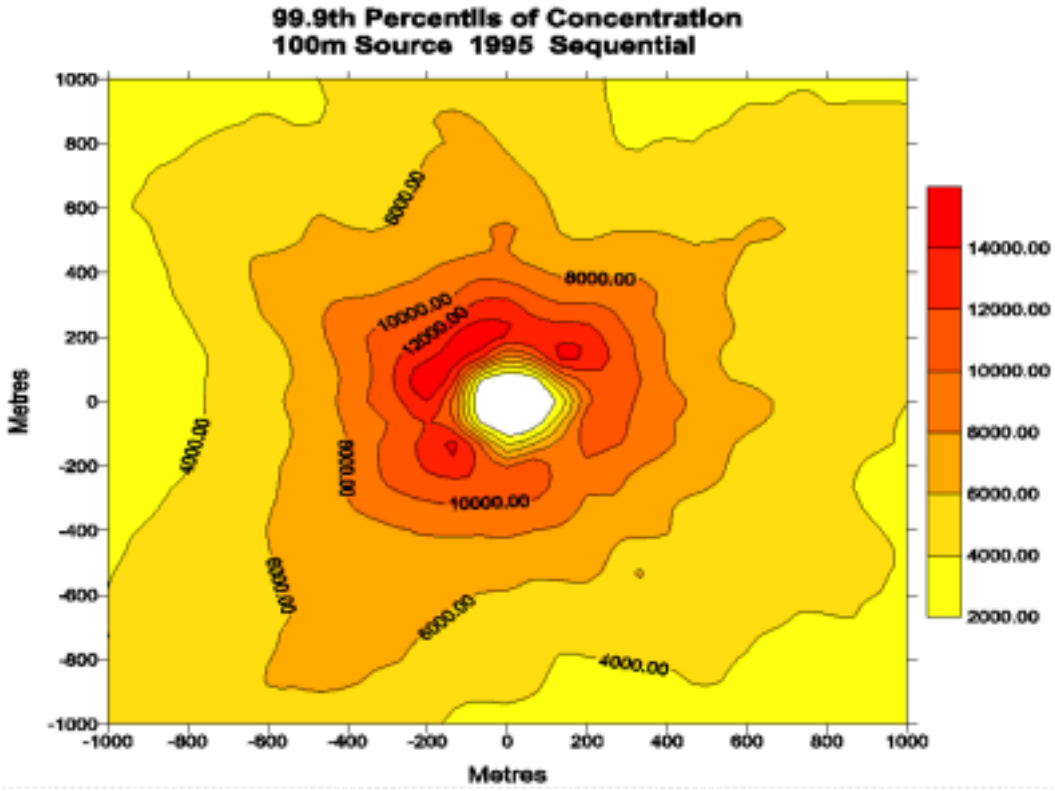

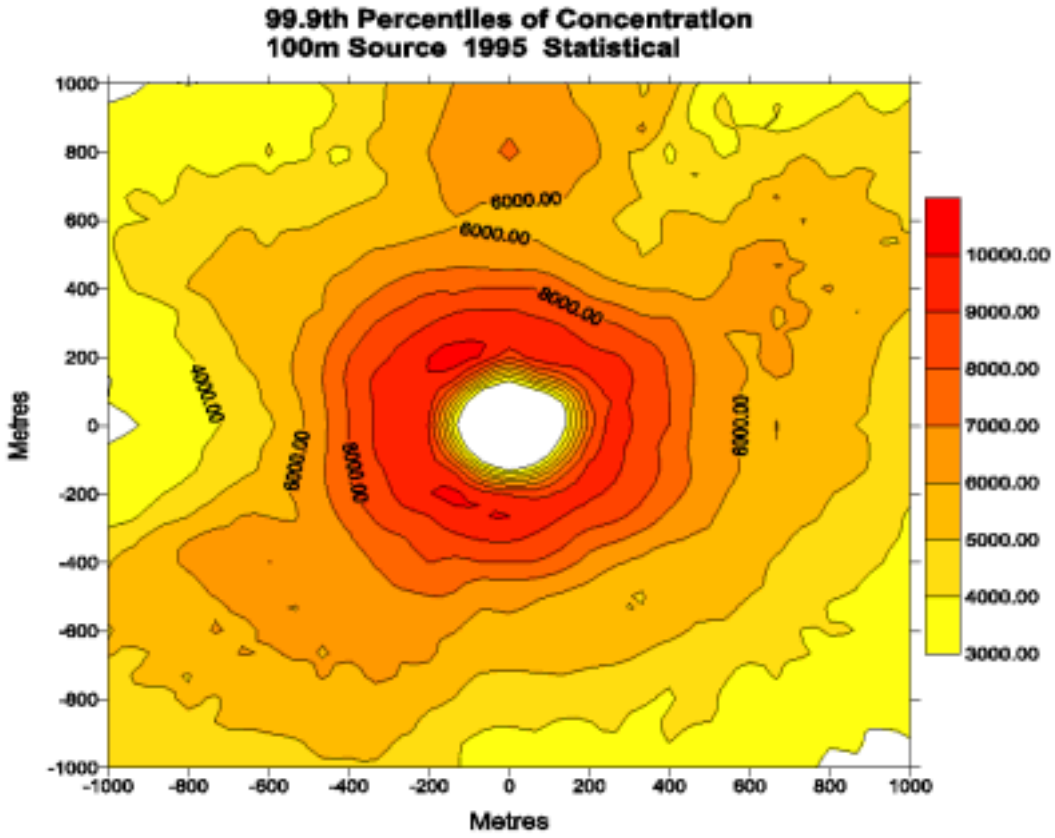

FIGURE E1e: 99.9th Percentiles of concentration for 100m source using 1995 sequential and statistical data

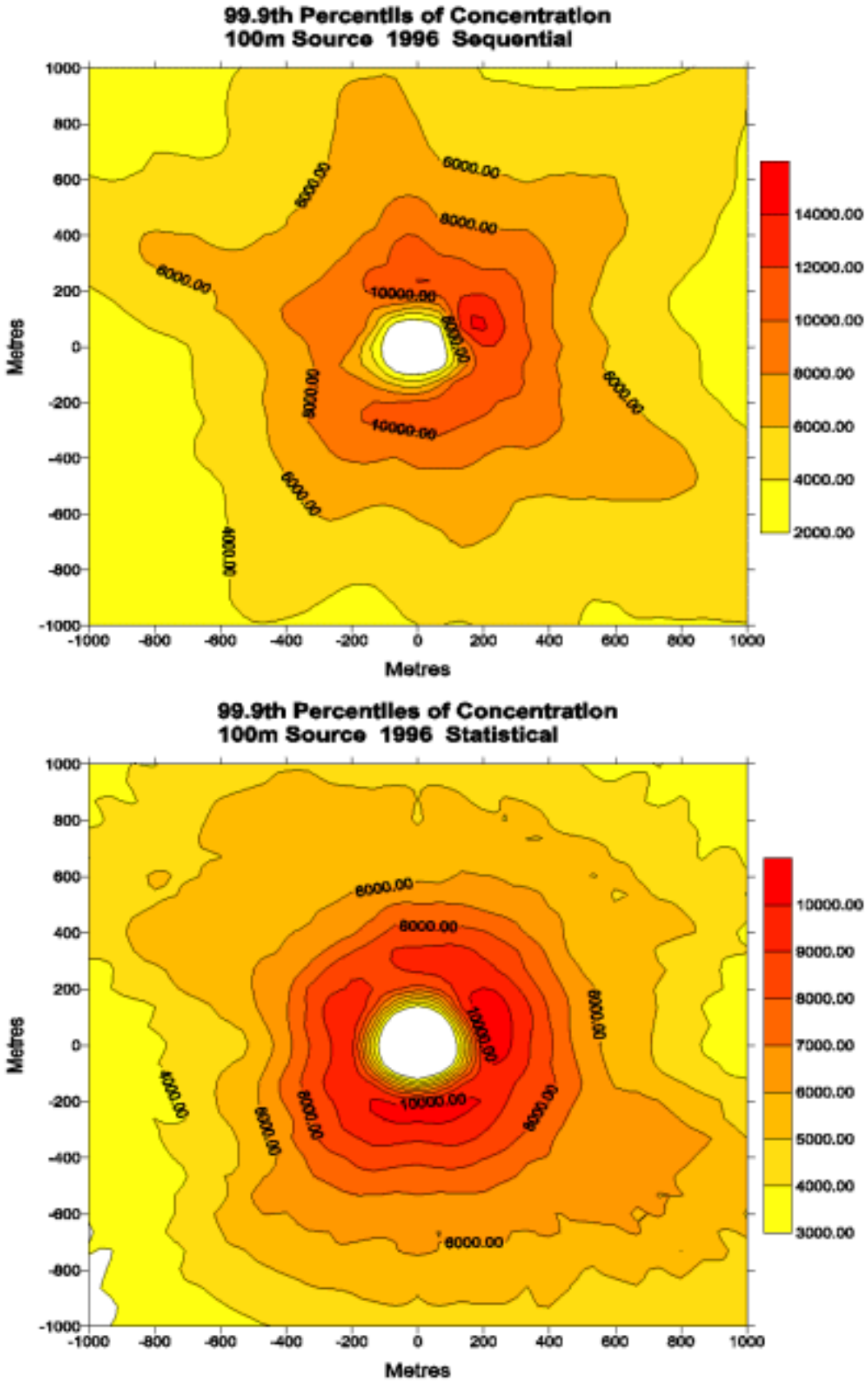

FIGURE E1f: 99.9th Percentiles of concentration for 100m source using 1996 sequential and statistical data

Figures 2a to 2f

Figures E2a to E2f

Case C

Release Height	Release Velocity	Release Temperature
75m	9m/s	15°C

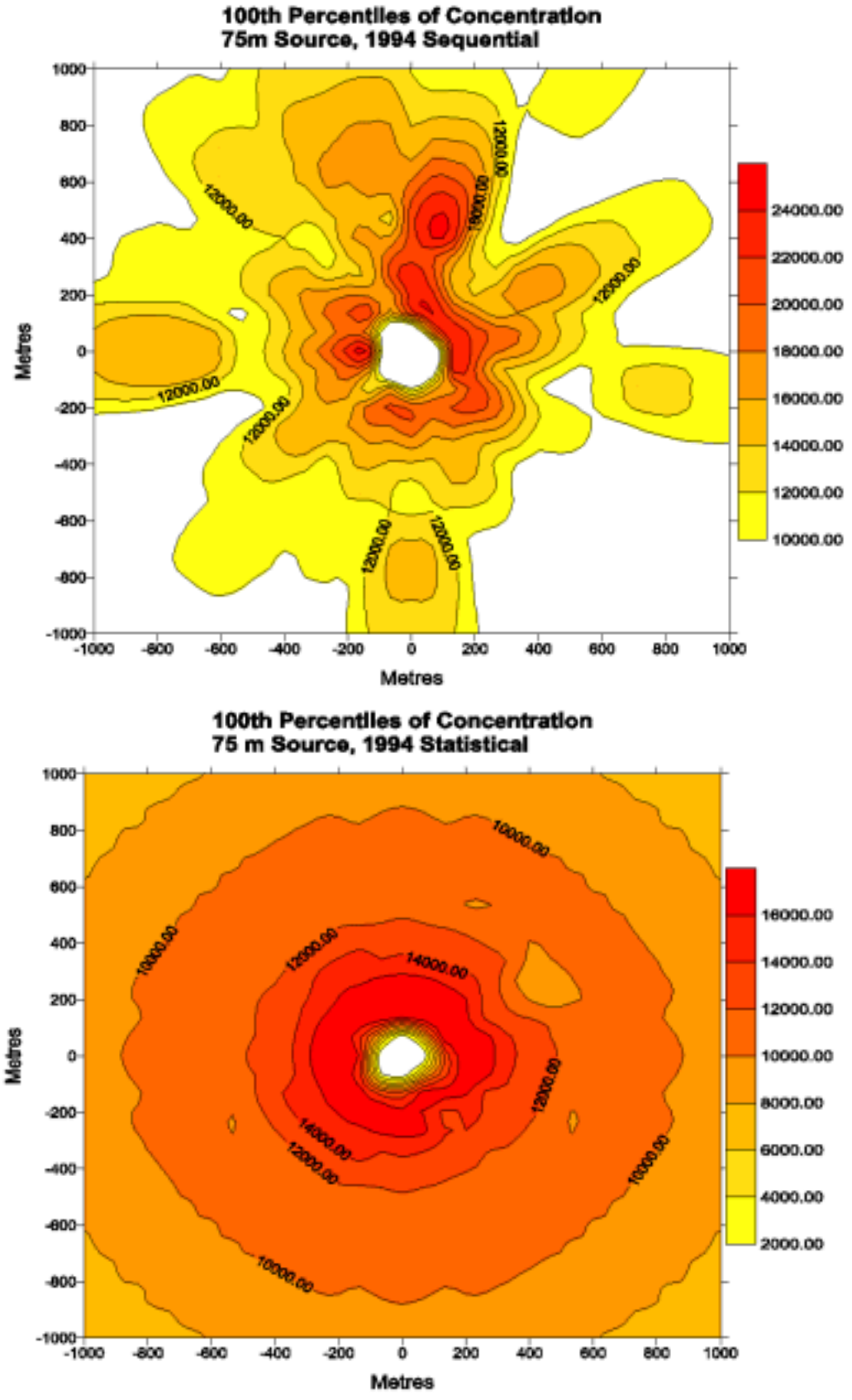

FIGURE E2a: 100th Percentiles of concentration for 75m source using 1994 sequential and statistical data

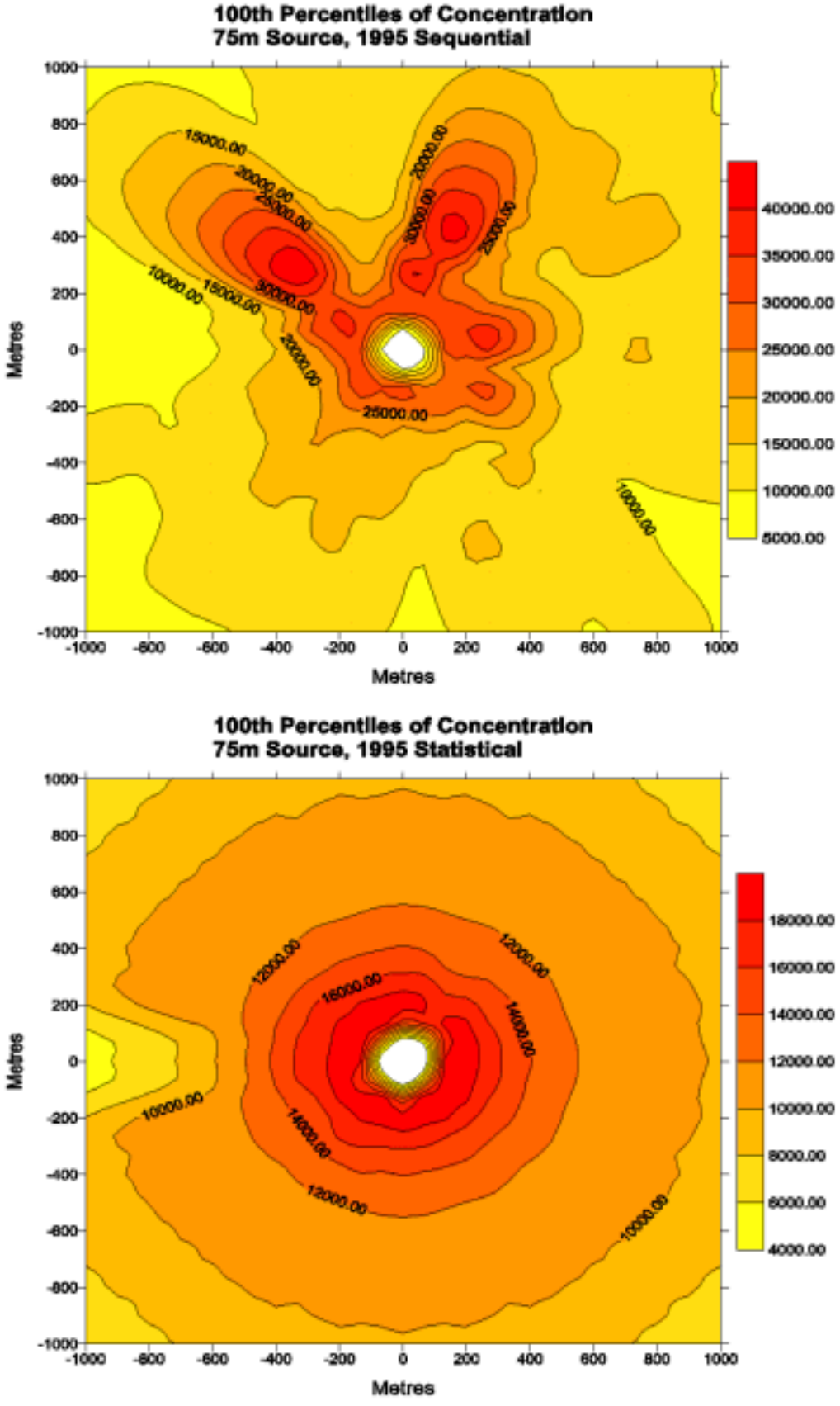

FIGURE E2b: 100th Percentiles of concentration for 75m source using 1995 sequential and statistical data

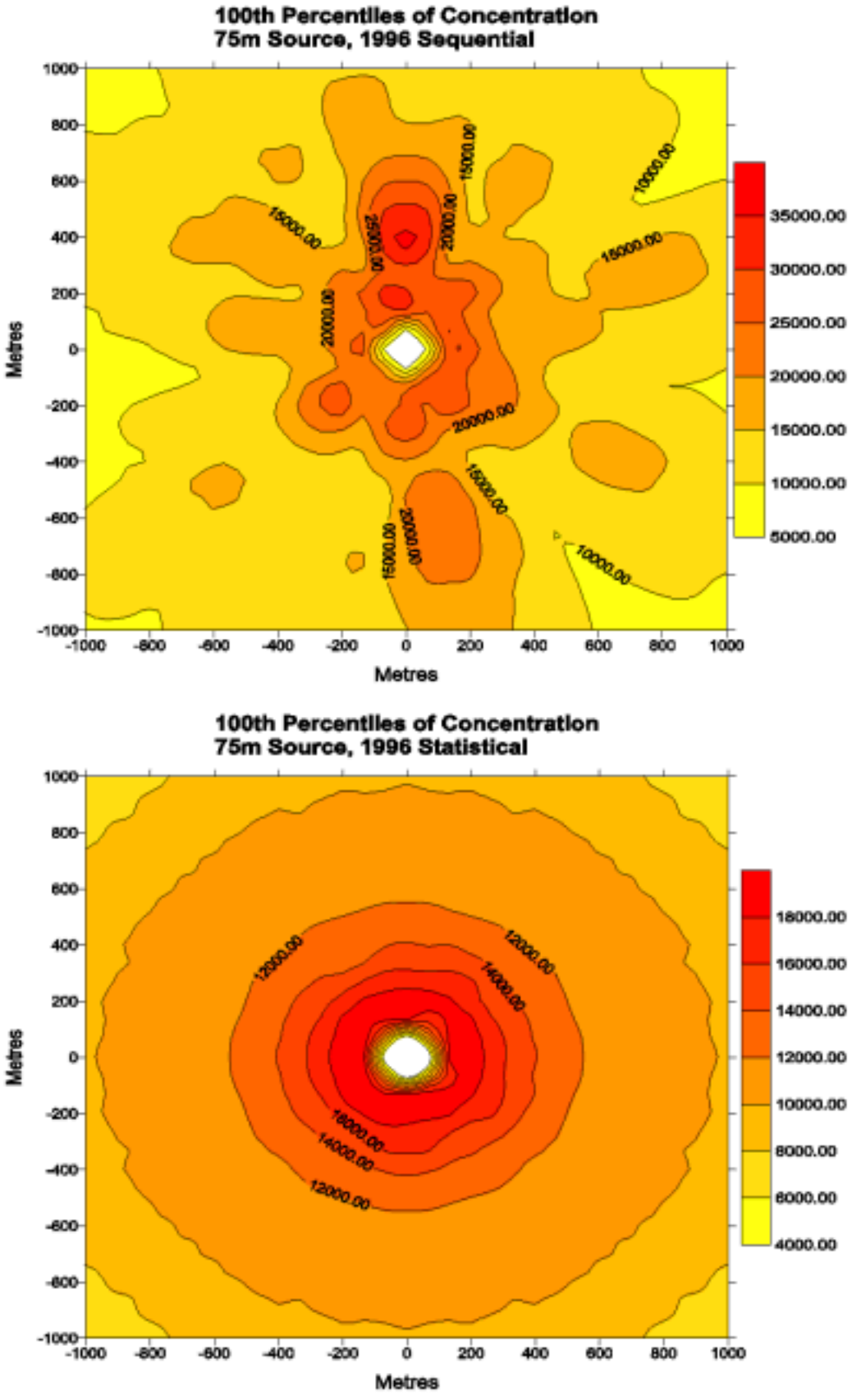

FIGURE E2c: 100th Percentiles of concentration for 75m source using 1996 sequential and statistical data

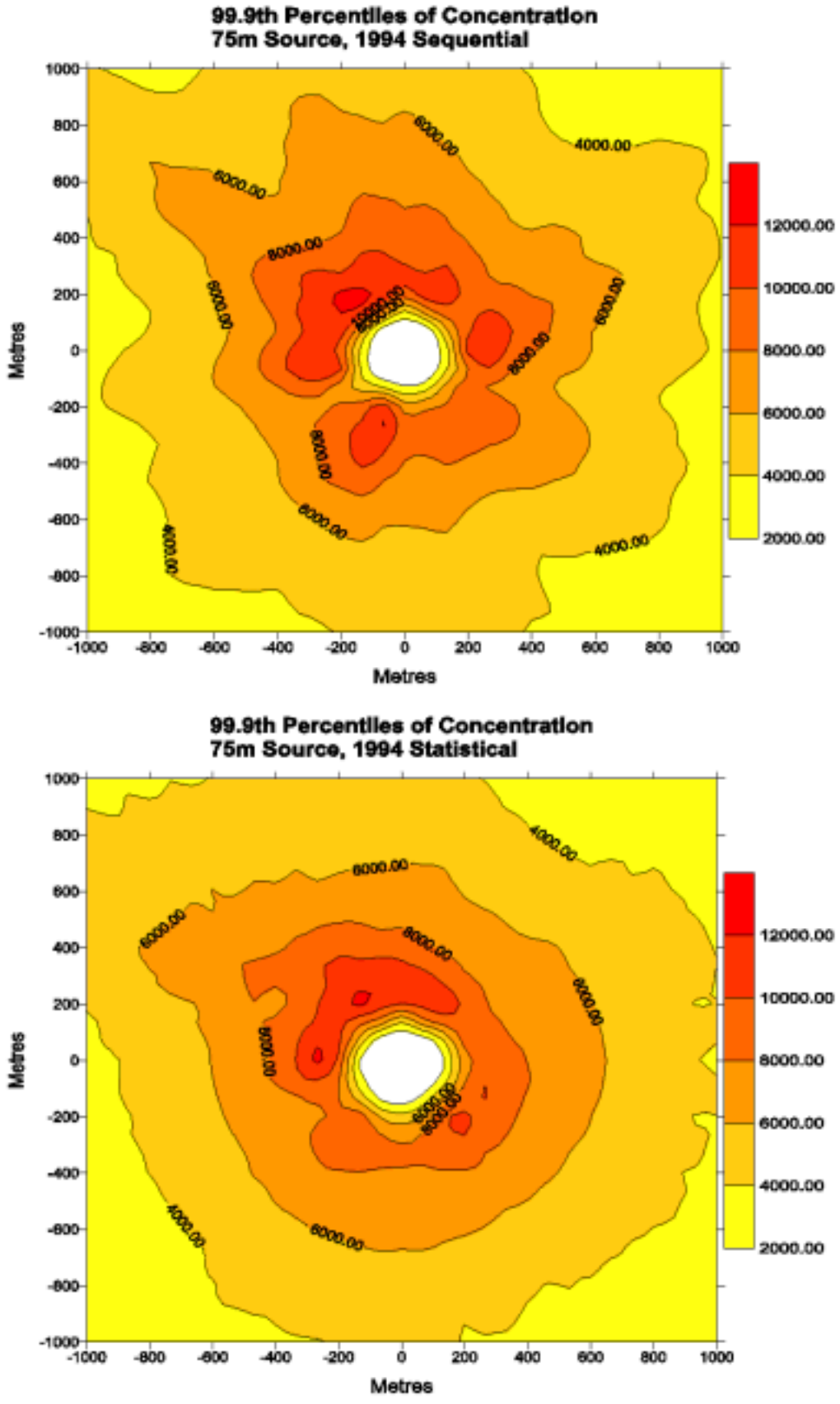

FIGURE E2d: 99.9th Percentiles of concentration for 75m source using 1994 sequential and statistical data

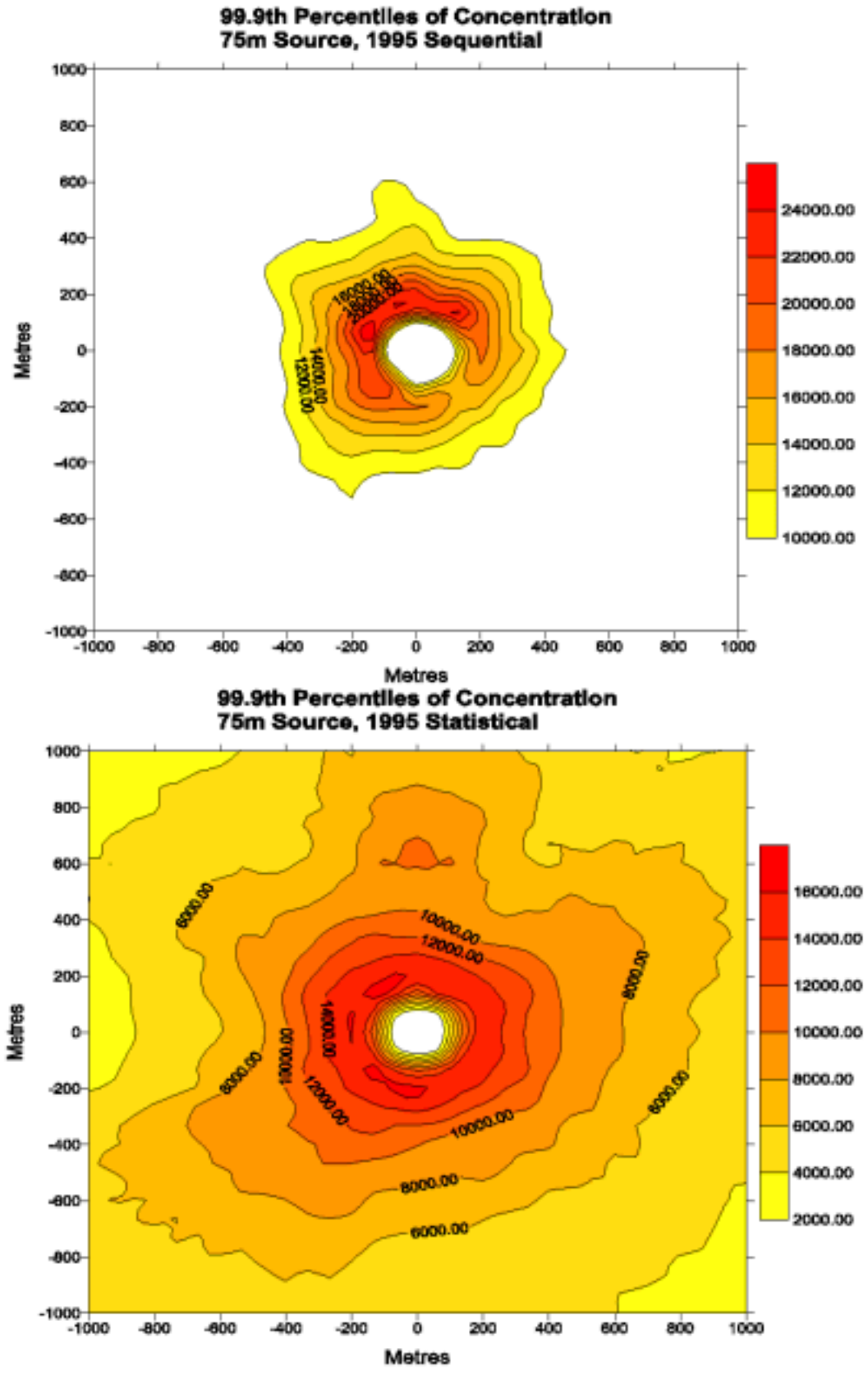

FIGURE E2e: 99.9th Percentiles of concentration for 75m source using 1995 sequential and statistical data

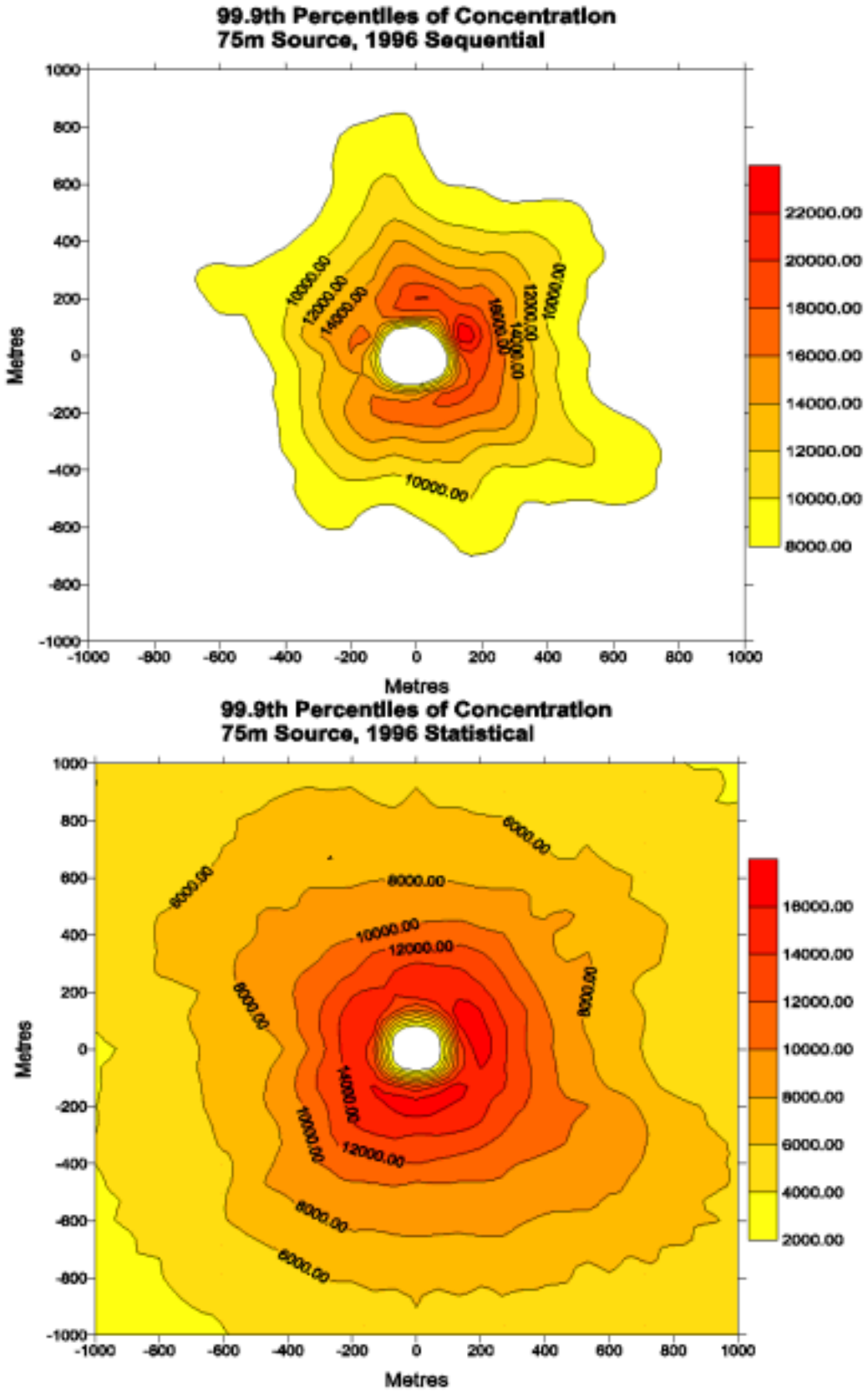

FIGURE E2f: 99.9th Percentiles of concentration for 75m source using 1996 sequential and statistical data

Figures E3a to E3f

Case E

Release Height	Release Velocity	Release Temperature
50m	9m/s	15°C

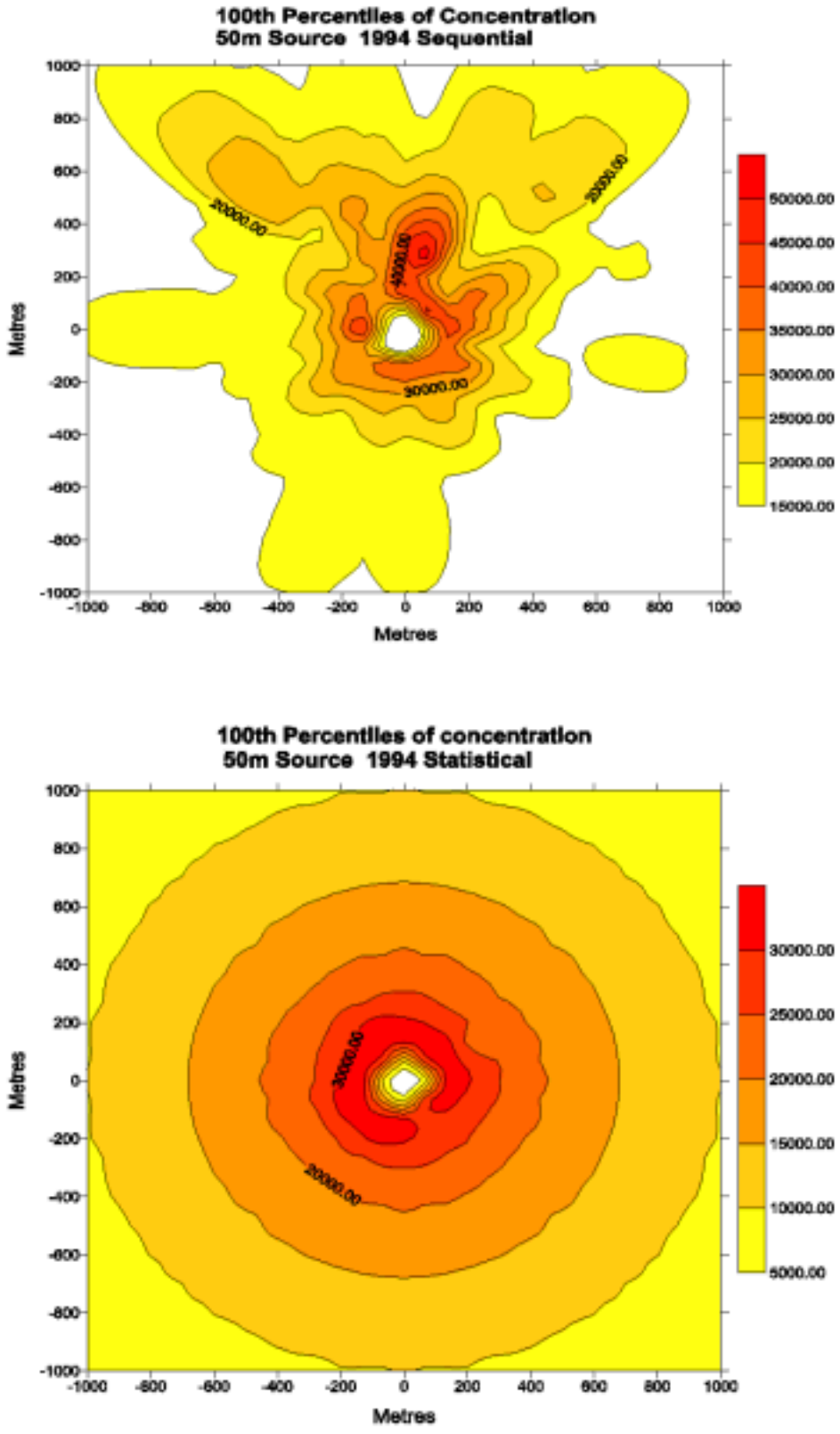

FIGURE E3a: 100th Percentiles of concentration for 50m source using 1994 sequential and statistical data

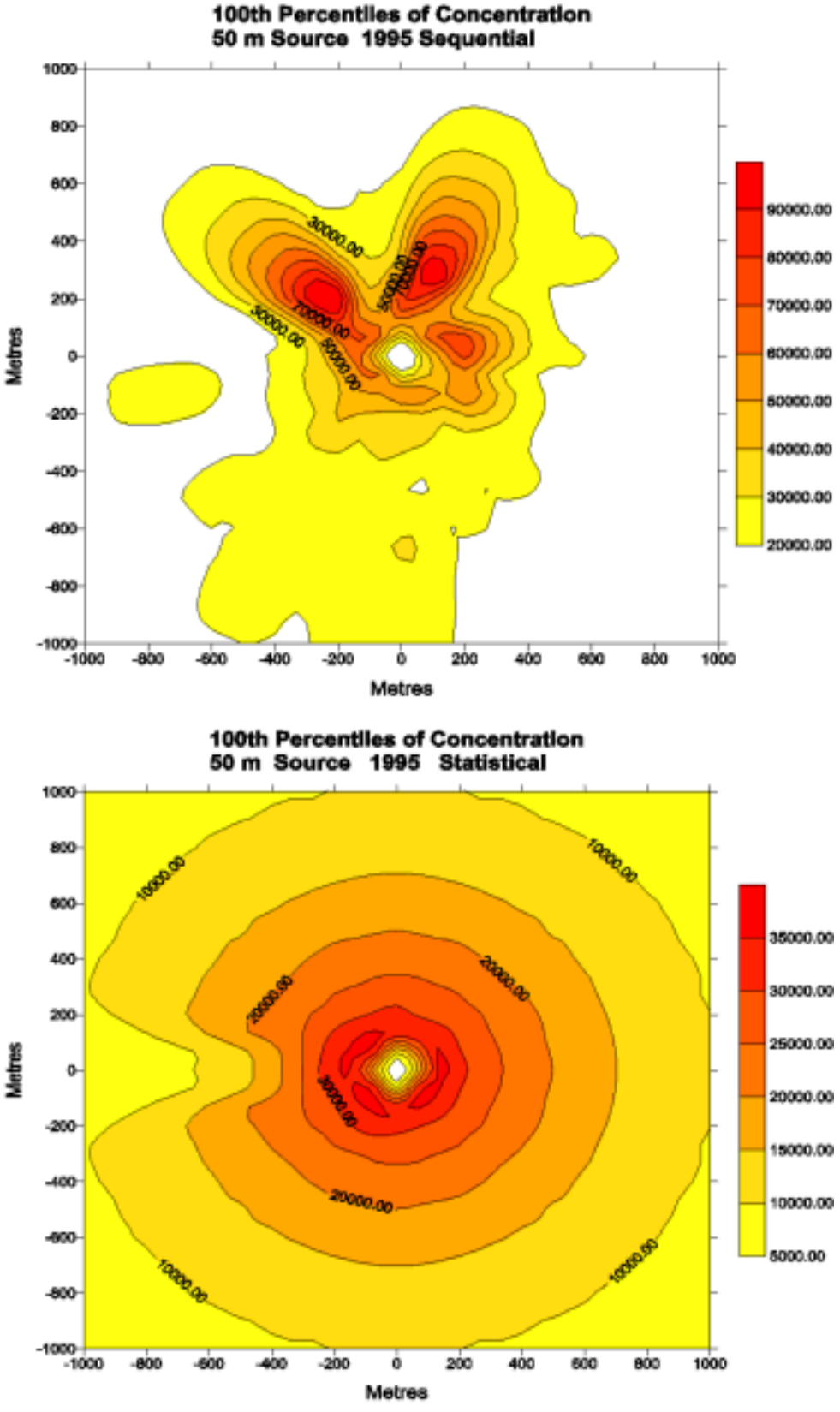

FIGURE E3b: 100th Percentiles of concentration for 50m source using 1995 sequential and statistical data

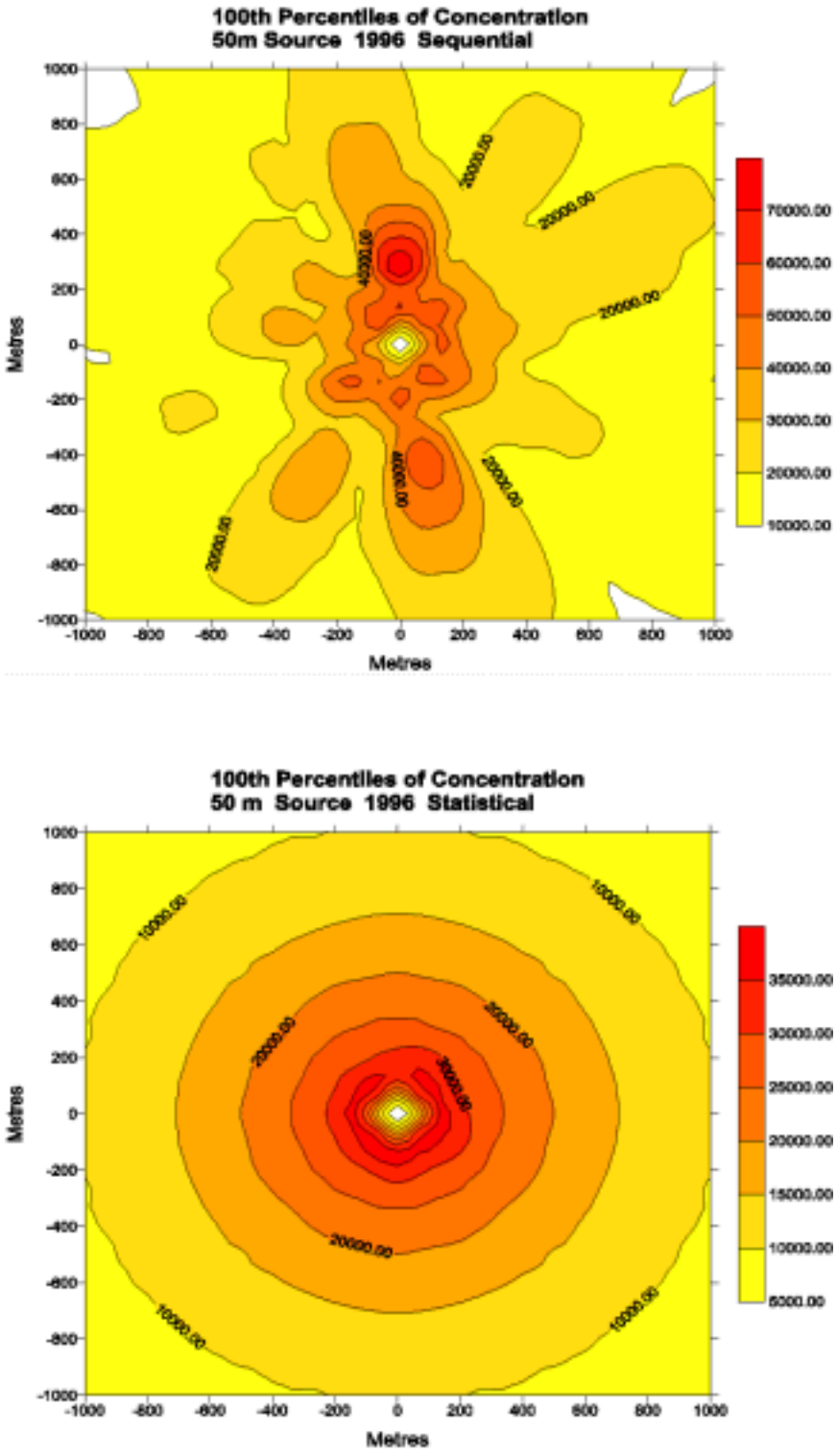

FIGURE E3c: 100th Percentiles of concentration for 50m source using 1996 sequential and statistical data

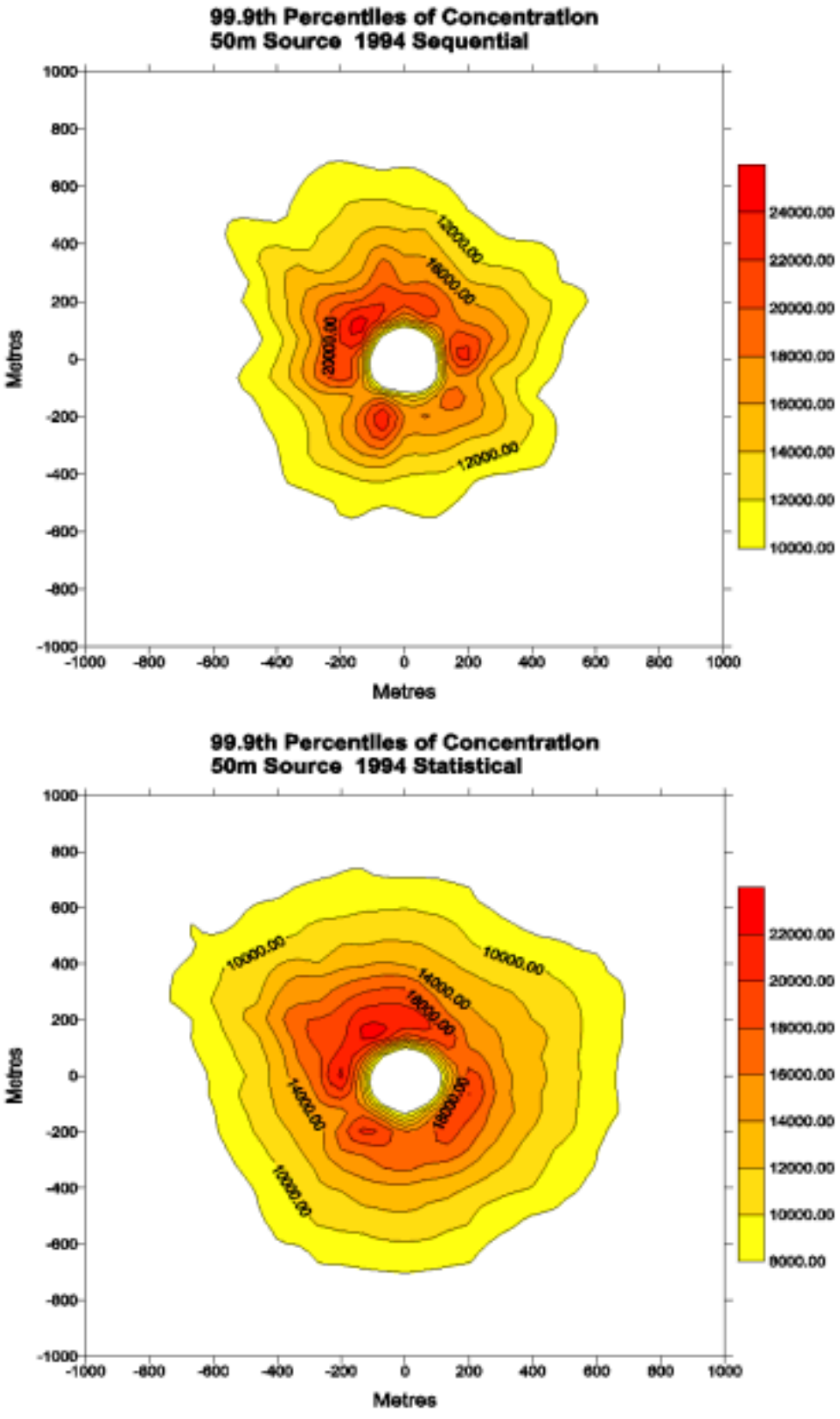

FIGURE E3d: 99.9th Percentiles of concentration for 50m source using 1994 sequential and statistical data

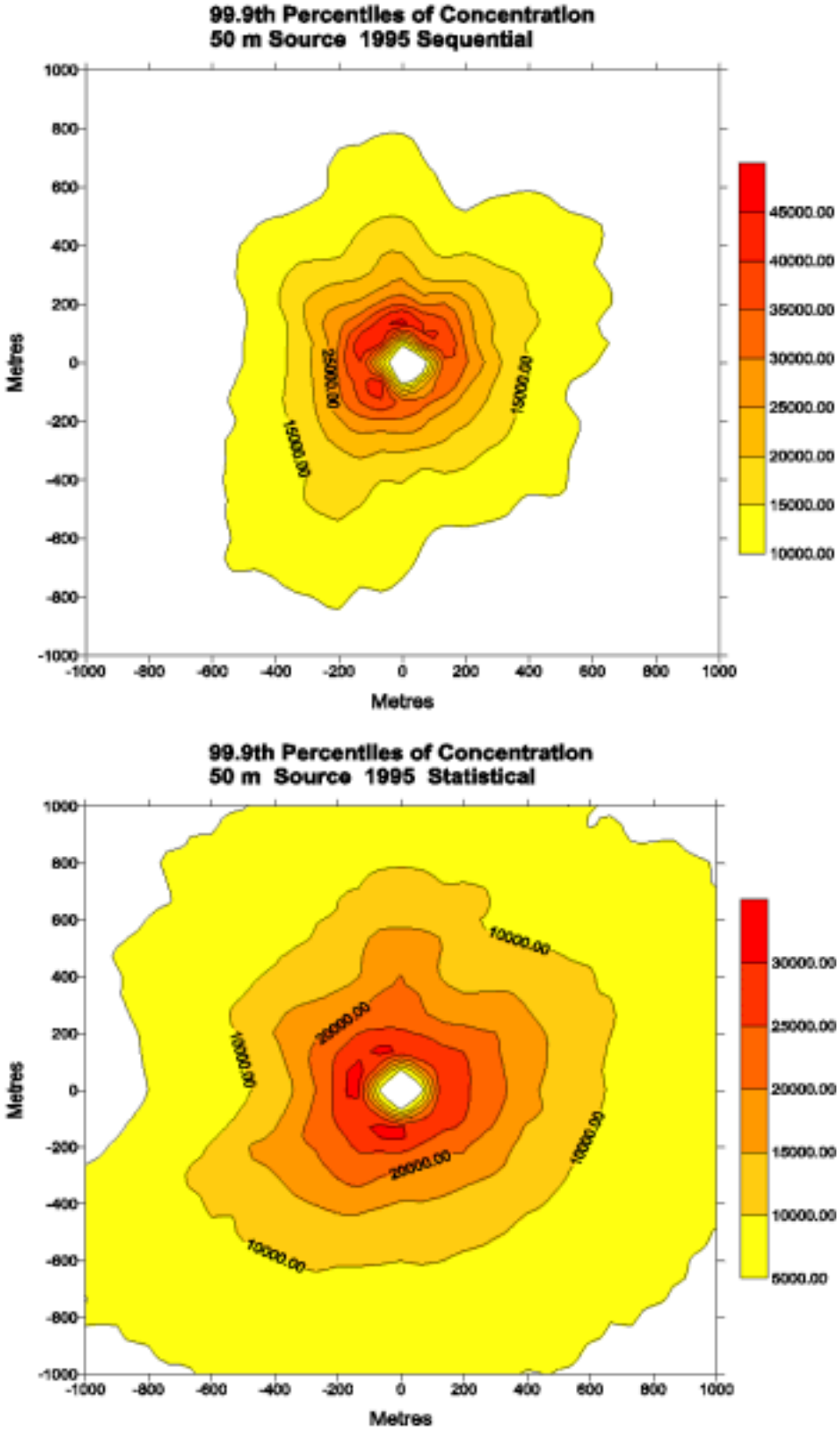

FIGURE E3e: 99.9th Percentiles of concentration for 50m source using 1995 sequential and statistical data

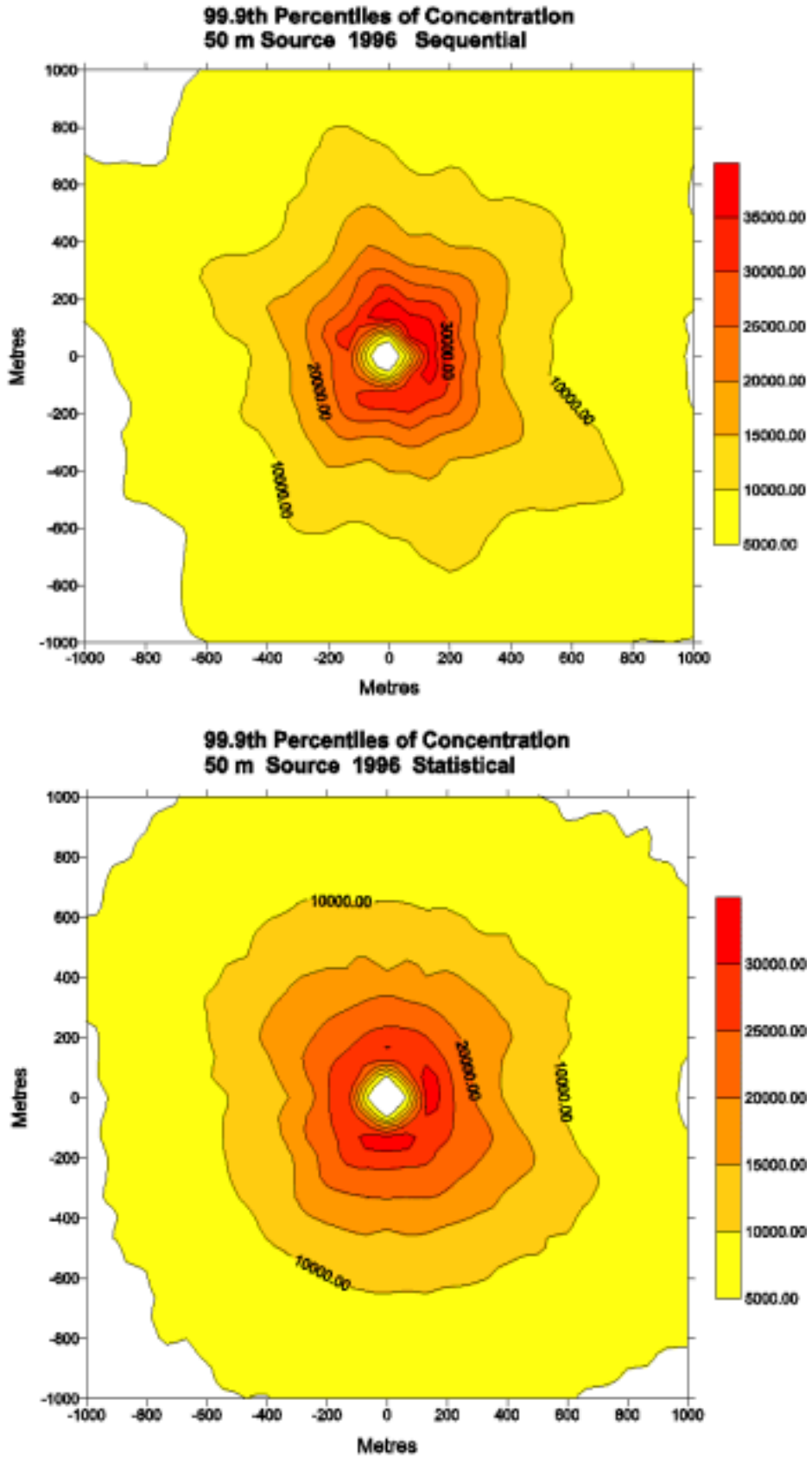

FIGURE E3f: 99.9th Percentiles of concentration for 50m source using 1996 sequential and statistical data

Figures E4a to E4f

Case G

Release Height	Release Velocity	Release Temperature
30m	9m/s	15°C

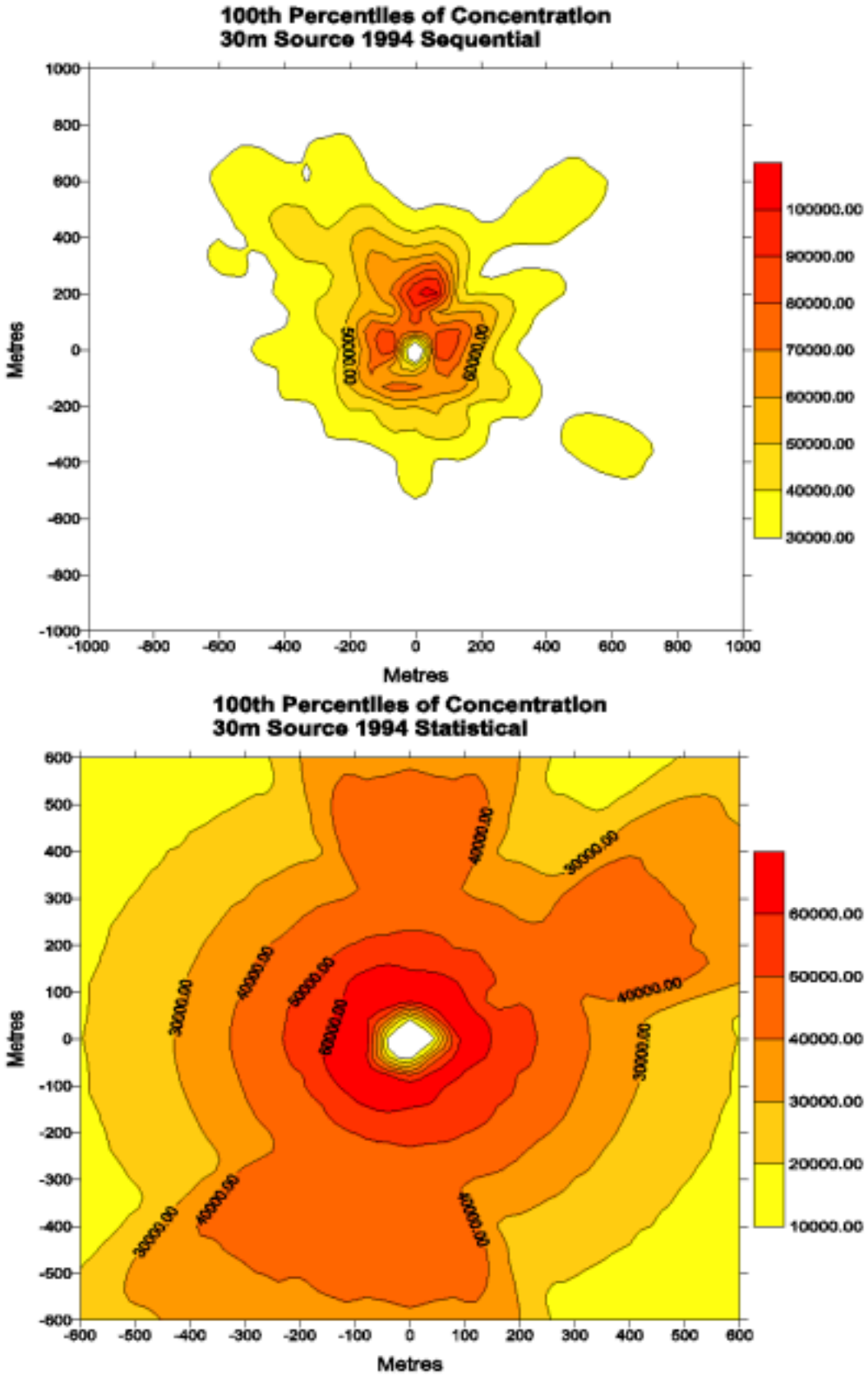

FIGURE E4a: 100th Percentiles of concentration for 30m source using 1994 sequential and statistical data

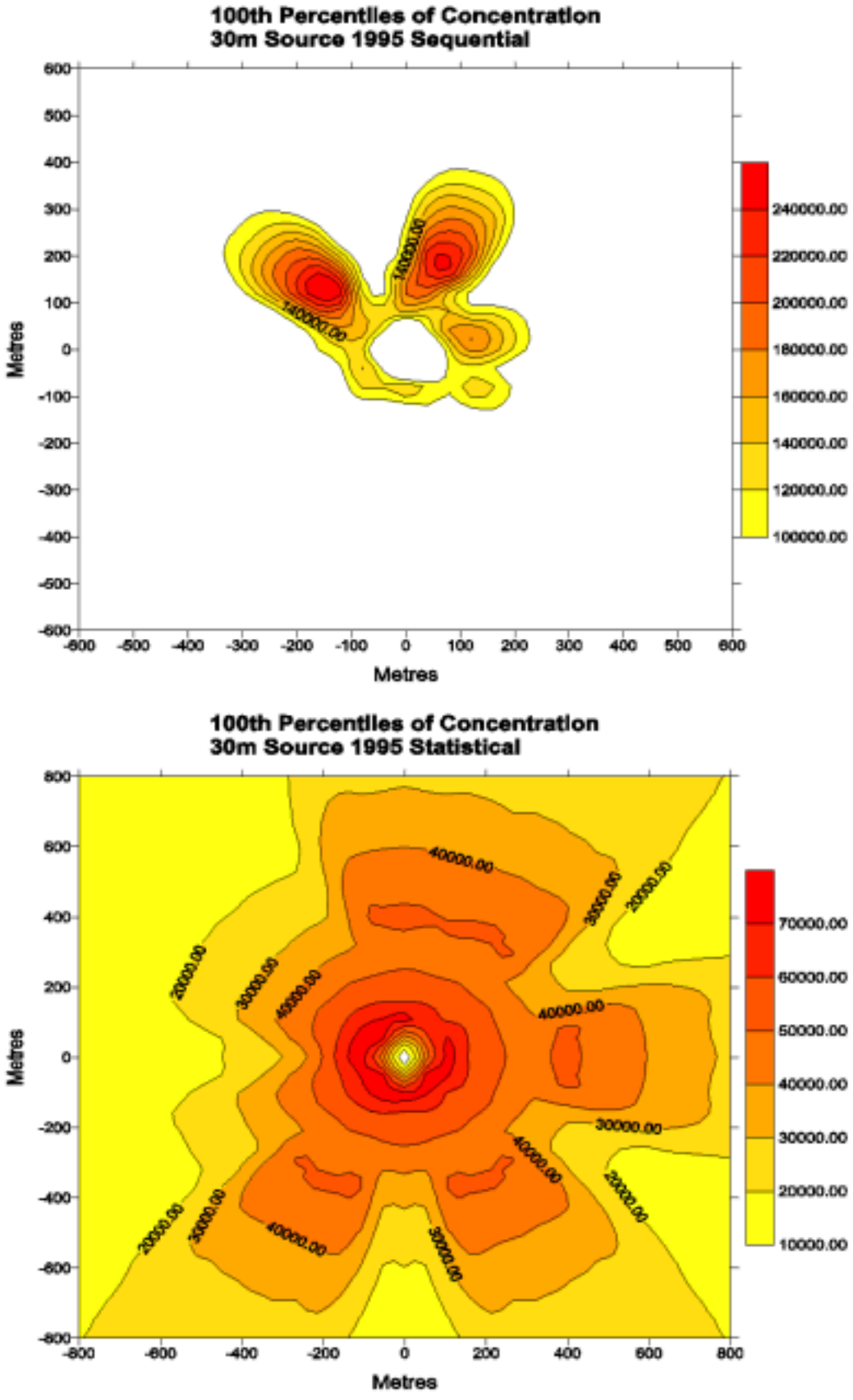

FIGURE E4b: 100th Percentiles of concentration for 30m source using 1995 sequential and statistical data

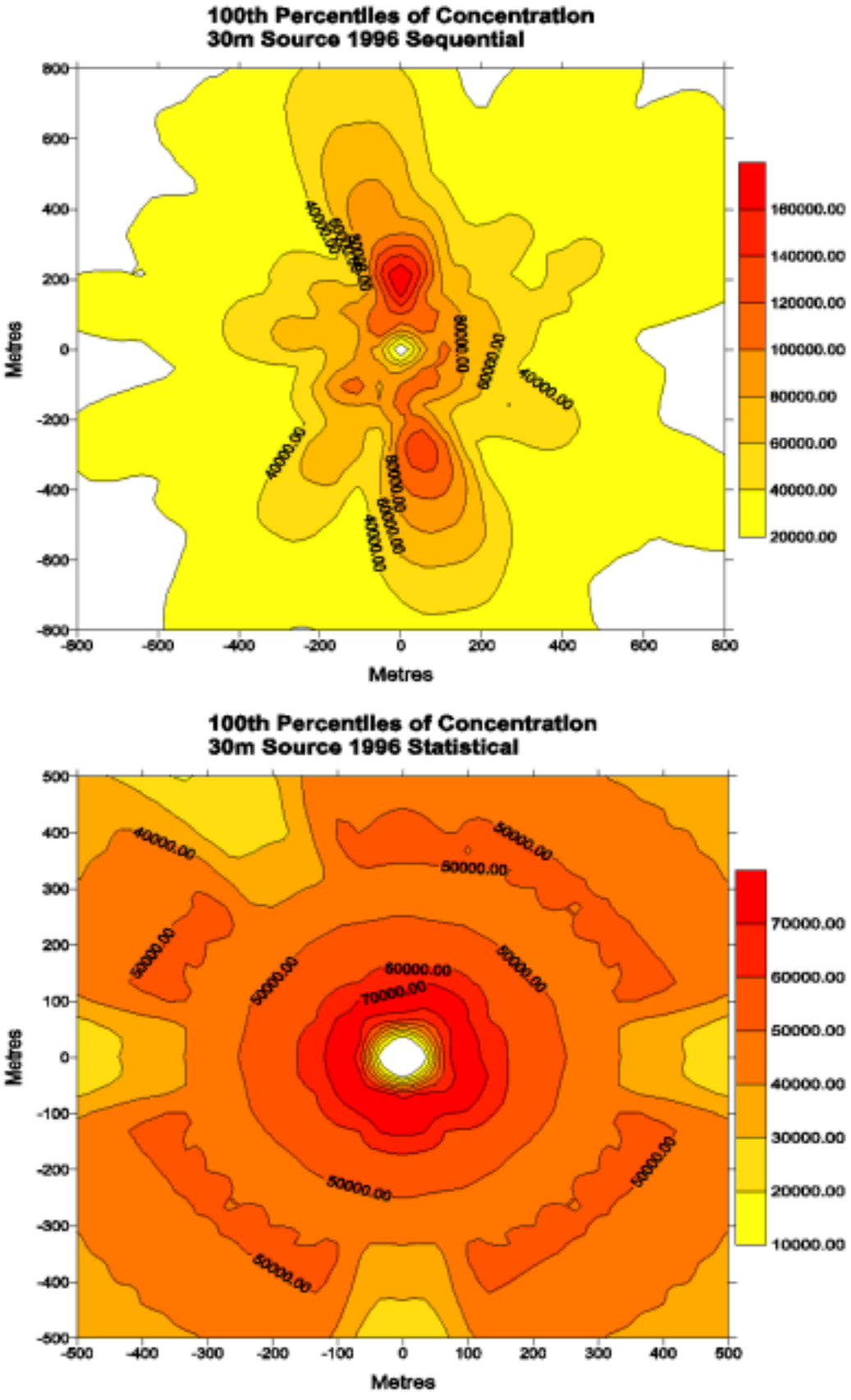

FIGURE E4c: 100th Percentiles of concentration for 30m source using 1996 sequential and statistical data

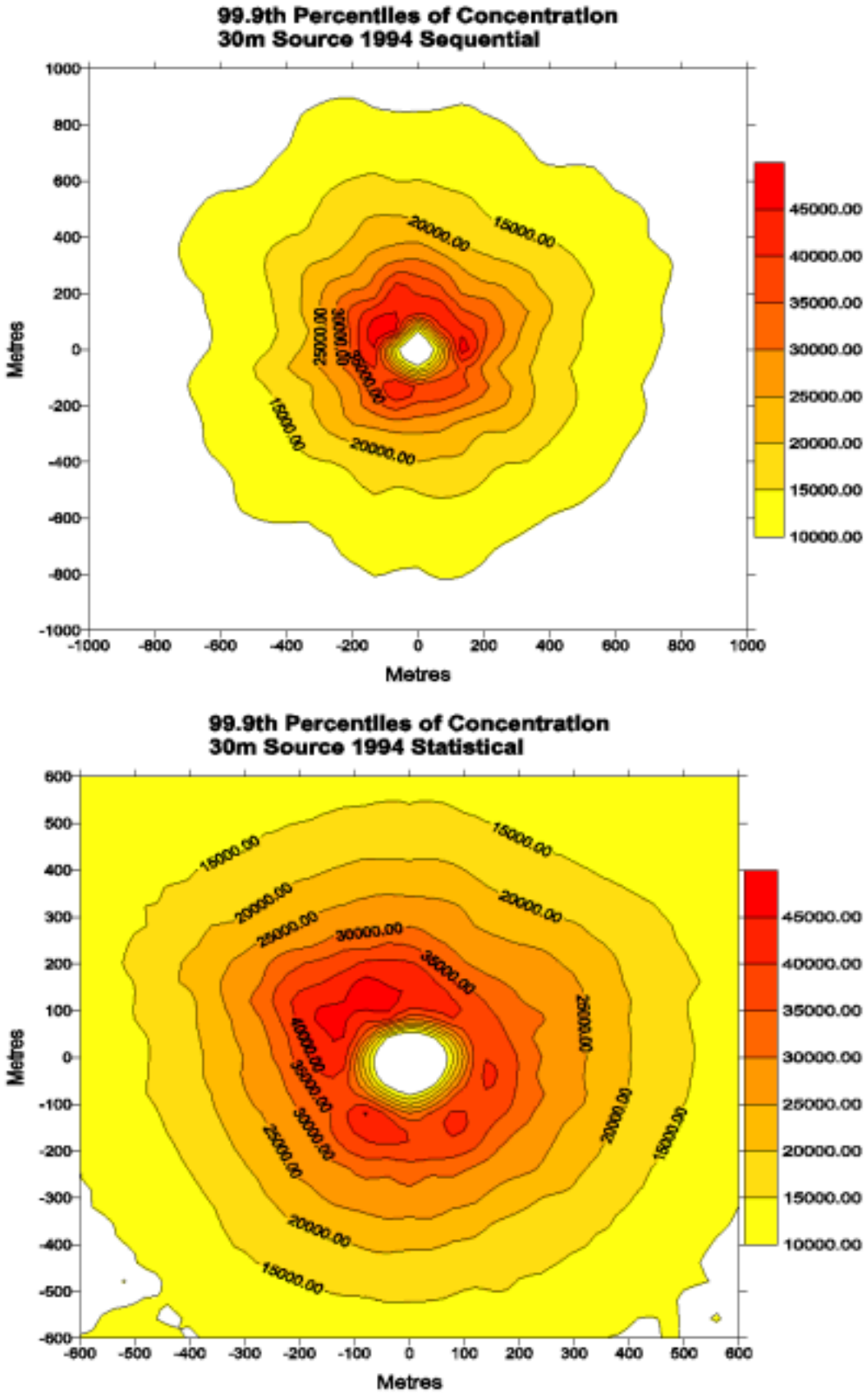

FIGURE E4d: 99.9th Percentiles of concentration for 30m source using 1994 sequential and statistical data

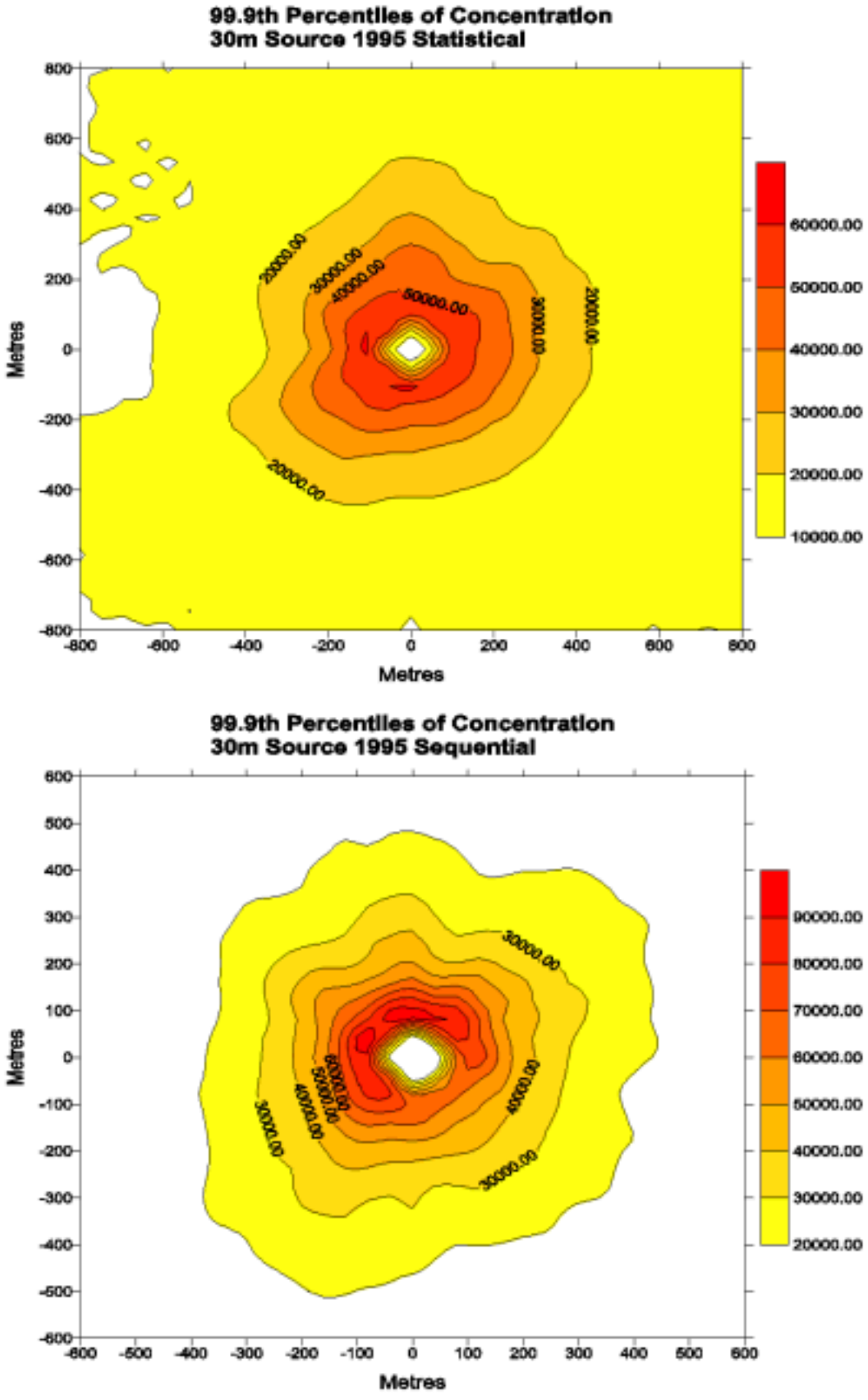

FIGURE E4e: 99.9th Percentiles of concentration for 30m source using 1995 sequential and statistical data

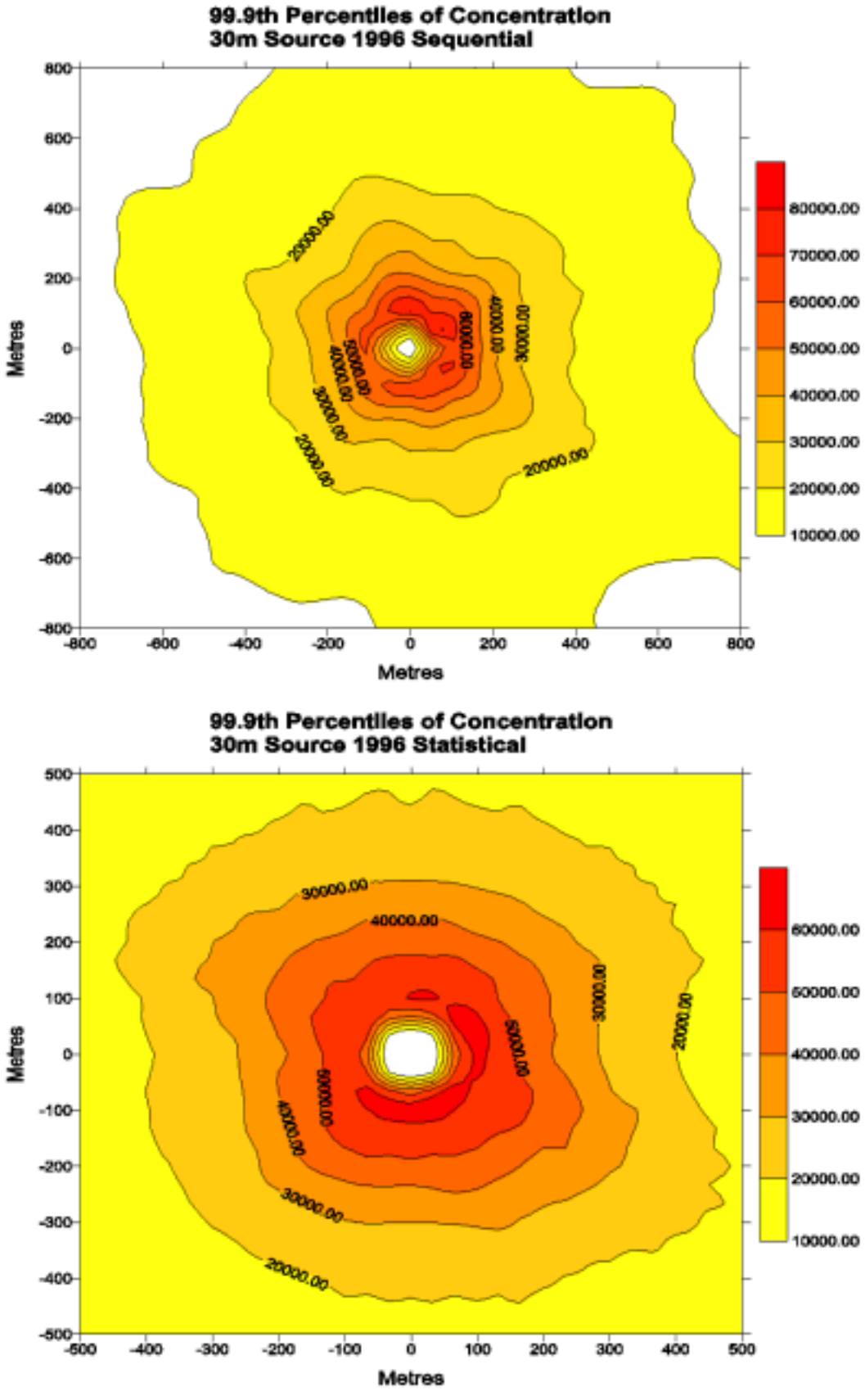

FIGURE E4f: 99.9th Percentiles of concentration for 30m source using 1996 sequential and statistical data

Figures E5a to E5f

Case I

Release Height	Release Velocity	Release Temperature
10m	9m/s	15°C

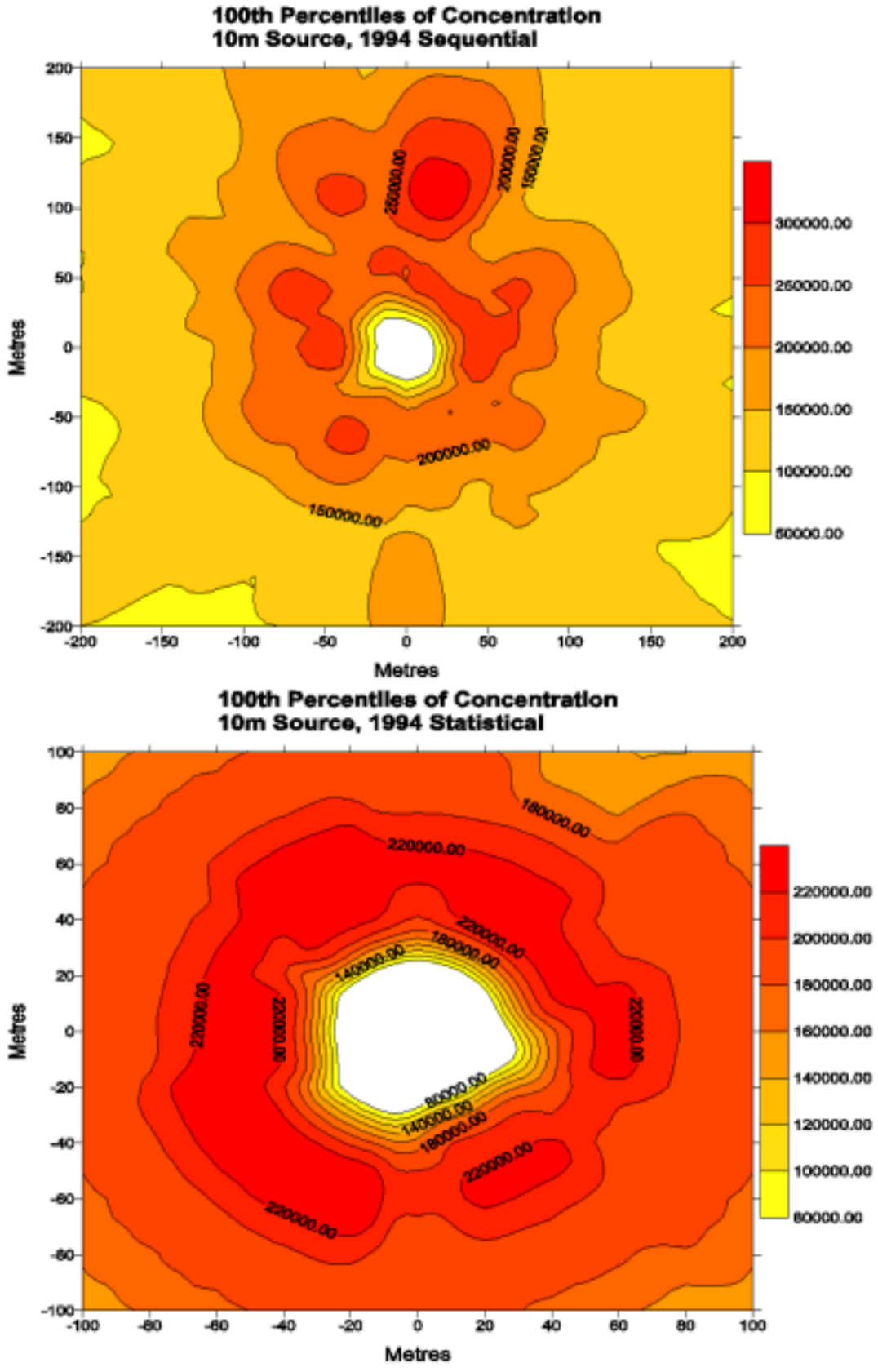

FIGURE E5a: 100th Percentiles of concentration for 10m source using 1994 sequential and statistical data

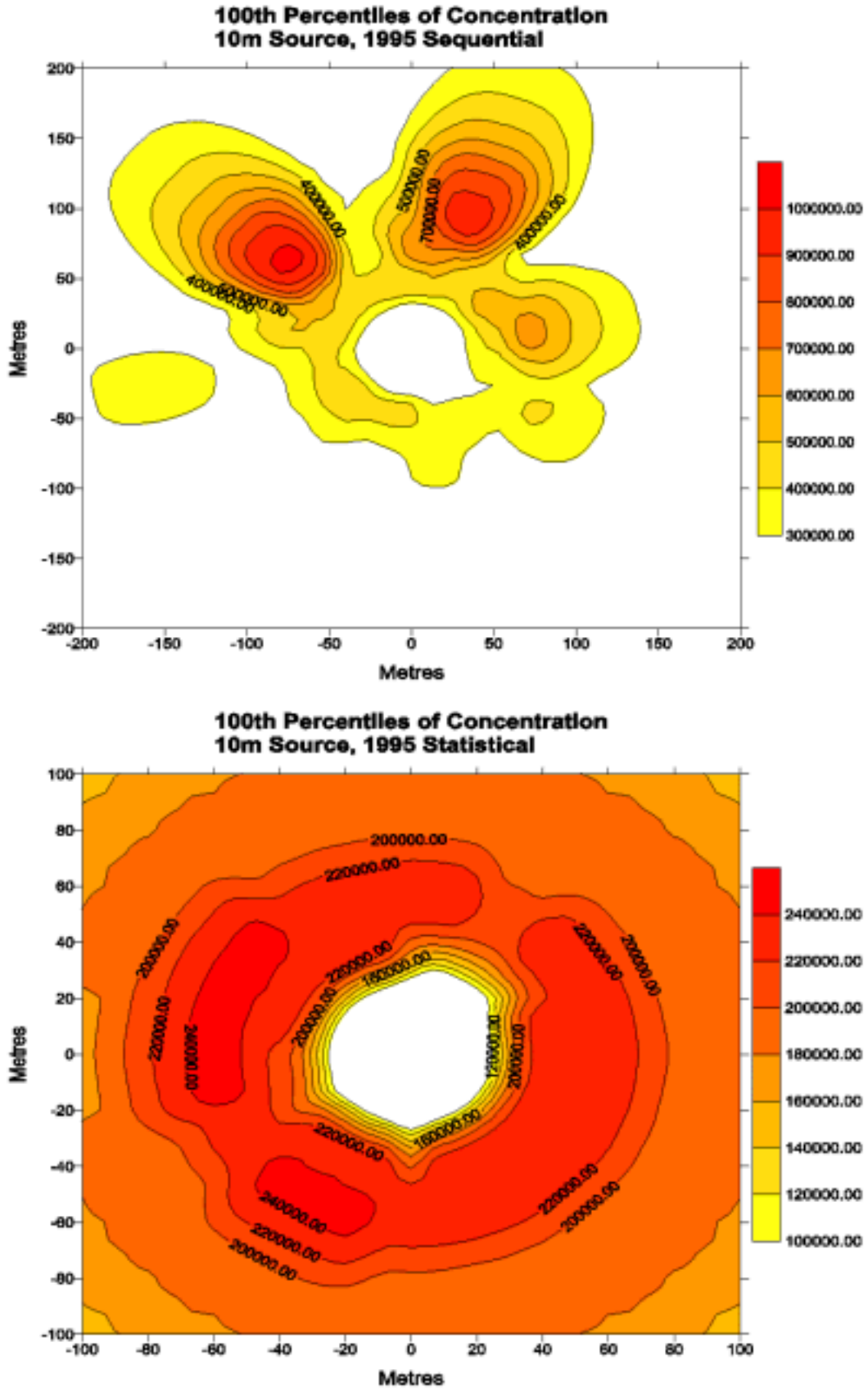

FIGURE E5b: 100th Percentiles of concentration for 10m source using 1995 sequential and statistical data

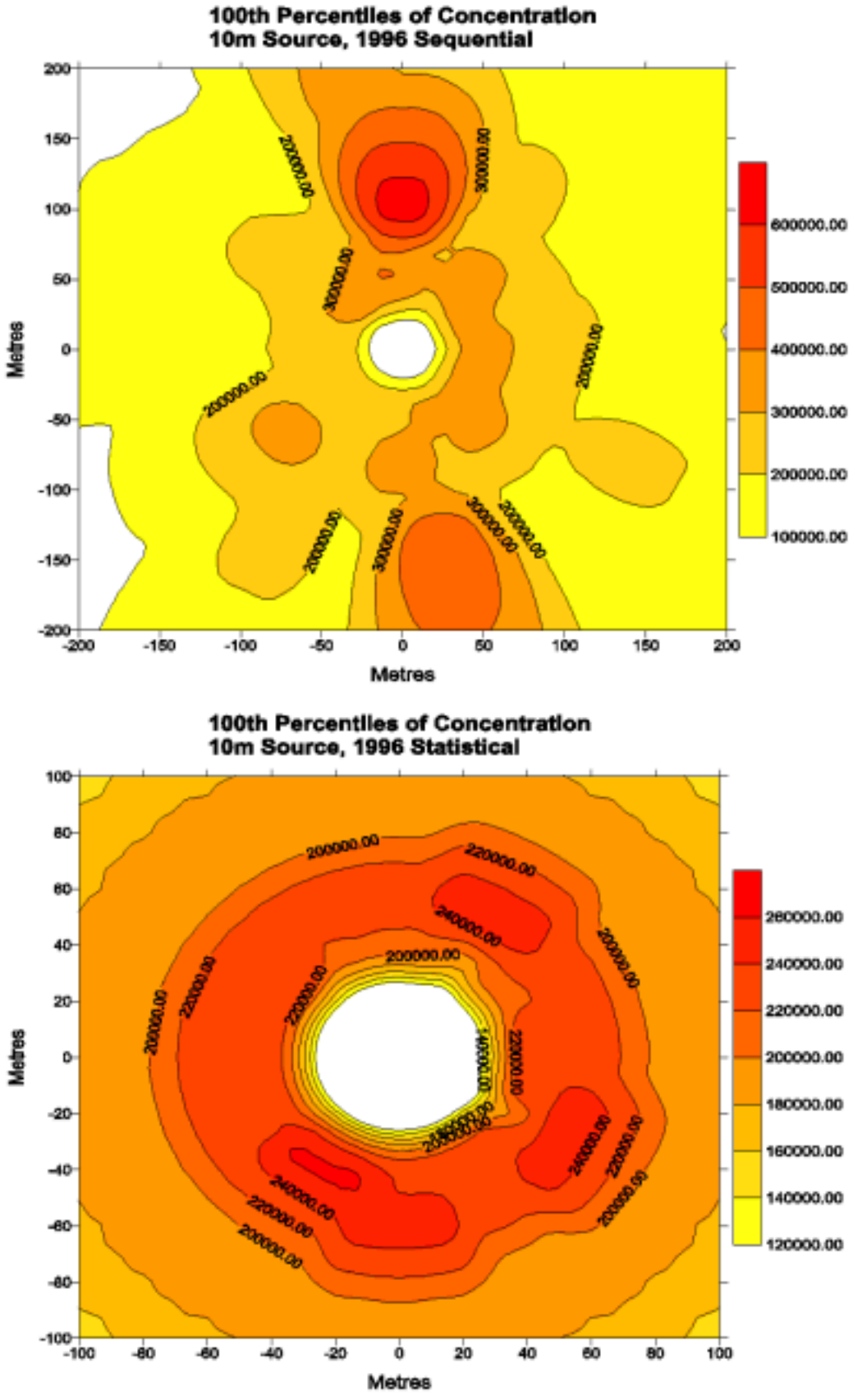

FIGURE E5c: 100th Percentiles of concentration for 10m source using 1996 sequential and statistical data

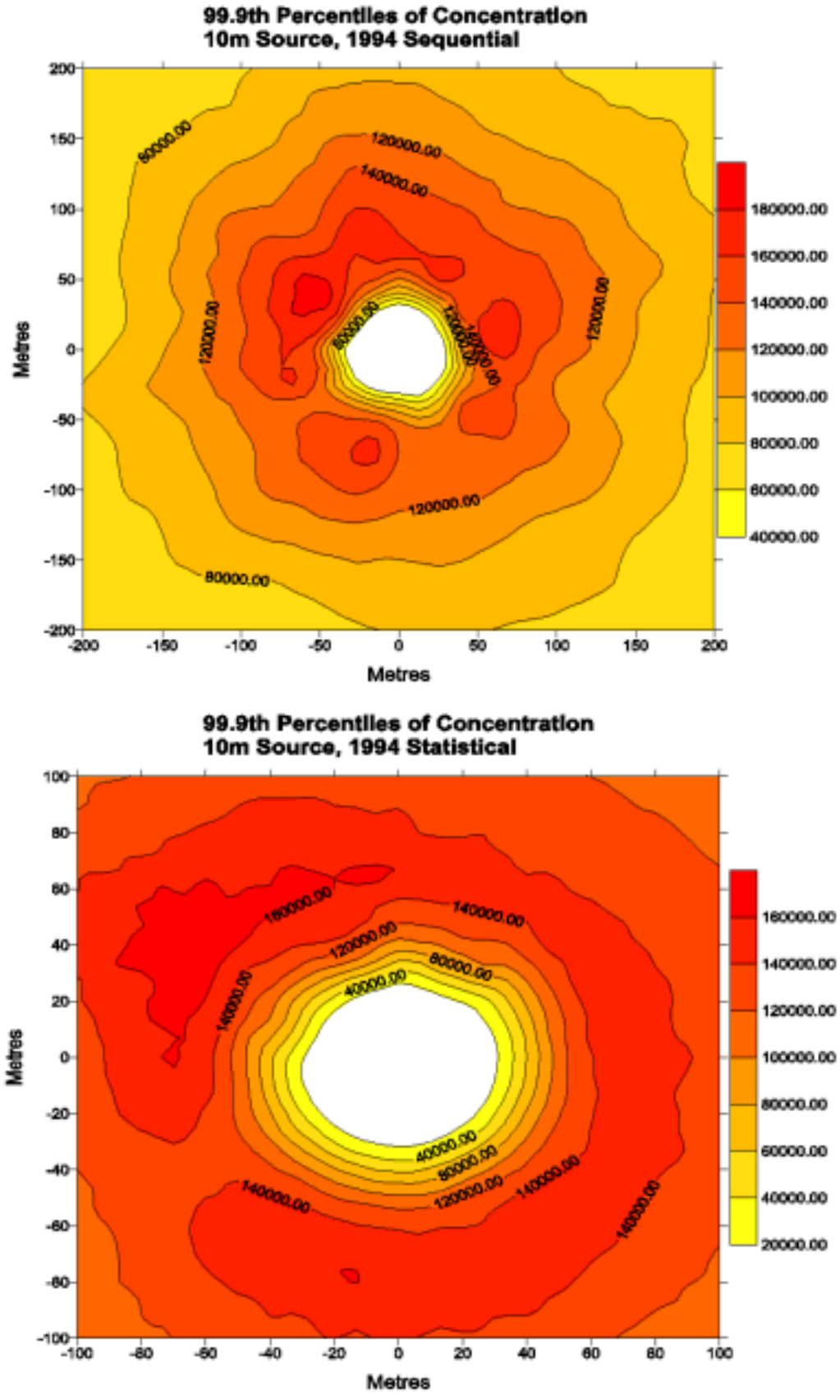

FIGURE E5d: 99.9th Percentiles of concentration for 10m source using 1994 sequential and statistical data

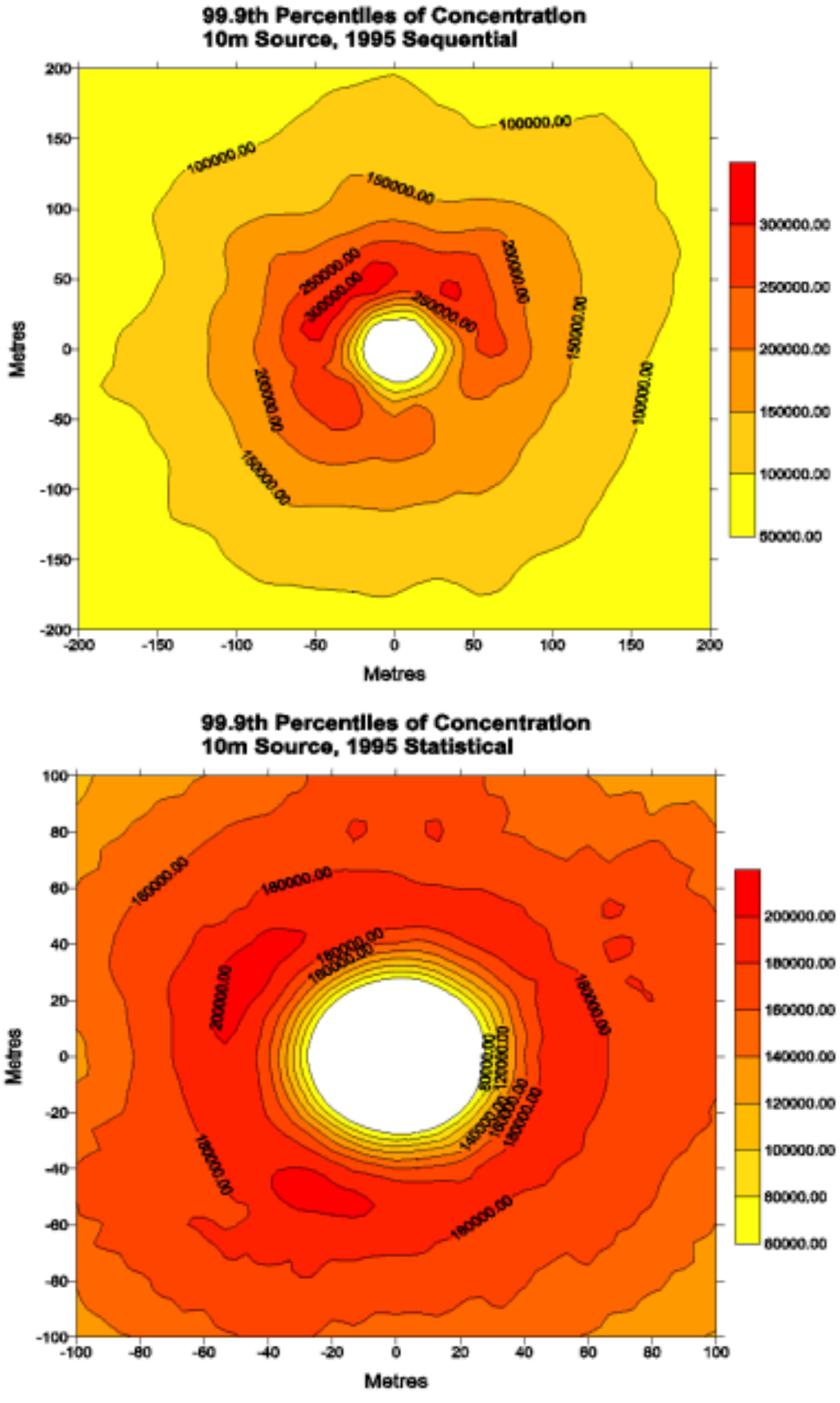

FIGURE E5e: 99.9th Percentiles of concentration for 10m source using 1995 sequential and statistical data

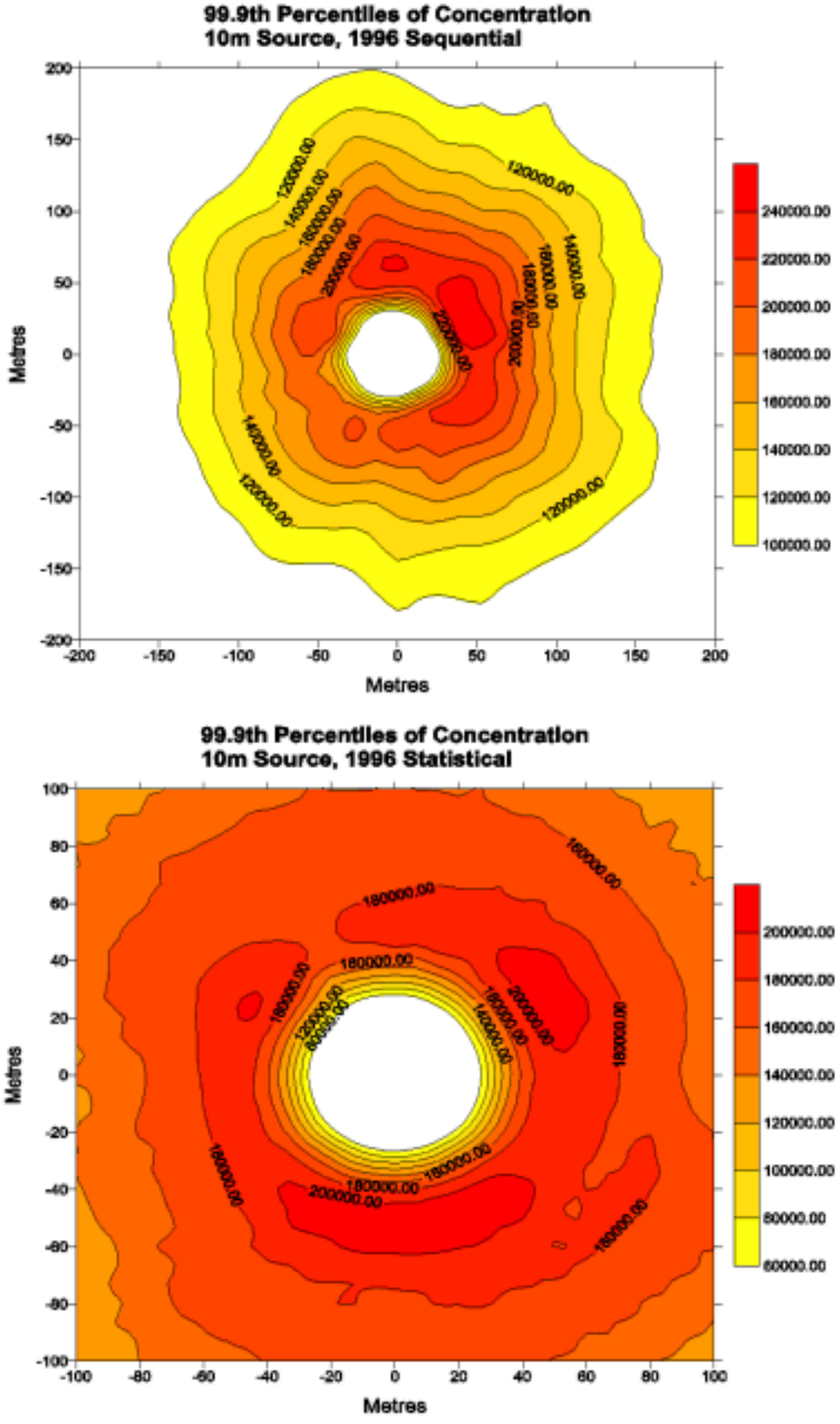

FIGURE E5f: 99.9th Percentiles of concentration for 10m source using 1996 sequential and statistical data

Figures E6a to E6f

Case K

Release Height	Release Velocity	Release Temperature
10m	15m/s	150°C

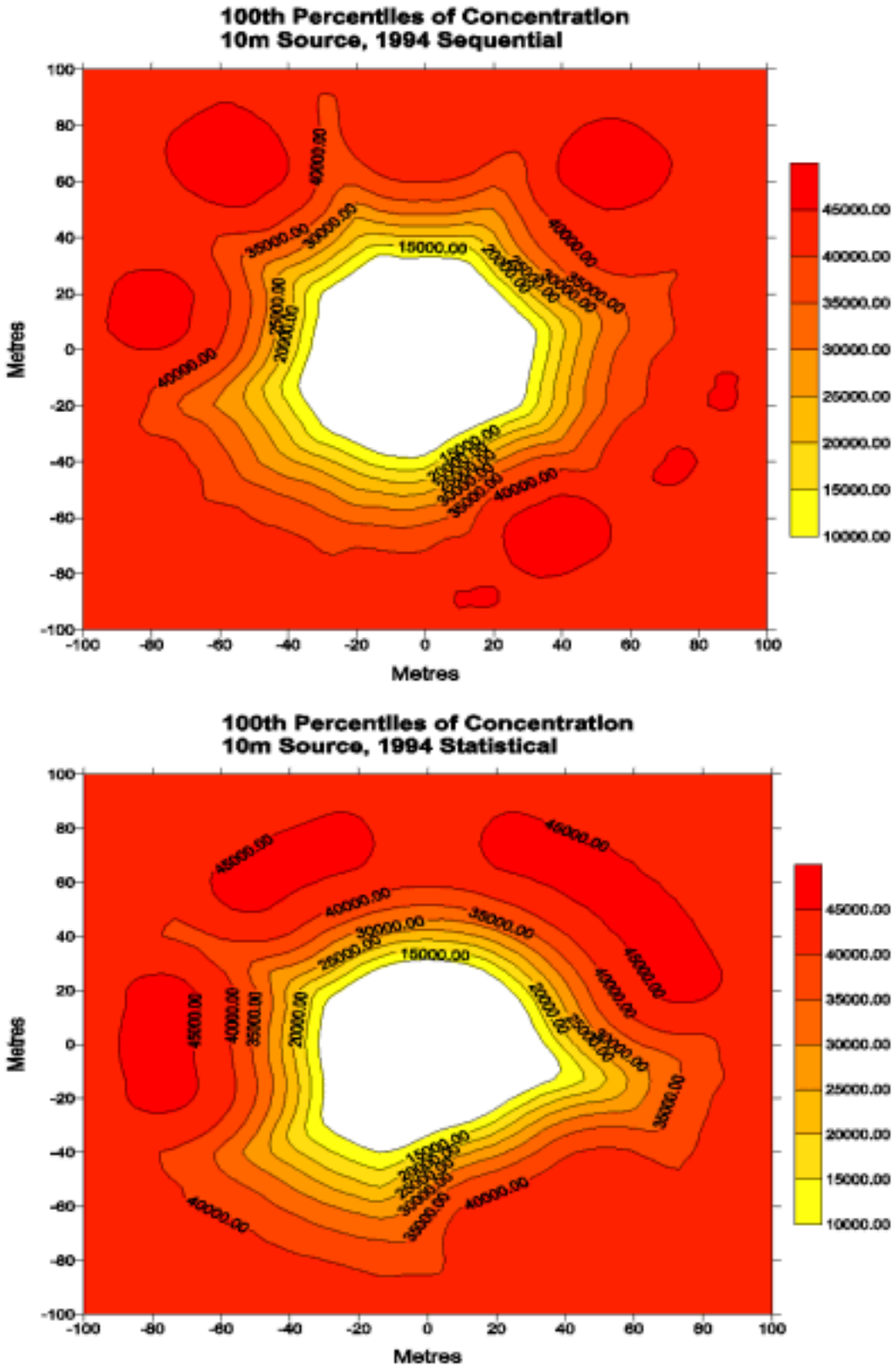

FIGURE E6a: 99.9th Percentiles of concentration for 10m source using 1996 sequential and statistical data

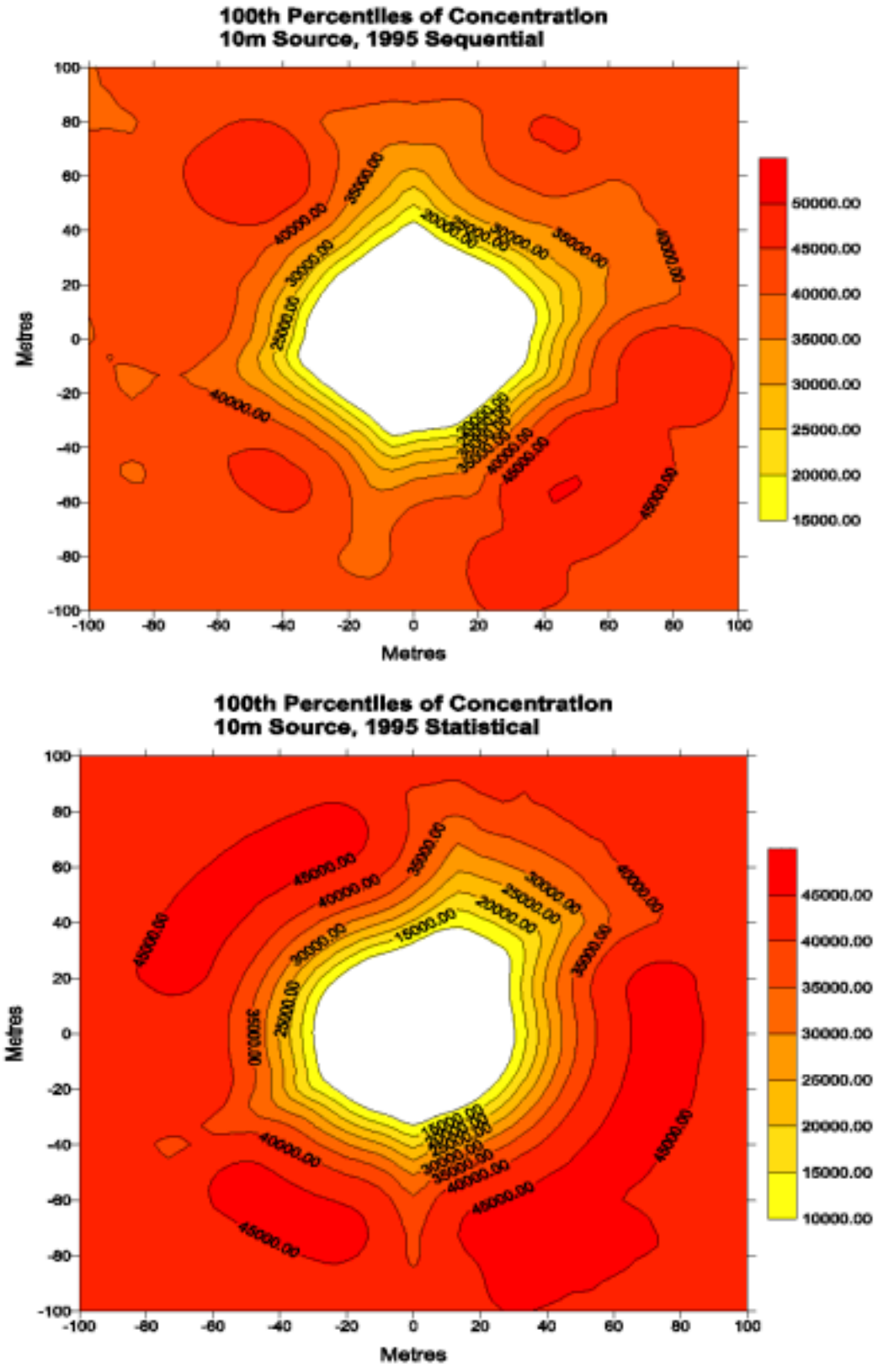

FIGURE E6b: 99.9th Percentiles of concentration for 10m source using 1996 sequential and statistical data

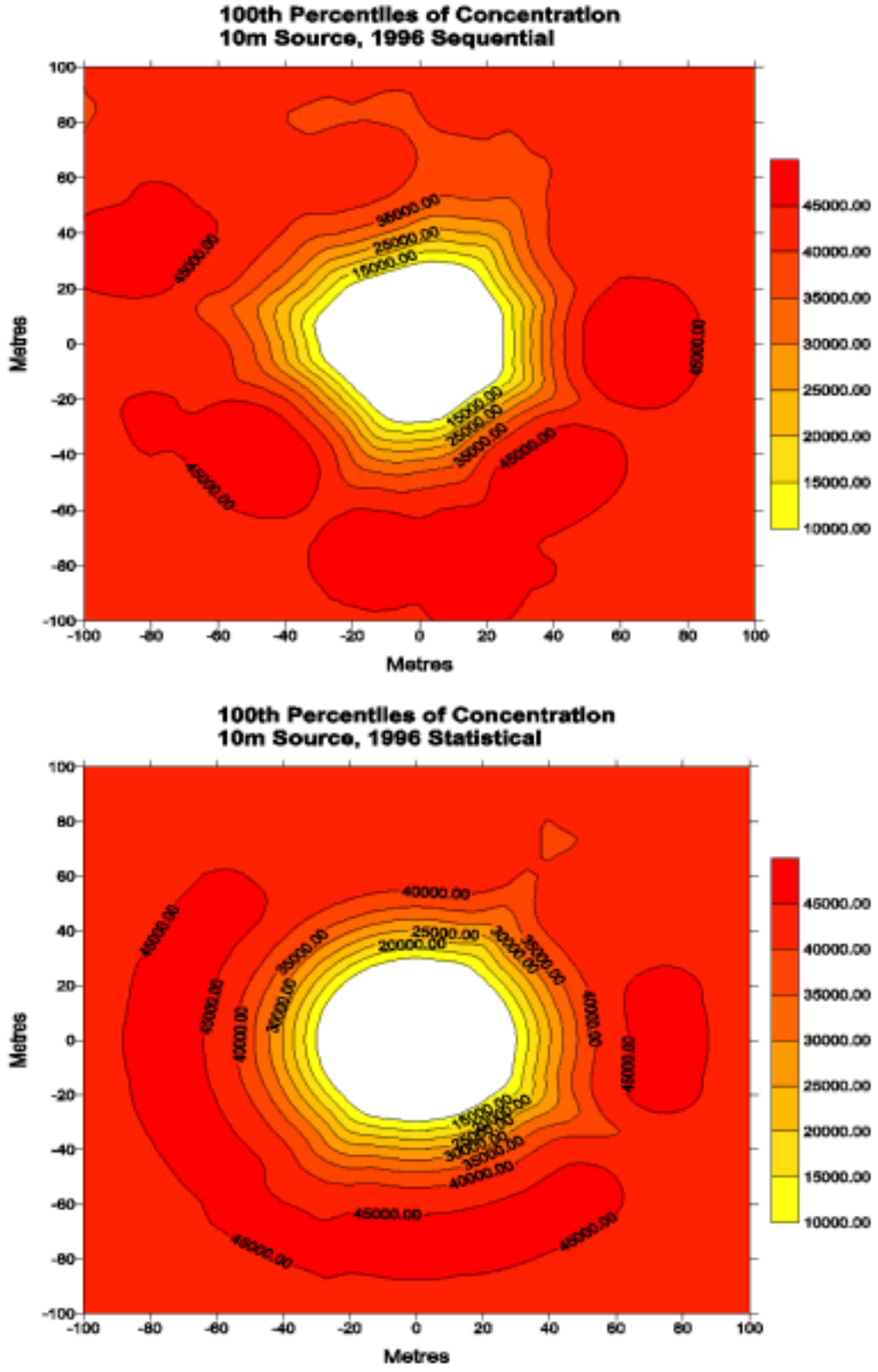

FIGURE E6c: 99.9th Percentiles of concentration for 10m source using 1996 sequential and statistical data

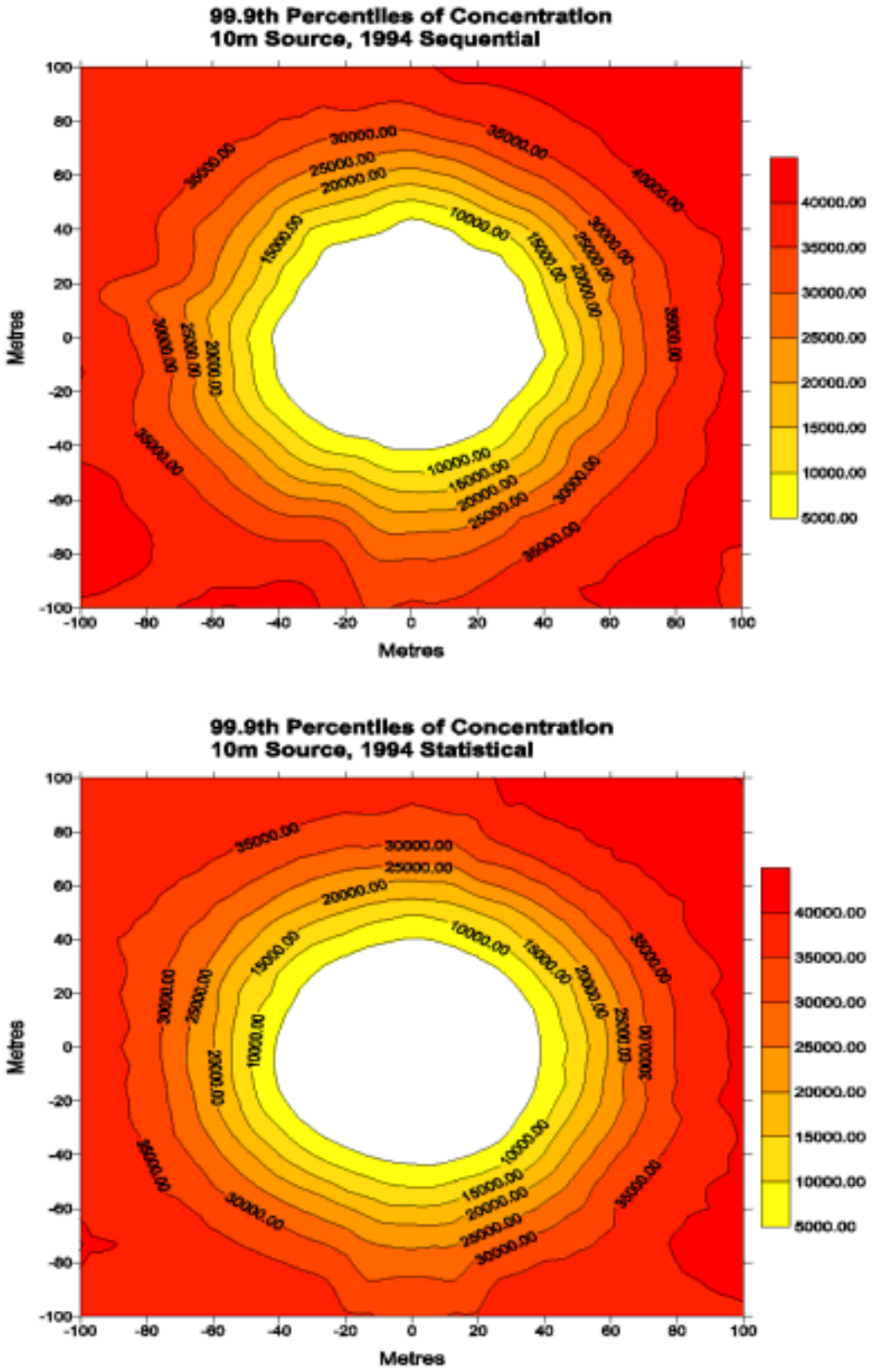

FIGURE E6d: 99.9th Percentiles of concentration for 10m source using 1996 sequential and statistical data

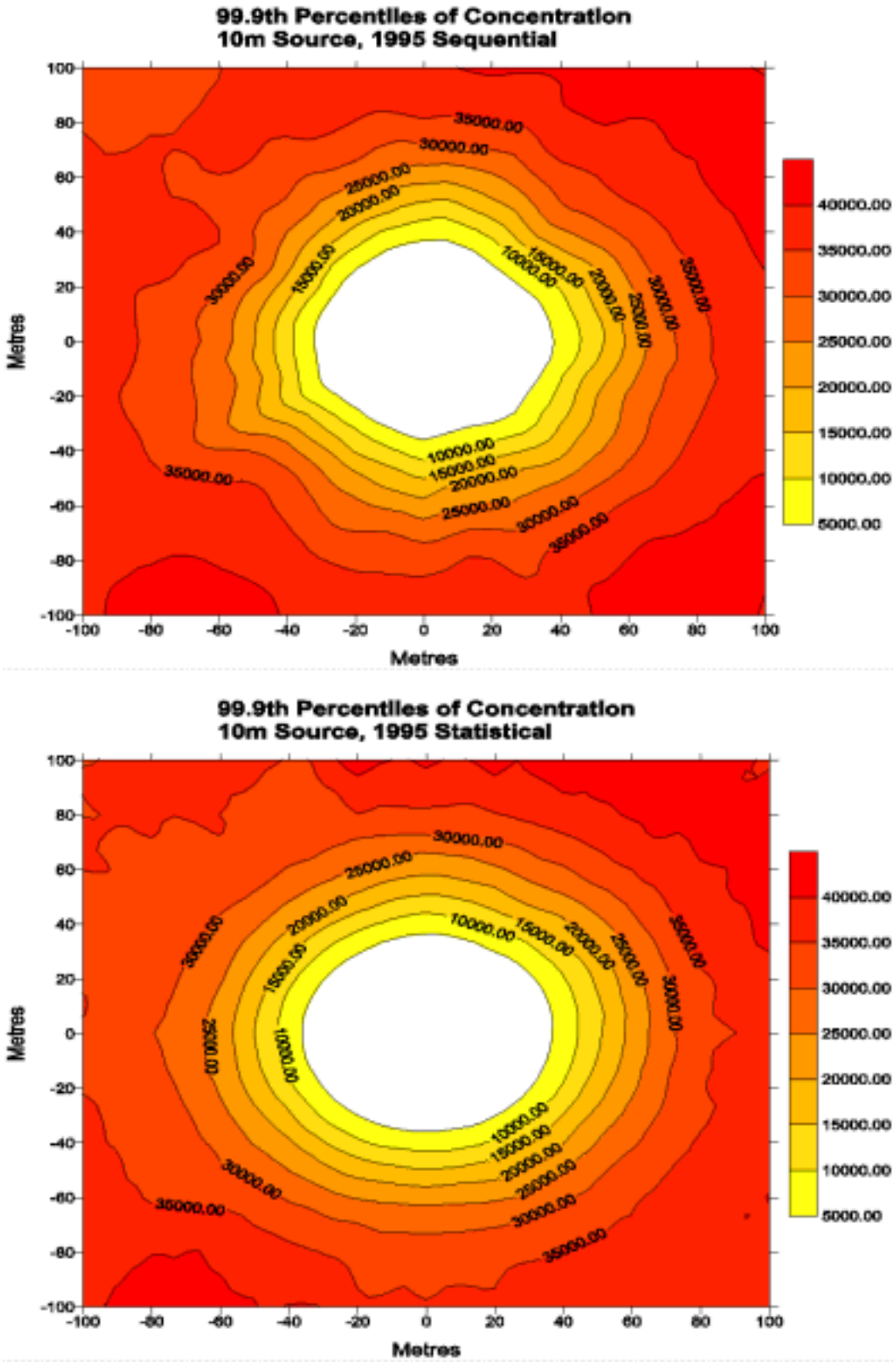

FIGURE E6e: 99.9th Percentiles of concentration for 10m source using 1996 sequential and statistical data

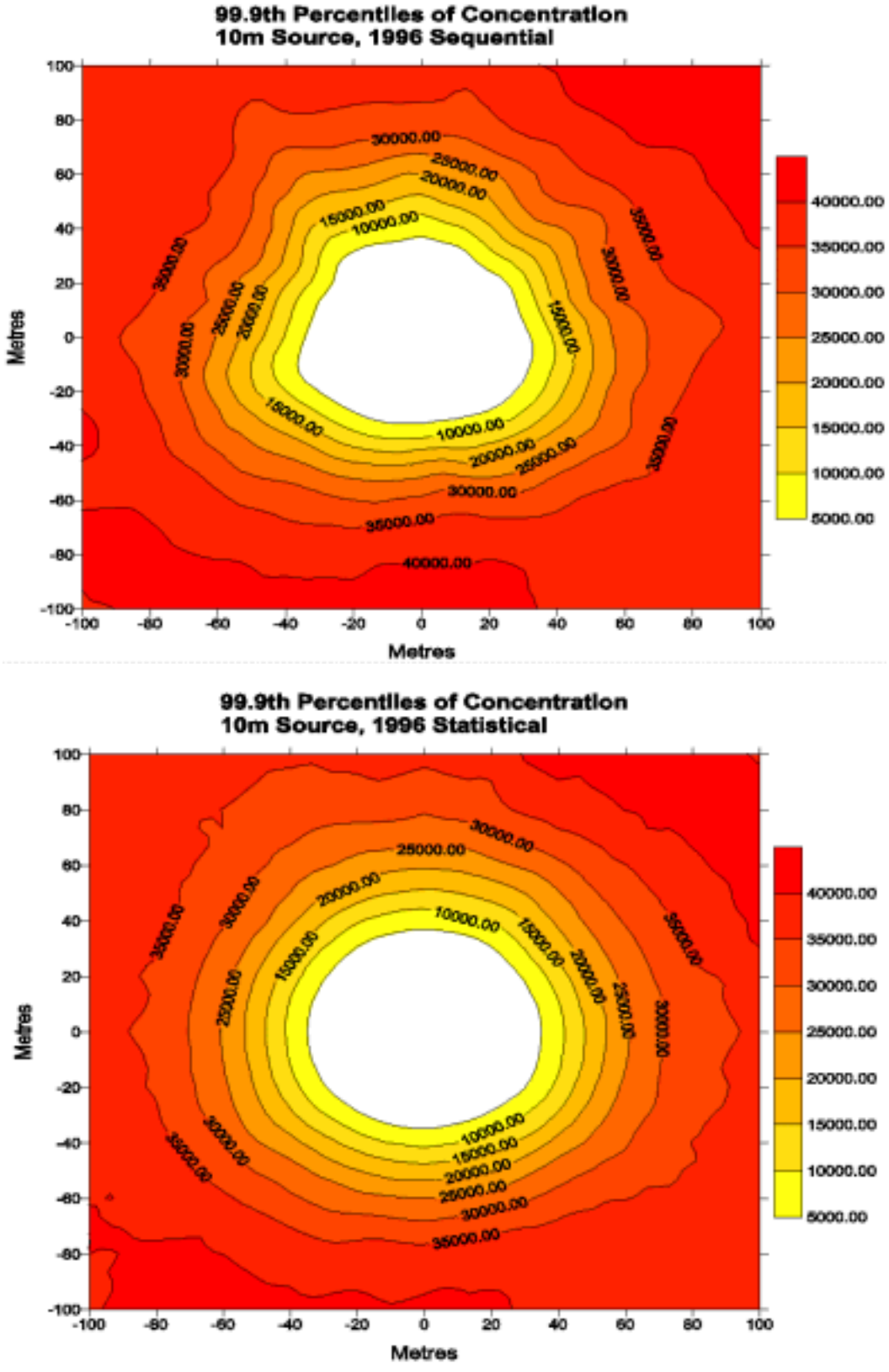

FIGURE E6f: 99.9th Percentiles of concentration for 10m source using 1996 sequential and statistical data

APPENDIX F

Figures F1a to F1f

Case A*

Release Height	Release Velocity	Release Temperature
100m	9m/s	15°C

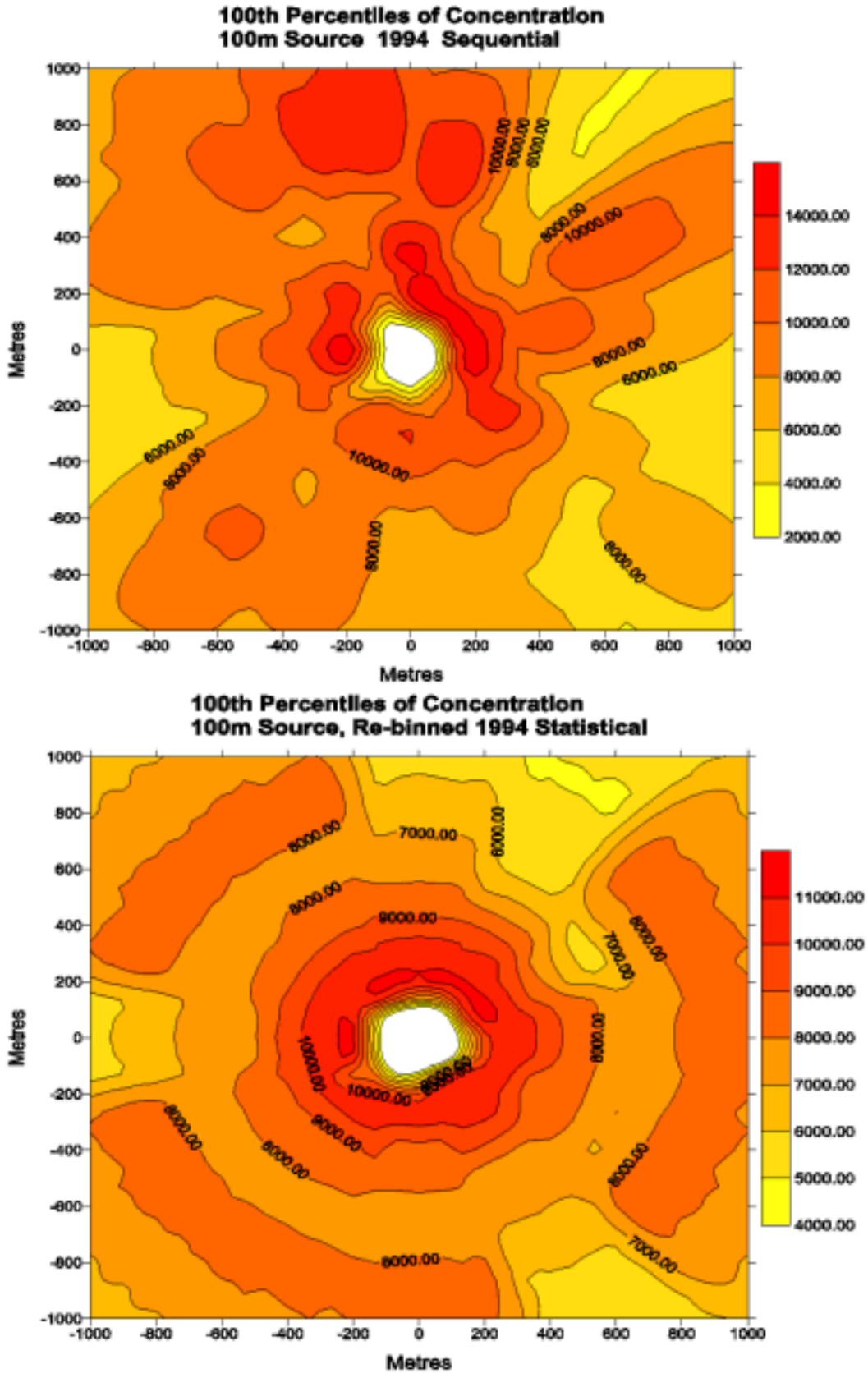

FIGURE F1a: 100th Percentiles of concentration for 100m source using re-binned 1994 statistical data and standard sequential data

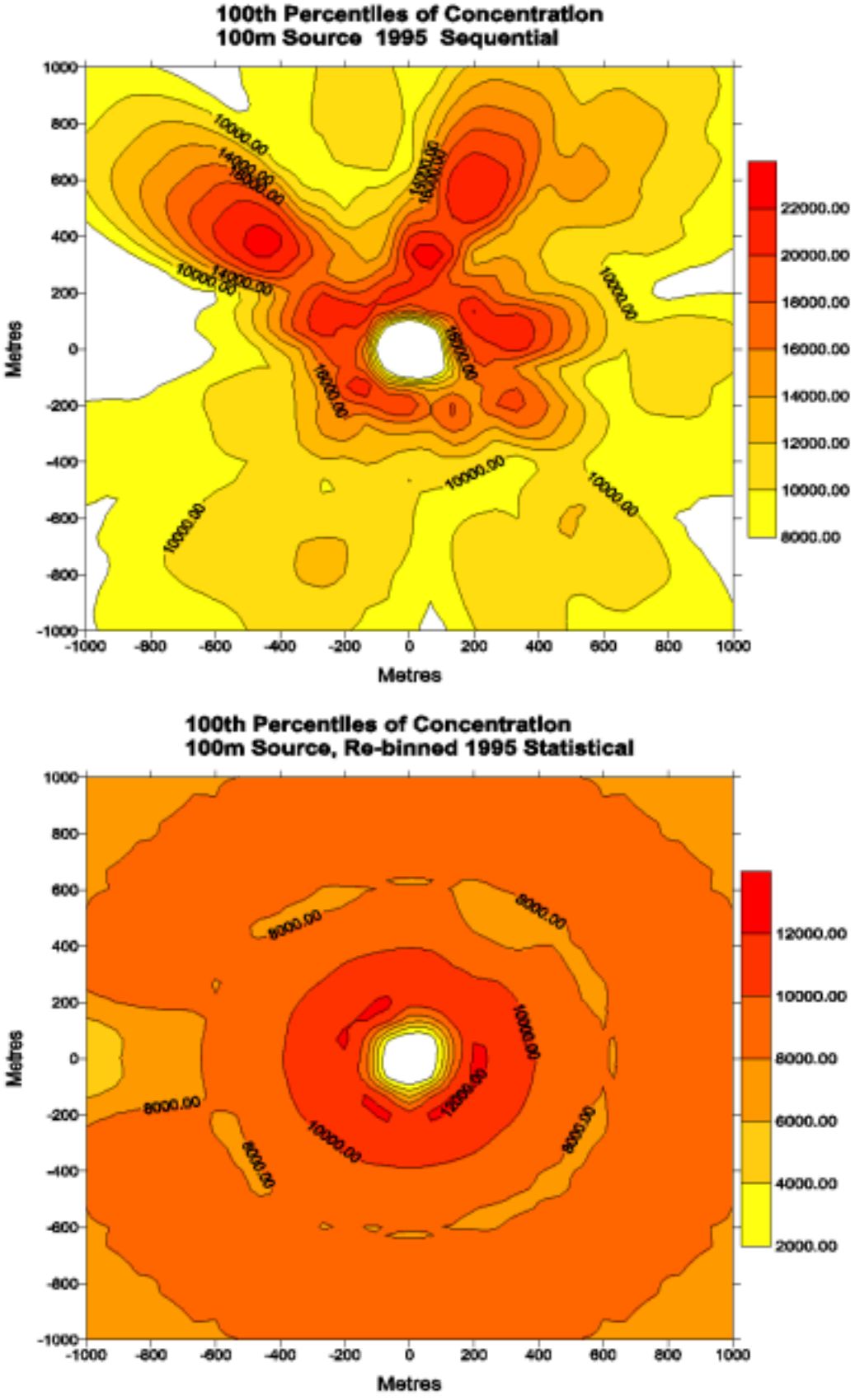

FIGURE F1b: 100th Percentiles of concentration for 100m source using re-binned 1995 statistical data and standard sequential data

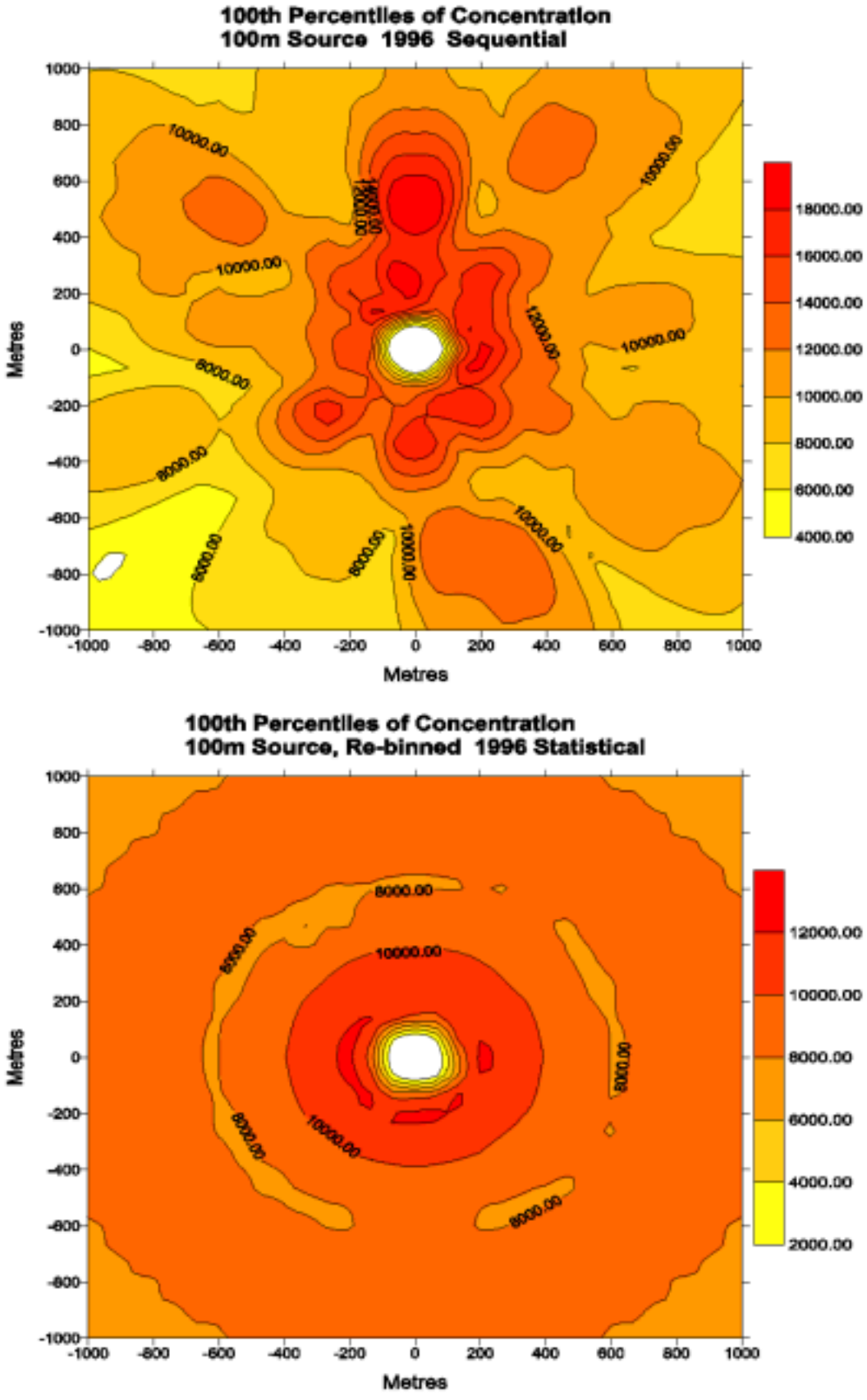

FIGURE F1c: 100th Percentiles of concentration for 100m source using re-binned 1996 statistical data and standard sequential data

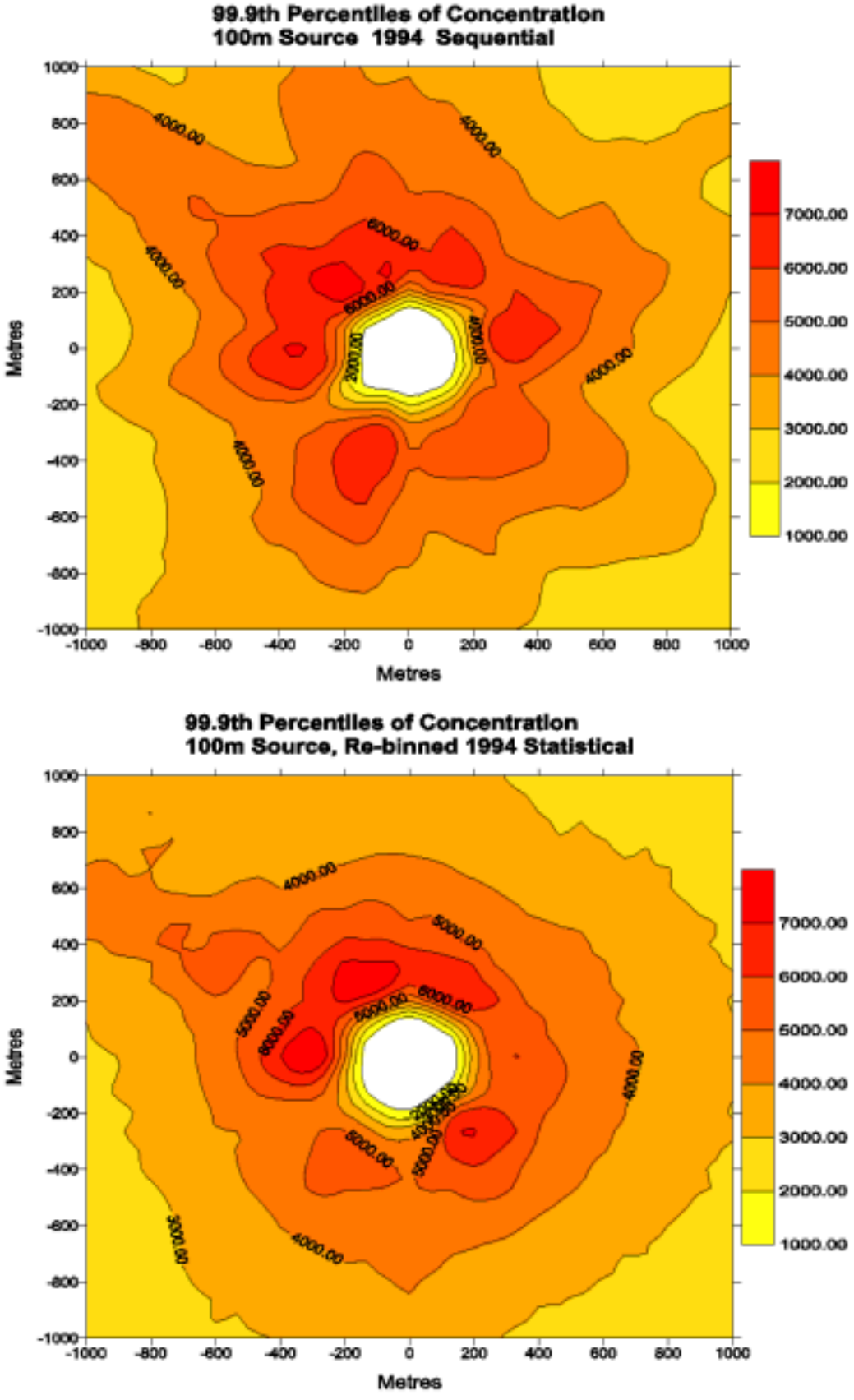

FIGURE F1d: 99.9th Percentiles of concentration for 100m source using re-binned 1994 statistical data and standard sequential data

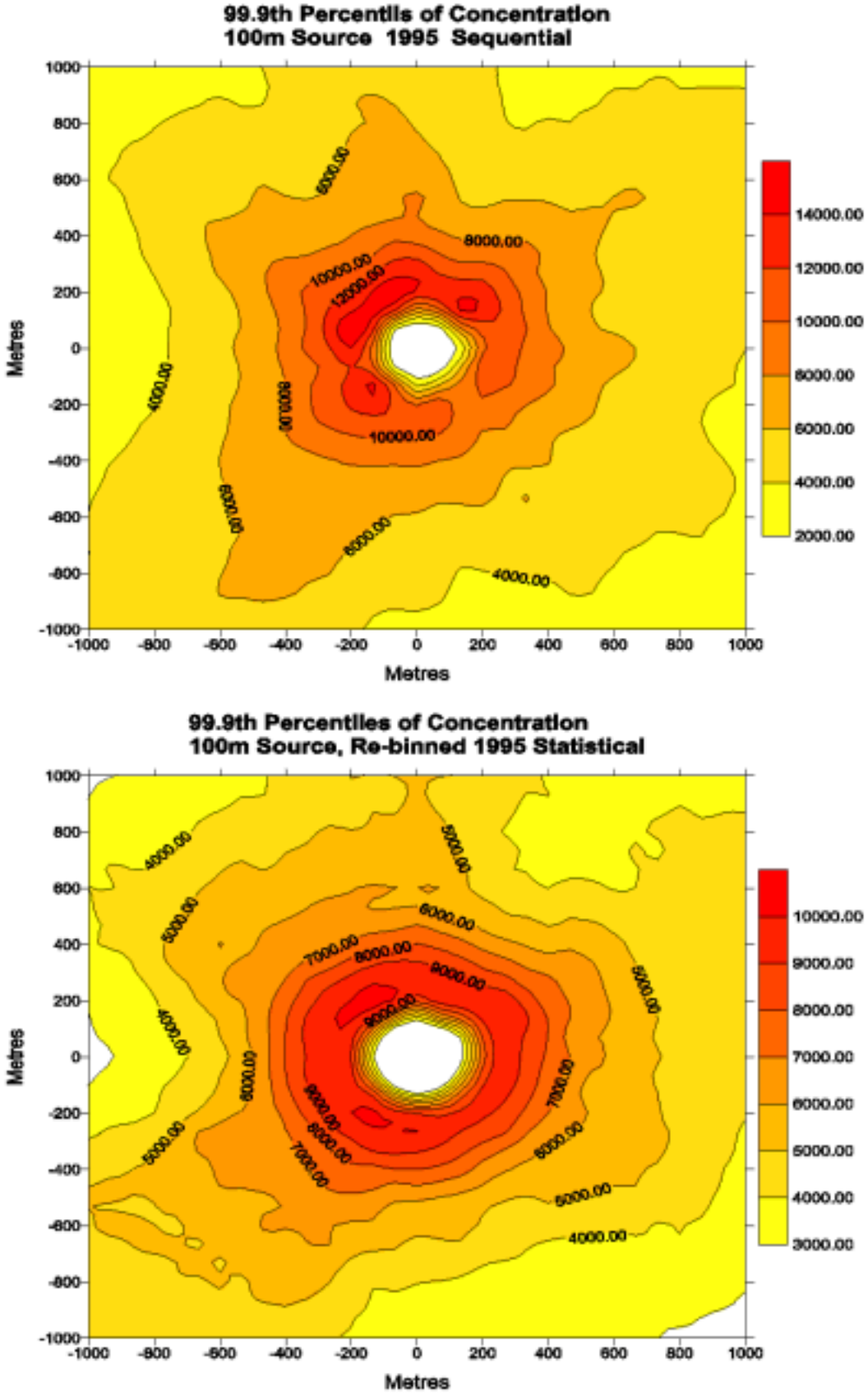

FIGURE F1e: 99.9th Percentiles of concentration for 100m source using re-binned 1995 statistical data and standard sequential data

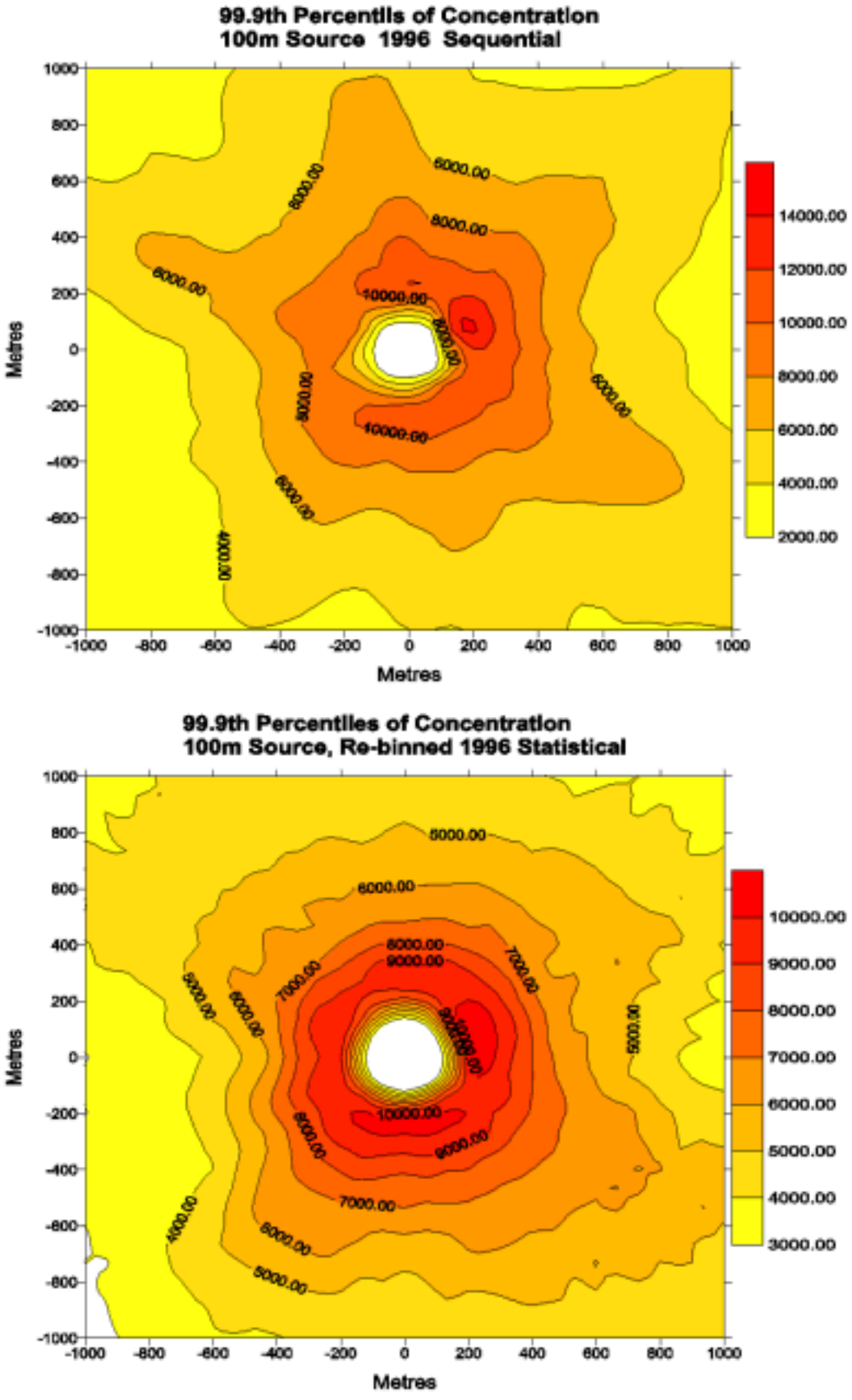

FIGURE F1f: 99.9th Percentiles of concentration for 100m source using re-binned 1996 statistical data and standard sequential data

Figures F2a to F2f

Case C*****

Release Height	Release Velocity	Release Temperature
75m	9m/s	15°C

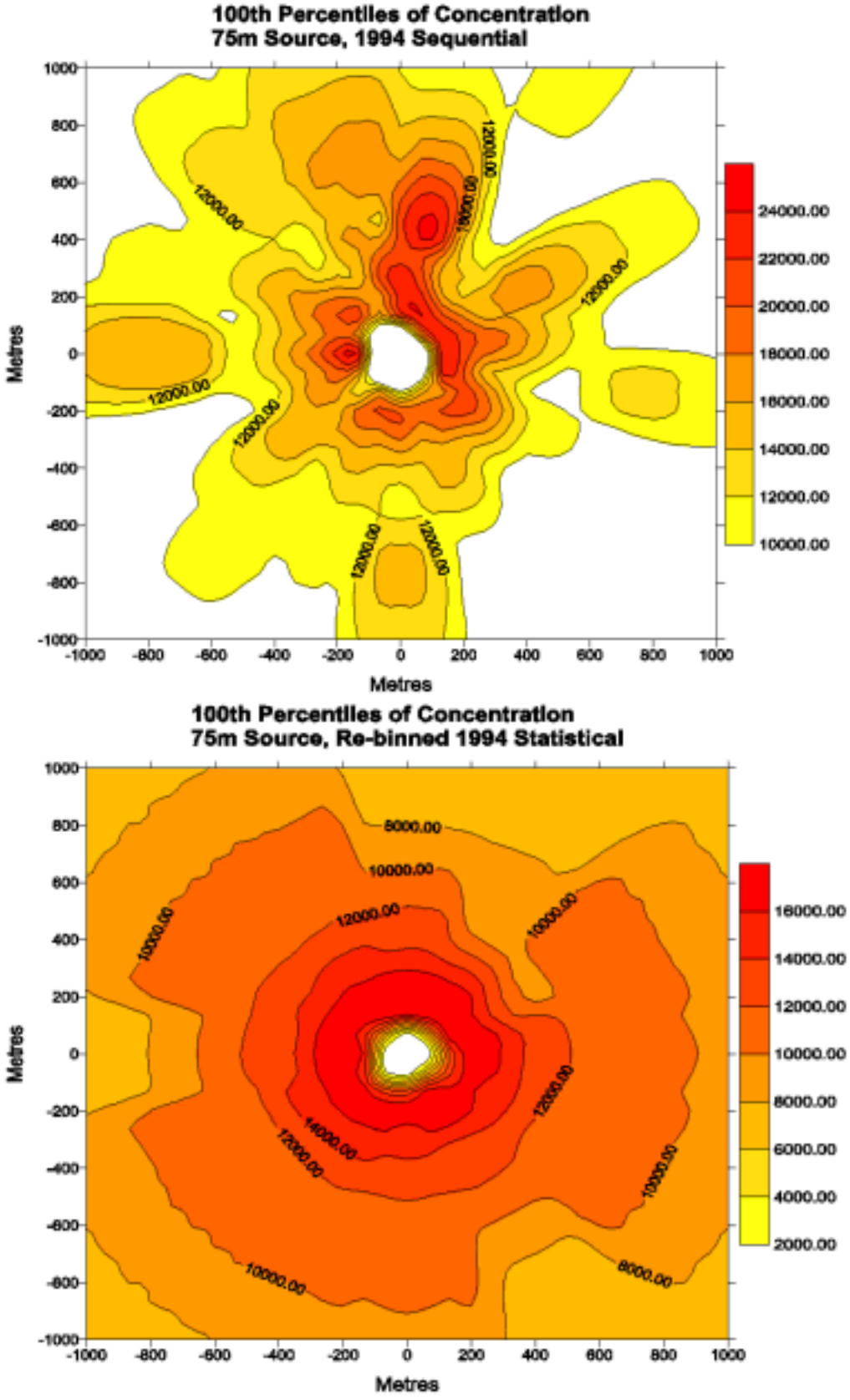

FIGURE F2a: 100th Percentiles of concentration for 75m source using re-binned 1994 statistical data and standard sequential data

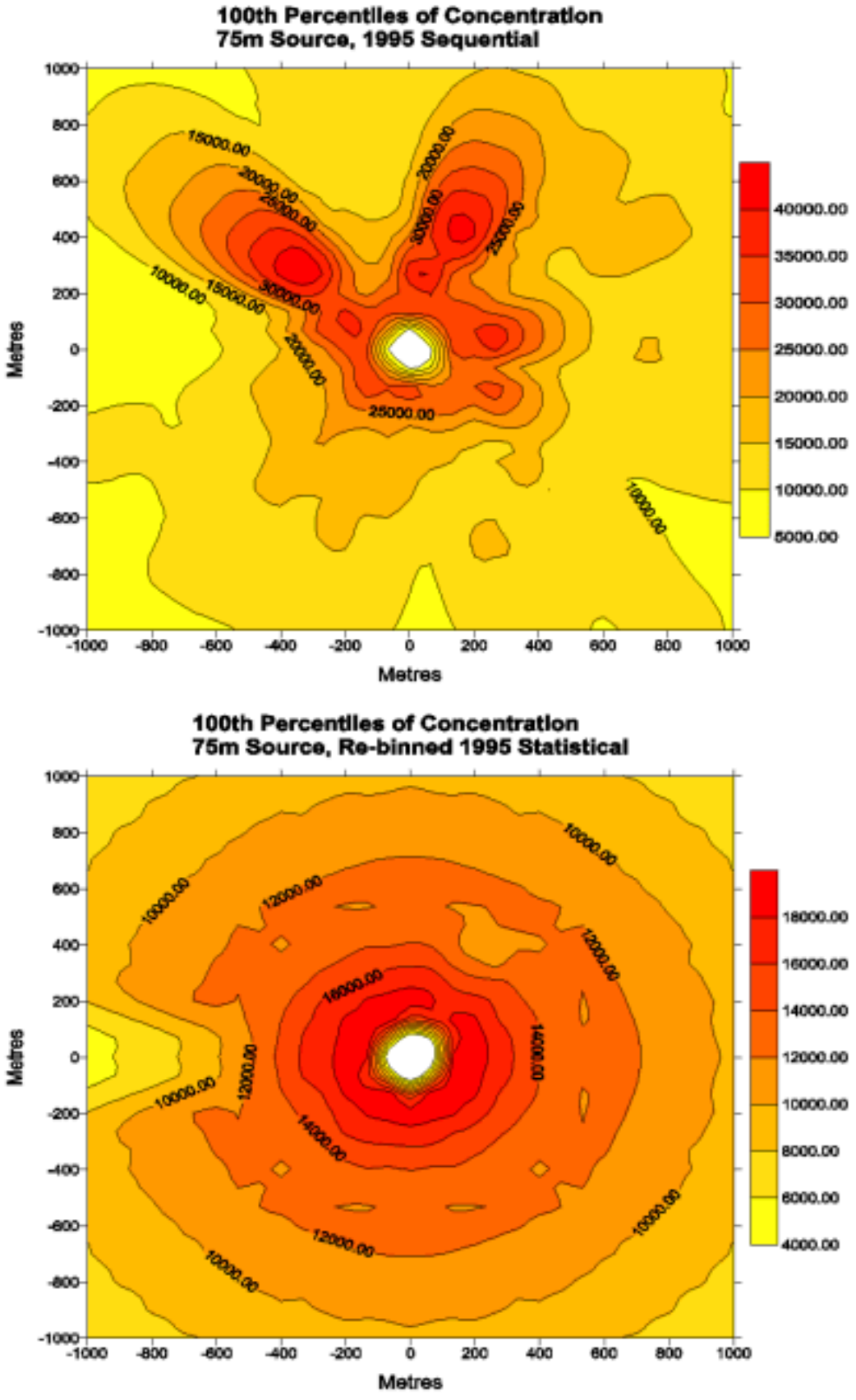

FIGURE F2b: 100th Percentiles of concentration for 75m source using re-binned 1995 statistical data and standard sequential data

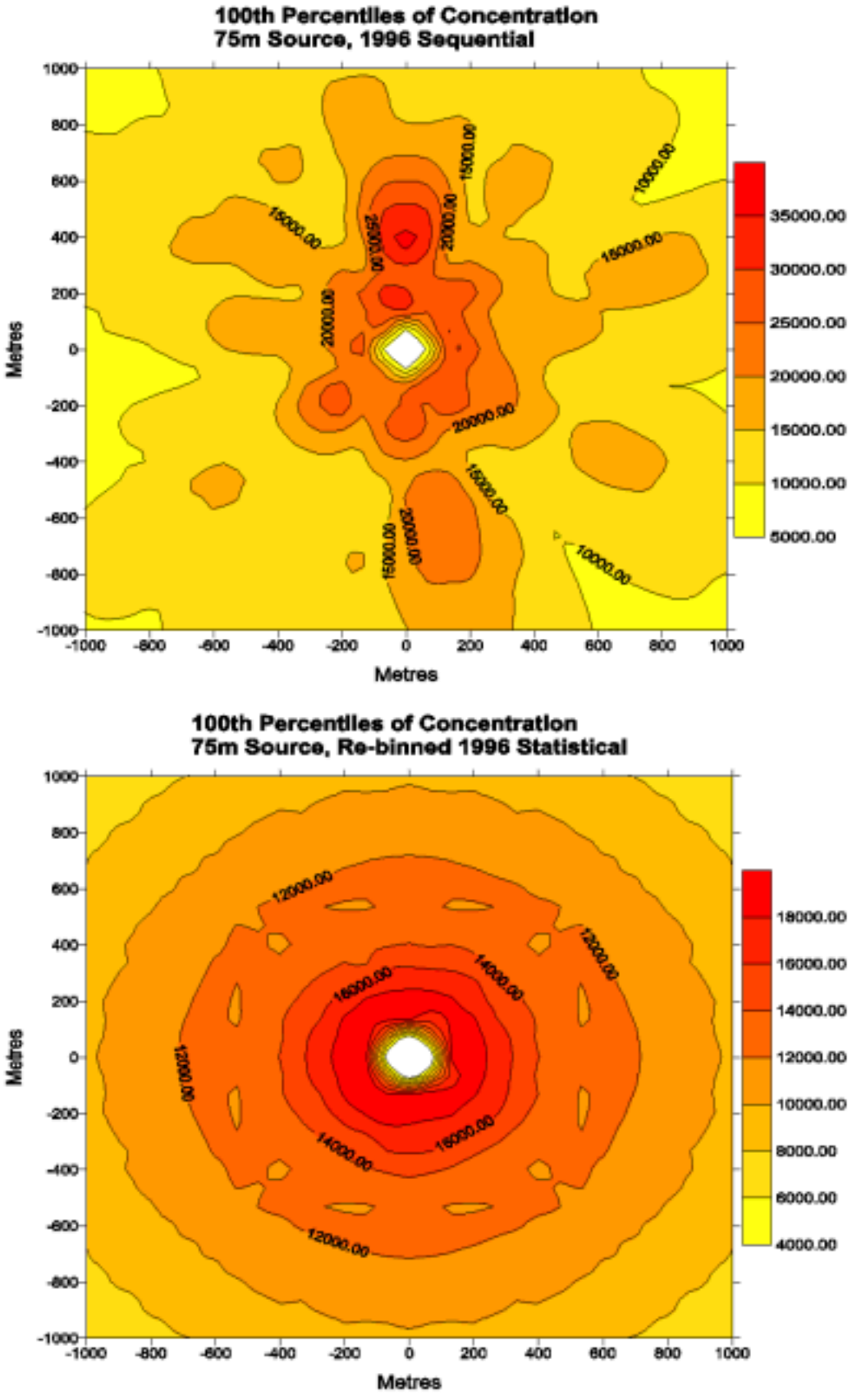

FIGURE F2c: 100th Percentiles of concentration for 75m source using re-binned 1996 statistical data and standard sequential data

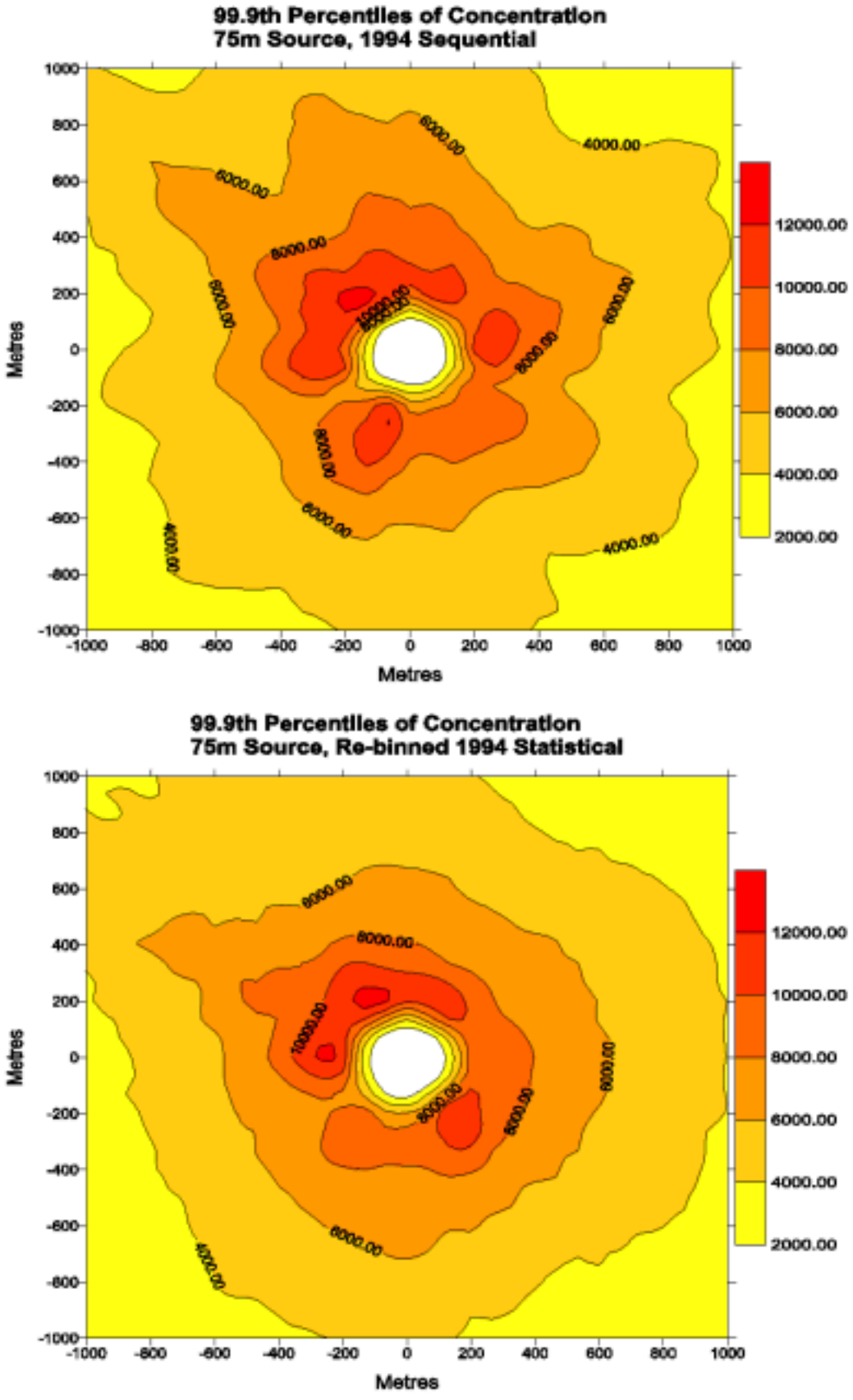

FIGURE F2d: 99.9th Percentiles of concentration for 75m source using re-binned 1994 statistical data and standard sequential data

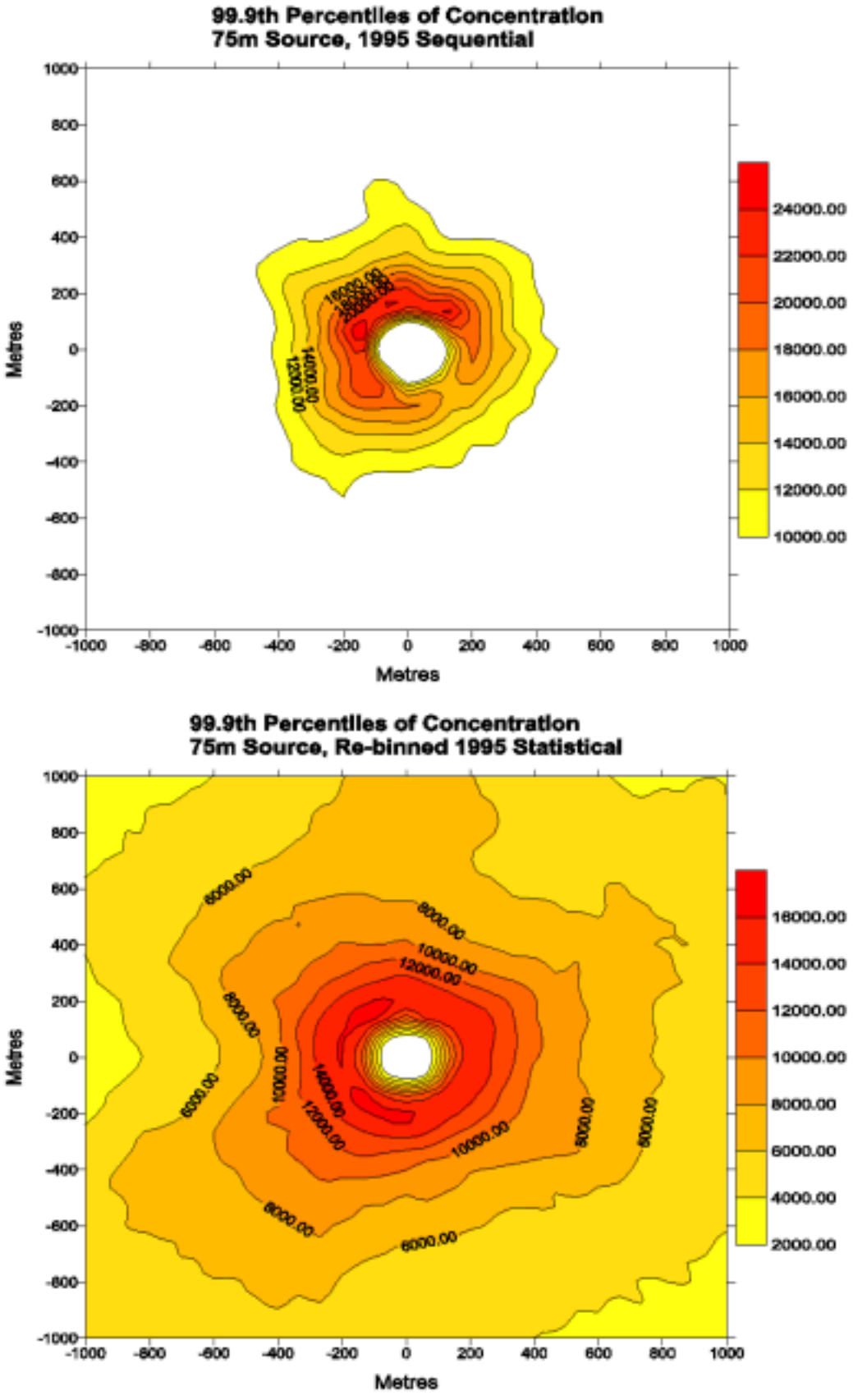

FIGURE F2e: 99.9th Percentiles of concentration for 75m source using re-binned 1995 statistical data and standard sequential data

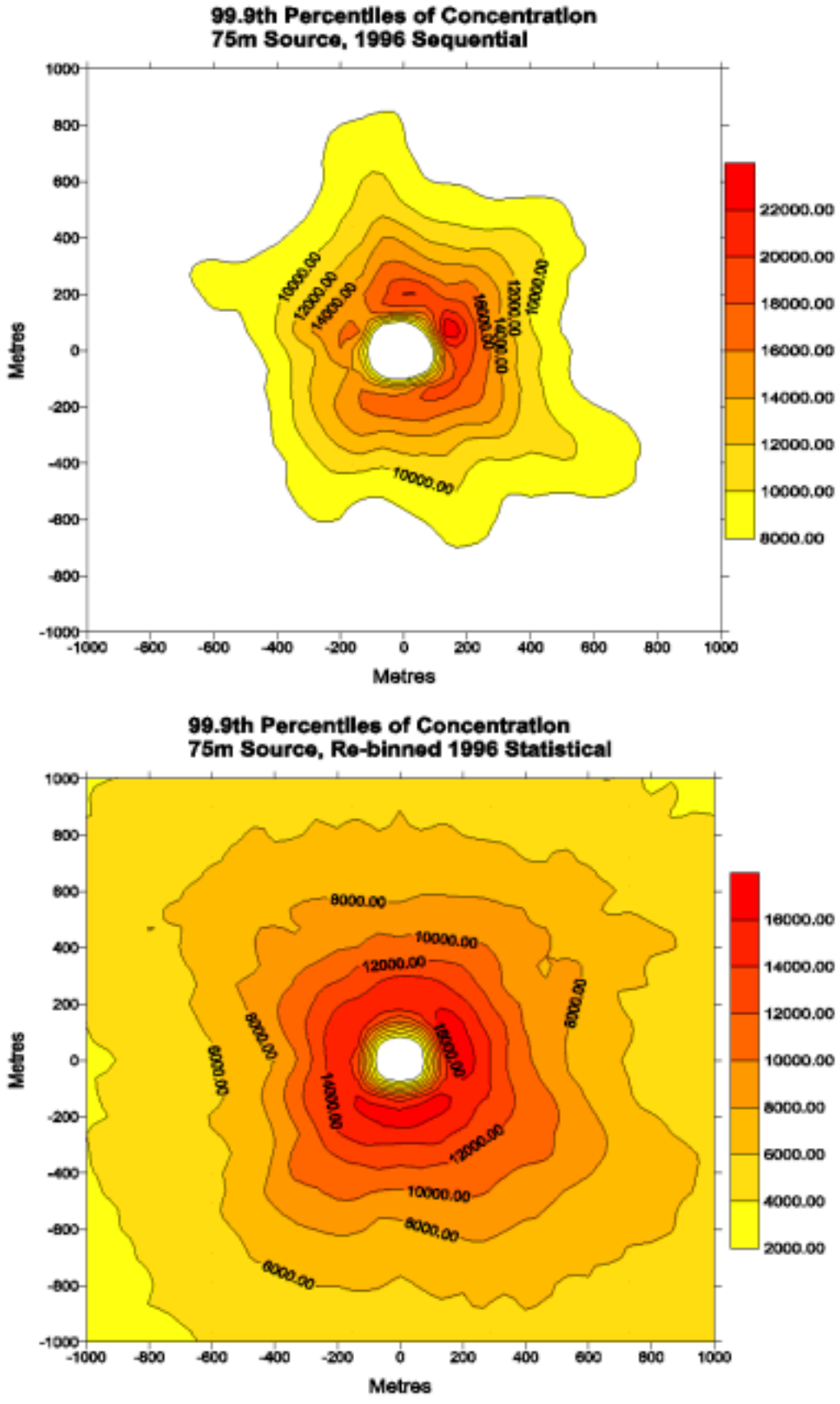

FIGURE F2f: 99.9th Percentiles of concentration for 75m source using re-binned 1996 statistical data and standard sequential data